Europa-Universität Flensburg

Optimization of
Energy System Design and Operation using
Multi-Objective Evolutionary Algorithms and
Mixed-Integer Linear Programming

Dissertation submitted by Cord Kaldemeyer, M.Eng.

in fulfilment of the requirements for the degree of
Doctor of Economics (Dr. rer. pol.)

Supervisors:

Prof. Dr. Olav Hohmeyer
Europa-Universität Flensburg

Prof. Dr.-Ing. Ilja Tuschy
Flensburg University of Applied Sciences

Flensburg, February 2021

Abstract

A global transition of energy supply systems towards more sustainability requires the detailed investigation of different future pathways to examine their technical, economical and environmental feasibility. In this context, the energy system design and operation is often subject of discussion between different stakeholders with conflicting perspectives. This demands for new methods to optimize different criteria simultaneously. Such a method for the multi-objective design and operation of energy supply systems is developed and applied to a set of diverse case studies in this thesis.

The here developed method combines the strengths of multi-objective evolutionary algorithms (MOEA) and linear programming (LP) or mixed-integer linear programming (MILP) techniques. Regarding the system design, the former is capable of handling non-linearities and enables a real Pareto-optimization. Concerning the system operation, the latter offers the advantage of solving to optimality and dealing with large numbers of decision variables and constraints. Furthermore, different cluster algorithms can be applied to reduce the model dimensionality and computational complexity via decomposition into representative partial models.

Different case studies demonstrate the broad range of method applications. In the first case study, a detailed compressed air energy storage system is optimized from an investor's perspective while considering technical and economical design objectives. In the second case study, a municipal district heating system is optimized from an operator's perspective regarding economical and environmental design objectives. As for the third case study, a multi-regional national power system is optimized from a central planner's perspective with regard to economical and environmental objectives. In summary, it can be demonstrated that the actual system design heavily depends on the considered optimization criteria and surrounding market environment.

This thesis shows that the proposed method allows for the optimization of arbitrary energy systems and gives deeper insights into the specific system's interrelations. It enables the modeller to answer a wide range of questions arround the design and operation of future energy supply systems in technical, economical and environmental dimension while preserving criteria from different stakeholder perspectives. In conclusion, the developed method provides a more solid decision basis for the transformation of energy supply systems when compared to existing methods that consider only one objective.

Acknowledgements

Statutory declaration

Ich erkläre hiermit an Eides Statt, dass ich die vorliegende Arbeit selbstständig verfasst und andere als in der Dissertation angegebene Hilfsmittel nicht benutzt habe; die aus fremden Quellen (einschließlich elektronischer Quellen, dem Internet und mündlicher Kommunikation) direkt oder indirekt übernommenen Gedanken sind ausnahmslos unter genauer Quellenangabe als solche kenntlich gemacht. Zentrale Inhalte der Dissertation sind nicht schon zuvor für eine andere Qualifikationsarbeit verwendet worden. Insbesondere habe ich nicht die Hilfe sogenannter Promotionsberaterinnen bzw. Promotionsberater in Anspruch genommen. Dritte haben von mir weder unmittelbar noch mittelbar Geld oder geldwerte Leistungen für Arbeiten erhalten, die im Zusammenhang mit dem Inhalt der vorgelegten Dissertation stehen. Die Arbeit wurde bisher weder im Inland noch im Ausland in gleicher oder ähnlicher Form einer anderen Prüfungsbehörde vorgelegt. Auf die Bedeutung einer eidesstattlichen Versicherung und die strafrechtlichen Folgen einer, auch fahrlässigen, falschen oder unvollständigen eidesstattlichen Versicherung und die Bestimmungen der §§ 156, 161 StGB bin ich hingewiesen worden.

Flensburg, Februar 2021

_____

Cord Kaldemeyer

Contents

1 Introduction

This chapter provides an overview of the thesis with its background, objectives and methods. First, the scientific gap within the scientific field of energy modeling is outlined. Secondly, the research objectives are formulated along with respective hypotheses followed by a delineation with regard to other research fields. Finally, a brief overview of the used methods and general procedures is given to guide the reader through the further course of the thesis.

1.1 Problem outline

The global transition towards sustainable and low-carbon energy supply systems requires the investigation of future trajectories from different perspectives as a base for a solid scientific discussion. Due to a development towards more cross-sectoral and decentralized structures, such energy systems imply a rising complexity regarding their technical, economic and socioeconomic dimensions [1, 2]. Insights into such complex systems can be retrieved by means of computer-based models to support the abovementioned discussion and decision processes with a quantitative base.

A variety of computer models implementing optimization methods can be used to investigate specific research questions. Among others, these models include economic dispatch models for capacity planning, unit commitment models for power plant dispatch and power flow models for electricity transmission network operation [3, 4, 5, 6]. Respective applications can be transnational investigations based on merely economic top-down equilibrium models or far more detailed technical investigation, which are used for local infrastructure planning based on technology-specific data in bottom-up models. Additionally, models can be adapted or linked in order to integrate different sectors such as electricity, heat and mobility with their cross-sectoral interdependencies.

Many of such models either seek for the optimal operation of an energy system like the dispatch of a fleet of renewable and fossil power plants to match a given electricity demand or the dimensioning of a local district heating system consisting of supply and storage technologies with respective capacities. Even if both objectives, specifically the operation and the design, are optimized simultaneously within combined models, in most cases only one objective, for example costs, emissions or technical metrics is regarded.

Consequently, generated results only deliver a decision base for a single stakeholder perspective with regard to the optimal system design and operation.

This one-sided investigation is often not beneficial in reality where decisions are made based on compromises between often conflicting stakeholder perspectives. As only one example, a local district heating network operator might be interested in building the most economical system layout, whereas a non-governmental organization might claim to select a layout at lowest emissions for the same supply task. Using two different models each considering only one objective might deliver completely different layouts which aggravates the finding of a good compromise solution between both objectives. This illustrates the need for new methods in the field of energy modeling which aim at the simultaneous optimization of operation and design with regard to multiple objectives.

1.2 Research objectives

Main goal of this thesis is the development of a new method which optimizes the design and operation of arbitrary energy systems with regard to multiple objectives. Such energy systems in turn are defined by a high degree of freedom in a technical, economical and environmental dimension which means that they can be described on different levels of technical, economical and environmental detail.

Apart from the actual method development, special emphasis will be put on a transparent method description which includes a generic implementation. From the definition of the main objective, several research questions are derived and to be answered in the course of the thesis:

1. Method development
   a) How can the design and operation of energy systems be optimized for multiple objectives?
   b) Which advantages are offered by the proposed method compared to existing methods?
   c) Which design patterns and concepts are valuable for a performant implementation?

2. Method application
   a) How can non-linear relations be considered within specific applications?
   b) How can model complexity and resulting runtimes be reduced?
   c) How can obtained results be related to existing system designs?
   d) Which algorithms and parameter sets are valuable in terms of different applications?
   e) Which range of applications can be identified for the proposed method?

The formulated research questions can be divided into two parts. The questions within the first part are related to the method development itself and thus of general nature. For this, in addition to the proposal of a suitable method, the method is delineated with regard to the scientific status quo. The questions in

the second part are related to the actual method application. Thus, the research questions are specific to the method applications or type of application. In conclusion, the formulated questions aim to elaborate the scientific value of both the method itself and its advantages in terms of specific applications.

1.3 Scope of thesis

In the scope of this thesis it is referred to optimization-based energy models as descibed in [1] or [7] as these are widely used within energy modeling due to their communicability and compact nature. For example, they can be represented only by an objective function, respective constraints and data as in [8]. Other articles compare respective models from different studies [9] and propose new evaluation frameworks [10]. Consequently, the advances of this thesis are related to this common definition of an energy model as a linear optimization based model which is able to cover an energy system in its economical, technical, environmental, temporal and spatial dimension. Additionally, methods from other fields such as evolutionary computing for hybrid models and complexity reduction through temporal or spatial clustering can be utilized as a complement. This definition links the modeling task closer to the methods used within the field of operations research where quantitative models and methods are developed and used in order to support decisions.

1.4 Course of action

This thesis describes a new method. Therefore, the structure is aligned to elaborate its scientific value as outlined in the following. After describing the state of research within the second chapter and summarizing the theoretical background in the third chapter, a new method which optimizes the operation and design of arbitrary energy systems with regard to multiple objectives is proposed in the fourth chapter of the thesis. In the following three chapters, the method is applied to three case studies which differ in their economical, environmental and technical details and thus demonstrate the broad range of applications. Finally, the scientific value of both the proposed method and its specific case study application is elaborated within a detailed discussion, based on the research questions formulated above. This described course of action within this thesis is shown in Figure 1.1.

Within the method development the focus is put on describing a generalized optimization architecture between two methods in detail. For the design optimization, multi-objective evolutionary algorithms (MOEAs) are applied in order to optimize design parameters within energy systems. These can for example be represented by installed capacities, technical or operational characteristics. Moreover, design parameters are related to a specific operational optimization model which is realized within a linear program (LP) or mixed-integer linear program (MILP). Respective operational models are re-calculated and
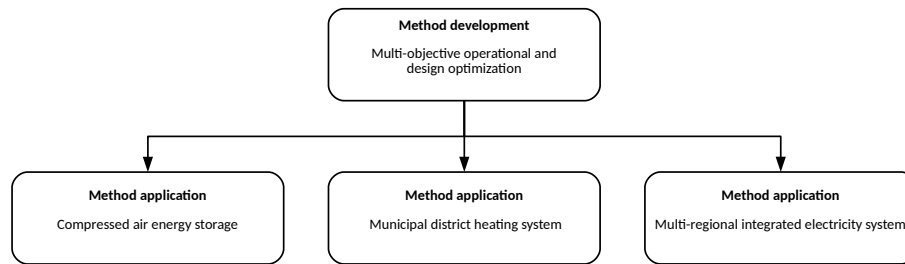
Figure 1.1: Course of action regarding the method development and applications.

asserted for different design parameters with regard to multiple objectives within the evolutionary algorithm. Additionally, clustering algorithms are applied to the input data of the operational models in a pre-processing step in order to reduce the size of the optimization problem.

A method application within three case studies demonstrates the general applicability of the method and serves to elaborate the scientific value. In the first case study, a compressed air energy storage (CAES) is optimized on a day-ahead electricity market from a potential investor's perspective. In this context, the design of the charging and discharging unit specifically the installed capacity of the compressor and the turbine are optimized with regard to a economical and technical objective based on a detailed technology model. In the second case study, components of a municipal district heating (DH) system in northern Germany are optimized at a higher level of abstraction but with multiple other technologies such as peak load boilers (PLB) and thermal energy storages (TES). For this, the installed capacities of power to heat (PtH) and combined heat and power (CHP) components are dimensioned in terms of an economic and environmental objective. In the third case study, a multi-regional power system with several technologies is optimized with regard to costs and emissions by the example of the power system of Kazakhstan. Therefore, optimal wind and solar capacities in single regions are determined allowing insights on possible future energy system designs. Finally, the results are related to the current power system design.

2 State of research in energy system modeling

This chapter describes the current state of research and the classified research needs. Initially, different types of energy models are discussed as defined in the scope of this thesis. Then the state of research in terms of existing methods and applications is outlined focussing on existing applications similar to the case studies within this thesis and some other applications are discussed briefly. Finally, the resulting research needs are defined.

2.1 Model classification

Problems to be solved in optimization based energy modeling are broad and sometimes include multiple sectors. In this context, models are often grouped by their underlying method, for instance linear programming or mixed-integer programming, or by their functionality, for example operational or investment optimization [11, 12, 13]. The latter has been used in a study, which groups energy models or problems to be solved by their concrete modeling capabilities [9]. Such model types include economic dispatch (ED), unit commitment (UC), power flow calculation (PF) or investment planning (IP) models for one or multiple periods. The differences between these models will be outlined briefly in the following to work out a clear definition to be used within the futher course of this thesis.

Although several classical textbooks on the modeling of electricity markets and systems exist based on economic theory [3, 6, 5, 4], there is no clear single definition of the terms ED and UC. Kirschen and Strbac use the terms economic as well as optimal dispatch and unit commitment but without giving a sharp definition [6]. Within Harris et al. ED is defined as the cost-effective management of a group of utilities to combine their generating and transmission facilities of delivery [4, p.176] but without further specification. Moreover, Biggar and Hesamzadeh refer to a similar definition using the term optimal dispatch and further divide models based on the consideration of a demand like using an inelastic electricity demand curve [3, p.97 f.] and the type of cost modeling for instance with constant variable generation costs [3, p.99 f.]. The term optimal dispatch is used as a synonym for an ED problem. Further, a UC problem is defined as the decision whether or not to bring a generating unit into a position where it is ready to produce output in the presence of startup costs [3, p.114] which are not regarded within the related ED problem.

In contrast, Wood, Wollenberg and Sheblé give a precise definition of both ED and UC [5, p.147 f.]. According to this definition, an ED problem aims to find the optimum operating policy for a set of units that is assumed to be already connected to an electricity or energy system. A UC problem in turn is more complex. Assuming a set of available units and a forecasted demand which has to be covered, the UC problem aims at finding a subset of these units to be used in order to serve the demand at minimum operating costs. This adds the dimension of space and time as it determines specific units and may be extended to include an entire optimization period. Moreover, it is more difficult to solve mathematically as it involves integer variables which capture the state of single units. These are for example binary variables which are used to capture states such as starts or shutdowns with respective costs or to define minimum loads and runtimes. Consequently, an ED problem can be interpreted as a subproblem of an UC problem [5, p.148].

Although different definitions for a UC problem exist some common elements can be identified. The existence of a time horizon in which decisions have to be made based on a forecast of a load and other time-dependent values. This time horizon is typically short-term up to a week with a time increment or resolution of less than one hour. Furthermore, UC involves a set of units at specific energy production cost and technical constraints as well as some representation of a grid or balance. Optionally, additional constraints, for example for the system reliability or revenues, can be defined. Based on this, decisions to be made encompass commitment decisions, specifically whether a unit is switched on, production decisions like how much energy is produced by a unit and network decisions such as how much energy is transfered between two network nodes at a specific date. For more information about different problem types and solution techniques it is referred to [14] and [15] in this place.

Models for the investment planning (IP problems) of new capacities within an economy are subject to many studies with specific research questions and also covered by classical text books [3, 16]. Within [3, p.181 ff.] the question of the computation of the socially efficient level of investment in generation and consumption is addressed. In this context, investment planning in the sense of the abovementioned problem types typically includes an ED or UC problem and aims at finding the optimal dispatch and the optimal mix and level of investment as stated by Biggar and Hesamzadeh [3, p.182]. In addition, the concept of "screening curves" to find the optimal level of capacities and operational hours for multiple technologies in order to reach maximum welfare is introduced under given assumptions such as an inelastic demand and well-defined fixed and variable cost for all units.

A different angle for an investment is given by an individual investor's perspective. Biggar and Hesamzadeh [3, p.199 ff.] analyze an investment from an independent generation entrepreneurs' perspective with the result that under some assuptions decentralised investment decisions will lead to an optimal level and mix of generation investment [3, p.203 ff.]. Also, the concept of duration curves is used again in order to explain different market types such as energy-only or capacity markets. Within Kirschen and Strbac

investment from a potential investor's perspective is analyzed purely from the economic point of view using average price assumptions and capacity factors [6, p.205 ff.]. Here, the case of single investment as well as the comparison of investments like using the incremental internal rate of return is presented by means of price duration curves along with some examples. The investment in transmission might also be included in an IP and is outlined by Kirschen and Strbac for different methods [6, p.227 ff.].

The modeling of electricity transmission networks with their respective constraints and power flows is widely covered. Existing power flow models and solution techniques are for instance given in [3, p.141 ff.], [5, p.253 f.] and [4]. In many cases a DC load flow model is used as a approximation of the original AC system, which would require a more complicated set of equations to be modelled [5, p.144]. As stated by Stoft "Most of the basic properties of AC power flows that are needed to design markets can be understood in terms of this essentially DC model, but some important phenomenon are purely AC in nature." [16], which enables a reasonable modeling of the physical network also in ED, UC and IP models. This also includes the possibility of combined ED, UC, IP and PF models for instance in a multi-regional model which simultaneously optimizes the investment and unit commitment with regard to the power flow in the network. Here, not only electricity but also multiple sectors like heat and transport can be integrated within a common model as described by concepts such as multi-energy systems [17] or energy hubs [18, 19]. Other synonyms for those systems are multi-vector energy systems or multi-carrier energy systems and have been described with a respective concept and software to describe and solve them [9]. In the course of this, all concepts allow for an inclusion of multiple sectors by means of a set of the abovementioned models.

In this thesis, the following model classification is used: An operational model (OM) is defined by an ED or UC model with optional inelastic demands for different commodities such as electricity, heat or transport. It is capable of capturing the dimensions of time and space and optionally offers an integration of PF as described in [5]. Further, multi-objective operational model (MOM) extends an OM by allowing for multiple objectives. In comparison, a design model (DM) seeks for optimal parameters of an energy system such as generation, storage or transmission capacities or internal technical parameters without using an OM and thus a detailed consideration of time and often space. A design model that extends a DM by allowing for multiple objectives is defined as a multi-objective design model (MDM). Furthermore, combined design and operational model (CDOM) combines an OM and DM using the same method and consequently is formulated as an IP similarly to the definition in [3, p.181 ff.]. Here, multi-objective combined design and operational model (MCDOM) extends a CDOM by allowing for multiple objectives with regard to the design optimization. In contrast, hybrid design and operational model (HDOM) combines an OM and DM using different optimization methods for both objectives, each regarding only one objective. Finally, a multi-objective hybrid design and operational model (MHDOM) extends an HDOM by allowing for multiple objectives with regard to the design optimization. The used model classification is summarized in Table 2.1.

Table 2.1: Model classification used in the scope of this thesis. Marks: x/- = fully/not applicable.

Model type	Model shortcut	Operational optimization	Design optimization	Multiple objectives	Different methods
Operational model	OM	x	-	-	-
Multi-objective operational model	MOM	x	-	x	-
Design model	DM	-	x	-	-
Multi-objective design model	MDM	-	x	x	-
Combined design and operational model	CDOM	x	x	-	-
Multi-objective combined design and operational model	MCDOM	x	x	x	-
Hybrid design and operational model	HDOM	x	x	-	x
Multi-objective hybrid design and operational model	MHDOM	x	x	x	x

The last two and in particular the latter are subject to the method development within this thesis. They are characterised by the quality that an "inner" operational optimization is embedded within an "outer" design optimization with either one or multiple objectives. Resulting operational costs and other results such as the optimal dispatch from the decision variables of the "inner" part can be included within one or more objectives of the "outer" part. This in turn means that respective optimal designs with regard to one or multiple objectives are optimal with respect to a mono-objective operation. This does not guarantee to reach a global optimum of the design with regard to the operation as it would be realized within a CDOM or MCDOM. On the other hand, it provides a flexible coupling of different models and the possibility to correctly deliver concave and convex parts of Pareto front within multi-objective design problems. See [20, p.530] for the underlying problem using aggregation methods for example in CDOMs such as in [21] or [22]. It has to be mentioned that it would principally be possible to also list single hybrid operational or design models here. But as these seem to be very rare in literature and are not subject of this thesis these are omitted here for the sake of conciseness.

2.2 Current state of research

It becomes clear that a broad range of models exist that can be applied to answer different types of questions within the field of energy supply systems. As the set of possible model applications is almost unlimited, in the following, the focus is directed on methods related to the ones outlined above. Further, the set of applications is limited to the field of the three selected case studies which are compressed air energy storage, district heating systems and multi-regional power systems.

Method development

Comparisons of modeling tools for the analysis of energy supply systems with a high share of renewable energies (RE) are provided by [12] and [11]. In [11] various modeling tools were compared with the conclusion that most of these tools are adequate to analyze future challenges within energy systems. Besides the requirement to chose a holistic view and integrate multiple sectors in future studies, the study emphasizes the need for more transparency in the field of energy modeling. While similar reviews for the integration of RE on different levels of detail [12] exist , [11] focuses more on optimization based planning tools and includes some open models of the last generation as described in [9].

Methods and approaches for the optimal design of hybrid RE systems with conventional backup capacities are reviewed in [23]. According to the authors, one of the most important issues related to these systems is the optimal sizing of different components in order to meet all energy demands at possible minimum investment and operating costs. For this, different sizing approaches are compared and analyzed in detail. Among commercial tools with heuristic solvers different population based approaches such as genetic algorithms (GA), particle swarm optimization (PSO) and others are reviewed with the result that these are capable of making significant contributions to higher RE penetration.

Optimization-based planning of distributed energy resources (DER) with respect to different objectives is analyzed in [24]. The review includes about 80 papers and outlines mono-objective methods in the first part and analyzes concepts and methods for multi-objective optimization in the second part. The authors argue that appropriate planning methods with multiple objectives in technical, environmental and economic dimensions are able to represent the stochastic nature of RE and the grid network. Thus, they are able to provide deeper insights into properties of DER. A review of multi-objective optimization of energy systems by means of evolutionary algorithms (EA) is given by [25]. The study analyzes about 50 papers and concludes that only a few studies optimize many entities of energy systems. The most popular methods seem to be different variants of genetic algorithms and particle swarm optimization.

Method application

There are numerous studies focusing on different aspects of CAES. Most studies are focused on integration effects of RE in specific energy systems or on business cases for potential operators by means of specific models. Many models are used for an operational optimization of concepts within a single market whereas only a few are capable of integrating multiple market environments. Some models focus on sole design optimization without considering intertemporal variation of time-related quantities such as resource prices or variable feed-in from RE. In the scope of this thesis the focus is put on techno-economic studies which investigate specific technical setups under given economic assumptions.In the following, the selection of major works in this field is delineated from the case study within this thesis according to different criteria which are the underlying model type, used methods and model details. Table 2.2 shows an overview of relevant studies in the field of CAES modeling. A detailed discussion of the underlying sources is provided in Section E in the appendix.

The vast majority of studies is based on classical operational models which are based on mixed-integer or linear programming methods. For instance, in [26] or [27] rather detailed MILP models are applied to analyze the technology in combination with wind energy and possible markets for electricity and control reserve, respectively. Both use unit commitment constraints where the latter uses a higher level of detail by means of including partial load conditions and ramping constraints. Although both models apply similar model types, the focus in [26] is on the effect of the storage system concerning wind integration from a system perspective where [27] demonstrates how a storage can participate in multiple markets while at the same time reducing wind curtailment, but from an operators perspective without an integration of other system states. Different studies such as [28], [29] or [30] deal with similar questions but with other methods applied for the operational optimization. Other studies focus on the design optimization with or without a further consideration of the economic environment. In [31] a multi-objective genetic algorithm optimization is applied on the design parameters of an underwater CAES system, where the roundtrip efficiency, cumulative costs and operating profit are optimized simultaneously. However, the operation is optimized only for a period of 24 hours based on average hourly electricity prices. Similarly, in [32] components of a CAES system attached to a wind farm are optimized without an operational optimization. In contrast, in [33] a HDOM is proposed where the operation is optimized using a MILP model which is embedded within an EA for the design optimization to size different components.

In conclusion, it can be stated that no MOM, CDOM, MCDOM or MHDOM has yet been applied within the field of CAES modeling. Except for the study which applies an MDM [31], no multi-objective and data clustering approaches are applied within techno-economic CAES models. Finally, although there are various technology perspectives of CAES, this diversity is not reflected within the current model landscape.

Table 2.2: Summary of relevant studies in CAES modeling. Marks: x/o/- = fully/partly/not applicable.

Reference	Model type								Used methods					Model details			
	OM	MOM	DM	MDM	CDOM	MCDOM	HDOM	MHDOM	(MI)LP	EA	MOEA	Other	Data clustering	UC constraints	Detailed components	Open modeling	Published dataset
[30]	x	-	-	-	-	-	-	-	-	-	-	x	-	x	o	-	-
[31]	-	-	-	x	-	-	-	-	-	-	x	-	-	-	x	-	-
[34]	x	-	-	-	-	-	-	-	x	-	-	-	-	x	-	-	-
[35]	x	-	-	-	-	-	-	-	-	-	-	x	-	-	x	-	-
[36]	x	-	-	-	-	-	-	-	x	-	-	-	-	x	-	-	-
[37]	-	-	-	-	-	-	-	-	x	-	-	-	-	x	o	-	-
[38]	x	-	-	-	-	-	-	-	x	-	-	-	-	x	-	-	-
[39]	x	-	-	-	-	-	-	-	x	-	-	-	-	x	x	-	-
[40]	x	-	-	-	-	-	-	-	x	-	-	-	-	x	x	x	-
[41]	x	-	-	-	-	-	-	-	x	-	-	-	-	x	o	-	-
[42]	x	-	-	-	-	-	-	-	x	-	-	-	-	x	-	-	-
[32]	-	-	x	-	-	-	-	-	x	-	-	-	-	-	-	-	-
[43]	x	-	-	-	-	-	-	-	-	-	-	x	-	x	o	-	-
[44]	x	-	-	-	-	-	-	-	x	-	-	-	-	x	x	-	-
[28]	x	-	-	-	-	-	-	-	-	-	-	x	-	-	-	-	-
[29]	x	-	-	-	-	-	-	-	-	-	-	x	-	-	-	-	-
[45]	x	-	-	-	-	-	-	-	-	-	-	x	-	x	-	-	-
[46]	x	-	-	-	-	-	-	-	-	-	-	x	-	-	-	-	-
[26]	x	-	-	-	-	-	-	-	x	-	-	-	-	x	-	-	-
[47]	-	-	x	-	-	-	-	-	-	x	-	-	-	-	x	-	-
[27]	x	-	-	-	-	-	-	-	x	-	-	-	-	x	o	-	-
[48]	-	-	x	-	-	-	-	-	-	-	x	-	-	-	x	-	-
[49]	x	-	-	-	-	-	-	-	x	-	-	-	-	x	-	-	-
[33]	-	-	-	-	-	-	x	-	x	x	-	-	-	x	-	-	-

Studies within the field of district heating involve the investigation of different technologies of current or future systems. Respective techno-economic studies have a long tradition whereas newer studies are focusing increasingly on the integration of RE and energy efficiency. Within the following scientific delineation, the focus is put on techno-economic studies which utilize optimization models for at least either the operation or design of a system. As the focus is put on the applied method, the concrete set of technologies or primary energy supply is of secondary importance. Table 2.3 shows an overview of relevant studies in the field of DH modeling. A detailed discussion of the underlying sources is provided in Section E in the appendix.

As opposed to studies within the field of CAES, many studies focus on the design and operation of DH systems with regard to one or multiple objectives. Here, mostly mixed-integer linear programming methods or evolutionary algorithms are applied standalone or in combination. For instance, in [21] the design and operation of a multi-energy system with seasonal energy storage is optimized by means of a CDOM which makes use of the ϵ-constraint method (cf. Section 3.3). Similarly, in [50] the design and the operation of an urban combined heat and power distributed generation system is optimized using the weighted sum method.Hybrid methods which utilize MOEAs in combination with a simulation model for the operation are applied [51]. Moreover, MHDOMs which apply a combination of MOEAs and MILP models are used in a line of papers where data clustering methods are applied to reduce the overall runtime [52, 53, 54, 55, 56, 57]. The underlying MHDOM has initially been developed in a respective thesis [58]. Other studies focus on aspects like the integration of RE into DH systems and apply a sole operational optimization within respective OMs. For instance, in [59] the contribution of heat storage to the profitable operation of combined heat and power plants is investigated from a potential investor's perspective for a part of the district heating network of Berlin. Furthermore, in [60] a short-term model for the flexible operation of DH systems which include high shares of wind power is proposed. Finally, in [8] different approaches for the integration of flow temperatures in unit commitment models of future DH systems are tested regarding their impact on the economical results.

In summary, it can be noted that a variety of models including mono- and multi-objective approaches is applied within the field of modeling DH systems. Apart from a selection of studies which apply OMs based on MILP, multiple studies apply CDOM, MCDOM or MHDOMs to optimize the system. For multi-objective approaches like MCDOM or MHDOMs, two methodical lines can be identified: On the one hand within MCDOMs "classical" methods such as the ϵ-constraint or weighted sums method are used in combination with MILP models for the operation and design. On the other hand, within MHDOMs, Pareto-based MOEAs are used for the design along with operational MILP models where some studies apply data clustering methods in order to increase the model runtime.

Table 2.3: Summary of relevant studies in DH modeling. Marks: x/o/- = fully/partly/not applicable.

Reference	Model type								Used methods					Model details			
	OM	MOM	DM	MDM	CDOM	MCDOM	HDOM	MHDOM	(MI)LP	EA	MOEA	Other	Data clustering	UC constraints	Detailed components	Open modeling	Published dataset
[61]	x	-	-	-	-	-	-	-	x	-	-	-	-	x	o	-	-
[8]	x	-	-	-	-	-	-	-	x	-	-	-	-	x	x	x	x
[50]	-	-	-	-	-	x	-	-	x	-	-	-	-	o	-	-	-
[59]	x	-	-	-	-	-	-	-	x	-	-	-	-	x	o	-	-
[62]	x	-	-	-	-	-	-	-	x	-	-	-	-	x	o	-	-
[63]	x	-	-	-	-	-	-	-	x	-	-	-	-	x	o	-	-
[60]	x	-	-	-	-	-	-	-	x	-	-	-	-	x	o	-	-
[52]	-	-	-	-	-	-	-	x	x	-	x	-	-	o	-	-	-
[53]	-	-	-	-	-	-	-	x	x	-	x	-	-	o	-	-	-
[54]	-	-	-	-	-	-	-	x	x	-	x	-	-	-	-	-	-
[56]	-	-	-	-	-	-	-	x	x	-	x	-	x	-	o	-	-
[55]	-	-	-	-	-	-	-	x	x	-	x	-	x	-	o	-	-
[57]	-	-	-	-	-	-	-	x	x	-	x	-	x	-	o	-	-
[21]	-	-	-	-	-	x	-	-	x	-	-	-	x	o	o	-	-
[64]	-	-	-	-	x	-	-	-	x	-	-	-	-	x	x	-	-
[51]	-	-	-	-	-	-	-	x	-	-	x	x	-	-	o	-	-
[65]	-	-	-	-	x	-	-	-	x	-	-	-	-	x	o	-	-
[66]	-	-	-	-	-	x	-	-	x	-	-	-	-	x	-	-	-
[67]	-	-	-	-	-	-	-	x	x	-	x	-	-	x	-	-	-
[68]	-	-	-	-	-	x	-	—	x	-	-	-	-	x	-	-	-
[69]	x	-	-	-	-	-	-	-	x	-	-	-	-	x	o	x	-
[22]	-	-	-	-	-	x	-	-	x	-	-	-	-	x	x	-	-
[70]	-	-	-	-	-	x	-	-	x	-	-	-	-	x	x	-	-
[71]	-	-	-	-	-	-	x	-	x	-	-	x	-	-	x	-	-
[72]	-	-	-	-	-	x	-	-	x	-	-	-	o	x	x	-	-
[58]	-	-	-	-	-	-	-	x	x	-	x	-	-	o	x	-	-

Compared to CAES and DH systems, research on multi-regional and other systems covers a wider range of topics from national multi energy systems (MES) to the detailed design of single coal and natural gas power stations. Some studies include different types of energy storage in the analyzed systems in order to provide a certain degree of flexibility and potential integration of RE. As in the field of DH systems, there are numerous studies wherefore the focus in this field is put mainly on studies that use (combined) multi-objective approaches similar to the one proposed in Chapter 4. Table 2.4 shows an overview of relevant studies in the field of modeling multi-regional and other systems. A detailed discussion of the underlying sources is provided in Section E in the appendix.

As mentioned, most of the selected studies apply MCDOMs, HDOMs and MHDOMs depending on the specific research questions. For example, [73] apply a MCDOM for integrated energy systems based on a multi-objective MILP model and the method of weighted sums which is published in detail within another publication. Further, in [65] the authors propose a HDOM for the component sizing, and placement in multi-energy microgrids based on mixed integer linear programming. MHDOMs which include multiple objectives are applied for different systems on different levels of detail. For instance, within a series of publications [74, 75, 76] the energy system simulation tool EnergyPLAN is coupled to a MOEA in order to find better system designs with regard to different objectives. The respective hybrid model is similar to the one proposed in another the study [51]. Similarly, in [77] the authors suggested a detailed simulation model that is embedded within a MOEA to size components within a hybrid microgrid. In contrast, in studies such as [78], [79] and [80, 81] optimization methods are used for the operational optimization. Other studies apply OMs and MDMs CDOM within different research fields. In [82] a national energy model and a power system model are linked to utilize the strengths of both model types. Further, in [83] a generic formulation for the operational and topological optimization of MES is proposed. Respective MDMs for different types of energy and power systems are proposed by [84], [85] and [86]. Within another study a CDOM implements the concept of energy hubs [19].

It becomes clear that combined and hybrid approaches are applied frequently within the field of modeling multi-regional and other systems in order to optimize the system operation and design. In this context, mono- as well as multi-objective approaches are used within MCDOMs, HDOMs and MHDOMs. As explained, a wide range of different applications is covered, especially through hybrid approaches within MHDOMs. These enable a coupling of arbitrary specialized models when compared to MCDOMs which require a problem definition within a single model. Nonetheless, data clustering methods are used only rarely to deal with model complexity.

Table 2.4: Summary of relevant studies in modeling multi-regional and other systems.
Marks: x/o/- = fully/partly/not applicable.

Reference	Model type								Used methods					Model details			
	OM	MOM	DM	MDM	CDOM	MCDOM	HDOM	MHDOM	(MI)LP	EA	MOEA	Other	Data clustering	UC constraints	Detailed components	Open modeling	Published dataset
[84]	-	-	-	x	-	-	-	-	-	-	x	-	-	-	x	-	-
[87]	x	-	-	-	-	-	-	-	x	-	-	-	-	x	-	-	-
[88]	x	-	-	-	-	-	-	-	x	-	-	-	-	x	-	-	x
[85]	-	-	-	x	-	-	-	-	-	-	x	-	-	-	-	-	-
[82]	x	-	-	-	-	-	-	-	x	-	-	-	-	x	-	-	-
[89]	-	-	-	-	x	-	-	-	x	-	-	-	-	x	-	-	-
[21]	-	-	-	-	-	x	-	-	x	-	-	-	x	x	x	-	-
[83]	x	-	-	-	-	-	-	-	-	-	-	x	-	-	-	-	-
[19]	-	-	-	-	x	-	-	-	-	-	-	x	-	-	-	-	-
[78]	-	-	-	-	-	-	-	x	-	-	x	x	-	-	-	-	-
[90]	x	-	-	-	-	-	-	-	-	-	-	x	-	-	x	-	-
[80]	-	-	-	-	-	-	-	x	-	-	x	x	-	-	x	-	-
[81]	-	-	-	-	-	-	-	x	-	-	x	x	-	-	x	-	-
[86]	-	-	-	x	-	-	-	-	x	-	-	-	x	-	x	-	-
[51]	-	-	-	-	-	-	-	x	-	-	x	x	-	-	-	-	-
[65]	-	-	-	-	-	-	x	-	x	-	-	-	-	-	x	-	-
[74]	-	-	-	-	-	-	-	x	-	-	x	x	-	-	-	-	-
[75]	-	-	-	-	-	-	-	x	-	-	x	x	-	-	-	-	-
[76]	-	-	-	-	-	-	-	x	-	-	x	x	-	o	o	-	-
[91]	-	-	-	-	-	x	-	-	x	-	-	-	-	o	-	-	-
[92]	-	-	-	-	-	x	-	-	x	-	-	-	-	o	-	-	-
[93]	-	-	-	-	-	x	-	-	x	-	-	-	-	o	-	-	-
[73]	-	-	-	-	-	x	-	-	x	-	-	-	-	o	-	-	-
[79]	-	-	-	-	-	-	-	x	x	-	x	-	x	-	x	-	-
[77]	-	-	-	-	-	-	-	x	-	-	x	x	-	-	x	-	-

2.3 Resulting research needs

On the basis of the state of research, it becomes clear that future RE systems are facing an increasing complexity. Consequently, the models themselves have to tackle these future challenges in their temporal and spatial dimension which is outlined in [1]. The reproducability of computational experiments and thus overall transparency is an issue. In this connection, the particular need for open models and data transparency is highlighted by [7]. A series of publications demonstrates only a few possible solutions towards open energy science among many others [9, 10, 94, 95]. In addition, decision support for problems within energy system design and operation are often characterized by contradictory objectives and subject to a high level of uncertainty.

These issues and the increasing complexity of real problems are not or only partly addressed by existing classical decision support models such as OM, DM, CDOM and their multi-objective variants. In comparison, MHDOMs offer advantages as they are able to consider multiple objectives and help to identify fundamental relationships. By providing an entire set of Pareto-optimal solutions to the decision makers, these methods allow for a deeper understanding of the design problem including the system operation. However , these methods have rarely been described generically for arbitrary algorithms and energy systems and do not address the issue of open modeling and data transparency. This results in a demand for new methods in order provide a better decision base from different perspectives within the process of shaping future energy systems. Based on the problems and challenges outlined above, such new methods should:

- optimize both the design and operation of energy systems simultaneously,
- take into account multiple objectives,
- be flexible in terms of different applications and problem types,
- deal with an increasing complexity of future energy systems,
- allow for a generic and transparent method description,
- present their models transparently and use open source software,
- publish underlying models and data under a permissive license.

Some of the analyzed studies indicate that a combination of MOEAs and (MI)LP models has proven to be particularly powerful to create effective MHDOMs, especially when combined with clustering algorithms. Currently, this combination of methods has only been applied within the field of district heating systems in respective studies by Fazlollahi et al. [56, 96, 57]. A structured, generic and transparent combination of MOEAs, (MI)LP models and different clustering algorithms has not been applied yet to the field of compressed air energy storage, multi-regional or other systems. This issue is addressed within this thesis by the development of a respective method and its application to a broad spectrum of problems, namely a CAES, DH and multi regional power systems.

2.4 Selected methods and applications

The question how the outlined research needs can be addressed leads to a selection of adequate methods and applications in order to elaborate the added value. These are outlined in the following for both the method development itself and its possible applications.

Method development

The proposed hybrid optimization method combines two methods to optimize an energy system's design and operation with regard to different objectives. For the optimization of an energy system's design, flexible and derivative-free "black-box solvers" for global optimization are able to handle one or multiple objectives and constraints. Consequently, this family of algorithms can be used to optimize different properties of energy systems . For the optimization of an energy system's operation, LP and MILP models are well suited to model ED and UD problems with only one objective effectively at a sufficient level of detail [14, 15]. Thus, both optimization approaches are combined and the operational optimization which realized as LP or MILP is embedded within a surrounding design optimization based on an EA or MOEA. Furthermore, complexity of operational models can be reduced by means of data clustering algorithms which are able to reduce the dimensions of time and space by representing the data of the original problem by single clusters.

In three selected case studies, different MOEAs are applied in the design part. In the CAES case study, the prominent Nondominated Sorting Genetic Algorithm (NSGA-II) is applied in order to use a robust well-established algorithm. For the district heating case study, the Multi-objective Evolutionary Algorithm based on Decomposition (MOEAD/D) is used. In the third case study which models a multi-regional power system, Non-dominated Sorting Particle Swarm Optimization (NSPSO) is applied to optimize the system design. This selection of a diverse set of algorithms from genetic algorithms to population based methods in the design part, aims to demonstrate that the general function principle of the hybrid method is independent of specific algorithms. In the operational part, either mixed-integer programming or linear programming models are used. The further is used in the first two case studies and the latter is applied in the last case study in order to show that the operational part is not limited to specific model types. Simultaniously, three different cluster algorithms are applied across the three case studies in order to reduce the overall model runtime. For this, k-means, k-medoids and hierarchical clustering are applied on the data of the respective operational model which likewise demonstrates the general usability of arbitrary clustering algorithms.

Method application

The general applicability of the method for a broad range of applications is demonstrated within the different case studies ranging from detailed technical to large and spatially resolved models. This aims to demonstrate how different systems can be solved flexibly by using the architecture of a master and slave problem for the design and operation, respectively, using different combinations of systems and algorithms. Different combinations of objectives and design variables aim to deliver valuable and unexpected insights into respective interrelations between both. Furthermore, the question which algorithms and parameter sets are valuable in terms of different applications, which can be addressed. Finally, the concept of using different case studies allows to focus on specific highlights in each application. This shows which numbers and types of objectives, decision variables, technical, temporal and spatial resolution can be chosen for similar systems which allows a higher degree of transferability compared to only one application.

In the first case study, method is applied with a model of a CAES plant on a high level of technical and economical detail. Two fitness functions are defined within the design process to optimize the plant design in an economical and technical dimension. Furthermore, the focus is put on the question how non-linear relations can be taken into account. Within the second case study, the applicability to a diverse set of technologies is demonstrated by means of the application to a municipal heating system. Two fitness functions are defined to optimize the system design in an economical and environmental dimension. The focus is put on the question how complexity can be reduced and how this affects the obtained results. In the third case study, an increased number of technologies is modelled using the power system of Kazakhstan. For the design optimization, an economic and an ecological design objective are selected. Within this case study, the focus is put on the comparison of the current system design to the set of Pareto-optimal system designs in the solution space. This aims to elaborate the method's added value by delivering new insights to the decision maker.

2.5 Scientific contribution

Within the state of research, a compact overview of optimization methods applied to energy systems is provided along with a description of the currently existing research gap. Moreover, a general outline of the proposed method is provided within the last section. In the first part of this section, the method's added value is highlighted by emphasizing its unique features. Further, the scientific contribution of the method application within different case studies is outlined in the second part.

Method development

The method for the design and operation of energy systems proposed in the scope of this thesis combines two well-suited methods in order to solve complex problems by decomposing them into subproblems. An energy system's design is optimized through evolutionary algorithms while its operation is realized using (mixed-integer) programming as it is especially suited to model the system dispatch. The operation is optimized regarding one objective in temporal or potentially spatial dimension which captures the operational characteristics of real systems. These are mostly operated based on (marginal) costs and can also include regulary penalties or incentives. Within the design optimization a global metaheuristic search algorithm quickly explores the search space and investigates good system designs.

This issue of often contradictory objectives within energy system design and operation is addressed by including multiple objectives in the design optimization. An entire set of Pareto-optimal design solutions with additional consideration of the system's operation is offered to the decision makers. This allows for a deeper understanding of the design problem and helps to identify fundamental relationships. The hybrid approach which links evolutionary algorithms and linear programs has advantages over the often applied weighted sum (cf. [22] or [73] as only two examples) and ϵ-constraint method variants (cf. for instance [21] or [66]) as it delivers concave and convex parts of a Pareto-front (cf. [20, p.530]) and does not require special knowledge of the problem to determine parameters such as weights or suitable ϵ-values a priori (cf. [97]). Moreover, the usage of evolutionary algorithms is flexible in terms of the chosen objective functions (e.g. non-linear functions) and decision variables (e.g. continuous or integer).

The method itself can be adapted flexibly in terms of different applications. Various technologies such as renewable, storage, and distribution systems can be modelled in the operational part. Additionally, resource or other constraints like emission limits for a specific optimization period can be added. Within the design optimization, multiple fitness functions can be defined for instance in economical, technical or ecological dimensions and exchanged quickly. Respective design variables can be integrated with single domains such as continuous or integer if needed. This also allows to optimize structures using binary variables like decisions about whether a component or subsystem is build or not.

Increasing complexity of future energy systems across all potentially coupled sectors with different energy services can be captured. Higher shares of decentralized intermittent RE demand for higher temporal and spatial resolutions which can be integrated by means of the method. If needed, data clustering allows to reduce the problem size while at the same time the system's characteristics can be preserved. Moreover non-linearities can be included in the pre- or post-processing phase of the operational level. Examples would be the integration of non-linear cost terms for capacity expansion as in [79] or the pre-processing of technical characteristics which is demonstrated in Section 4.2.

While existing MHDOMs are described in multiple studies of which some apply (MI)LP [52, 53, 54, 55, 56, 96, 57, 58, 79] and some other methods such as simulation [78, 80, 81, 51, 74, 75, 76, 77] for the operational modeling, a generic and detailed description of the combination of MOEAs and (MI)LP models along with a description of the implementation has not been provided yet. However, due to the good communicability of compact (MI)LPs in combination with MOEAs, a combination of both can be described generically. Such a description is outlined in Sections 4.2 and 4.3 for arbitrary algorithms and energy systems.

The particular need for open models in the sense of open science is highlighted by [7]. Some possible other solutions towards open energy modeling are proposed in [9, 10, 94, 95] among many others. Consequently, the implementation of the proposed method and case studies is realized by means of free and open software which has partly been published previously [9] while the additional implementations are made available under a compatible license. This way of organizing different pieces of software into compatible and documented packages along with its underlying data allows for reproducability and a high level of transparency.

Method application

To delineate the method application in the first case study, a compact overview of CAES research related to this thesis is provided in Table 2.2. Summarizing, the presented case study contributes to the current research landscape through the following features. First, complexity is reduced by applying data clustering algorithms on the input parameters. This allows an efficient repeated solving of the problem and easier interpretation of the input data like only looking at typical periods. Secondly, multiple objectives are considered simultaneously in the optimization process. Except for the works of [47] and [48] which solely focus on design optimization this has not been realized so far in combination with compressed air energy storage. Thirdly, the energy system operation and design are optimized simultaneously. Up to now, both have only been linked in [33] within a mono-objective optimization. A multi-objective approach for both domains does not exist yet. Finally, special emphasis is put on transparency and reproducability which is achieved by publishing the model along with data. Although the reproducabilty of experiments is a key issue in science, many studies do not publish their models and data which is discussed in Chapter 3 and particularly in [7].

Further, a compact overview of district heating systems research related to this thesis is provided in Table 2.3 in order to delineate the method application in the second case study. Summarizing, the presented case study contributes to the current research landscape through the following features. At first, a high level of accuracy is realized by formulations within the operational optimization which are based on static thermodynamical modeling. Except for the works of [58], this has not been combined with a multi-objective design optimization yet. Secondly, a realistic behaviour within technology modeling is

improved through unit commitment constraints within the operational optimization. To the date of writing, this has not been linked with a multi-objective design optimization except for the works of [58] and [67]. However, within these studies, the focus is not put on a generic description of the underlying method. Thirdly, accessability and reusability is fostered by choosing an open modeling approach. Finally, the issue of lacking transparency is addressed like in the first case study by publishing the model along with all underlying data.

Finally, the value of a method application for a multi-regional power system is evaluated within Table 2.4. Within the third case study, a contribution to the current research landscape is delineated as follows. In [90], [80], and [81], a MHDOM is applied only to a specific single technology such as a specific type of power plant, whereas [51], [74],[75] and [76] apply the model to multiple energy nodes with a simulation model for the operation. In contrast to [78] which applies a MHDOM for gas and electricity network planning, the third case study uses a multi-node model with investment in generation capacity. Within [79] a MHDOM is applied on the household level using a similar approach and [77] applies a MHDOM on the level of a microgrid. The third case study contrasts the above mentioned by applying the method within a MHDOM that integrates a multi-regional power system model for the country of Kazakhstan. Here, the focus is on renewable capacity expansion with regard to the levelized costs of electricity and relative emissions from power generation. The model builds upon the general model in [88] in combination with respective data [98] and multiple extensions with regard to renewable generation data. Finally, this combination of model and its application to the power system of Kazakhstan is unique according to the current state of science.

3 Modeling, optimization and data clustering

This chapter provides the theoretical background for the subsequent method development and its application. An overview of different modeling problem types is given and subsequently the foundations of the used optimization and data clustering methods are explained in their fundamental aspects.

3.1 Problem types in modeling

Modeling tasks can be described by means of different problem types which vary in their nature and can be classified differently. In this thesis, the black box model of computer systems is used to distinguish between different types as outlined in [99]. Referring to this, any computer-based system can be described as a system that takes an input and processes this through a computational model. The model is not specified and thus referred to as a "black box". Its purpose is to represent aspects which are relevant to specific real world application and deliver a relevant output. A black box view of systems distinguishes between the actual model input, the model itself, and the output. Depending on which of these is known, three problem types can be determined: optimization, modeling, and simulation. Each of these is explained in the following in detail according to the definitions from [99] to highlight the differences and be precisely defined in the scope of this thesis.

In optimization problems the model is known along with a description of the desired output, wheras the task is to find the input(s) leading to this output. The output side is labelled "specified" instead of "known" because the optimal value might not be known and could be defined implicitly for example as "the lowest costs in terms of all considered variants". Respective problems usually occur in design and engineering. One example of this type is the famous traveling salesman problem which is an abstract representation of many specific real world problems such as finding good routes to deliver goods or sheduling machines in production processes.

In contrast, within modeling or system identification problems the input and output are known and the goal is to find a model which connects the input with the output. In other words, the goal is to find a causal relationship between the input and output data and to generalize from this to explain yet unseen situations. For instance, one could try to explain the price on wholesale electricity markets in terms of different price drivers such as the electrical demand, wind, solar or conventional power plant feed-in. Based on historical

data one could find a mathematical model which explains the output depending on the input, for instance by applying a regression model. In this context, it has to be mentioned that modeling problems can also be transformed into optimization problems. One could think of a regression model, whose parameters have to be adjusted as good as possible. In this case, the overall model accuracy expressed by some metric can be defined as objective and model parameters as decision variables of the optimization problem.

Finally, in simulation problems, the model of the system as well as at least parts of the input are known, whereas the output is unknown. Simulation can be useful in many real-world applications where it is too expensive or even not possible to perform a real experiment. An example could be a traffic simulation, where different mobility alternatives in a specific region are compared along with different transport infrastructures like road and railway systems. Performing the real experiment would not be possible in this case or at least be expensive and politically unjustifiable. Comparing different alternatives in computer simulations with input data on traffic demand and infrastructure along with a good model is cheaper and also repeatable for different assumptions.

For optimization problems, complexity grounds in the problem's dimensionality resulting from its number of decision variables and their respective domain. The latter in turn determines the number of possible values and the possible algorithms to solve the problem itself. This leads to the second aspect which is the runtime of the algorithm i. e. the number of steps or time it takes until an algorithm terminates. Prominent definitions of problem hardness relate a problem's size to the actual running time of an algorithm to solve it in the worst case [100]. This runtime expressed depending on the problem size can be interpreted as an upper bound of the runtime and be polynomial or even superpolynomial. This might happen when the worst-case runtime is given as an exponential function which allows to group problems into different classes depending on their hardness [99]. This again leads to the requirement of problem reduction which in turn is based on the concept that a suitable (possibly irreversible) mapping can be found which transforms a hard problem into a softer one.

3.2 Mixed-integer linear optimization

As mentioned before, any optimization problem consists of at least one objective function that is to be minimized or maximized along with a set of optional constraints. The following explanations are based on the consistent definitions for different problem types in [101, p.14 ff.]. Given a number of continuous variables n_c and a number of discrete variables n_d within a vector $x^T = (x_1, ...x_{n_c})$ and $y^T = (y_1, ...y_{n_d})$ respectively, an objective function $f(x, y)$, n_e equality constraints $h(x, y)$ and n_i inequality constraints $g(x, y)$ an optimization problem can be defined as mixed-integer nonlinear optimization problem if at least one of the functions $f(x, y)$, $g(x, y)$ or $h(x, y)$ is nonlinear and at the same time $n_c > 0$ and $n_d > 0$.

A formal definition of such a problem according to [101, p.14 ff.] is given in Equation 3.1 and outlined in the following along with some additions and further explanations.

$$
min \left[f(x, y) \left| \begin{array}{cc} h(x, y) = 0 & h : X \times V \rightarrow \mathbb{R}^{n_e} & x \in X \subseteq \mathbb{R}^{n_c} \\ g(x, y) \geq 0 & g : X \times V \rightarrow \mathbb{Z}^{n_i} & y \in V \subseteq \mathbb{Z}^{n_d} \end{array} \right. \right] \tag{3.1}
$$

In this case the continous subset $X \subseteq \mathbb{R}^{n_c}$ and discrete subset $V \subseteq \mathbb{Z}^{n_d}$ are related to the domain of the respective continous and discrete decision variables $x \in X$ and $y \in V$ where equality constraints are defined via $h : X \times V \rightarrow \mathbb{R}^{n_e}$ and inequality constraints via $g : X \times V \rightarrow \mathbb{Z}^{n_i}$. A special subtype of these problems with only linear relations between the decision variables which are defined to be either real or integer valued is called mixed-integer linear program (MILP). If the subset for y only consists of discrete values for example $\{-3.0, 0.25, 1, 17.3, ...\}$ the problem is called discrete optimization problem which can be formulated as MILP by means of binary variables [101]. Every vector $x_\oplus^T = x^T \oplus y^T$ which fulfills the defined constraints is called feasible point wheras the set of all feasible solutions is called feasible region S. A pair of vectors (x, y) is called optimal solution if it is feasible and $f(x, y) \leq f(x', y')$ for all feasible solutions $(x', y') \in S$ which also yields that it is possible to have multiple optimal points which in turn represent a solution of the problem.

Depending on their objective function $f(x, y)$, equality and inequality constraints $h(x, y)$ and $g(x, y)$ and number of continous and discrete variables n_c and n_d the general definition according to 3.1 delivers special types of optimization problems [101]. Among them and relevant in the scope of this thesis are linear programs (LP) and mixed-integer linear programs as explained above. Within an LP the objective function is defined as $f(x, y) = c^T x$ with $h(x, y) = Ax - b$ and $g(x, y) = x$ and thus $n_d = 0$. For a MILP the objective reads $f(x, y) = c^T x_\oplus$ with $h(x, y) = Ax_\oplus - b$ with $g(x, y) = x_\oplus$ and consequently $n_d \geq 1$. In this definition the coefficient matrix with m rows and n columns is defined as $A \in M(m \times n, \mathbb{R})$ with a right hand side for the constraints $b \in \mathbb{R}^m$ and a so called cost vector $c \in \mathbb{R}^n$. Here, the number of columns is defined as sum of continuous and discrete variables $n = n_c + n_d$.

Any minimization problem can be converted into a maximization problem by changing the algebraic sign of the objective function. Changing the algebraic sign of inequality constraints in turn changes the relation between both expressions as a $\leq$ relation can be converted into a $\geq$ relation and vice versa. An equation can in turn be defined via two inequalities using $\leq$ and $\geq$ to relate two expressions. Moreover, decision variables are bounded by lower and upper bounds so that $l_c \leq x \leq u_c$ for continuous variables and $l_d \leq y \leq u_d$ for discrete variables including binary variables which are bounded by zero and one. For further reading on the basics of operations research, linear optimization and modeling techniques please refer to [101], [102] and [103].

If a model is described as an LP or MILP, it can be solved using a single algorithm or a combination of different ones. The oldest and probably most popular one used within linear programming is the

simplex algorithm by Dantzig [101]. The term "linear programming" describes methods to achieve the best outcome for LPs. Roughly speaking, starting with a feasible solution, this algorithm iterates through the feasible region *S* asserting feasible points as long as no better point can be found [103]. As explained, in this context it is also possible that multiple optimal points represent a solution to the minimization or maximization problem. While having to fulfill additional integer constraints, MILP problems are solved using different methods. Among others, the LP-based branch-and-bound algorithm [103, p.142 ff.] is a prominent example and utilizes linear programming methods to iterate towards feasible integer solutions. The research field of solving MILPs via respective algorithms is still very active and many improvements have been made in the last decade. As some of these the concepts of presolve, cutting planes, heuristics, and parallelism can be mentioned, where the combination and specific implementation depends on the respective mathematical solver. An extensive review would go beyond the scope of this thesis and therefore it is referred to respective literature [101, 102, 103].

3.3 Multi-objective optimization

The field of multi-objective optimization focuses on a class of problems where not only one objective but many objectives are optimized simultaneously. These multi-objective optimization problems (MOP) often occur in real world problems and do not have one optimal but many solutions. Therefore, a single solution is defined by its performance in relation to several, possibly conflicting objectives [99, p.195]. As one example, a bridge can be optimized in terms of its strength and costs where the first objective is to be maximized and the second to be minimized. It is obvious that not all objectives can be fullfilled at the same time and there must be situations where an improvement of one objectives leads to a deterioration of another objective. Thus, the goal is to find a set of good solutions in terms of multiple objectives which can be interpreted as best compromises to the problem. In turn, this set of solutions delivers a good decision base in terms of the regarded objectives.

In literature, the term multi-objective optimization is also known as Pareto, vector, multi-criteria or performance optimization. For reasons of consistency, within this thesis it is throughout referred to multi-objective optimization. As the scientific field of multi-objective optimization is growing permanently, numerous books covering the basic concepts and newest improvements are published. For reasons of consistency, the relevant concepts for this thesis are outlined based on [20] along with some amendments from [99] and the well-defined introductions from [104] and [105]. Based on these, a MOP is described in its general form by Equation 3.2.

$$min \left[f(x) \right] = min \left[f_1(x), f_2(x), ..., f_k(x) \right] \tag{3.2}$$

As described, this vector of k objective functions $f_i(x)$ which in turn depend on a vector of decision variables x is to be minimized simultaneously where no explicit minimum as for a mono-objective problem exists [20, p.518]. This explained absence of a classical minimum as for a mono-objective function leads to a redefinition of the term optimality for multi-objective problems. Due to the existence of multiple objectives, there are many ways to measure the quality of solutions and thus the solver itself. One basic concept of multi-objective optimization which is also used by some MOP solving algorithms is the concept of Pareto optimality which is defined after [20, p.519 f.] in the following.

A point x^* dominates x if $f_i(x^*) \leq f_i(x)$ for all $i \in [1, k]$ and at the same time $f_j(x^*) < f_j(x)$ for at least $j \in [1, k]$. In other words x^* is at least as good as x for all objective values and better than x in at least one objective value. In this context the notation $x^* \succ x$ indicates that x^* dominates or is superior to x. Moreover, a point x^* weakly dominates x if $f_i(x^*) \leq f_i(x)$ for all $i \in [1, k]$ which means that x^* is at least as good as x for all objective values. This implies that a dominating point at the same time weakly dominates the same point. Howover, this weak domination is expressed by the notation $x^* \succeq x$. The case of a nondominated point x^* which is also called noninferior, admissible or efficient is defined by the relation that there is no point x that dominates it. Formally, this relation can be described as in Equation 3.3. For more details on the concept of dominance such as the dominance level among solutions using the concept of ϵ dominance, it is referred to [20, p.522], as it would go beyond the scope of this thesis.

$$x^* \, is \, Pareto \, optimal \iff \nexists x : (f_i(x) \leq f_i(x^*) \, for \, all \, i \in [1, k] \, , and \tag{3.3}$$
$$f_j(x) < f_j(x^*) \, for \, some \, j \in [1, k])$$

The Pareto set P_s contains all Pareto optimal points or Pareto points where a Pareto optimal point x^* is defined as one that is not dominated by any other point x in the search space. This means that there exists no point x that dominates it and $\nexists x : f_i(x) \leq f_i(x^*)$ for all $i \in [1, k]$ and at the same time $\nexists x : f_j(x) < f_j(x^*)$ for some $j \in [1, k]$. Thus, the Pareto set which is also called efficient or admissible set is defined as in Equation 3.4.

$$P_s = \left\{ x^* : \left[\nexists x : (f_i(x) \leq f_i(x^*) \, for \, all \, i \in [1, k] \, , and \right. \tag{3.4}$$
$$\left. f_j(x) < f_j(x^*) \, for \, some \, j \in [1, k]) \right] \right\}$$

However, the Pareto or nondominated front P_f which is also called nondominated set contains all function vectors $f(x)$ which correspond to the Pareto set P_s. This leads to the definition after Equation 3.5 which differetiates the front from the set defined in 3.4 which is often not realized in literature according to [20, p.520]. Moreover, it has to be noted that Equation 3.5 allows for the case that $f_i(x^*) = f_i(x)$ which yields

that either of both is nondominated with respect to each other and consequently neither one dominates the other.

$$P_f = \{f(x^*) : x^* \in P_s\} \tag{3.5}$$

There are several methods to find Pareto front approximations $\hat{P}_f$ with regard to the true Pareto front P_f or even the true Pareto front itself. Some of these methods do not explicitly use the concept of Pareto dominance while others are based on respective indicators to different extents. For instance, methods such as aggregation methods combine the objective vector of a MOP into a single and thus scalar function using weights for the different functions [105]. However, if not extented by suitable goal attainment techniques this method does not deliver the true Pareto front if it is concave or has concave parts [106]. Moreover, this technique can only be applied if objective functions can be converted into each other and is therefore not applicable for all types of optimization problems. Finally, obtained results are dependent on the used weights, which need to be specified a priori and complex preferences of different decision makers cannot be represented. Other popular methods such as lexicographic ordering, boundary intersection methods, gender based approaches or the frequently used ϵ-constraint method are described in the respective literature [99, 20, 105, 104]. The latter is simple to implement and is shown to deliver efficient solutions if the solution to the ϵ-constraint problem is unique [107]. An improved version of the method called augmented ϵ-constraint method which is able to detect efficient Pareto sets is proposed for continuous [108] and integer problems [109]. However, one issue using this approach is that decisions about which objective to be minimized, which bounds to be selected for the other objective and what steps to be chosen between respective bounds have to be made. This might be problematic for complex problems with many values where there might be no feasible solution for the choices.

Another possibility is the usage of evolutionary algorithms (EAs) from the field of bio-inspired search heuristics. Such algorithms tailored to multi-objective optimization provide an effective method in obtaining the Pareto optimal set [97]. Originating in the 1960ties, evolutionary algorithms are applied widely to solve non-convex and combinatorial numerical optimization problems. Briefly explained, they use different paradigms from natural evolution, which are selection, recombination, and mutation to evolve a population consisting of individuals (decision vectors x) towards optimal or near-optimal solutions [105]. EAs which are specially suitable to solve multi-objective problems are called multi-objective evolutionary algorithms (MOEA). These are typically designed to approach sets of Pareto optimal solutions which are distributed across the Pareto front P_f. In this context, the selection schemes are adjusted with regard to single-objective optimization algorithms in a way that good Pareto fronts are obtained. The number of developed methods in this field has grown rapidly since the 1990ties [105].

The fast growing number of MOEAs can be grouped according to different criteria. As one example [99, p.200 ff.] distinguishes between nonelitist, elitist and decomposition approaches. The term elitism here describes keeping the best individuals of a generation unchanged when creating the next generation or population. The term decomposition describes the division of the main problem into several subproblems which targets different parts of the Pareto front. In contrast, in [105] it is distinguished between Pareto based, indicator based and decomposition based MOEAs. The first describes the usage of ranks between solutions to create a new population, whereby the latter utilizes other indicators such as the hypervolume indicator [110] during the evolutionary process [111]. The general scheme of an evolutionary algorithm is visualized in Figure 3.1.
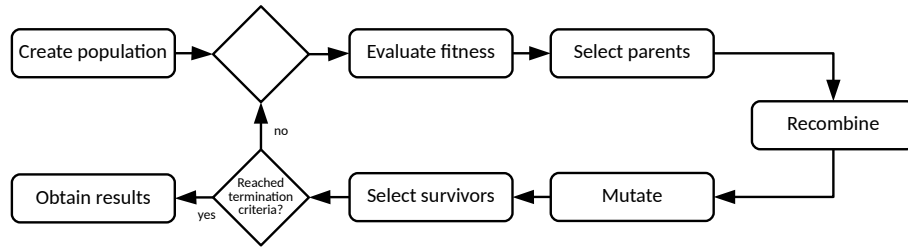
Figure 3.1: General scheme of an evolutionary algorithm as activity diagram.

As explained, within multi-objective optimization non-dominated fronts should be improved over time. Within this process the term exploration rougly speaking is the generation of new populations in yet uncovered regions of the search space, whereas the term exploitation describes the concentration of the search close to already explored good solutions [99, p.41 ff.]. According to [20, p.28 f.] intelligence includes the proper balance of both properties in terms of the problem at hand to be successful. The abovementioned quality of solutions can be measured by several indicators or so-called performance metrics which are studied in numerous publications [110, 112, 113, 114, 115]. Especially in [110] a broad overview of different performance metrics along with their applications and properties is given.

In the scope of this thesis, the hypervolume metric is used as a performance indicator as it covers the exploration and exploitation and is most commonly used according to [110]. The hypervolume indicator (also known as Lebesgue Measure or S-Metric) measures the accuracy and diversity of a solution [110]. In the following the definition of Simon [20, p.525 ff.] is outlined to remain consistent with the definitions described above. For Q Pareto front approximations $\hat{P}_f(q)$ for $q \in [1, Q]$ a vector of reference points $r = [r_1, ..., r_k]$ whose i-th components are larger than those of the points in the Pareto front approximation is computed. A single entry in this vector of reference points is described as follows

$$r_i > \max_q \left[\max_{x \in \hat{P}_n(q)} f_i(x) \right] \tag{3.6}$$

where the hypervolumes S' related to the reference point can then be calculated via

$$S'(\hat{P}_f(q)) = \sum_{j=1}^{M(q)} \prod_{i=1}^{k} (r_i - f_i(x_j(q))) \tag{3.7}$$

Hereby $M(q)$ represents the number of points within the approximation of the q-th Pareto front while $x_j(q)$ is the j-th point in the q-th approximation of the Pareto set. Larger hypervolumes therefore indicate better approximations of the real Pareto front as the algorithm explores the search space by evolving the population. After this initial exploration phase, the hypervolume typically increases at lower rates as the fronts are exploited.

Calculating this measure can, however, be time-consuming. This makes efficient and approximate methods important and thus has brought up a range of descriptions which differ in their mathematical definition and speed [114, 115, 116, 117]. In the scope of this thesis, which deals with two-dimensional optimization problems, the hypervolume definition from [117] is used with a referrence point as described in [116]. In the following, this hypervolume definition is referred to using the symbol HV. Methods for the effective calculation of higher dimensional hypervolumes are covered in [114] and [115] but exceed the scope of this thesis.

3.4 Data clustering algorithms

Modeling energy systems is a complex task because the dimensions of time and space have to be regarded in a specific model. As only one example, the transformation towards low-carbon energy systems is a driver for more decentralized and thus spatially distributed renewable systems, which at the same time induce a higher intermittency on the spatial scale. As a result, models which are often defined as optimization problems increase in their complexity. Consequently, respective solvers show higher runtimes as the runtime is directly influenced by the problem size expressed by the number of matrix rows and columns.

Different options exist to reduce complexity. For example, a reduction on the spatial scale can be realized by aggregating different nodes in an energy system model [17]. Another possibility is the reduction of nonlinearities or discontinuities leading to non-convex optimization problems by reduced technology models as described in [18, 64]. A further reduction method is the temporal aggregation of time series into typical periods. These typical periods are meant to represent the original periods and can be obtained by picking them manually (which includes a component of randomness) or systematecally using clustering algorithms. The latter are a promising option to tackle increasing complexity because they allow a reduction of the problem while preserving its characteristics.

As explained above, the goal of time series aggregation is to find groups of similar periods of a defined length within an original time series. This group is then represented by one of its periods based on a method-specific criterion. In most methods, the grouping itself is based on distance measures of the attributes of a group member whereas in the first step a pre-processing of the input data is required for a correct grouping. This pre-processing typically includes a normalization process. In the second step the groups are created using a suitable method and in an optional step extreme periods, for instance winter periods with high heat demands or summer periods of extremely hot days, can be added. This can be of importance, especially within problems where a specific technical design has to be found, as it might lead to an under- or oversizing of regarded technologies. For a thorough analysis of this phenomenon please refer to [118]. In a final step, the obtained cluster periods have to be adapted to match the average values of the original time series.

There are numerous measures to compare the obtained cluster periods and the observed data. Common "classical" statistical error measures with regard to forecast errors are reviewed in [119], leading to the conclusion that each error measure has its own advantages and disadvantages, which can lead to an inaccurate evaluation. Thus, the authors strongly recomment to use more than one measure to assess errors appropriately. Moreover, there are measures such as the Davies–Bouldin index [120] specifically designed to evaluate how well the clustering is done. In terms of clustering related to energy modeling, measures specifically designed for cluster methods are used in [121] and [96].

In contrast to this, within energy modeling many authors use classical statistical measures for different types of models. In this context, often the root-mean-square error (RMSE) as well as the mean absolute error (MAE) are used. Related to cluster result evaluation within energy research, the former is used in [122], [123], [124, p.55 ff.] and [118] in different variants. In this case a variant means the specific application, such as the application on duration curves of the modelled and obtained data as in [118]. Due to their frequent usage and their easy interpretability, the latter are chosen to evaluate results in the scope of this thesis and explained in the following.

The RMSE can be used to measure the differences between n values which are generated or predicted by a model and the observed values where deviations have a high weighting. Depending on whether these calculations are performed over the data used for estimation or computed from a sample these differences are either called residuals or errors. Overall, the RMSE can be interpreted as a single measure of predictive power, which aggregates the magnitudes of the deviations or errors. Therefore, it can be used to measure accuracy, to compare errors for different methods or models or for a specific dataset. In contrast, it cannot be used to compare between different datasets as it is a scale-dependent measure. The definition for the RMSE is given by Equation 3.8.

$$RMSE = \sqrt{\frac{\sum\limits_{i} (\hat{y}_i - y_i)^2}{n}} \tag{3.8}$$

As opposed to the RMSE, the MAE measures the difference between n values without a strong emphasis on deviations. Refererring to the definition above, the MAE is stated as the average distance between the model and observed values by taking the mean of all absolute differences. It also can be used to measure accuracy, compare errors for different methods or models as it is scale-depending only for a specific dataset and not among different ones. The formal definition for the MAE is given by Equation 3.9.

$$MAE = \frac{\sum\limits_{i} |\hat{y}_i - y_i|}{n} \tag{3.9}$$

Both dimensional measures RMSE and MAE can be converted to a non-dimensional measure using normalization. It then is commonly prefixed by a letter N or R for relative NRMSE or NMAE. Using normalization also facilitates a comparison between different datasets as the scale is unspecific. One drawback of normalization is the lack of definitions on how to normalize the data, which has led to different types of normalization in the literature. As an example choices for the normalization can include the range taken by the difference of the maximum and minimum value or the mean value of the modelled or observed values. Because the range is a often chosen option it is defined in Equation 3.10. Either the modelled or observed values can be used for the calculation and the dimensional measure is divided by the range y^{range}.

$$y^{range} = max(y) - min(y) \tag{3.10}$$

Both metrics can be used to measure accuracy or compare errors. They are negatively-oriented scores, which means that lower values are better and can range from zero to ∞ and are indifferent to the direction of errors. The RMSE is generally larger or equal to the MAE and with a difference increasing with the variance in sample deviations. If both are equal, all errors are of the same magnitude. Depending on their different properties, both metics can be chosen for a specific application. As explained, RMSE gives a higher weight to large errors because errors are squared and averaged before taking the square root. This indicates, that it is more useful if large errors are undesired and should be penalized. If this is not the case, the MAE can be chosen as it is easier to understand and interpret because of its simplicity. Within the further course of this thesis, the MAE is used as a main error metric whereas the RMSE is calculated and checked additionally.

4 Multi-objective optimal design and operation of energy systems

Within this chapter the proposed method and its implementation is described in detail. After providing an overview in the first section, the method and its hybrid optimization approach is outlined along with some theory. Subsequently, the developed software architecture and implementation are described in detail independently of the programming language that is chosen for the implementation. Within the last section, the general implementation framework is described based on previous work.

4.1 General method outline

Based on the previously outlined research needs, a new hybrid optimization method is proposed in order to provide a better decision base for different stakeholder perspectives within future energy systems. Similarly to the description in [73], this method will provided answers to questions like: "What is the most effective way of designing and operating energy systems to deliver different energy services with regard to different criteria such as costs, system reliability or emissions?". Such energy systems could include heat, electricity and mobility with respective availabilities of primary resources and demands in spatial and temporal resolution. Within these systems, decisions about when to invest in technologies, where to locate them, what energy resources to use and where, how and when to convert them to deliver the energy services required could be investigated, along a broad range of other applications.

The proposed hybrid optimization method combines two well known optimization methods for different applications, namely the optimization of an energy system's design and operation in its core. As already stated in [14] and [15] LP and MILP models are well suited to model ED and UD problems, i.e. the operation of energy systems. Moreover, flexible and derivative-free "black-box solvers" for global optimization are able to handle one or multiple objectives and constraints and can be used to optimize different properties of energy systems such as the energy system design. Thus, both are combined and the operational optimization realized as LP or MILP is embedded within a surrounding design optimization based on an EA or MOEA. In an optional step, complexity can be reduced by means of clustering algorithms, which are able to reduce the operational model in its temporal and spatial dimension by repre-

senting the data of the original problem by single clusters. Figure 4.1 gives an overview of the proposed method with its single steps.
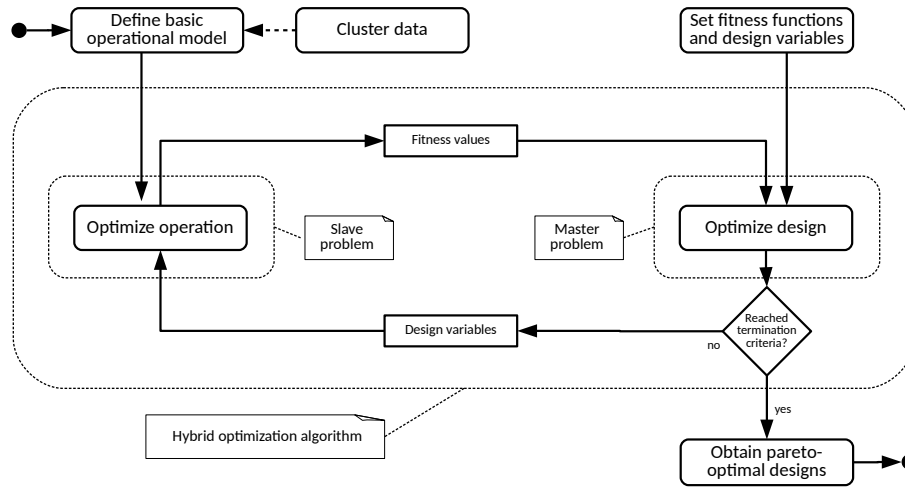
Figure 4.1: Overview of proposed hybrid optimization method.

Similarly to [67] the hybrid optimization method consists of two optimization levels. On the main or master level a design optimization is conducted while the sub or slave level conducts an operational optimization. Arbitrary MOEAs can be used on the master level and optimize design variables such as installed capacities or topologies like the number of pressure stages in a compressor. A design loop in the MOEA can be started, if an operational model is created and respective fitness functions and design variables are set up. This design loop optimizes design variables with regard to one or multiple objectives and terminates after a certain criterion, which can be defined a priori. Examples for this could be a certain number of generations or a specific hypervolume that is reached. If multiple fitness functions are used within a MOEA the designs obtained are Pareto-optimal in terms of these objectives. Otherwise, the obtained design is only optimal in terms of one objective in the case when a single-objective EA is applied.

Evolutionary algorithms are often applied with considerable amount of problem experience and knowledge, which allows to find good solutions that are near to the optimum. As described in Section 3.3, EAs are very good at quickly investigating the search space (exploration) but less good at fine-tuning solutions (exploitation). In other words, such algorithms quickly reach solutions close to the optimum, but are in tendency slow when it comes to reaching solutions very close to the real optimum, which is partly due to the stochastic nature of the search itself. As noted in [99, p.168], in some cases a combination of an evolutionary and a heuristic method can resolve this problem and performs better than either of its "parent" algorithms. In this context, the proposed method shares this property in the sense that the second

component in the hybrid architecture is a deterministic solver for (mixed-integer) linear programs, which is able to detect the real optimum for the operation of an energy system.

As described in [99] the hybridization of evolutionary algorithms with other techniques is motivated by numerous factors. One of these is the fact that many complex real world problems can be decomposed into subproblems, for which exact methods or at least very good heuristics may already be available [99, p.167 f.]. Using a combination of appropriate methods for these subproblems adds value in these cases as each method can use its advantages on a specific subpart of the original problem. By means of this, the proposed method allows to solve complex problems by decomposing them into several subproblems which are solved by a combination of well-suited algorithms. In this regard, an additional data clustering, which is applied to the operational model a priori can also be interpreted as decomposition, because it represents an original problem through smaller subparts. This combination of algorithms aims to deliver valid or even better solutions to the original problem than applying a single algorithm. The added value for specific problem types is supported by the fact that no overall successful and efficient general problem solvers exist, which is also indicated by the No Free Lunch theorem [100, 125]outlined in the introduction.

4.2 Hybrid optimization approach

As explained in the general outline, the method consists of two different algorithms which optimize an energy systems design and operation with regard to one or multiple objectives. Consequently, a detailed method description can be provided using layers for the different algorithms with a suitable interface between them. Figure 4.2 shows a detailed description of the proposed hybrid optimization architecture within an activity diagram. The activity diagram is modelled by means of the unified modeling language (UML) in order to provide a standardized representation.

Initially, an operational model is created based on given data, which can be clustered a priori. After this, a population of so-called design models is created as a first step of the applied evolutionary algorithm. A design model itself includes one or multiple operational models, specifically linear programs and additional methods, which can be used within the (MO)EA. Among others, these include methods to return fitness values, change decision variables or return lower and upper bounds. Within this process of creating an initial population, a seed of random numbers within a given range is used to create single design models. This means that different initial designs like minimum or maximum capacities are set for all individuals within the created population. In this context, the initial random numbers of the design decision variables are set within their respective lower and upper bounds to start with a diverse initial population.

After creating an initial population of design models, this population is evolved within a suitable (MO)EA. For this, within every evolutionary advance, different steps are applied. In the first step, one or multiple fitness values are evaluated for each individual before selecting and recombining parents in the second
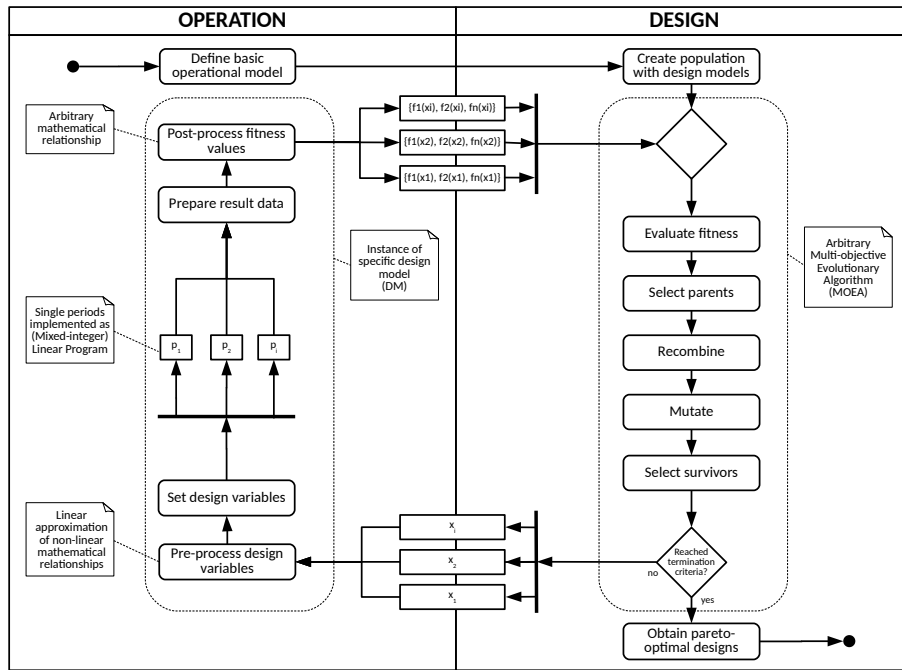
Figure 4.2: Detailed hybrid optimization architecture as activity diagram.

and third step. Arbitrary schemes can be applied for both the parent selection and recombination. Possible variants like the nondominated sorting genetic algorithm (NSGA-I, NSGA-II and NSGA-III) are a rank-based selection with a uniform crossover, but these generally depend on the chosen EA or its parametrization. This also holds for a subsequent mutation of the child generation and a respective selection of survivors. For different schemes and algorithms it is referred to standard literature such as [99] or [20] in this place, as these are highly individual and possibly differ on two implementations of the same algorithm.

In the operational part all design models within the population are optimized parallely regarding their operation. Each individual in the population of the design model contains a vector of decision variables x_i with respective given boundaries. As the worst-case runtime of respective (MI)LPs scales exponentially with the problem size, a parallellized optimization leads to a significant increase in performance. This will be illustrated in the last case study. An additional pre-processing can be applied to the design models depending on the values of the decision variables. For example, if the nominal capacity of a thermal power plant is changed, this directly impacts the operational behaviour and thus several coefficients in the linear program, which can be adapted before running the operational optimization. Using this additional step also allows for a treatment of nonlinearities in the (MI)LP because it allows for a "good" linear fit which includes the possibility to use piecewise-linear expressions for better approximations. In this context it must be pointed out that all operational models or periods are stored within a design model and only created once. During the design optimization itself, only parameters are changed on the model.

This eliminates the necessity to re-build the model within single runs and consequently has a significant impact on the runtime as only relevant parts of the operational models are changed.

After the optional pre-processing stage, design variables and other preprocessed data are changed on all individuals before their operation is optimized for all contained periods. This general case of multiple periods can be used if an entire optimization should be represented by different clusters. Examples could be to represent a year by four different weeks or modeling a "rolling horizon", where a year is optimized week by week. In either case the result data is pre-processed in a subsequent step, either by means of respective cluster weights or unweighted in the case of equally occuring periods. After optimizing all periods, fitness values are calculated for all individuals based on the prepared operational result data. Arbitrary fitness functions can be defined a priori and use either operational results or other data as arguments. These vectors of individual fitness values f_n, which in turn depend on the decision variable vectors x_i, are then returned into the (MO)EA to create a new generation until results are returned when a pre-defined criterion is met.

Fitness evaluation process

Figure 4.3 shows that the evaluation process of a single individual involves different steps of which some are optional. The design of a suitable generic and at the same time performant process is crucial as it represents a bottleneck in terms of the computational effort and therefore overall algorithm performance. A respective generic concept for the fitness evaluation process is developed and is illustrated in Figure 4.3. The illustration refers to the left part of Figure 4.2 between the passed decision vectors and fitness function evalutions but on a higher level of detail.

In the initial loop of the design optimization, the design problem has to be set up by defining fitness functions with a suitable fitness data structure. The fitness data structure provides all data that is needed to calculate the fitness values. This means that both parameters and decision variables in terms of design and operation have to be included. In order to save memory and computational resources, parameters are only added once in the initial step, whereby operational decision variables are updated in all following steps.

When the optional pre-processing stage has finished all design variables are set on the design model. As explained above, this includes for example upper bounds of energy conversion units but possibly also other parameters like coefficients of performance for different heat pump designs or load ranges. Everything that depends on a design decision variable can be adapted on the design model in this step, which in turn includes one or more operational models. Consequently, a design decision variable within the (MO)EA is a parameter, upper bound, index set or other component within the (MI)LP model. Interdependencies of design variables have to be treated in the pre-processing becasue otherwise infeasibilities
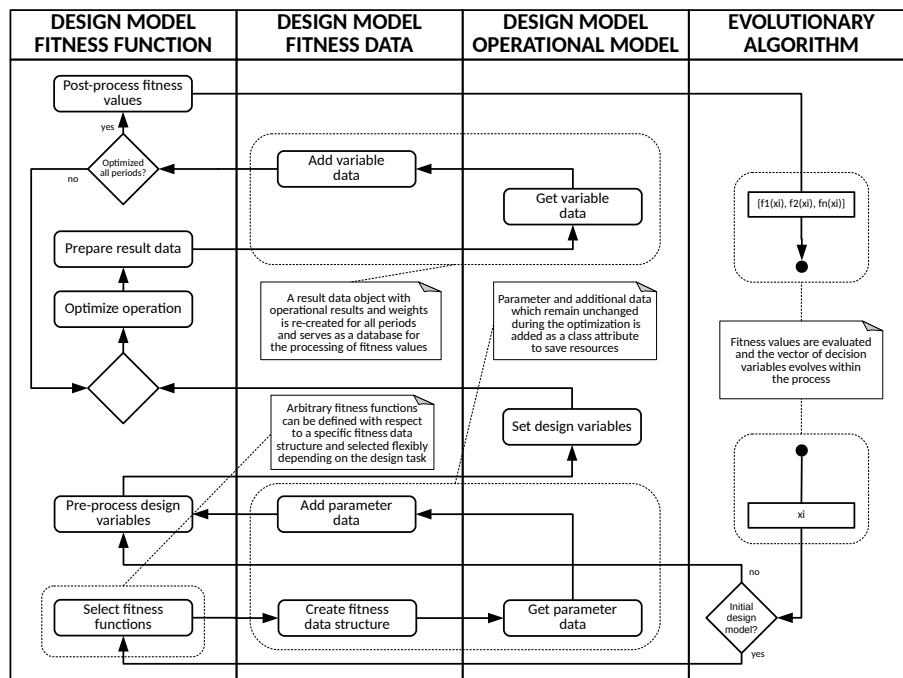
Figure 4.3: Fitness evaluation process in a single design model as activity diagram.

of the operational model might occur. For instance, if the rated capacity of a storage system is a design variable and an assumption within the operational model is that the storage's filling level is at 50 % of the rated capacity in the beginning and end of every optimization period, this initial and final filling level has to be adapted when the design variable is updated. Otherwise, there may be cases when these filling levels exceed the capacity, which leads to a constraint violation in the operational model and thus an infeasible problem.

Subsequently, the operation is optimized for one or multiple periods while the fitness data structure is updated using the decision variables of the single periods. These are contained within an operational model with their weights in the case of a preliminary data clustering. Keeping the data and related weights in a tabular or spreadsheet structure enables an easy processing, because new columns or rows can be added flexibly by multiplying operational results with their respective weight. This allows for a simple and intuitive calculation of different metrics to be used within a subsequent fitness calculation that returns the actual values of the individual to the design optimization.

Performance optimization

Parallel computing is applied to speed up the entire design optimization process. This is indicated by the interface between the operation and design layer in Figure 4.3. This concept of dividing a given task into

different independent units to be processed in parallel can lead to significant reductions of the overall runtime and is an indispensable tool of modern computer science [126]. Because of the improved computational capacities, much research is done to utilize parallelization for different types of optimization algorithms in both practical and theoretical science [127, 128, 129, 130]. This has led to a multitude of existing approaches and different classification schemes of which the following will be used in the scope of this thesis.

According to [126], there are three classes of parallelization within optimization that differ in the approach in which parallel computing is used to speed up the optimization algorithm. In the first class, parallel computing is used to speed up the computation of the objective function value for single solutions. This is most practical in cases where such calculations require a certain amount of computational effort. Because the assertion of objective functions is at the core operation of every optimization process, gains in execution time of this operation directly translate into a shorter optimization process itself and often a linear speed-up [126]. As parallelism only affects the objective function, no changes have to be made on the optimization algorithm itself.

In the second class of approaches, parallelism is used to simultaneously evaluate multiple solutions as one typical step of an optimization algorithm and especially algorithms with populations of many candidate solutions like evolutionary algorithms. Similarly to the calculation of objective values, their actual evaluations for different sets of solutions are completely independent, which also enables a parallel execution. This results in a linear speed-up and shortening of the overall runtime. As in the case of a parallel computation of objective values, this only requires simple adaptions of the original sequential algorithm. Both approaches described do not require any significant changes to the original optimization algorithm but lead to a significant gain in computational speed.

The third class of approaches is related not only to speeding up the processing, but introduces new search strategies by keeping parallel populations that are able to interact. One example is the coarse-grained or island model parallelization scheme in the field of genetic algorithms. This algorithm produces many co-existing populations from which individuals are exchanged at certain time intervals through migration between islands. While the first two classes lead to a significant increase in computational speed at a low expense in implementation, the approaches from this third class are used to improve the algorithm performance. Although there is evidence that the third class leads to obtaining better results than using equivalent multi-start schemes or parallel optimizations without migration, it is omitted in the scope of this thesis as it would require the adaption of specific algorithms and thus prevent their interchangeability. For more information please refer to [126].

Besides the opportunity to optimize the computational speed of the design optimization expressed by the runtime per evaluated individual, other methods can be used to optimize the algorithm with regard to the convergence speed. Apart from the possibility to use specific strategies like migration, good start solu-

tions can be used with sufficient knowledge about the problem because these are "closer" to the optimum than random seeds and consequently require less steps to discover the optimum. In [80] additional points are determined as initial guesses after initial runs to obtain better results for previously complex and sparse Pareto fronts. Following this concept, the final Pareto front is constructed from all previous runs. Other possibilities are offered by parameter studies that are specifically available for different problem types and algorithms [131, 132, 133, 134, 135] or can even be optimized on a higher level in a meta optimization [136, 137]. Another possibility is the formulation of the problem itself, for instance by means of the objective function, the presence or absence of constraints and their structure, the domain of the decision variable as continuous or integer or their number.

So far, the focus of the performance optimization is put on the design optimization, which includes multiple individual design models consisting of one or more operational models. As explained above, these operational models are created only once in the initial phase of the design optimization and then updated and solved within subsequent steps. Depending on the model type like LP or MILP and the nature of the problem, several other possibilities can be used to reduce the solving time. Similarly to the formulation of the design problem, the formulation of the operational problem has a large impact on the solution time. For instance, if a unit commitment problem is formulated as MILP with many binary and other integer variables over a horizon of an entire year, it is very likely to perform much worse than a respective formulation as LP because of the additional restrictions which require more effort to solve the problem. Besides this, multiple other techniques can be applied. For instance, warmstarts where specific start values for variables are given, sparse index sets which allow a denser formulation of the problem or decomposition techniques can be used for specific problems. As there are many acceleration options and these mostly depend on the problem itself, it is referred to respective standard literature in this place [101, 102, 103], while applied techniques and their implications are discussed within the case studies. Finally, the problem itself can be reduced in its dimension by means of an upstream data clustering which will be discussed within the following.

Data clustering process

Complexity can be reduced through suitable data clustering. The criteria for the clustering depend on the problem at hand. Where storage characteristics with respective load cycles exists in a modelled energy system, an appropriate data clustering has to be conducted in order to determine the cluster period length and the right number of cluster periods. Initially, the data of the respective storage system has to be analyzed, i.e. the unclustered original time series with its contained cycles and their duration. Apart from a manual analysis, algorithms can be helpful in this context because they provide a structured standardized way to process the data and help to gain deeper insights. One method to realize this is the usage of a cycle detection algorithm as proposed by [138] that is implemented in a freely available software package [139].
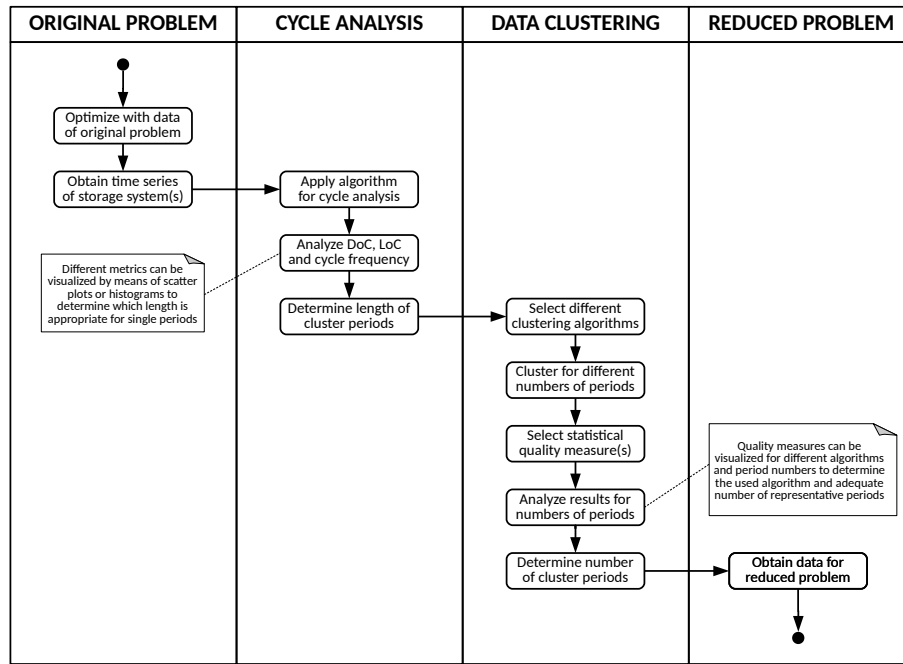
Figure 4.4: Data clustering process for systems with storage or other intertemporal characteristics.

This algorithm can be used to detect cycles in a time series along with their respective depth-of-cycle (DoC) and duration. Also, it delivers results for the DoC which are identical to the well known rainflow-counting algorithm with the advantage of also delivering a length-of-cycle (LoC). Providing structured information about the characteristics of a storage system, a standardized procedure can be applied to determine the adequate cluster period length and number of clusters. Other options are the application of discrete fourier transformation [118, 140] or the simple definition of a cycle as two passages or the average value. However, the results obtained from these will be more difficult to interpret or lack intermediate cycles. Figure 4.4 shows the developed standardized procedure that is used in this thesis and outlined in the following.

In the first step of the procedure, an operational optimization with the unclustered original time series is performed. In a second step, the time series of the contained storage technologies are analyzed by means of the abovementioned algorithm which delivers the cycle DoC and LoC for one or multiple systems. By analyzing the LoC in combination with the related magnitudes, a choice about the cluster period length can be made. Using this cluster length, the number of clusters to represent the original time series is determined in the next step. For this, a suitable measure for the cluster quality has to be selected, for instance as described in Equations 3.8 and 3.9. By calculating one or multiple measures for different numbers of clusters and even different cluster algorithms, a good choice on the number of clusters and the algorithm can be made. The question about how many clusters have to be chosen is up to the decision maker and always a trade-off between model accuracy and runtime. Finally, the results can be obtained
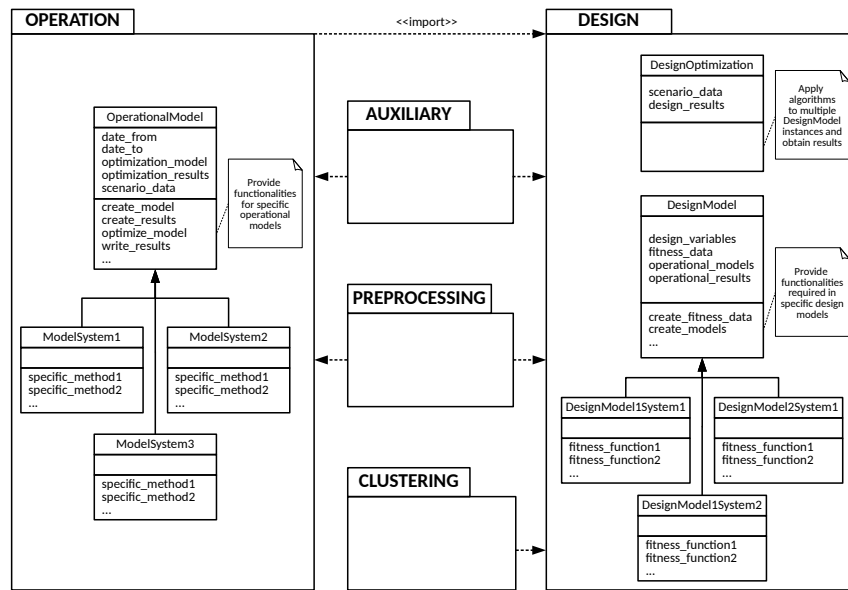
Figure 4.5: Hybrid optimization architecture within independent and interdependent packages.

and integrated within the final model for the design and operational optimization. This approach differs from approaches in the literature in which the optimum of the design optimization is known a priori [118] while an optimum of a multi-objective design optimization is not known in advance and would require other distance metrics. Moreover, it is not applicable for seasonal storage or has to be adapted in this case. For the question on how to represent seasonal storage within energy system models based on clustered data please refer to [141].

4.3 Generic software architecture

The proposed hybrid optimization approach is realized in a suitable software architecture that is independent of its actual implementation. Similarly to the developed optimization architecture and fitness evaluation process, special emphasis is put on the development of a flexible architecture that allows a coupling of different algorithms along with a parallelized design optimization. The introduced structure that divides different steps and procedures into an operational and a design part is applied likewise to structure different components of the overall architecture. This developed architecture is illustrated as an abstract package and class diagram in Figure 4.5. Both, the operational and the design part are realized in single packages and the package for the operational optimization can be used by itself to optimize energy systems in terms of their operation. Furthermore, additional packages such as functionalities for the pre- and post-processing or data clustering can be imported and used flexibly in both parts.

Within a base class for different operational models, all mutual properties are kept and additional methods provided in order to process a respective object. For instance, the start and end dates of an optimization period are kept as an attribute of type date and time along with the mathematical model (LP or MILP), scenario data that is used to build the model and results which are added when a model is optimized. Other methods are provided to construct and optimize the model in combination with methods to process the results. This generic base class in turn serves as a parent class for concrete energy system models with additional attributes or methods. For example, an energy system that is used to model a local battery infrastructure based on RE might hold methods to calculate different metrics. This concept of subclassing concrete energy system instances from a base model ensures that a specific set of attributes and methods is available for all models and can be used flexibly in other packages.

In the design optimization package, a base class for specific design models is provided similarly to the operational package. This class contains all information and procedures that are needed to construct a design model that includes one or multiple operational models. For instance, if five representative periods are obtained from the data clustering procedure, these are used to instantiate five operational models in a design optimization object whereby their single operational results are aggregated as described in Figure 4.4. Design variables are stored as an attribute and refer to single components which are changed on the contained design models via respective methods. Such methods include the creation of the underlying fitness data structure, the initial creation of the operational models or methods to actually solve these models and process their results. Because these attributes and methods are also fixed for all design models, they can be used to access design models within other parts of the software. Specific design models can be derived from this class and implement their own fitness functions. In this connection, different design models can either be used for different or the same operational model or models when calculating different scenarios for the same energy systems or using different objectives. This allows for a flexible usage and adaption of design models depending on the purpose. Finally, instances of these models can be used in a design optimization class that creates one or more populations with individuals consisting of multiple design models and applies algorithms to evolve these in terms of one or multiple objectives before collecting the final results.

The advantages of object-oriented design lie especially in its modular and flexible structure which allows to model arbitrary energy systems as instances of the same basic structure. Energy systems can be optimized by themselves regarding their operation and optionally be optimized with regard to design parameters. This optionality can also be reflected in a respective packaging structure that includes one or multiple other packages as a dependency which in turn enables a streamlined installation process. Also, an object-oriented design allows for a separation of model and data. Through this, single instances of operational or design models can be created by datasets which are passed into the constructor of respective classes. This enables a flexible usage of both packages depending on the specific situation.

4.4 Implementation framework

An implementation of the proposed architecture can partly be realized based on previous work. In addition, new concepts have to be developed and combined with existing ones from other areas. While a standalone operational optimization can be realized in the solph package of the Open Energy Modelling Framework (oemof) [9, 142], the scientific library PyGMO [126] is applied for a parallelized design optimization. Small contributions for multi-objective capabilities are added to the library during the course of this thesis [143]. The data clustering is realized by means of the package tsam which is proposed and validated in an article [118] along with an another package that is developed in the scope of this thesis and located in oemof [139]. The development of a generic software architecture and its application through suitable interfaces between the abovementioned packages is a core achievement in this thesis. An overview of the software that is implemented in the scope of this thesis is provided in Table 4.1. In addition to the new development and improvement of existing open source projects, wrappers arround third party packages are written in order to leverage their applicability. Each software component is implemented as a single Python package and archived digitally by means of a digital object identifier on the platform Zenodo which is financed and supported by the European Commission [144]. A brief description of the implemented software and the way it is used in the scope of this thesis is provided in the following.

Table 4.1: Overview of software implemented in the scope of this thesis.

Description	Package name	Contribution	Reference
MOEA compatible branch of oemof.solph	oemof	Improvement	[145]
Application starter for OMs	asom	Own development	[146]
Application starter for (M)HDOMs	ecom	Own development	[147]
Algorithm for cycle detection in time series	cydets	Own development	[139]
Data clustering and analysis	zms_clustering	Own wrapper	[148]
Pre-processing of CAES system	zms_caes_model	Own development	[149]
Pre-processing of DH system	zms_heat_models	Own development	[150]
Generic visualization of data	zms_plotting	Own development	[151]

The operational optimization is implemented in the Open Energy Modeling Framework which has initially been proposed as a novel approach to energy system modeling, representation and analysis. It provides a toolbox to construct complex energy system models and is published open source under a free licence. Based on a collaborative development processes, the framework supports a high level of participation, transparency and principles of open science in energy system modeling. Energy systems can be described in a generic graph-based topology that enables to flexibly model complex cross-sectoral

systems and include different modeling approaches. Thus, the framework can be seen as a multi-purpose modeling environment for energy modeling and analysis at different scales. In contrast to the abstract graph-based energy system representation in the solph package [9] that is used for the operational optimization, a concrete representation of energy systems is chosen in the scope of this thesis. This means that single technologies, energy balances or other constraints are expressed through their commonly used sets of equations or inequalities. Within the single case studies, additional identifiers are added for parameters and decision variables. In addition, different sets and indices are introduced in order to distinguish between technologies. In order to use oemof.solph and respective operational models in MOEAs, a customized branch [145] is created and adapted for mutable optimization parameters. This allows for a direct access of OM parameters by means of references within the MOEA. Moreover, an implementation of the CAES model in the first case study is added to the branch. A command line application starter for the organization and usage of respective models is proposed in a single package [146]. It also includes all operational models and clustered data that are used in the scope of this thesis.

The design optimization is based on the PyGMO optimization library which can be used for massively parallel optimization. Built around the idea of providing a unified interface to describe optimization problems, it distinguishes between an actual mathematical problem description and subsequent solution. It consequently allows to apply different optimization algorithms and at the same time enables their easy deployment in massively parallel environments. Existing optimization algorithms such as simplex methods, sequential quadratic programming or interior points methods as well as bio-inspired and evolutionary algorithms can be applied to solve different types of problems. Furthermore, different algorithms can be mixed easily to create combined algorithms via the asynchronous, generalized island model as described in [126]. The package allows to model and solve constrained, unconstrained, continuous and integer optimization problems with one or multiple objectives that provide flexibility in the design optimization. A respective command line tool that integrates the abovementioned application starter in order to create (M)HDOMs based on evolutionary algorithms is proposed in another package [147]. Here, the abovementioned custom branch and application starter published in [145] and [146] are dependencies and required to use the package.

All data clustering is realized by means of the tsam package that is realized as a Python package that uses different machine learning algorithms for the aggregation of typical periods. The package can be applied to different types of time series that are often needed within energy models. These typically include weather or load data or both simultaneously. Through this, the computational effort for energy models can be reduced significantly by aggregating their input time series and therefore the complexity of the model itself. A package that implements an algorithm to detect cycles in a times series along with their respective DoC and LoC is developed in this thesis. It is maintained as a standalone oemof package [139] and implements an algorithm that is proposed in [138], which gives a precise definition of a cycle. A package for the data clustering itself and additional analysis such as the automatic calculation

of different metrics or visualization of the clustered data is realized as a wrapper arround the tsam package and proposed in [148].

As indicated in Table 4.1, several auxilliary packages are used for different other tasks. For example, two separate packages are used to pre-process model parameters within the first [149] and second case study [150]. Moreover, a package for uniform plotting is applied for data visualization [151]. All packages are located in Python's scipy ecosystem [152]. Most important of these are the numpy, pandas and matplotlib packages that offer capabilities for numerical mathematics, data analysis and visualization. This software implementation in a high-level language lowers barriers for the usage and contribution for example by means of collaborative development in the scope of oemof. The mere availability of different libraries for a language facilitates the implementation of all crucial tasks along the modeling chain. Furthermore, interfaces to other languages can be used to extend capabilities if needed. For further discussion of the usage of free and open software and data in the light of open science please refer to [9, 10, 7, 95].

5 Case study - Compressed air energy storage

This chapter describes the application of the method on a compressed air energy storage plant that is operated on a wholesale electricity market. First, an overview of the case study is provided. Then, the underlying models for the design and operation are described in detail. For this, all technical and economic parts of the system are discussed where necessary. Finally, a specific setup is chosen and modelled and the results of this are discussed.

5.1 Case study overview

Future low-carbon energy systems demand for an integration of high shares of volatile RE. This can be realized by the use of storage technologies among other supporting measures. Compressed air energy storage (CAES) is a promising option among these technologies with different existing technical concepts and a high level of maturity [153]. Furthermore, there are various market environments in which these concepts can be embedded and operated in order to utilize their flexibility. Therefore, decision support tools for different concepts and market environments are required to improve the planning of future energy systems of which some are highlighted in the state of research. One well known concept is a diabatic CAES with an additional recuperation in the expansion part that is successfully operated in McIntosh, USA [154]. Figure 5.1 shows a schematic diagram of such a diabatic CAES plant that includes a recuperaton of the flue gases in the expansion part.
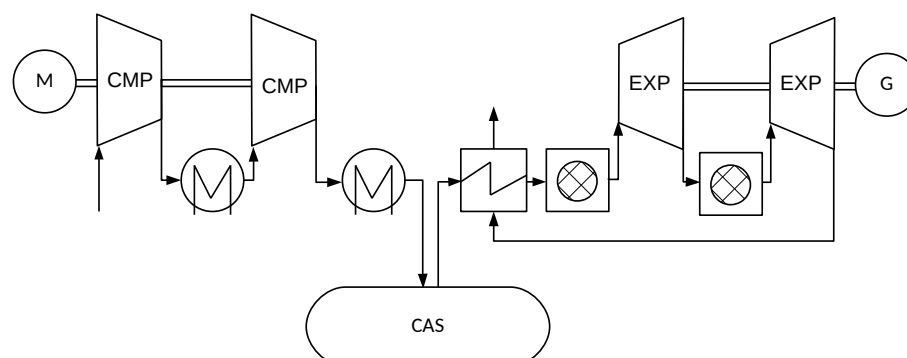
Figure 5.1: Schematic diagram of a diabatic CAES plant with recuperator.

An operation of the compression or charging part consisting of one or multiple compressors involves a certain input of electrical power to compress air from ambient pressure to a higher pressure level. The mass flow into the storage is decreasing with rising pressure level while the compression power remains constant. Heat is released into the environment during the compression but can potentially be used in other concepts. In contrast, the expansion or discharging part requires heat supply to generate power output that can be delivered to the grid. As a connection between the compression and expansion part, the level of the air storage is influencing both, the compression and the expansion part in its operational behaviour.

In theory, to make an investment decision, the planner must calculate the long-term marginal cost of the plant and have a forecast of the price at which the output of the plant might be sold. Hence, the expected rate of return must be included in the calculation and for the special type of storage system, not only the price for sold electricity but also for purchased electricity must be included. In the presence of an energy only market, the building of a storage is a rational decision, as long as the storage system benefits from charging at low price regimes and discharging at high price regimes based on forecasted price time series. In a liberalized electricity market, this reasoning is applicable to investments in storage capacity similarly as for regular power plants [6, p.206].

In practice, the investment decision for a new plant is more complex and includes various factors. For instance, uncertainty caused by construction delays or fluctuations in the price of fuels or electricity can affect the marginal costs of the plant. Furthermore, the long term development of wholesale electricity prices is difficult to forecast because of multiple uncertain factors like changes in demand, new technologies or competitors entering the market. Thus, the planning of conventional power plants is often only possible when backed by upstream and downstream contracts that guarantee fixed prices for both the fuel supply and the electrical energy being sold [6, p.206]. Such mechanisms cover at least a part of the price risks that cannot be controlled by the plant operator. This risk is even higher in the case of an energy storage system operated in an electricity only market. This is because not only the fuel price or price at which electricity is sold impacts the economic viability, but also the spread expressed by the difference between low and high prices and the frequency of price change has a strong impact on the economical results [39, 40, 29, 28].

Apart from the investigation of a storage's business economy other objectives like the overall storage efficiency are of interest to the decision maker. Therefore, the proposed method is applied to investigate both the business economy and storage efficiency of a diabatic CAES system based on a detailed modeling of costs and technical characteristics. Different scenarios for possible price developments at wholesale electricity markets are modelled in order to represent different future trajectories. These include the level of RE in the electricity system or changes in the overall electricity demand. Based on these scenarios, different result sets for the dimensioning can be analyzed in terms of multiple objectives providing more

information for the decision maker. As also stated in [5, p.199], a large number of independent generation entrepreneurs on the market is assumed whereas the investment of a single actor has a negligible effect on the market price. Moreover, it is assumed that the storage is a price-taker meaning that it does not influence the market price by its operation.

Three price scenarios are modelled based on spot market prices of the European Power Exchange (EPEX SPOT) of the year 2014. It has been demonstrated that the profitability of a CAES system strongly relies on revenues from the control reserve market and would not survive in current energy only markets [39]. It is therefore assumed that the price spread changes in future and that stronger spreads lead to a higher profitability of the system. This approach of using different spreads has already been used in [39] and is shown for a period of three days in Figure 5.2.
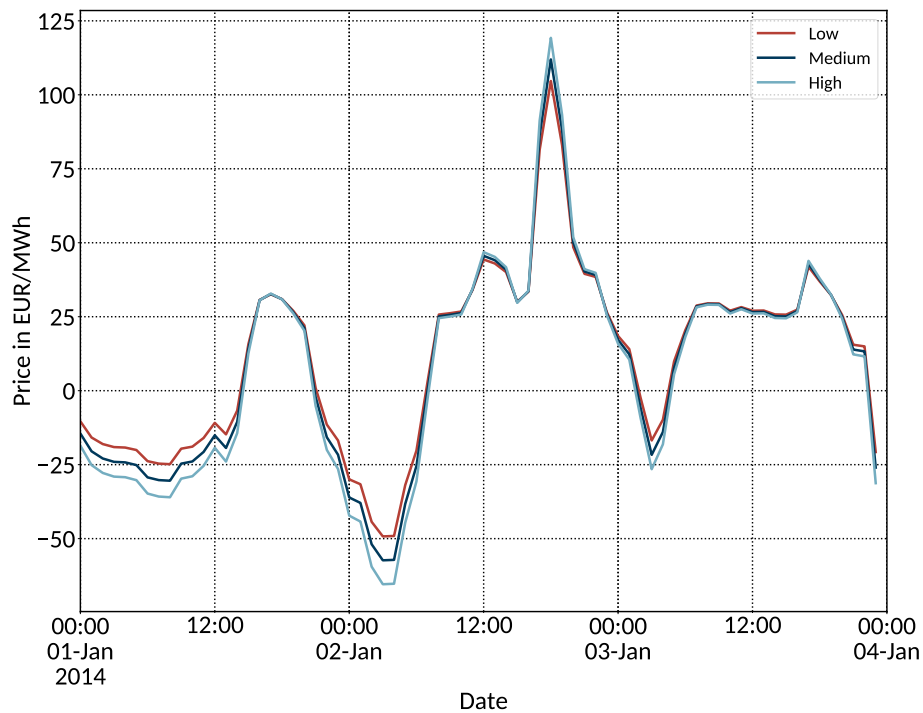
Figure 5.2: Power market scenarios representing different stages of future energy supply systems.

In this context, spreads of different magnitudes can be interpreted as different pathways of future energy systems. These are caused by higher levels of RE, changes in electrical demand or different volatile characteristics in the system. The prices are scaled by amplifying around their mean value by using a scaling factor according to Equation 5.1.

$$c_t^{elm,sca} = f^{sca}(c_t^{elm} - \overline{c}^{elm}) + \overline{c}^{elm} \tag{5.1}$$

Every scaled value $c_t^{elm,sca}$ of the time series is calculated by multiplying the difference between the mean value $\overline{c}^{elm}$ from the actual original value c_t^{elm} with an arbitrary scaling factor f^{sca} and adding an intersect which is also given by the mean value $\overline{c}^{elm}$. The actual scaling is realized after the data clustering process and applied to all single clusters. For the low, medium and high scenario shown in Figure 5.2, the scaling factor f^{sca} is set to 2.5, 2.75 and 3, respectively.

5.2 Model creation and outline

An overview of used symbols, subscripts and identifiers for the following model description is provided in the nomenclature. These are used to specify variables and parameters in the following model description. All needed sets and indices are defined in Expressions 5.2 and 5.3. It is important to mention that the formulation holds for arbitrary sets. This means that the formulation holds for any number of time steps and periods.

$$t \in T \quad \text{Index and set of all time steps} \tag{5.2}$$

$$p \in P \quad \text{Index and set of all representative periods} \tag{5.3}$$

For the sake of clarity, a sign convention is used within the modeling part. Within the operational optimization model, all decision variables and depending expressions are set in uppercase letters whereby parameters that are known in advance are set in lowercase letters. Due to the hybrid modeling approach, both decision variables and parameters of the operational model can be integrated into the design optimization model. Thus, an operational parameter can become a design variable (cf. Equations 5.8 and 5.9) which in turn determines an operational decision variable (cf. Equations 5.16 and 5.17 as only two examples).

Design model

Two fitness functions are defined in the design process to optimize the plant design in an economical and technical dimension. As stated in [155, p.46], the economic plant performance is far more sensitive to the ratio of the compression and expansion power than to storage volume. Thus, the capacities of the further are determined as decision variables in the optimization process. Within the first objective function, the net present value (NPV) of the plant is maximized. As a classical indicator for an investment decision, it includes the investment and operational costs as well as the expected rate of return. In the second objective function, the overall storage efficiency η^{caes} is maximized as it is a common measure to compare storage technologies in different contexts.

Consequently, the multi-objective design optimization problem can formally be described according to Expression 5.4. It results in an unconstrained non-linear multi-objective optimization problem whose decision variables are parameters of a mixed-integer operational model which is repeatedly solved to deliver dispatch results that are used to calculate the design objectives.

$$max \; [C^{npv}, \eta^{caes}] \tag{5.4}$$

Further, the general formulation of the NPV in the first fitness function is shown in Equation 5.5 and outlined below.

$$C^{npv} = -C^{cpx,total} + \sum_a \left(\frac{C^{opx,total} - C^{orv,total}}{(1+i)^a} \right) \tag{5.5}$$

The NPV applies to a series of cash flows that occur at different times between now and the future. It accounts for the value of money at a specific time and allows for an evaluation and comparison of different investment projects or products. The capital expenditure or capital expense (CAPEX with symbol cpx) occurs when the initial investment is made and has to be repaid by the difference between the operational expenditure or operational expense (OPEX with symbol opx) and operational revenues (OREV with symbol orv) over the investment's lifetime. Both, the OPEX and OREV are discounted by its time value and adapted by the expected rate of return which has to be defined a priori by the investor. For the concrete investment in a potential CAES plant, the CAPEX are defined according to Equations 5.6-5.11.

$$C^{cpx,total} = C^{cpx,inv,total} + C^{cpx,bop} \tag{5.6}$$

$$C^{cpx,inv,total} = C^{inv,cmp} + C^{inv,exp} + C^{inv,cas} \tag{5.7}$$

$$C^{inv,cmp} = \left(\frac{\overline{p}^{cmp}}{\overline{p}^{cmp,ref}} \right)^{0.6} c^{inv,cmp,ref} \tag{5.8}$$

$$C^{inv,exp} = \left(\frac{\overline{p}^{exp}}{\overline{p}^{exp,ref}} \right)^{0.6} c^{inv,exp,ref} \tag{5.9}$$

$$C^{inv,cas} = v^{cas} c^{cas,inv} \tag{5.10}$$

$$C^{cpx,bop} = C^{cpx,inv,total} s^{bop} \tag{5.11}$$

For the initial investment, costs for the actual plant and the balance of plant (BOP) are included within the CAPEX. As explained in the method description, these can be modelled in various ways e.g. by means of non-linear cost characteristics which account for cost degressions based on scale effects. Thus, an
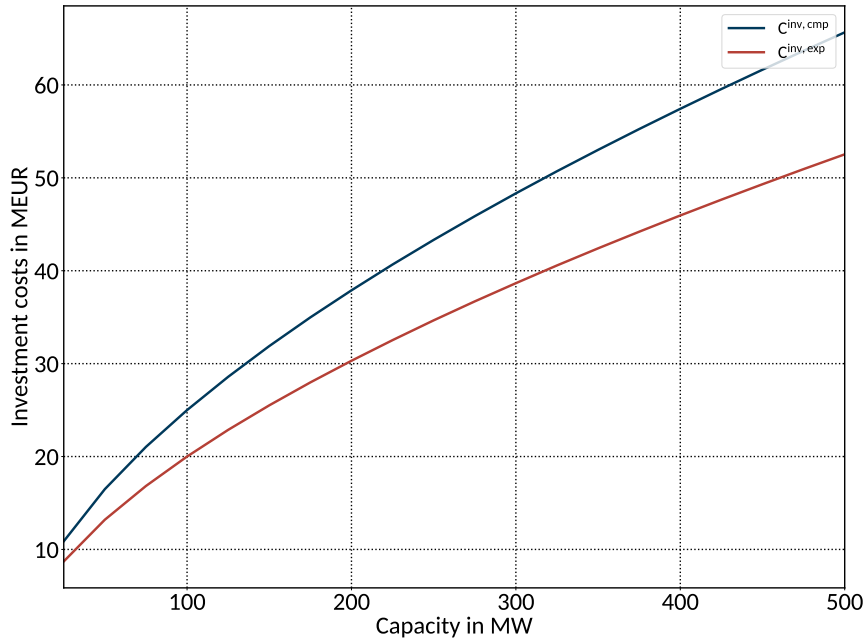
Figure 5.3: Non-linear investment costs for turbomachinery within the range of 50-500 MW based on a reference value approach similarly to [156, p. 48].

estimation of the turbomachinery costs for the compression and expansion part is chosen and grounds on a reference value approach. It is similar to one used in [156, p. 48] which is based on standard literature [157, 158] and illustrated in Figure 5.3.

Within the model, installation costs $c^{ref,inv}$ for a reference component of capacity $\overline{p}^{ref}$ have to be defined a priori and are scaled by the installed capacity of the component at hand $\overline{p}$. Moreover, costs for the creation of a cavern $c^{cas,inv}$ with a certain volume v^{cas} are considered along with the BOP which are expressed as share s^{bop} of the initial investment costs $C^{cpx,inv}$. This allows for a flexible usage in the modeling because only the capacity for a specific design case $\overline{p}$ can be used as a functional argument. This cost estimation approach is often used to estimate component costs in power engineering. The exponent of 2/3 or roughly 0.6 describes the case of a cubically increasing benefit at quadratically increasing costs. A typical example for this behaviour would be a gas tank with cubically increasing volume (benefit) and quadratically increasing surface area (costs) related to the diameter.

Similarly, to the CAPEX, the occuring OPEX are modelled based on different cost expressions. These include expenses for personell $C^{opx,per}$ as share of the investment costs for the compression and expansion s^{per}, insurance costs $C^{opx,ins}$ and maintenance costs $C^{opx,mnt}$ which are both determined in relation to the overall investment costs by means of the factors s^{ins} and s^{mnt}, respectively. In order to calculate the costs related to the operation on the electricity market, expression $C^{opx,elm}$ is used to model different cost components. Costs for purchased electricity $c_{p,t}^{elm}$ as well as variable costs $c_{p,t}^{cmp,var}$ by the compres-

sion part $P_{p,t}^{cmp}$ are added to the fuel costs $c_{p,t}^{fuel}$ for the heat supply in the expansion part $\dot{Q}_{p,t}^{exp,in}$ and respective costs for emission certificates $c_{p,t}^{emi}$. All single cost expressions within the OPEX are described within Equations 5.12-5.16.

$$C^{opx,total} = C^{opx,per} + C^{opx,ins} + C^{opx,mnt} + C^{opx,elm} \tag{5.12}$$

$$C^{opx,per} = (C^{cpx,cmp} + C^{cpx,exp})s^{per} \tag{5.13}$$

$$C^{opx,ins} = C^{cpx,inv}s^{ins} \tag{5.14}$$

$$C^{opx,mnt} = C^{cpx,inv}s^{mnt} \tag{5.15}$$

$$C^{opx,elm} = \sum_p \omega_p (\sum_t (P_{p,t}^{cmp}\tau(c_{p,t}^{elm} + c_{p,t}^{cmp,var}) + \dot{Q}_{p,t}^{exp,in}\tau(c_{p,t}^{fuel} + c_{p,t}^{emi}))) \tag{5.16}$$

In contrast to OPEX, OREV are calculated as illustrated in Equation 5.17 based on the optimal dispatch which includes the option of clustered data. Occuring revenues are calculated by summing over single periods p with a respective weight ω_p and all time steps t for each respective plant k. Revenues are generated by selling electricity generated in the expansion part $P_{p,t}^{exp}$ at specific costs $c_{p,t}^{elm}$ with an optional bonus $c_{p,t}^{exp,var}$.

$$C^{orv,total} = \sum_p \omega_p (\sum_t P_{p,t}^{exp}\tau(c_{p,t}^{elm} + c_{p,t}^{exp,var})) \tag{5.17}$$

As a second objective, the plant's overall efficiency is optimized as a technical measure. Within the classical definition of a storage's cycle efficiency, the overall energy output is related to the respective input [155, 39]. The former is the electrical work when operating the expansion part, the latter is represented by the electrical work in the compression part and an additional fuel supply in the expansion part. Another definition for a storage efficiency of diabatic CAES concepts is proposed in [159] in order to compare a CAES plant with other storage technologies. This approach assumes that the fuel could possibly be used in another conventional peak load plant and is implemented in Equation 5.18.

$$\eta^{caes} = \frac{W^{exp} - W^{exp,in,ref}}{W^{cmp}} \tag{5.18}$$

As can be seen, the numerator is defined by the electrical work when discharging the storage W^{exp} minus the electrical work of the reference plant $W^{exp,in,ref}$. The difference of both measures is related to the electrical work of the compression part W^{cmp} similarly to the classical efficiency definition. Electrical work when discharging the storage is defined by Equation 5.19 as follows by the weighted sums over all periods.

$$W^{exp} = \sum_p \omega_p \left(\sum_t P^{exp}_{p,t} \tau \right) \tag{5.19}$$

The required additional heat supply in the expansion part is defined by Equation 5.20. Here, an additional fuel supply $W^{exp,in,ref}$ is assumed to be possibly used by an alternative power plant. It consists of the heat supply $\dot{Q}^{exp,in}_{p,t}$ multiplied by an efficiency of a conventional power plant $\eta^{ref,cpp}$ which can be determined flexibly depending on the specific use case. For instance, an efficiency $\eta^{ref,cpp}$ of 35 % could represent a gas turbine while an efficiency $\eta^{ref,cpp}$ of 55 % could represent a combined cycle extraction plant where the former leads to a higher overall storage efficiency η^{caes} and the latter to a lower.

$$W^{exp,in,ref} = \sum_p \omega_p \left(\sum_t \dot{Q}^{exp,in}_{p,t} \tau \eta^{ref,cpp} \right) \tag{5.20}$$

One advantage of using a reference approach is the possibility to relate the storage efficiency to other technologies that are used in the system. It solves the problem of coupled products as the storage's electricity output is not related to the sum of electricity and heat into the storage which makes it impossible to determine a direct relation between both. For more information on this difficulty, it is referred to [159] in this place. Finally, the electrical work of the compression part is formulated in Equation 5.21 similarly to the expansion part.

$$W^{cmp} = \sum_p \omega_p \left(\sum_t P^{cmp}_{p,t} \tau \right) \tag{5.21}$$

Operational model

The operational model integrates economical data such as prices for fuel, sold electricity and technical data for different components. Regulatory framework mechanisms can be integrated in the compression and expansion part by adding specific costs e.g. for final consumer charges or additional bonus payments. Output data is delivered in time series which capture the storage dispatch, fuel consumption and other metrics such as the pressure in the air storage. Figure 5.4 provides an overview about the basic structure and input and output data.

A MILP formulation and the assumption of perfect foresight are applied for the operational modeling. This combination is commonly used for similar unit commitment problems and in respective studies [39, 40, 37, 38, 43]. This case study proposes and applies a new and more flexible formulation for

INPUT DATA ⟹ **OPTIMIZATION** ⟹ **OUTPUT DATA**

Compression and expansion

Maximum capacities
Minimum capacities
Efficiencies
Emission factors
Fixed generation costs
Variable generation costs
Plant availabilities
Start costs
Minimal runtimes
Minimal downtimes
Operational characteristics

Storage

Maximum pressure
Minimum pressure
Initial stored mass

Market environment

Heat prices
Power prices
Fuel prices
Emission prices
Energy tax
Consumer charges
Support mechanisms

Unit commitment of compressed air energy storage in specific market environments

$$\min \left\{ f(\mathbf{x},\mathbf{y}) \;\middle|\; \begin{array}{l} \mathbf{h}(\mathbf{x},\mathbf{y}) = 0 \\ \mathbf{g}(\mathbf{x},\mathbf{y}) \geq 0 \end{array} \right.$$

$$\mathbf{h}: X \times V \to \mathbb{R}^{n_e}$$
$$\mathbf{g}: X \times V \to \mathbb{Z}^{n_i}$$

$$\left. \begin{array}{l} \mathbf{x} \in X \subseteq \mathbb{R}^{n_c} \\ \mathbf{y} \in V \subseteq \mathbb{Z}^{n_d} \end{array} \right\}$$

Hourly power supply
Hourly heat supply
Hourly power consumption
Hourly fuel consumption
Caused emissions
Storage pressure
...

Figure 5.4: Structure of the operational model for the CAES case study.

diabatic CAES plants when compared to the one proposed in [40]. It is able to represent operational differences through formulations of the following parts: compression (CMP), mass storage (CAS) and expansion (EXP). Although in real systems these parts may consist of multiple components like different compressor stages or storages, these are represented as one aggregated part in the model . This allows for a flexible adaptation to different concepts.

The developed abstract CAES technology model is shown in Figure 5.5 and illustrates the contained physical variables. From this abstract technology model, relations between the physical streams can be derived for the process of mathematical modeling. For instance, the mass flow fed into the CAS is related to the compression power and cavern pressure. Moreover, these technical measures can be integrated in an economical context by embedding the compression or expansion power in an electricity market or other environment. All relations will be outlined in detail in the operational model description.

Assumptions made in the model are as follows: The operation is optimized under perfect foresight which means that prices which are typically based on forecasts are known in advance and remain constant. This means that no uncertainty is considered in the model. Moreover, the turbine's fuel consumption in the expansion part and related costs depend linearly on the supplied electrical power. Partial load and a dependency on the pressure in the air storage is modelled for the compression part whereas a throttling to a constant pressure is applied in the inlet of the expansion part. Furthermore, no detailed start or shutdown costs and runtime restrictions are modelled.

Finally, the model definition is given for a single representative period without an index for the period p as this index is only used for multiple operational models in the design model. If not mentioned ex-
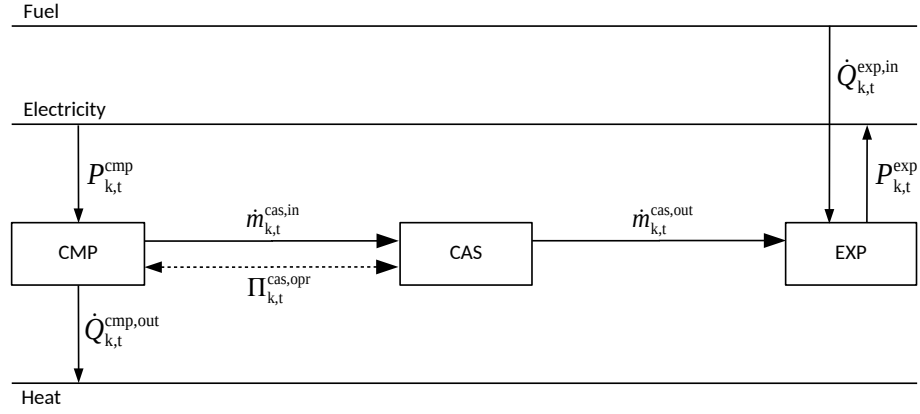
Figure 5.5: Abstract technology model of a diabatic CAES plant.

plicitly, all (non-heat) capacities are assumed to be electrical capacities in the following. The objective function in general form can be described in 5.22 by means of the described indentifiers, indices and sets. It consists of single expressions for costs and revenues which are outlined in Equations 5.23-5.24. Costs for fuel, emission certificates and purchased electricity are defined in 5.23 whereas revenues for purchased electricity are captured in 5.24. As already described in the design model, variable costs for the compression and expansion part can be added flexibly in order to model additional costs or bonuses. This is realizedby means of the parameters $c_{c,t}^{cmp,var}$ and $c_{c,t}^{exp,var}$, respectively.

$$min \left[\sum_t (C_t - R_t) \right] \tag{5.22}$$

$$C_t = P_t^{cmp} \tau (c_t^{elm} + c_t^{cmp,var}) + \dot{Q}_t^{exp,in} \tau (c_t^{fuel} + c_t^{emi}) \tag{5.23}$$

$$R_t = P_t^{exp} \tau (c_t^{elm} + c_t^{exp,var}) \tag{5.24}$$

Constraints for the technical description of the compression part are outlined from Inequality 5.25 to Equation 5.28. Inequalities 5.25 and 5.26 ensure that the compressor power is either set to zero or within a load range between the minimum and maximum power output by means of a binary status variable Y. The relation between compression power, mass flow and storage pressure is described in 5.27 through a plane that results from a linearization of their non-linear physical relationship. Finally, the compression heat flow is captured in Equation 5.28 and related to the occuring mass flow.

$$P_t^{cmp} \leq Y_t^{cmp} \overline{p}^{cmp} \qquad \forall t \tag{5.25}$$

$$P_t^{cmp} \geq Y_t^{cmp} \underline{p}^{cmp} \qquad \forall t \tag{5.26}$$

$$\dot{m}_t^{cmp} = a^{cmp} Y_{,t}^{cmp} + b^{cmp} P_t^{cmp} + c^{cmp} (Z_t^{cmp} + \underline{\pi}^{cas} Y_t^{cmp}) \qquad \forall t \tag{5.27}$$

$$\dot{Q}_t^{cmp,out} = P_t^{cmp} d^{cmp} - \dot{m}_t^{cmp} e^{cmp} \qquad \forall t \tag{5.28}$$

Within Expression 5.27, the abovementioned binary status variables ensure that the mass flow equals zero if the compression part is not operating. In this place, it has to be noted on parameter $\underline{\pi}^{cas}$ in Equation 5.27, that the cavern pressure is modelled by means of a minimum storage pressure $\underline{\pi}^{cas}$ and a working pressure above this minimum value $\pi_t^{cas,opr}$ which is limited by a maximum working storage pressure $\overline{\pi}^{cas,opr}$ in Inequalities 5.33 and 5.34. This formulation allows for an application of a "Big-M" type method which is commonly used if the continuous variable is bounded with zero by the lower bound as it is the case for the working storage pressure. As a result, Equations 5.29-5.32 serve to resolve the product of the continuous variable for the working storage and the compression status variable by introducing an auxiallary continuous variable. This formulation ensures that the mass flow is set to zero if the compression part is not operated.

$$Z_t^{cmp} \leq \overline{\pi}^{cas,opr} Y_t^{cmp} \qquad\qquad \forall\, t \qquad\qquad (5.29)$$

$$Z_t^{cmp} \leq \pi_t^{cas,opr} \qquad\qquad \forall\, t \qquad\qquad (5.30)$$

$$Z_t^{cmp} \geq \pi_t^{cas,opr} - (1 - Y_t^{cmp})\overline{\pi}^{cas,opr} \qquad\qquad \forall\, t \qquad\qquad (5.31)$$

$$Z_t^{cmp} \geq 0 \qquad\qquad \forall\, t \qquad\qquad (5.32)$$

The abovementioned relationship between compression power, mass flow and storage pressure is visualized in Figure 5.6 for the design parameters of the Huntorf CAES plant in Germany. All red data points represent the real physical relationship whereby the plane shows the resulting linear approximation. It can be seen that a good approximation is achieved within the defined load range of 50-100 % with increasing deviations next to the minimum and maximum load.

This effect of stronger deviations next to the lower and upper bound of the feasible capacity has to be regarded in the design optimization which changes the installed capacity and thus the physical relationship. Here, only one linear fit e. g. for the maximum feasible capacity would lead to strong deviations in terms of the plant behaviour and thus inaccurate results. Consequently, the linear approximation has to be computed for every design case in a pre-processing step for the operational model (cf. Figure 4.2) and can be compared to an approach illustrated in [64]. The physical model is published as an installable Python package and published online [149].

Mass storage constraints are provided from Inequality 5.33 to Equation 5.36, respectively. As described above, Inequalities 5.33 and 5.34 hereby define the upper and lower bound of the working storage pressure. Equation 5.35 describes an intertemporal constraint which links the actual pressure to the pressure of a preceding time step. Additionally, mass flows from and into the storage are multiplied with the initial mass which is expressed according to the ideal gas law based on the cavern volume, initial pressure and temperature multiplied with the gas constant. This reflects that the formulation of the mass flow is normalized. Temporal losses can be accounted for by means of a temporal efficiency which is included
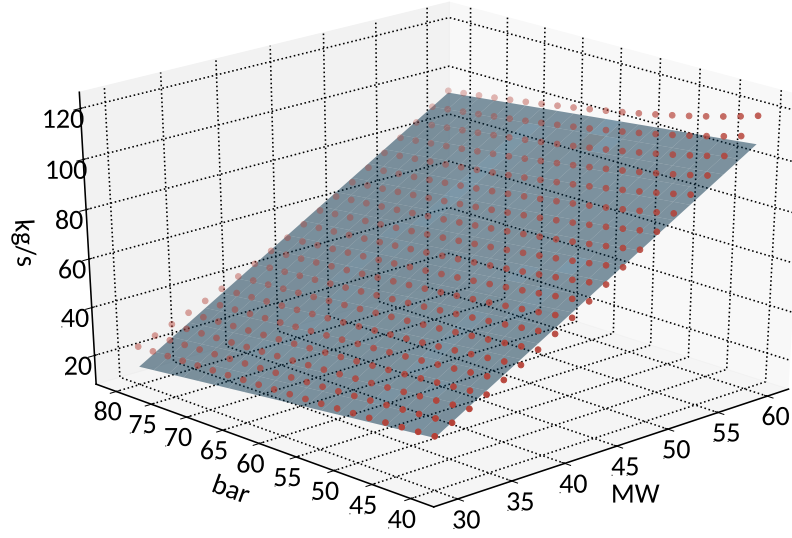
Figure 5.6: Linear fit of compression part for design parameters of the plant in Huntorf.

in the first summand. Finally, Equation 5.36 equates the pressure in the first and last time step to enable a model usage in cases where the energy content in the initial and final state has to be equal. This can be the case within a rolling optimization or when multiple representative periods are used in the design optimization.

$$\pi_t^{cas,opr} \leq \overline{\pi}^{cas,opr} \qquad\qquad \forall\, t \qquad (5.33)$$

$$\pi_t^{cas,opr} \geq 0 \qquad\qquad \forall\, t \qquad (5.34)$$

$$\pi_t^{cas,opr} = (1 - \eta^{tmp,cas})\pi_{t-1}^{cas,opr} + 3600\frac{RT^{0,cas}}{p^{0,cas}v^{cas}}(\dot{m}_t^{cmp} - \dot{m}_t^{exp}) \qquad \forall\, t \in T \setminus \{t^1\} \qquad (5.35)$$

$$\pi_t^{cas,opr} = \pi^{0,cas} \qquad\qquad \forall\, t \in \{t^1, t^{max}\} \qquad (5.36)$$

The expansion part is modelled from Inequality 5.37 to Equation 5.40. Within the first two equations, a load range similarly to the one in the compression part is defined. Furthermore, the relation between the mass flow and expansion power is defined by Equation 5.39 based on the assumption that the pressure before the turbine inlet is throttled to a constant value. Within Equation 5.40 the fuel heat flow is linked to the air inflow. This modeling technique which is applied to model the mass flow and expansion power is commonly used to divide a depending mathematical quantity into a constant and variable block [160]. For instance, a specifically high fuel consumption occurs when a unit is switched on and operates at minimal load. This specific fuel consumption decreases when increasing towards maximum load as the ratio of the fixed block and the variably produced quantity decreases.

$$P_t^{exp} \leq Y_t^{exp} \overline{p}^{exp} \qquad\qquad \forall\, t \qquad\qquad (5.37)$$

$$P_t^{exp} \geq Y_t^{exp} \underline{p}^{exp} \qquad\qquad \forall\, t \qquad\qquad (5.38)$$

$$\dot{m}_t^{exp} = P_t^{exp} a^{exp} + Y_t^{exp} b^{exp} \qquad\qquad \forall\, t \qquad\qquad (5.39)$$

$$\dot{Q}_t^{exp,in} = P_t^{exp} c^{exp} + Y_t^{exp} d^{exp} \qquad\qquad \forall\, t \qquad\qquad (5.40)$$

A simultaneous operation of the compression and expansion part is prevented in Inequality 5.41. As both status variables are binary, the inequality assures that no more than one status variable can be activated in a certain time step. This formulation avoids situations where the operational part and expansion part are operated simultaneously because the operation of both parts is indifferent in terms of the economical objective. In reality, such operational states would not occur as they would not be rational.

$$Y_t^{cmp} + Y_t^{exp} \leq 1 \qquad\qquad \forall\, t \qquad\qquad (5.41)$$

On the other hand, the same behaviour can be enforced by adding specific costs for the startup of the plant along with different auxialliary constraints for a more detailed model. Nevertheless, such formulations are not applied in this place as the focus is put on the newly proposed model. For common formulations in unit commitment models, it is referred to respective literature in this place [160, 15, 59, 161, 140].

5.3 Model and algorithm setup

After a generic model description, the actual model is set up for the case study. For this, in the first section, all economic and technical model parameters are outlined. Afterwards, the process of data clustering is explained based on the model parametrization. Finally, a brief overview of the chosen algorithm setup is given.

Model parametrization

As explained within the description of the design model, the storage's NPV and efficiency are selected as design objectives. Further, the electrical power of compression part $\overline{p}^{cmp}$ and expansion part $\overline{p}^{exp}$ are varied on the operational model and optimized during the design optimization. An overview of the selected objectives and decision variables is provided within Table 5.1 along with their symbol, unit and respective range.

Table 5.1: Overview of design objectives and decision variables for the selected CAES system.

Model component	Symbol	Unit	Possible range
Objectives			
Net present value	C^{npv}	MEUR	$\mathbb{R}$
Roundtrip efficiency	η^{caes}	%	0..100
Decision variables			
Electrical capacity of compression part	$\overline{p}^{cmp}$	MW	10..3000
Electrical capacity of expansion part	$\overline{p}^{exp}$	MW	10..3000

There are numerous sources for costs of CAES systems of which some relate to real systems whereas others make assumptions for future developments [162, 163, 164, 165, 166, 167, 155]. The different cost components highly depend on the individual technical concept including turbomachinery or air storage. A detailed overview of CAES costs in comparison to other storage technologies is provided in a comprehensive literature overview [166]. Within this case study, costs are modelled based on assumptions from a respective study [39] with the addition that the occuring turbomachinery costs are modelled on a higher level of detail by means of Equation 5.7. This allows to account for size effects concerning the installed turbomachinery capacity in the design optimization. Table 5.2 provides an overview of economic model parameters for the selected CAES system.

Investment cost assumptions for turbomachinery can be considered as rather optimistic given the price ranges in [165] but are still in the lower range defined in [164] and [163]. Cost assumptions for the installation of a cavern are rather moderate and similar to the ranges defined in [167] and [164]. Variable

Table 5.2: Overview of economic model parameters for the selected CAES system.

Parameter	Unit & reference	Value
Investment costs		
Reference power compression	MW	100
Reference costs compression	MEUR	25
Specific costs for compression	EUR/kW	250
Reference power expansion	MW	100
Reference costs expansion	MEUR	20
Specific costs for expansion	EUR/kW	200
Recuperator	EUR/kW	40
Cavern	EUR/m³	60
BOP and others	% of total investment costs	50
Operational costs		
Fuel costs	EUR/MWh	20
Final consumer electricity charges	EUR/MWh	1.9
Personell costs	% of turbomachinery costs	1
Insurance costs	% of total investment costs	0.85
Fixed costs for maintenance	% of total investment costs	1
Variable costs for maintenance	EUR/MWh el. production	3.5
Others		
Lifetime	a	30
Discount rate	%	5

fuel costs for gas are fixed at a price slightly above the mean European Gas Index (EGIX) for the years 2014-2018 [168] along with final consumer electricity charges of the compression part. The latter are assumed to be identical with pumped hydro storages [169] as these share many common features. An overall plant runtime of 30 years can be considered as rather pessimistic because the plant in Huntorf has been operated successfully for almost 40 years now [170] with a retrofit of the expansion part in the year 2006. This practical experience is supported by higher estimations for the runtime in other studies [165]. All other cost assumptions are chosen based on the abovementioned study [39].

As described above, a different underlying technical model than in [39] is used for the description of the operational model. According to Figure 5.1, a two-stage setup with each a lower and higher stage is chosen for both the compression and expansion part. Moreover, fuel is saved by recuperating heat from the higher pressure part of the expansion. An overview of all technical model parameters for the investigated system is provided in Table 5.3.

Table 5.3: Overview of technical model parameters for the selected CAES system.

Parameter	Unit	Value
Compression		
Isentropic compressor efficiency	%	90
Motor efficiency	%	97
Maximum temperature LP stage	°C	226
Maximum temperature HP stage	°C	460
Expansion		
Isentropic efficiency turbine	%	90
Heat transfer efficiency	%	80
Combustion efficiency	%	90
Generator efficiency	%	98.5
Maximum temperature HP stage	°C	490
Maximum temperature LP stage	°C	945
Storage		
Pressure range	bar	40-80
Pressure losses	%	0
Efficiency of reference plant	%	35
Other components		
Mechanical efficiency	%	99

For the compression part, an isentropic compressor efficiency of 90 % and motor efficiency of 97 % is assumed similarly to [39]. The maximum temperatures are assumed with 226 and 460 °C, respectively. For the expansion part, an isentropic turbine efficiency of 90 % is assumed along with a heat transfer efficiency of 80 % and a combustion efficiency of 90 % which can be interpreted as conservative. Further, a generator efficiency of 98.5 % is estimated which can be considered as rather optimistic when compared to other studies [171]. The temperatures in both stages of the expansion part are slightly different compared to the real plant, with 538 °C in the first and 871 °C in the second stage of the expansion, respectively. A closer comparison reveals that the first stage temperature is lower whereas the second stage temperature is higher when compared to the original plant.

For the air storage, the selected pressure range is slightly higher and ranges from 40-80 bar when compared to the real plant in McIntosh with a pressure range from 46-76 bar [155] whereas possible pressure losses are neglected. An efficiency of 35 % is assumed for a reference plant and represents an alternative fuel utilization in a gas turbine process (cf. Equations 5.18-5.21). This assumption can be considered as rather conservative as it tends to bring up higher storage efficiencies when compared to the assump-

tion of a higher reference efficiency e.g. for a combined cycle extraction turbine. Finally, a mechanical efficiency of 99 % is assumed for all turbomachinery components. All abovementioned technical parameters except for the defined pressure range are contained implicitly in the operational model as these are expressed by respective coefficients in the compression or expansion part. In contrast, all economic parameters listed in Table 5.2 are included explicitly as parameters in the design and operational model.

Data clustering

Due to the MILP formulation of the operational model which uses additional binary variables to describe the characteristics of different components, complexity is be reduced to decrease the runtime of a single operational optimization model. Following the approach described in the method development (cf. Figure 4.4), different steps are applied to determine an adequate length of the representative periods and an adequate number of time steps. Within a first step, an operational model with a fixed dimensioning similar to the one in Huntorf is optimized for an optimization period of one year in order to analyze the cycles of the system. Figure 5.7 shows the performed cycle analyis which yields the respective DoC and LoC.
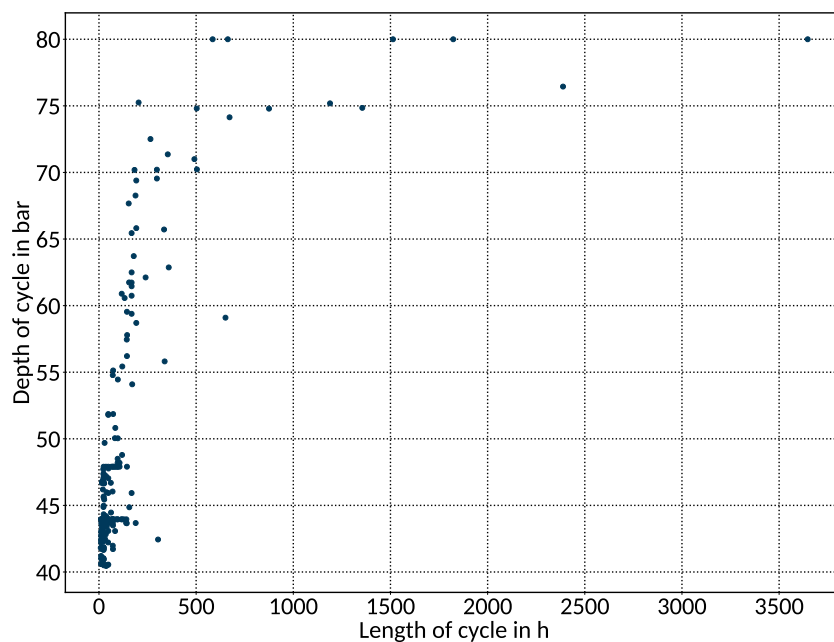
Figure 5.7: Depth and length of CAES cycles for an optimization period of one year in the scenario with intermediate spreads. Figures 9.1 and 9.2 in the appendix show corresponding distributions for both quantities.

It can be seen that most cycles have a LoC of less than three days with only a minor share having a LoC larger than one week. Moreover, longer cycle durations correlate with higher DoCs. Furthermore, a clear

accumulation of comparably small intra-day and multi-day cycles resulting from the diurnal electricity price profiles can be observed. The latter is supported by Figures 9.1 and 9.2 in the appendix which show corresponding distributions. As a result, this allows for a comparably low number of time steps per period which is set to 72 h. Since the initial and final filling level of the storage are set to be equal and in this case at a value of 50 % of the entire storage capacity, this allows for sufficient flexibility in terms of dis- and recharging in single operational periods. This is mainly because in previous optimization runs with representative periods of 24 or less hours, this equality constraint for the storage level (cf. Equation 5.36) often forced the storage not to operate.

After determining the length of the underlying representative periods, the number of representative periods is determined. For this, the MAE is chosen as a statistical measure and calculated for different cluster algorithms and numbers of periods. As explained in Section 3.4, the MAE is applied to the duration curves due to their frequent usage and interpretability. This implies that errors are not specifically penalized as it would be the case for the RMSE. Figure 5.8 shows the MAE between annual original and cluster electricity price duration curves for a different number of representative periods.
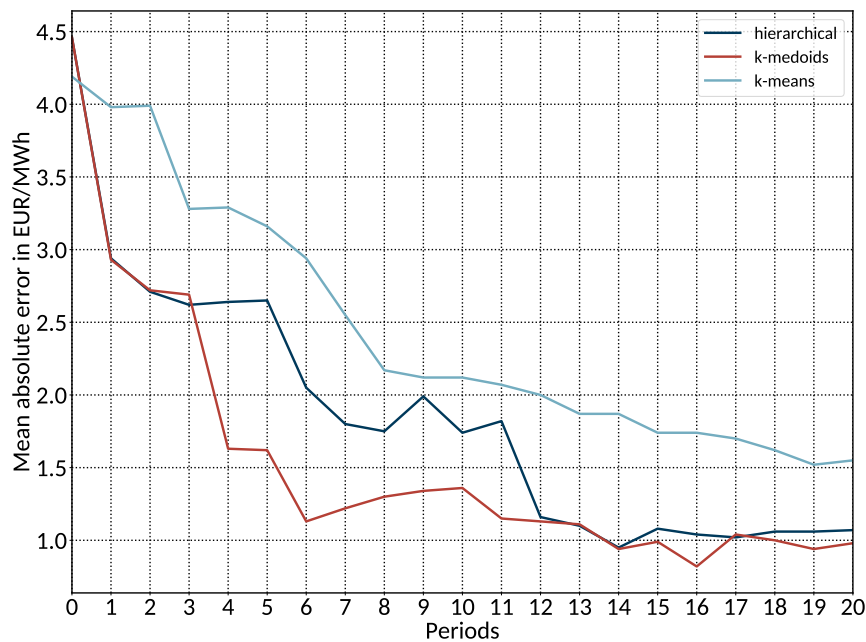
Figure 5.8: Mean absolute error between annual original and cluster electricity price duration curves in the scenario with intermediate spreads for a different number of representative periods of each 72 h.

The selected clustering algorithms perform differently on the respective datasets, and in this case the k-mediods algorithm gives the best results for the selected statistical quality measure. This is mainly because the medoids represent more fluctuations and peaks compared to centroid-based methods which partially average them out [118]. Moreover, it can be seen that a high increase in accuracy can already

be achieved with a small number of periods whereas the effect decreases significantly when adding more periods into an area where only small improvements in accuracy are achieved. In conclusion, an original time series for an entire year in hourly resolution can be expressed by less than 7 representative periods of each 72 hours at a MAE of less than 1.5 EUR/MWh for the duration curves.

A summary of the statistical distributions for the selected representative periods is shown in a boxplot in Figure 5.9. Here, the lower, middle and upper lines of the box represent the 25 %, 50 % and 75 % or first, second (median) and third quartile. Whiskers are drawn at a distance of 1.5 of the interquartile range (IQR) or at the minimum or maximum value if there are no values beyond 1.5 x IQR. Further, possible outliers below or above 1.5 x IQR are marked as dots below and above the whiskers.
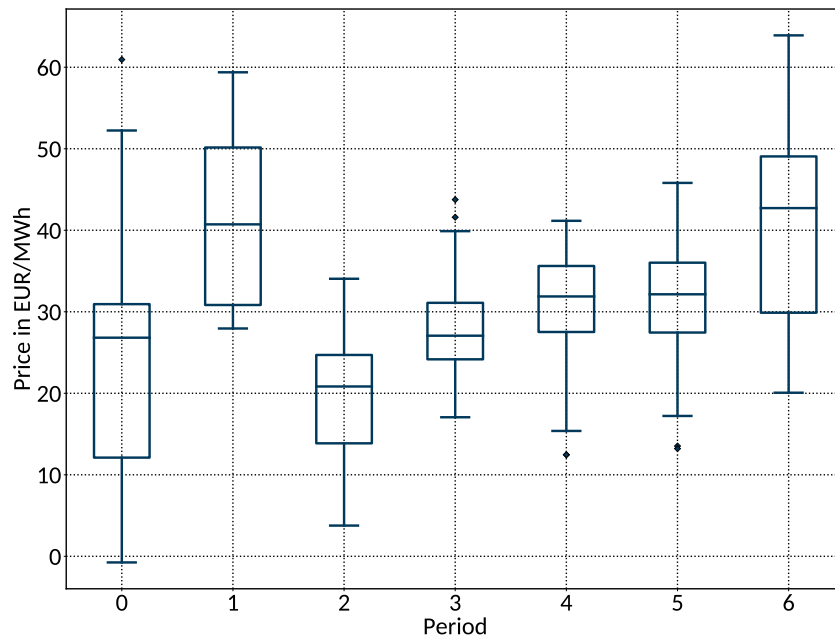
Figure 5.9: Boxplot of selected representative periods of each 72 h for the electricity prices in the scenario with intermediate spreads using the k-medoids clustering algorithm. Figure 9.5 in the appendix shows the corresponding time series.

It becomes clear that a diverse set of periods is derived from the clustering process in order to represent different price developments. For instance, comparably high fluctuations are represented in period 0, 1, 2 and 6 on different price levels. Moreover, period 3, 4 and 5 capture intermediate prices with a lower share of fluctuation. This also relates to the MAE which is shown in Figure 5.8. A very small but diverse set of clusters would already be sufficient to represent a large portion of price variability for example by period 0, 2, 4 and 6. Adding more periods only has a comparably minor influence with regard to the MAE as period 1 is similar to period 6 and periods 3 and 5 are similar to period 4. Nevertheless, all periods are taken into account for the combined optimization as the runtime for the LP/MILP within a single

operational optimization is mainly influenced by its matrix dimensions (cf. Figure 9.17). As a result, the number of representative periods only has a rather linear impact on the runtime.

Algorithm setup

In the design optimization part, the solid and widely used MOEA NSGA-II [172] is applied. Despite its initial publication in the year 2002 it still has a great value as a blackbox optimizer and is applied as a standard algorithm for many real-world applications. Offsprings are generated using a type of crossover and further mutation. Following generations are selected based on the comparison of nondominated fronts and crowding distance. Besides suitable parameter sets for different standard problems in the original publication [172], meanwhile various parameter sets for different problem types are investigated in other studies [136].

As explained in the method development, an island model for parallel optimization is applied in the design optimization. Each island has exactly one population consisting consisting of single individuals which is evolved during the optimization process. Since no migration between these islands is implemented, this process is equal to repeated optimization runs from a results perspective as the results are aggregated and asserted when all experiments are finished. Nevertheless, this parallel execution enables an accelerated performance of the entire optimization process due to a better utilization of computational resources. Table 5.4 summarizes the parameter selection for the MOEA.

Table 5.4: Parameter selection for the multi-objective evolutionary algorithm NSGA-II.

Parameter	Symbol	Unit	Value
Number of individuals in population	n_i	-	24
Number of islands	n_p	-	20
Number of generations	n_g	-	150
Crossover probability	p_c	%	0.95
Distribution index for crossover	η_c	-	10
Mutation probability	p_m	%	0.01
Distribution index for mutation	η_m	-	50

As stated in [173], the selection and tuning of parameters for EAs is problem specific and can be challenging because parameters interact in highly non-linear ways. For problems which only include a few decision variables, the number of individuals in a population would typically also be smaller than for a large problem with possibly hundreds or thousands of decison variables. For the CAES problem at hand, a number of individuals in each population n_i of 24 is proven to deliver good results after a comparison with multiple runs for other population sizes. Moreover, a number of islands n_p of 20 is used in order to

obtain denser Pareto fronts as single populations often only cover certain areas of the front. A number n_g of 150 generations is chosen which is higher than in other similar studies [174]. Nevertheless, this ensures a reasonable convergence towards the real Pareto front. Finally, standard values for the parameters p_c, η_c, p_m and η_m according to [143] are found to be deliver good results after testing against different other combinations of parameter settings. For further reading on the selection of parameter sets it is referred to [173] in this place.

Within the operational optimization, default solver settings are changed in order to speed up the calculation of single models. As explained in the method development, a design model might include several operational models depending on the determined number of clusters. The actual problem description as LP or MILP in arbitrary structure determines the complexity and required solving speed. Due to the existence of multiple binary variables in multiple representative periods, the following settings are applied to the solver: the mixed-integer gap is set to 0.03 or 3 % and a timeout of 7200 seconds is defined to solve the operational model. This means that the solution process is stopped if it has not finished by this time and a new individual is created for the next generation.

5.4 Results and discussion

Design results are obtained by applying the described model for the three analyzed future power market scenarios. As described in the case study overview in Section 5.1, these scenarios are based on scaled electricity spot market prices and chosen to represent different possible stages of future energy supply systems. In this context, different scaling factors lead to different levels of fluctuations or spreads which increase with higher factors. The obtained Pareto-fronts are illustrated in Figure 5.10 for all scenarios. For reasons of clarity, only denser parts of the solution space are shown which means that solutions with a net present value lower than -80 MEUR and compressor capacities below 50 MW are not included in the figure.
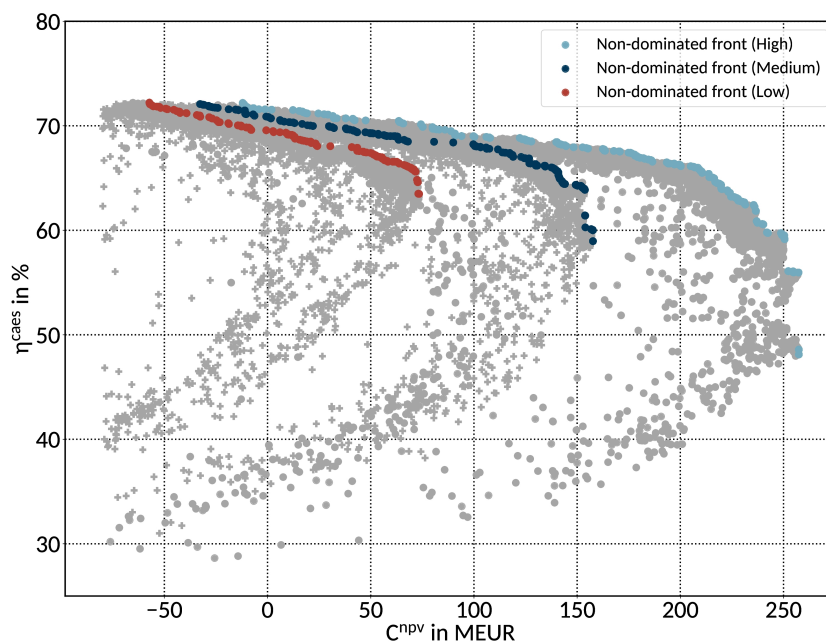
Figure 5.10: Pareto fronts for the analyzed power market scenarios.

It becomes clear that the algorithm in the design optimization converges quickly towards scenario-specific fronts as the areas with solutions far from the Pareto-front are only covered sparsely. The density of solutions increases from the lower left to the upper right towards the color-coded Pareto-front as the algorithm evolves the underlying populations. By looking at the appearance of the different fronts, it gets clear that different market environments have a strong impact on the derived solutions. Different design cases lead to very different solutions regarding both objectives. As for the first scenario with the lowest spreads, the NPV remains throughout negative with comparably high storage efficiencies. This changes in the second scenario with partly positive NPVs and a wider range of efficiencies. Finally, in the third scenario, a positive NPV is achieved for almost all design cases with and even broader range of efficiencies. These results demonstrate that the specific storage design has a strong impact on both,

economical and technical objectives which in turn depend on the realized dispatch. Overall, the achieved efficiencies are sligthly higher than literature values for similar concepts investigated in[155, p.32] or [39]. This stems from the assumption of a lower reference efficiency (cf. Table 5.3) but the obtained results still lie within the expected range depending on the actual design case.

Scenario "Low"

A more precise analysis of the design results illustrates the interdependencies between objectives and design variables. For the analysis, both objective axes of Figure 5.10 are kept to focus on a single Pareto-front whereas the depending design parameters are applied to a second y-axis. A respective "zoomed" overview for the first scenario with the lowest spreads and thus lowest resulting NPV is illustrated in Figure 5.11.
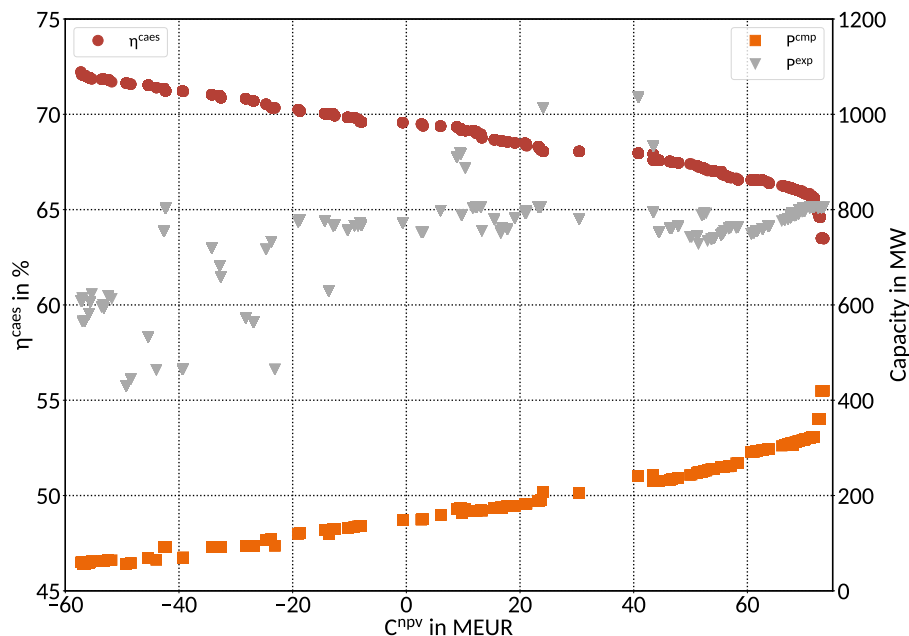
Figure 5.11: Pareto front and design parameters for scenario "Low".

As expected from Figure 5.10, the plant is not economical in many design cases in the low-spread scenario. Better values for the NPV are achieved with higher compressor capacities. In contrast, when a high storage efficiency is still of importance, lower capacities for the expansion part seem to be beneficial while leaving the compression capacity almost at its lower bound. As illustrated by Figure 5.6 in section 5.2, the specific compression work decreases with the actual pressure in the cavern. As a result, an overall lower pressure level in the cavern realized by a large expansion part is beneficial for the storage efficiency. This is because more mass can be charged into and later on discharged from the storage using the same

compression work (cf. Equation 5.18). In other words, an increasing expansion capacity leads to a higher efficiency in the compression part when the overall capacity of the compression is kept constant.

Scenario "Medium"

A different relation between both objectives and design variables is shown in Figure 5.12 for the second power market scenario with intermediate spreads.
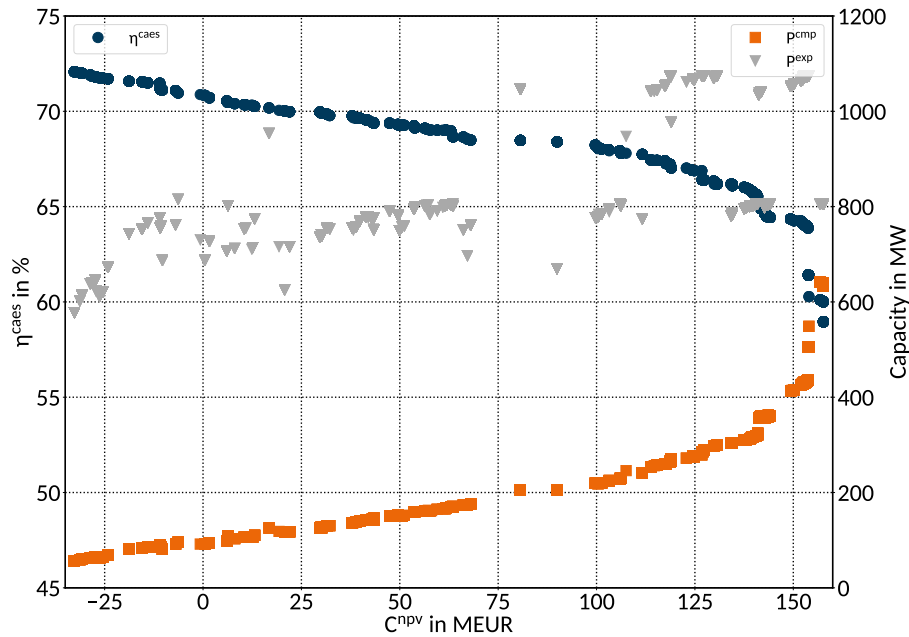
Figure 5.12: Pareto front and design parameters for scenario "Medium".

Compared to the first scenario, the NPV increases from negative to positive values with an increasing capacity of the compression part. Further, the ratio between compression and expansion decreases slightly towards a higher NPV. Nevertheless, this ratio is not constant but variable in certain areas of the front like the area between an NPV of 50-100 MEUR. Thus, there seem to be areas in which extra capacity in the expansion part is beneficial in an economic sense. On the other hand, additional capacity in the expansion part is not penalized within the model with regard to the efficiency as opposed to the compression part which includes losses from partial load. Thus, such areas have to be regarded against this background and rather be interpreted as a trend. As for the efficiency, additional capacity in the compression part leads to higher shares of partial load and thus lower resulting efficiencies. In conclusion, it can be seen that additional compression capacity is beneficial in an economic sense while reducing the overall storage efficiency due to higher shares of partial load. Moreover, it is generally beneficial to select a compression part capacity within a range of approximately 0.1 and 0.5 in relation to the expansion part, depending on the actual preferences of the decision maker.

Scenario "High"

Different results for the dimensioning are achieved in the third power market scenario with high spreads which is shown in Figure 5.12.
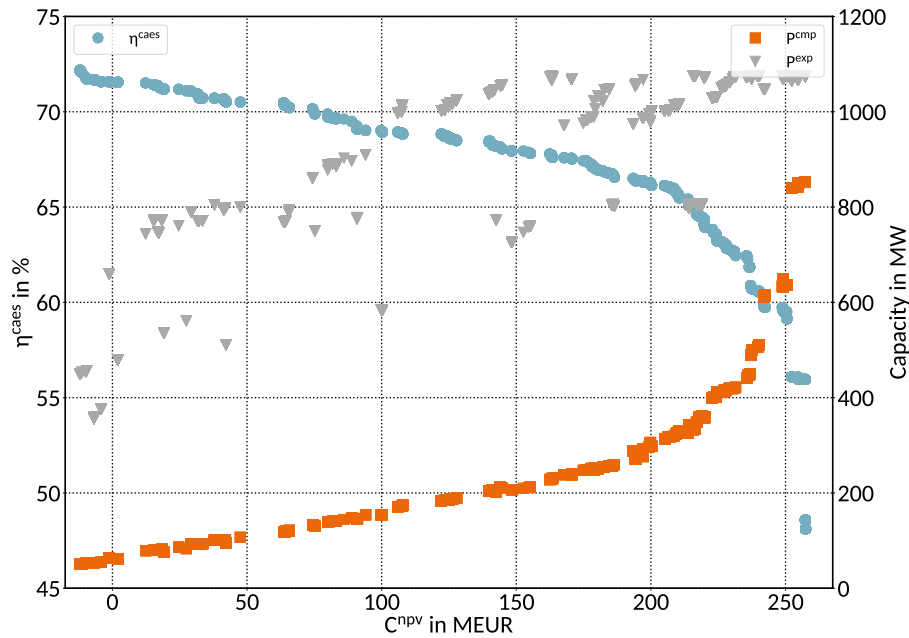
Figure 5.13: Pareto front and design parameters for scenario "High".

Similar to the second scenario, the NPV increases with a higher capacity of the compression part with the difference that the achieved NPVs are generally higher. Exactly as with the second scenario, an increasing compressor size reduces the overall storage efficiency due to higher shares of partial load. Nevertheless, the ratios between the compression and expansion part are different compared to the second scenario, especially in the area with higher NPVs which are achieved at ratios of approximately 0.5 to 0.75. This changed ratio is mainly caused by a stronger operation of both parts which is induced by higher incentives through lower and higher electricity prices. As in the second scenario, this comes at the expense of storage efficiency and the actual dimensioning depends on the individual preferences of the decision maker. Both ratios that are found in the second and third power market scenario differ from values that are found in existing literature as the actual dimensioning is strongly influenced by the chosen objective(s) and assumptions. For instance, in [155, p.46], an optimal compression to expansion power ratio of 1.75 is found to be beneficial which means that the installed capacity for the compression is almost twice the capacity of the expansion, independently of the storage volume. Nevertheless, the study investigates an adiabatic concept with additional revenues from negative control reserve markets. This induces a strong operation of the compression part due to high revenues [27] which could be confirmed

by other studies [40]. Moreover, the performed optimization is mono-objective and only considers the NPV to be maximized.

System operation

Extensive tests are applied to the operational model in order to validate its functionality for different design cases. Tests include the defined load ranges of the compression and expansion part as well as the storage level with regard to the charging and discharging operation. Moreover, additional constraints such as the equality of the initial and last filling level are checked. Finally, the general behaviour with regard to the market operation is analyzed and illustrated in Figure 5.14 for a selected design case.
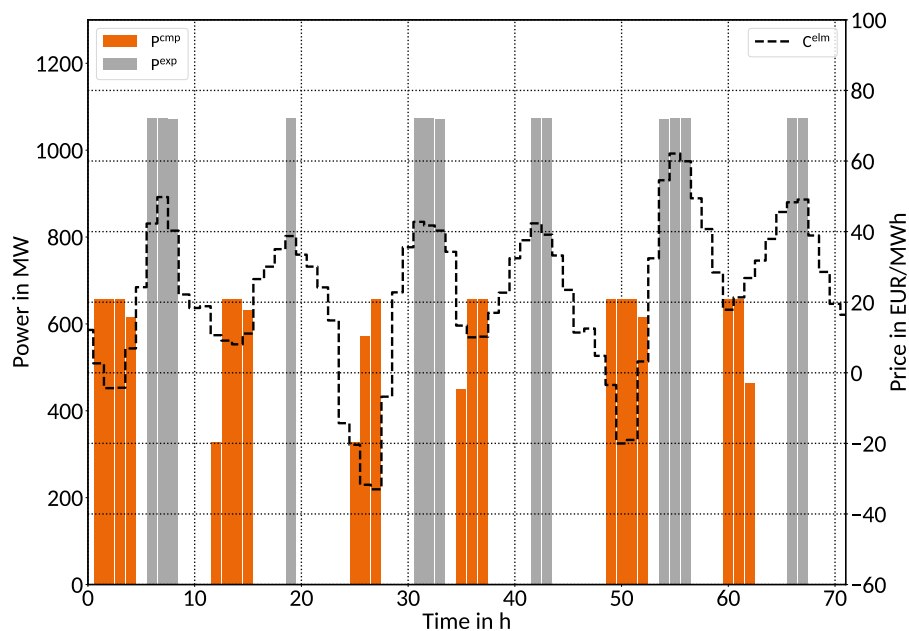
Figure 5.14: Unit commitment for a design case within a cluster of scenario "High".

It can be seen that both, the compression and expansion part operate as expected with regard to the surrounding market environment. The system is charged when electricity prices are low and discharged then electricity prices are high. Pre-defined load ranges are satisfied as both parts are either turned off or operate between minimum and maximum load. As the load of the compression part also depends on the filling level of the air storage (cf. Equation 5.27), this relation is also visible in the results for the compressor operation with differing load conditions. In contrast, the electricity production in the expansion part is only modelled depending on the mass flow (cf. 5.39) and thus shows no partial load behaviour. In conclusion, the operational model is validated successfully for its applicability under varying system design cases.

As explained above, these different design cases lead to a diverse set of objective values which are directly affected by the actual system operation. The partial load behaviour of the compression part which depends on the actual storage pressure has a direct influence on the efficiency. For reasons of interpretability, the minimum storage pressure $\underline{\pi}_k^{cas}$ and working pressure $\overline{\pi}_k^{cas,opr}$ which are included in the model (cf. Equation 5.27) are aggregated by means of the real pressure π^{cas} in the following. Figure 9.3 in the appendix shows exemplary duration curves for both expansion, compression and storage part for the selected design case with a low efficiency of 57.92 %. Besides a strong influence of the partial load in the compression part, the operation is affected by the design variables in combination with the respective power market scenario. In this connection, higher levels of plant utilization are induced by stronger price fluctuations and vice versa.

Model performance

Finally, the overall model performance in terms of computational runtime and solution quality is analyzed. Besides the described compact formulation of the operational model and performed data clustering, the former is realized by tweaking parameters of the evolutionary algorithm. The latter are outlined in Table 5.4 and include parameters such as the population size, number of populations and overall evolutions. As these likewise affect the solution quality, a good compromise between both, solution speed and quality, has to be found. For this, within the modeling process, different combinations of parameters are evaluated in terms of the overall and intra-generational runtime and solution quality. The former is illustrated in Figure 9.6 in the appendix and amounts for about 20-40 minutes per generation and about 100 hours in total on machine with 12 Intel® Xeon™ E5-2620 v4 CPUs at 2.10 GHz clock speed and 64 GB RAM.

The quality of obtained solutions is measured by tracking the hypervolume indicator (cf. Equation 3.7) and number of non-dominated individuals per generation and island. Both figures are shown examplarily for the selected parameter setup in Figure 9.7 and Figure 9.8 in the appendix, respectively. As described within the foundations, the design algorithm shows a typically explorative behaviour in the first generations (hypervolume indicator) and exploits the front in later generations (non-dominated individuals) whereas the performance differs between the different populations. For this reason, it is found to be beneficial to rather run many islands in parallel in order to obtain dense Pareto-fronts. However, the parameter setting could be improved even further by other approaches such as parameter tuning before or control during the optimization run as described in [99, p.136 ff.].

5.5 Case study conclusions

This case study demonstrates that the developed method can be applied to optimize design parameters of a specific CAES concept with regard to different objectives. The optimization is based on a detailed techno-economical operational model that is validated against literature values. For this, the developed model includes partial load conditions and keeps track of non-linear cost effects as well as operational characteristics that are dynamically changed for different design cases. As already noted, within investigations on the dimensioning of other technologies in similar models [64], the partial load behaviour can have a significant impact on the optimal design. Thus, the flexibility of the proposed hybrid method, which uses a dynamical fit in the pre-processing of specific design cases, provides a methodical advantage due to the higher level of achieved accuracy. Moreover, non-linear costs for different component sizes are regarded in the post-processing of the operational optimization. This concept is superior to approaches that apply linearization techniques like piecewise linear (PWL) functions based on special ordered sets (SOS) for the cost modeling [175, 21]. This aspect of modeling at a higher level of accuracy is of special interest in future energy supply systems with increasingly complex technologies like fuel cells [64]. Overall, the algorithm setup selected for the case study using the combination of NSGA-II and a MILP performs well and can be used on regular desktop computers. This is realized through the concepts of data clustering, parallelization and other performance measures that are applied to the selected solution algorithms. Further, the model is scaled onto a computational cluster to obtain results at a higher level of detail.

By analyzing the appereance of the different Pareto-fronts, it becomes clear that different market environments have a strong impact on the derived solutions due to a different dispatch of the compression and expansion part. Consequently, different design cases lead to very diverse solutions regarding both objectives. These results underline that the specific technical design of the storage has a strong impact on the realized dispatch and consequently both objective values. Thus, the method provides deeper insights into the interdependence of design parameters and objective values under different market conditions. This is an advantage over classical mono-objective methods that often only investigate specific design cases [39, 40, 175, 28, 29] although the dimensioning has a strong impact on the results. Solution sets that are identified in the multi-objective optimization are superior because dominated solutions with inferior objective values are discarded during the optimization process. Consequently, the resulting Pareto-fronts provide a better decision base because preferences of different stakeholders can be considered and discussed. This is of special interest in future energy supply systems where the fitting of energy storage, supply and demand will be a recurring task. Nevertheless, current framework conditions do not bring up business cases for bulk energy storage, which is why the undelying price series are scaled in order to bring up profitable design cases.

From a practical point of view, it becomes clear that no CAES plant can survive in the current day-ahead electricity market in Germany because it is organized as an energy only market with comparably low spreads. This has also been demonstrated in previous studies [39, 40, 155, 27] . The current situation might change with increasing spreads on the market when a high level of volatility is needed if no additional remuneration like capacity payments or revenues from other markets are available [155, p.45]. In contrast to such additional remuneration schemes, some economists argue that electrical energy should be treated like any other commodity. This means that electricity is traded on a free market without price caps and centralized mechanisms for controlling or encouraging investments in generation or storage [16]. It is also argued that the averaging of network charges over time results in inefficient usage and investment decisions in local generation [3, p.205 ff.] which adapts the same market priciples on parts of the underlying infrastructure. In contrast, other economists argue that relying solely on price spikes in such markets is unlikely to bring up enough generation capacity [6, p.220]. Further, it is argued that consumers do not purchase electrical energy only, but consume a service with a certain level of reliability. Finally, both theoretical positions have their relevance and could implement respective policy frameworks for energy storage that will be needed in future energy systems with high shares of RE.

6 Case study - Municipal district heating system

This chapter describes the method application on a typical municipal district heating system. For this, an overview of the case study is provided in the first place. After this, the entire model building process including the design and operational model is described in detail. Subsequently, a specific setup is chosen and optimized before results are interpreted in the last step.

6.1 Case study overview

District heating systems play a central role in decarbonizing energy systems because these systems can provide flexibility to the electricity supply with high shares of volatile RE. For such complementary heating systems, the concept of 4th generation district heating (4GDH) was developed [176] in order to transform current centralized, inefficient and fossil based systems into renewable, decentralized and energy efficient ones. In order to increase the system's overall energy efficiency and integrate RE or waste heat potentials, lower flow temperatures are a crucial element besides a combination of different and more flexible heating technologies. Moreover, other elements like large scale seasonal storage, biomass conversion and low energy buildings can complement these systems.

The planning and assessment of systems like these requires adequate models that capture the underlying economical and technical characteristics. These models are subject to different objectives which encompass economical targets like the system's NPV or heat production costs, technical objectives like the system's energy efficiency and environmental objectives like the system's net emissions. Among others, questions to be answered are which technologies are to be chosen, how these are dimensioned and how respective setups perform under different boundary conditions such as resource costs and political frameworks. Different stakeholder perspectives are often conflicting, a multi-objective approach which integrates different objectives offers advantages in this context.

In this case study, a typical mid-sized third generation municipal DH system is optimized based on available data for the city of Flensburg in northern Germany. Considered heat production technologies can be different types of gas-fueled cogeneration plants like internal combustion engines (ICE), back-pressure turbines (BPT) or combined cycle gas turbines (CET), heat pumps (HP) as well as an electric boilers (EHB) and a gas-fired peak load boilers (PLB). In combination with a thermal energy storage (TES) that

adds flexibility to the system, these technologies serve an overall heat demand through a respective heating network. Electricity is purchased from and delivered to the electricity network based on prices on the day-ahead electricity market. A schematic diagram of the analyzed municipal district heating system with its underlying possible components is shown in Figure 6.1.
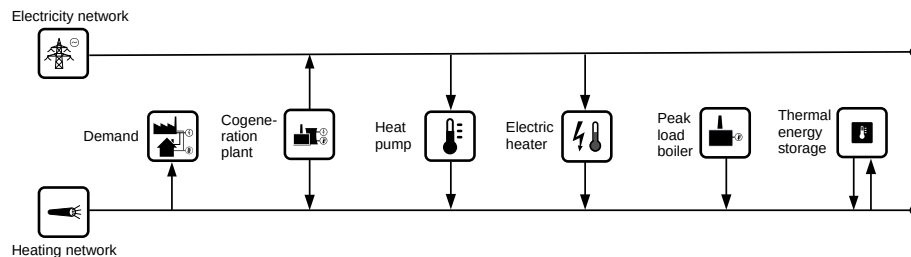
Figure 6.1: Schematic diagram of a typical municipal district heating system of the third generation.

The shift from fossil based cogeneration plants towards power to heat (PtH) technologies like efficient heat pumps and electric heaters requires a suitable political framework to bring these technologies into a competitive position. The economic operation of a PtH unit is essentially determined by the price at which electricity can be purchased. This price in turn consists of different components like taxes, fees, submissions and levies which depend on various factors such as the technical or economical settings in which the plant is operated. In the transformation process towards a less carbon intense and a finally carbon neutral energy supply system, it is being argued that there should be no discrimination against single technologies in the future. This could lead to a discontinuation or adaption of the payments to support CHP plants and reduced final consumer charges for PtH technologies.

In the following, three exemplary different power market scenarios for the year 2030 [177] model the electricity prices and resulting emissions in the surrounding national electricity system. The marginal generation costs of the LP model of the power system are interpreted as prices at the wholesale electricity market, similar to the approach chosen in [178]. In the first scenario "2030-A" the assumption is that the increase of renewable electricity generation is relatively low, whereas it increases progressively in the scenario "2030-C". Furthermore, in an additional scenario "2030-C-climate", a higher price for carbon of 100 EUR/t is assumed in addition to the increased share of renewable electricity production. These different assumptions are also reflected in the electricity prices and emissions resulting from the model, which are shown in Figure 9.9 and 9.10 in the appendix. Finally, the installed national power plant capacities are shown in Figure 6.2. All data and assumptions are provided in a respective data package that has been published online[177].

Different electricity prices and emissions in the energy system are assumed to have a strong impact on the use of CHP and PtH technologies and the resulting dimensioning. Therefore, the three scenarios can be
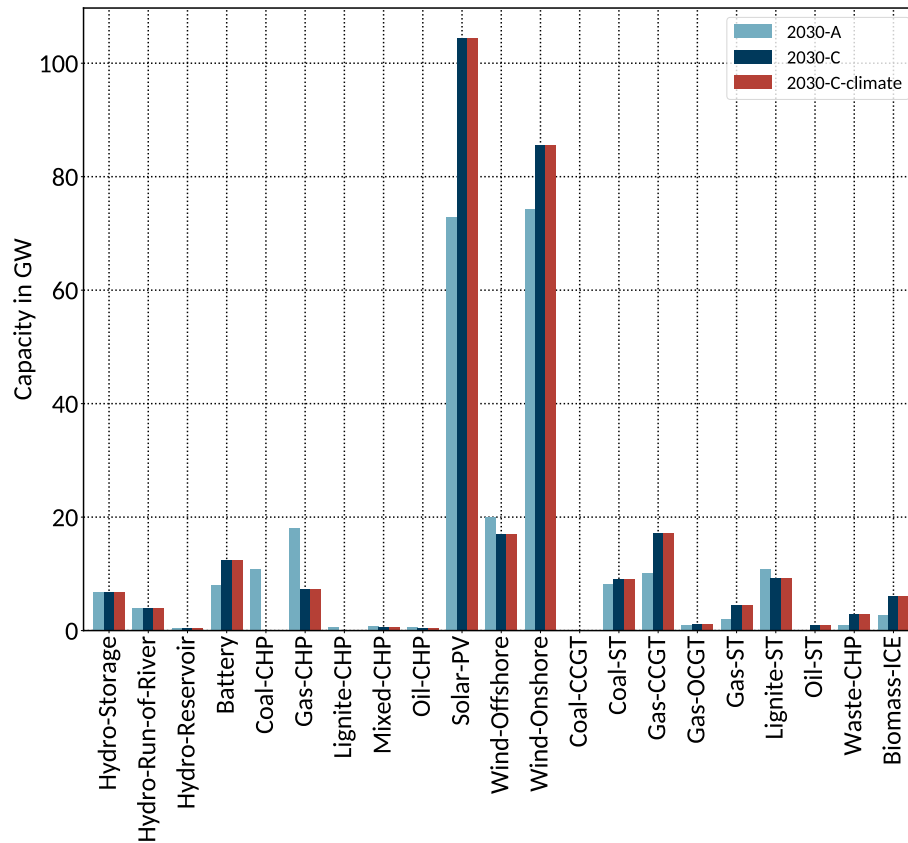
Figure 6.2: Installed capacities for the German energy system in different power market scenarios for the year 2030.

interpreted as different extremes which show the effect of potential adaptions of the regulatory framework. In contrast to the different electricity prices and system emissions, all other assumptions remain constant in the different scenarios and are outlined in detail in Table 6.6 (in Chapter 6.3, p. 93).

6.2 Model creation and outline

Similarly, to the first case study, an overview of used symbols, subscripts and identifiers is provided in the nomenclature. All needed sets and indices are defined in Expressions 6.1-6.8. The formulation again holds for an arbitrary number of units and time steps. Subsets and empty sets for the case of a non-existent unit can also be covered using this approach. For the following model description, the same sign conventions as within the first case study are used (cf. Section 5.2).

$$t \in T \quad \text{Index and set of all time steps} \tag{6.1}$$

$$c \in C \quad \text{Index and set of all CHP units} \tag{6.2}$$

$$d \in D \quad \text{Index and set of all heat demands} \tag{6.3}$$

$$h \in H \quad \text{Index and set of all heat pumps} \tag{6.4}$$

$$e \in E \quad \text{Index and set of all eletric boilers} \tag{6.5}$$

$$b \in B \quad \text{Index and set of all peak load boilers} \tag{6.6}$$

$$s \in S \quad \text{Index and set of all thermal storages} \tag{6.7}$$

$$g \in G \quad \text{Index and set of all heat production units } (G = C \cup H \cup E \cup B) \tag{6.8}$$

Design model

Two fitness functions are defined to optimize the heating system design in an economical and environmental dimension. As analyzed in respective studies [179, 180], the actual system design e.g. towards higher shares of CHP or PtH capacity can have a stong impact on the overall economic and environmental performance whereby a TES provides flexibility to decouple the system's electricity production and consumption time-wise. Thus, the installed CHP and PtH facilities and their respective dimensioning are selected as decision variables in the design optimization process. Further, within the first objective, the levelized costs of heat (LCOH with symbol $lcoh$) as a classical indicator for an investment decision into a heating system are minimized. Moreover, within the second objective, the relative operational emissions of heat (REOH with symbol $reoh$) capture the carbon footprint of the system per produced unit of heat and are likewise minimized.

The resulting multi-objective design optimization problem can be described as in Expression 6.9 where decision variables are again parameters of a mixed-integer operational model. As opposed to the first case study, the unconstrained problem is linear because no non-linear expressions such as cost degression effects are considered for the different heating system components. A possible approach for their integration has already been presented in the first case study whereas the focus here is put on the integration of multiple technologies.

$$min \left[C^{lcoh}, E^{reoh} \right] \tag{6.9}$$

The general formulation of the LCOH within the first fitness function is illustrated in Equation 6.10 and outlined below.

$$C^{lcoh} = \frac{-C^{npv}}{Q^{dch}}$$
(6.10)

The overall levelized costs of heat are defined as the ratio of the net present value and the discounted heat (DCH). Here, the NPV is modelled according to Equation 6.11 by means of different cost expressions for the investment and operation of the system over the expected lifetime. Further, additional revenues from electricity production are included in single expressions. As an initial investment is negative, the algebraic sign is changed in expression 6.10 as high NPVs lead to high LCOE and vice versa.

$$C^{npv} = -C^{cpx,total} + \sum_a (\frac{C^{opx,fix,total} + C^{opx,var,total} - C^{orv,total}}{(1+i)^a})$$
(6.11)

Similarly to the first case study, investment costs occuring in the initial period are modelled within the CAPEX and outlined from Equation 6.12-6.17 whereby the symbol cpx represents capital expenditures.. These encompass cost expressions for all system components which are related to the installed electrical or thermal capacity depending on the respective component. For CHP plants, the electrical capacity without district heating (denoted by the symbol $wodh$) is taken. For instance, costs for CHP components $C^{cpx,inv,c}$ and heat pump components $C^{cpx,inv,h}$ are related to the nominal electrical capacity whereas costs for electric heaters $C^{cpx,inv,e}$ and peak load boilers $C^{cpx,inv,b}$ are related to the thermal generation capacity. Further, costs for storages $C^{cpx,inv,s}$ are related to the overall storage capacity whereby the ratio between energy content and charging or discharging capacity is expressed by a fixed value.

$$C^{cpx,total} = C^{cpx,inv,c} + C^{cpx,inv,h} + C^{cpx,inv,e} + C^{cpx,inv,s} + C^{cpx,inv,b}$$
(6.12)

$$C^{cpx,inv,c} = \sum_c \overline{p}_c^{wodh} c_c^{inv}$$
(6.13)

$$C^{cpx,inv,h} = \sum_h \overline{p}_h c_h^{inv}$$
(6.14)

$$C^{cpx,inv,e} = \sum_e \overline{q}_e^{dh} c_e^{inv}$$
(6.15)

$$C^{cpx,inv,s} = \sum_s \overline{q}_s^{heat} c_s^{inv}$$
(6.16)

$$C^{cpx,inv,b} = \sum_b \overline{q}_{b,t}^{dh} c_b^{inv}$$
(6.17)

Operational fixed costs for each period are modelled likewise depending on the installed capacity of respective components according to Equations 6.18-6.23. As pointed out in the first case study, these costs consist of insurances, personnel expenses, rents and other items which occur in every period independently of the actual system operation. Here, the symbol opx represents operational expenditures.

$$C^{opx,fix,total} = C^{opx,fix,c} + C^{opx,fix,h} + C^{opx,fix,e} + C^{opx,fix,s} + C^{opx,fix,b} \tag{6.18}$$

$$C^{opx,fix,c} = \sum_c \overline{p}_c^{wodh} c_c^{fix} \tag{6.19}$$

$$C^{opx,fix,h} = \sum_h \overline{p}_h^{wodh} c_h^{fix} \tag{6.20}$$

$$C^{opx,fix,e} = \sum_e \overline{p}_e^{wodh} c_e^{fix} \tag{6.21}$$

$$C^{opx,fix,s} = \sum_s \overline{q}_s^{heat} c_s^{fix} \tag{6.22}$$

$$C^{opx,fix,b} = \sum_b \overline{q}_{b,t}^{dh} c_b^{fix} \tag{6.23}$$

Occuring variable costs for the system's operation are modelled in Equations 6.24-6.28 in the same way. Fuel, emission as well as other variable costs e.g. for maintenance are considered in the expression $C^{opx,var,c}$ for all CHP plants. As fuel and emission costs are related to the plant input, these are related to the heat flow into the plant whereby all other variable costs are related to the actual electricity production. Furthermore, operational costs for the electricity consumption in PtH components are modelled by means of expressions $C^{opx,var,h}$ for heat pumps and $C^{opx,var,e}$ for electric boilers. Similarly to the CHP plants, these could include costs for maintenance as well as other costs that are related to the electricity consumption. Finally, fuel and emission costs for peak load boilers can be captured by means of expression $C^{opx,var,b}$.

$$C^{opx,var,total} = \sum_p \omega_p \left(\sum_t (C^{opx,var,c} + C^{opx,var,h} + C^{opx,var,e} + C^{opx,var,b}) \right) \tag{6.24}$$

$$C^{opx,var,c} = \sum_c (\dot{Q}_{c,p,t}^{fuel} \tau (c_{c,p,t}^{fuel} + c_{c,p,t}^{emi}) + P_{c,p,t} \tau c_{c,p,t}^{var}) \tag{6.25}$$

$$C^{opx,var,h} = \sum_h P_{h,p,t} \tau (c_{p,t}^{elm} + c_{h,p,t}^{var}) \tag{6.26}$$

$$C^{opx,var,e} = \sum_e P_{e,p,t} \tau (c_{p,t}^{elm} + c_{e,p,t}^{var}) \tag{6.27}$$

$$C^{opx,var,b} = \sum_b \dot{Q}_{b,t}^{fuel} \tau (c_{b,p,t}^{fuel} + c_{b,p,t}^{emi} + c_{c,p,t}^{var}) \tag{6.28}$$

In addition, operational revenues $C^{orv,total}$ for selling electricity at the electricity market which are denoted by the symbol *elm* in the price $c_{p,t}^{elm}$ are regarded in Equation 6.29. Again, these are calculated for all CHP plants, time steps and periods along with their respective weight.

$$C^{orv,total} = \sum_p \omega_p \left(\sum_t \sum_c P_{c,p,t} \tau c^{elm}_{p,t} \right) \tag{6.29}$$

As explained above, in order to calculate the levelized costs of heat, the NPV is divided by the discounted overall heat load Q^{dh} in the disctrict heating system which is defined in Equation 6.30 in its general form i.e. when consisting of multiple loads.

$$Q^{dh} = \sum_p \omega_p \left(\sum_t \sum_d \dot{Q}^{dh}_{d,p,t} \tau \right) \tag{6.30}$$

Finally, this overall heat load is discounted as shown in Equation 6.31 for an integration in Equation 6.10 above.

$$Q^{dch} = \sum_a \frac{Q^{dh}}{(1+i)^a} \tag{6.31}$$

Within the second objective, the relative emissions of heat E^{reoh} are optimized as defined within Equation 6.32 by dividing the system's total emissions E^{total} by the overall heat load Q^{dh} as defined in Equation 6.30. In contrast to classical approaches from economic theory, here the emissions are calculated individually in another objective in order to track the actual carbon intensity of the system separately.

$$E^{reoh} = \frac{E^{total}}{Q^{dh}} \tag{6.32}$$

The system's total emissions E^{total} are outlined from Equation 6.33-6.38. Here, an approach similar to the one in [180] is chosen to account for emissions based on the hourly marginal emissions in the surrounding energy system e^{system} and the occuring local emissions which result from the specific fuel emissions e^{fuel}_c. The idea behind the approach is that all local emissions are accounted for in the first place whereby all electricity production from CHP is credited through negative emissions. The central assumption here is that no other additional power plant has to be switched on for the electricity production from CHP and thus emissions in the magnitude of the system emissions can be saved.

$$E^{total} = \sum_p \omega_p \left(\sum_t (E^{c,fuel} + E^{b,fuel} + E^{h,el} + E^{e,el} - E^{c,el}) \right) \tag{6.33}$$

$$E^{c,fuel} = \sum_c \dot{Q}_{c,p,t}^{fuel} \tau e_c^{fuel} \tag{6.34}$$

$$E^{b,fuel} = \sum_b \dot{Q}_{b,p,t}^{fuel} \tau e_b^{fuel} \tag{6.35}$$

$$E^{h,el} = \sum_h P_{h,p,t} \tau e^{system} \tag{6.36}$$

$$E^{e,el} = \sum_e P_{e,p,t} \tau e^{system} \tag{6.37}$$

$$E^{c,el} = \sum_c P_{c,p,t} \tau e^{system} \tag{6.38}$$

As explained above, in addition to the related fuel emissions from CHP plants $E^{c,fuel}$ and peak load boilers $E^{b,fuel}$, PtH emissions for heat pumps $E^{h,el}$ and electric boilers $E^{b,el}$ are accounted through electricity that is purchased from the surrounding electricity system at specific emissions e^{system}. As mentioned before, emissions from CHP electricity $E^{c,el}$ are credited based on the assumption that they are must-run capacities which replace other power plants in the system. This implies that the overall emissions heavily depend on the ratio between fuel emissions e_c^{fuel} and system emissions e^{system}. For instance, at low fuel emissions and high system emissions, the overall emissions are comparably low and vice versa. Further, these emissions also depend on the extent to which specific heat units are utilized. This reflects whether higher shares of PtH or CHP are used depending on the respective economic environment.

Operational model

To model the heat supply for all technologies, the overall operational revenues are maximized under technical restrictions. Apart from technical data on the demand and supply side, economical data such as costs for fuel and sold electricity are integrated into the model. Moreover, regulatory framework mechanisms can be considered on the input and output side of each unit. Output data is delivered in time series which capture the heat and power dispatch, fuel consumption and metrics such as storage filling levels. Figure 6.3 gives an overview about the basic structure and crucial input and output data.

As in the first case study, the optimization task is solved via a MILP model under the assumption of perfect foresight. This method is commonly used for similar unit commitment problems in the heat sector [69, 59, 60, 39]. Within this case study, again, an abstracted model of the heating system is chosen to represent general mathematical relations of all contained technologies in combination with economical restrictions. Whereas real systems practically consist of multiple components and partly show highly non-
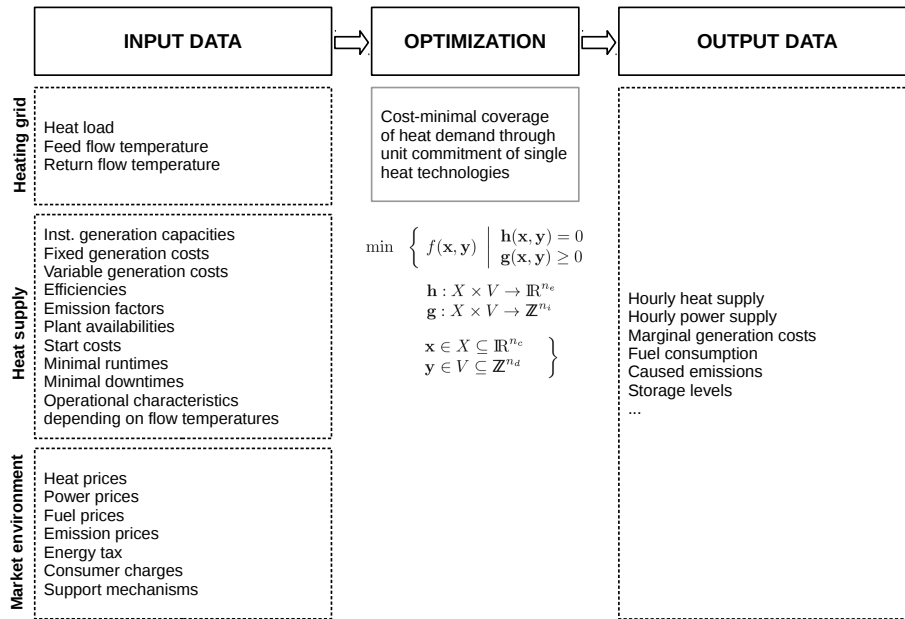
Figure 6.3: Structure of the operational model for the heating system case study.

linear and specific behaviour, a generic formulation is chosen to allow for a flexible adaptation to different concepts. Such an abstracted technology model is shown in Figure 6.4 and maps decision variables of single components to their physical input and output flows.
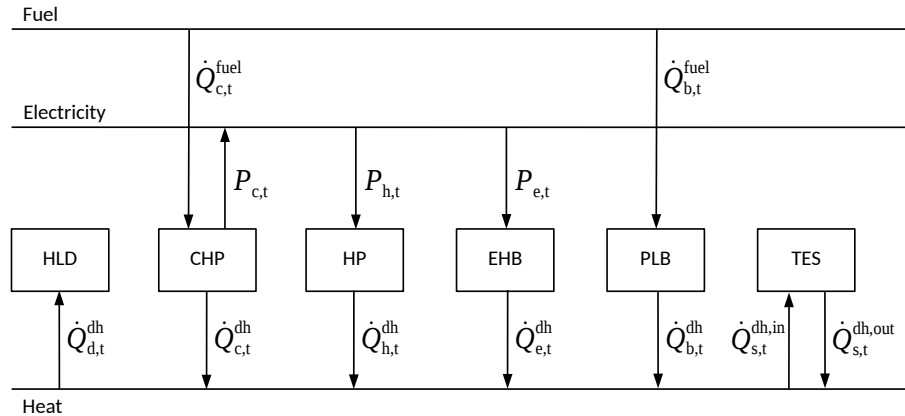
Figure 6.4: Abstract heating system model.

Classical energy conversion units that serve the heat load (HLD) might encompass different CHP plants such as back-pressure, motoric or combined-cycle plants powered by different fuels along with classic peak load boilers (PLB). Moreover, PtH technologies such as heat pumps or electric heating boilers might be integrated at a later stage in liberalized eletricity markets with higher shares of RE and respective low power prices or system service oppurtunities. Additionally, a TES allows for more flexibility when operating other units for instance storing energy through heat pump operation at low electricity prices.

Within the model, it is assumed that all consumers and units are connected in a grid single node. Flow temperatures and respective time-varying parameters such as flow dependent operational characteristics are not considered. As their effect on the results is comparably small [8], these are set constant over time in order to reduce the problem size.

The objective function is described in Expression 6.39 by means of the described indentifiers, indices and sets. Again, it consists of expressions for costs and revenues that are related to single technologies which are explained in Equations 6.40-6.44. Costs for CHP units are described in Expression 6.40 and consist of costs for fuel , CO_2certificates and other variable generation costs . In contrast, all revenues for delivered electricity are expressed in 6.41. Costs for other technologies are expressed likewise and related to the specific input and output quantities. In the following, all non-heat capacities are assumed to be electrical capacities.

$$min\left[\sum_t(\sum_c(C_{c,t} - R_{c,t}) + \sum_h(C_{h,t}) + \sum_e(C_{e,t}) + \sum_b(C_{b,t}))\right] \qquad (6.39)$$

$$C_{c,t} = \dot{Q}_{c,t}^{fuel}\tau(c_{c,t}^{fuel} + c_t^{emi}) + P_{c,t}\tau c_{c,t}^{var} + Y_{c,t}^{start}c_{c,t}^{start} \qquad (6.40)$$

$$R_{c,t} = P_{c,t}\tau c_t^{elm} \qquad (6.41)$$

$$C_{h,t} = P_{h,t}\tau(c_t^{elm} + c_{h,t}^{var}) + Y_{h,t}^{start}c_{h,t}^{start} \qquad (6.42)$$

$$C_{e,t} = P_{e,t}\tau(c_t^{elm} + c_{e,t}^{var}) + \dot{Q}_{e,t}^{dh}\tau c_{e,t}^{var} + Y_{e,t}^{start}c_{e,t}^{start} \qquad (6.43)$$

$$C_{b,t} = \dot{Q}_{b,t}^{fuel}\tau(c_{b,t}^{fuel} + c_t^{emi}) + Y_{b,t}^{start}c_{b,t}^{start} \qquad (6.44)$$

A central constraint of the defined heat supply task is the thermal load coverage at any point in time. This relation is expressed by an energy balance in Equation 6.45 which ensures that the heat demand is covered by all technologies. In addition to the generation units, within the last expression of the balance, all input and output heat flows from thermal storages are captured.

$$\sum_d\dot{Q}_{d,t}^{dh} = \sum_c\dot{Q}_{c,t}^{dh} + \sum_h\dot{Q}_{h,t}^{dh} + \sum_e\dot{Q}_{e,t}^{dh} + \sum_b\dot{Q}_{b,t}^{dh} + \sum_s(\dot{Q}_{s,t}^{dh,out} - \dot{Q}_{s,t}^{dh,in}) \qquad \forall\, t \qquad (6.45)$$

The modeling of CHP plants in Equations and Inequalities 6.48-6.52 follows a formulation from [181] which is adapted by two equations for flue gas losses in Equations 6.54 and 6.55, respectively. This adaption is made in accordance with one of the authors and has been tested extensively. Similar formulations for CHP plants can be found in [69, 60] and [182] whereby the latter provides a general overview about the modeling approaches for CHP plants in MILP models. The concrete model is explained briefly in the following whereby parameters and variables are aligned to the proposed naming convention.

$$\underline{\eta}_c^{wodh} = \frac{\underline{p}_c^{wodh}}{\alpha_c^1 + \alpha_c^2 \underline{p}_c^{wodh}} \qquad\qquad \forall\, c,t \qquad\qquad (6.46)$$

$$\overline{\eta}_c^{wodh} = \frac{\overline{p}_c^{wodh}}{\alpha_c^1 + \alpha_c^2 \overline{p}_c^{wodh}} \qquad\qquad \forall\, c,t \qquad\qquad (6.47)$$

$$\dot{Q}_{c,t}^{fuel} = Y_{c,t}\alpha_c^1 + \alpha_c^2 p_{c,t}^{wodh} \qquad\qquad \forall\, c,t \qquad\qquad (6.48)$$

$$\dot{Q}_{c,t}^{fuel} = Y_{c,t}\alpha_c^1 + \alpha_c^2(P_{c,t} + \beta_c \dot{Q}_{c,t}^{dh}) \qquad\qquad \forall\, c,t \qquad\qquad (6.49)$$

$$\dot{Q}_{c,t}^{fuel} \le Y_{c,t}\frac{\overline{p}_c^{wodh}}{\overline{\eta}_c^{wodh}} \qquad\qquad \forall\, c,t \qquad\qquad (6.50)$$

$$\dot{Q}_{c,t}^{fuel} \ge Y_{c,t}\frac{\underline{p}_c^{wodh}}{\underline{\eta}_c^{wodh}} \qquad\qquad \forall\, c,t \qquad\qquad (6.51)$$

$$\dot{Q}_{c,t}^{fuel} \le P_{c,t} + \dot{Q}_{c,t}^{dh} + \overline{L}_{c,t}^{fg,abs} + Y_{c,t}\underline{q}_c^{cond} \qquad\qquad \forall\, c,t \qquad\qquad (6.52)$$

$$\dot{Q}_{c,t}^{fuel} \ge P_{c,t} + \dot{Q}_{c,t}^{dh} + \underline{L}_{c,t}^{fg,abs} + Y_{c,t}\underline{q}_c^{cond} \qquad\qquad \forall\, c,t \qquad\qquad (6.53)$$

$$\overline{L}_{c,t}^{fg,abs} = \dot{Q}_{c,t}^{fuel}\overline{l}_c^{fg,rel} \qquad\qquad \forall\, c,t \qquad\qquad (6.54)$$

$$\underline{L}_{c,t}^{fg,abs} = \dot{Q}_{c,t}^{fuel}\underline{l}_c^{fg,rel} \qquad\qquad \forall\, c,t \qquad\qquad (6.55)$$

As described in [181], the plant-specific alpha coefficients are calculated by solving the system of linear equations given by Equation 6.46 and 6.47. These include the minimum and maximum capacities and efficiencies of the CHP unit without district heating. Subsequently, the alpha coefficients are used in Equations 6.48 and 6.49 to describe the relation between fuel inflow and electrical as well as heat outflow. A load range for the fuel inflow is described in Inequalities 6.50 and 6.51 based on a binary status variable for the operational mode. Moreover, Inequalities 6.52 and 6.53 define the relation between fuel inflow, flue gas losses and minimum condenser capacity. Respective flue gas losses are hereby related to the fuel inflow whereby the formulation is extented by Inequality 6.53 as well as Equation 6.54 and 6.55 as described above.

The chosen formulation is valid to model extraction turbines and motoric plants. Furthermore, a conversion of Inequality 6.52 into an equation also allows for a representation of back-pressure turbines. The explained extension with the last three expressions allows for a correct consideration of flue gas losses for all plant types. Inequality 6.53 and Equation 6.54 are used for internal combustion engines and otherwise omitted (cf. Figure 6.5 for the impact on the minimal heat extraction in the case of an ICE). For a detailed derivation of all physical relationships, it is referred to [181] in this place. Moreover, the entire formulation is ported into a branch of the framework [142] in this thesis (cf. Section 4.4 for the implementation). Finally, exemplary operational regions for different CHP types such as a combined extraction turbine, an internal combustion engine and a back pressure turbine are sketched in Figure 6.5 for the assumption of

constant supply temperatures. These operational regions may vary with changing supply temperatures whereby more examples can be found in respective publications [8, 180] and the initial formulation of the used modeling approach [181].
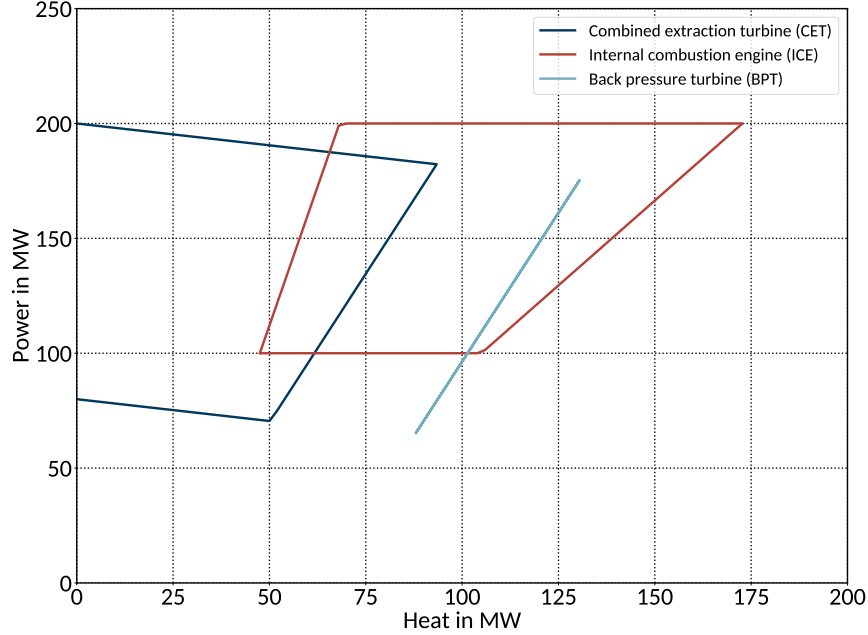
Figure 6.5: Exemplary PQ-diagrams for different types of CHP plants.

As demonstrated in [181] and [8], the linearization of technical characteristics leads to deviations in the border regions of the operational regions in comparison to the detailed (non-linear) thermodynamical modeling. Nevertheless, these deviations are comparatively minor when pre-calculated for every time step of the optimization horizon or approximated with good assumptions for the average values [8]. For a more detailed analysis on the effects for combined-cycle extraction turbines it is referred to [181].

Heat pumps are modeled via Equation 6.56 which relates the transferred output heat flow with the electrical power for the fluid compression. The operational area is described by a slope and a y-intersect which is activated by a status variable if a pump is operated. This means that the coefficient of performance can be defined in an arbitrary range without the need to pass the coordinate origin. As soon as the pump is turned off, the heat flow is set to zero through this relation. Moreover, the load range between a maximal and minimal load is defined through Inequalities 6.57 and 6.58.

$$\dot{Q}_{h,t}^{dh} = P_{h,t}\epsilon_h^m + Y_{h,t}\epsilon_h^b \qquad\qquad \forall\, h,t \qquad\qquad (6.56)$$

$$P_{h,t} \leq Y_{h,t}\overline{p}_h \qquad\qquad \forall\, h,t \qquad\qquad (6.57)$$

$$P_{h,t} \geq Y_{h,t}\underline{p}_h \qquad\qquad \forall\, h,t \qquad\qquad (6.58)$$

The chosen heat pump formulation diverges from a commonly used representation with constant coefficient of performance (COP) and no y-intersect used in [183] and [60] by adding more flexibility and detail to the model. In contrast, a more detailed formulation using piecewise-linear functions is provided in [184] but comes at the expense of a higher computational effort. In [183], the modeling of constant versus varying coefficients of performance is compared for compression heat pumps in a large scale system whereby the results state that the impact on the results is neglectable. Nevertheless, it is assumed to have a higher impact with smaller systems including fewer technologies and a higher variation in temperature levels.

Electrical boilers are described through Equation 6.59 which relates the transferred output heat flow to the eletrical input in a similar way as the heat pump description. The only difference in the operational area in contrast to the heat pump lies in the omitted y-intersect. A load range is defined in Inequality 6.60 and 6.61 respectively.

$$\dot{Q}^{dh}_{e,t} = P_{e,t}\eta^{th}_e \qquad\qquad \forall\, e,t \qquad\qquad (6.59)$$

$$\dot{Q}^{dh}_{e,t} \leq Y_{e,t}\overline{q}^{dh}_e \qquad\qquad \forall\, e,t \qquad\qquad (6.60)$$

$$\dot{Q}^{dh}_{e,t} \geq Y_{e,t}\underline{q}^{dh}_e \qquad\qquad \forall\, e,t \qquad\qquad (6.61)$$

Peak load boilers are described in Equation 6.62 and Inequalities 6.63 and 6.64 in the same way as electric boilers. Here, the output heat flow relates to the fuel inflow multiplied by the thermal boiler efficiency. Load ranges are defined on the output inflow as for the heat pump.

$$\dot{Q}^{dh}_{b,t} = \dot{Q}^{fuel}_{b,t}\eta^{th}_b \qquad\qquad \forall\, b,t \qquad\qquad (6.62)$$

$$\dot{Q}^{dh}_{b,t} \leq Y_{b,t}\overline{q}^{dh}_b \qquad\qquad \forall\, b,t \qquad\qquad (6.63)$$

$$\dot{Q}^{dh}_{b,t} \geq Y_{b,t}\underline{q}^{dh}_b \qquad\qquad \forall\, b,t \qquad\qquad (6.64)$$

Thermal energy storages are described in Equation 6.65 through an energy balance under the assumption of a perfect mixing in the same way as in [185], [186] and [61]. This intertemporal link between two states links every point in time with its predecessor. Temporal losses are accounted for by means of a temporal efficiency. Losses in heat transfer are integrated by respective efficiencies for heat transfer into and out of the storage. The actual thermal storage capacity is represented by the maximum amount of heat that can be stored and defined in Inequality 6.66. Implications of this commonly used modeling approach and alternative approaches are discussed in detail in [187] and [188]. This chosen formulation for a storage model allows to store and restore heat on different temperature levels because only heat flows are captured. If temperature restrictions have to be considered in the model, this could possibly be

realized by pre-calculated parameters like upper bounds for inflows depending on whether it is possible to transfer heat from or into the heating grid [8].

$$Q_{s,t} = Q_{s,t-1}\eta_s^{tmp} + (\dot{Q}_{s,t}^{dh,in}\eta_s^{dh,in} - \frac{\dot{Q}_{s,t}^{dh,out}}{\eta_s^{dh,out}})\tau \qquad \forall\, s,t \qquad (6.65)$$

$$Q_{s,t} \leq \overline{q}_s^{heat} \qquad \forall\, s,t \qquad (6.66)$$

$$\dot{Q}_{s,t}^{dh,in} \leq \overline{q}_s^{dh,in} \qquad \forall\, s,t \qquad (6.67)$$

$$\dot{Q}_{s,t}^{dh,out} \leq \overline{q}_s^{dh,out} \qquad \forall\, s,t \qquad (6.68)$$

Operational states for all units which enable the integration of start oder shutdown costs in the objective function are captured in Equations 6.69 and 6.72. A start variable is introduced by Inequalities 6.69 and 6.70 captures whether a specific unit is started at a specific point of time whereby Equation 6.71 and 6.72 provide information about shutdown states.

$$Y_{g,t}^{start} \geq Y_{g,t} - Y_{g,t-1} \qquad \forall\, g,t > 1 \qquad (6.69)$$

$$Y_{g,t}^{start} \geq Y_{g,t} - y_g^{init} \qquad \forall\, g,t = 1 \qquad (6.70)$$

$$Y_{g,t}^{stop} \geq Y_{g,t-1} - Y_{g,t} \qquad \forall\, g,t > 1 \qquad (6.71)$$

$$Y_{g,t}^{stop} \geq y_g^{init} - Y_{g,t} \qquad \forall\, g,t = 1 \qquad (6.72)$$

For very detailed models, the definition of minimum run- and downtimes allows for a more realistic representation of the technical behaviour such as the ramping up and down of a combined-cycle plant. Since the application of respective restrictions -especially when used in combination- can lead to undesired states of single units in the edge regions of an optimization period, this behaviour has to be taken into account. For this, the time steps at the beginning and end of an optimization period are aggregated in a single set to be treated separately. Equation 6.73 defines this set whereby in each case the larger edge region e.g. the maximum of up and downtimes is chosen.

$$T^{er} = \{t^1, ..., max(n^{up}, n^{down})\} \cup \{t^{max} - max(n^{up}, n^{down}), ..., t^{max}\} \qquad (6.73)$$

This extended formulation improves the approach proposed in [160] by defining clear states within the edge regions and thus prevents undesired states. This allows for a definition of minimum up and downtimes in Inequalities 6.74 and 6.75. In contrast, Equation 6.76 sets the initial unit state in the border regions. Again, the respective formulation has been ported in the framework within the scope of thesis (cf. Table 4.1).

$$(Y_{g,t} - Y_{g,t-1})n^{up} \leq \sum_{\vartheta=0}^{n^{up}} (Y_{g,t+\vartheta}) \qquad\qquad \forall\, g, t \in T \setminus T^{er} \qquad (6.74)$$

$$n^{down} \geq \sum_{\vartheta=0}^{n^{down}} (Y_{g,t+\vartheta}) + (Y_{g,t-1} - Y_{g,t})n^{down} \qquad \forall\, g, t \in T \setminus T^{er} \qquad (6.75)$$

$$Y_{g,t} = y_g^{init} \qquad\qquad \forall\, g, t \in T^{er} \qquad (6.76)$$

6.3 Model and algorithm setup

After a description of both, the design and operational model, a concrete example is set up in the case study. As within the first case study, all economic and technical model parameters are outlined within the first section. Subsequently, the data clustering process is explained followed by a brief overview of the chosen algorithm setup.

Model parametrization

As explained in the design model description, the heating system's LCOH and relative emissions of heat are selected as design objectives. For this, a setup similar to the one presented in [8] is chosen. The setup consists of a TES, two PtH technologies, which are a heat pump and an electric heater, as well as two CHP technologies, which are an internal combustion engine and a combined extraction turbine. These installed capacities along with their depending technical characteristics are chosen as design variables and varied on the operational model. An overview of the selected design objectives and decision variables is provided within Table 6.1 along with their symbol, unit and respective range.

Table 6.1: Overview of design objectives and decision variables for the selected district heating system.

Model component	Symbol	Unit	Possible range
Objectives			
Levelized costs of heat	C^{lcoh}	EUR/MWh	$\mathbb{R}$
Relative emissions of heat	E^{reoh}	g/kWh	$\mathbb{R}$
Decision variables			
Electrical capacity of CET	$\overline{p}_{cet}^{wodh}$	MW	0.001..500
Electrical capacity of ICE	$\overline{p}_{ice}^{wodh}$	MW	0.001..500
Electrical capacity of HP	$\overline{p}_{hp}$	MW	0.001..500
Thermal capacity of EHB	$\overline{q}_{ehb}^{dh}$	MW	0.001..500
Thermal capacity of TES	$\overline{q}_{tes}^{heat}$	MWh	10..3000

There are various sources for costs of heating system components whereby single cost components depend on the system at hand. A literature review of costs for different production units is provided within [165]. Further, a cost function for a sensible TES is given in [22]. In the following, costs are modelled based on own assumptions from previous studies [8, 179] as shown in Table 6.2. When compared to [165], investment cost assumptions for CHP plants are considered rather high. Further, it becomes clear that the installation costs for a HP exceed the ones of an EHB by far at similar annual fixed costs. Investment costs for a sensible TES, here a conventional hot water tank, are more than one order of magnitude lower.

For the storage, it is assumed that the input and output capacities represent the maximum capacity of the heat exchangers and amount to one fifth of the overall energy content of the storage. This assumption of a fixed ratio between both metrics allows for a simpler dimensioning of the storage as the input and output capacity are directly related to the energy content given by the thermal capacity with respective investment costs. As opposed to the CAES case study, no scale effects regarding the investment costs are considered as these can be highly individual and do not add any value to present the applied method.

Table 6.2: Overview of economic model parameters for the selected district heating system.

Parameter	Unit	Value
Investment costs		
Electrical capacity of CET	EUR/MW	1,000,000
Electrical capacity of ICE	EUR/MW	1,000,000
Electrical capacity of HP	EUR/MW	140,460
Thermal capacity of EHB	EUR/MW	80,000
Thermal capacity of TES	EUR/MWh	18,750
Fixed operational costs		
Per unit electrical capacity of CET	EUR/MW	30,000
Per unit electrical capacity of ICE	EUR/MW	10,000
Per unit electrical capacity of HP	EUR/MW	1,013
Per unit thermal capacity of EHB	EUR/MW	1,100
Per unit thermal capacity of TES	EUR/MWh	87.5
Variable operational costs		
Per unit electrical output of CET	EUR/MWh	4.5
Per unit electrical output of ICE	EUR/MWh	10
Per unit electrical input of HP	EUR/MWh	0.67
Per unit thermal output of EHB	EUR/MWh	0.5

Technical parameters for the CET, ICE, HP, EHB and TES are changed in the design optimization within a pre-processing package which is described in the implementation in Section 4.4 and Table 4.1, respectively. Nonetheless, a set of exemplary CHP parameters is illustrated in Table 6.3 for the initial design of the CET and ICE. As described in the description of the operational model, these can be calculated based on the descriptions in [181] and are changed dynamically within the abovementioned package. Likewise, parameters for the initial EHB and HP designs are provided in Table 6.4 and changed dynamically. The initial design of the TES and related parameters and are given in Table 6.5 through the capacities, efficiencies and temporal losses.

Table 6.3: Overview of initial technical model parameters for CHP plants.

Parameter	Description	Unit	CET	ICE
$\overline{p}^{wodh}$	Max. el. power without DH	MW	127.56	88.37
$\underline{p}^{wodh}$	Min. el. power without DH	MW	56.12	44.19
$\overline{\eta}^{wodh}$	El. efficiency without DH	%	52	44
$\underline{\eta}^{wodh}$	El. efficiency without DH	%	44	40
α^1	Coefficient for efficiency	-	36.32	22.12
α^2	Coefficient for efficiency	-	1.65	2
β	Power loss index	-	0.13	0
q^{cond}	Minimal condenser load	MW	8.99	0
$\overline{l}^{fg,rel}$	Flue gas loss at max. heat	%	19	16
$\underline{l}^{fg,rel}$	Flue gas loss at min. heat	%	-	41

Table 6.4: Overview of initial technical model parameters for PTH plants.

Parameter	Description	Unit	EHB	HP
ϵ^m	Slope of COP	-	-	-145.92
ϵ^b	Y-intersect of COP	-	-	3-52
$\overline{p}$	Maximum power	MW	-	127.44
$\underline{p}$	Minimum power	MW	-	80.8
η^{th}	Thermal efficiency	%	99	-
$\overline{q}^{dh}$	Maximum heat	MW	114	-
$\underline{q}^{dh}$	Minimum heat	MW	5.7	-

Table 6.5: Overview of initial technical model parameters for the TES.

Parameter	Description	Unit	Value
$\overline{q}^{heat}$	Maximum amount of heat	MWh	1,520
$\overline{q}^{dh,in}$	Maximum heat input	MW	63.33
$\overline{q}^{dh,out}$	Maximum heat output	MW	63.33
$\eta^{dh,in}$	Efficiency of heat input	%	99
$\eta^{dh,out}$	Efficiency of heat output	%	99
η^{tmp}	Temporal effiency	%	100

Further, all parameters that are related to the analyzed future scenarios are defined. These encompass assumptions for the energy system in Germany and Europe and are published online in a freely available data package [177]. Besides assumptions for installed generation (cf. Figure 6.2) and grid capacity, assumptions for different fuel types, emissions and power plant efficiencies are included within the dataset. Further, the marginal hourly emissions in the power system are calculated based on own assumptions and contained in the model input data [146] (cf. Table 4.1 in Section 4.4). In order to reflect a possible political shift towards higher shares of power to heat, final consumer charges for PtH are assumed to be zero and no bonus payments for CHP are guaranteed. This implies that both technologies are not subsidized or discriminated as both measures are often debated in energy policy. Finally, the most relevant parameters in the power system are provided in Table 6.6.

Table 6.6: Overview of parameters in the considered power system scenarios.

Parameter	Unit	Value
Scenario 2030-A		
Average system emissions	g/kWh	370
Average and median of electricity price	EUR/MWh	60.6 / 64.42
Average and maximum heat load in DH system	MW	135.94 / 383
Certificate price for CO_2	EUR/t	29.4
Scenario 2030-C		
Average system emissions	g/kWh	300
Average and median of electricity price	EUR/MWh	84.72 / 66.84
Average and maximum heat load in DH system	MW	135.94 / 383
Certificate price for CO_2	EUR/t	29.4
Scenario 2030-C-climate		
Average system emissions	g/kWh	220
Average and median of electricity price	EUR/MWh	121.81 / 106.1
Average and maximum heat load in DH system	MW	135.94 / 383
Certificate price for CO_2	EUR/t	100
Others		
Gas price	EUR/MWh	26.4
Emission factor for gas	t/MWh	0.2012
Final consumer charges for power to heat	EUR/MWh	0
Lifetime	a	20
Discount rate	%	5

As the scenarios are chosen to model trends from a slow expansion of RE in scenario 2030-A towards a rather quick expansion at higher carbon prices in scenario 2030-climate, this trend is also reflected in the resulting time series for the electricity price and system emissions. Where the electricity price rises from approximately 60 EUR/MWh to 121 EUR/MWh from scenario A to C-climate on average, the median is slightly lower for scenario C and C-climate as also a couple of "extreme" marginal generation costs are obtained from the model. Nevertheless, these lie within the range of other studies (cf. [178] for more information). An opposite trend can be observed in the emissions which are decreasing with higher shares of RE in the system from 370 g/kWh to 220 g/kWh in the climate scenario. At this point, it should be noted that the carbon and gas prices in the scenarios are harmonized with the assumptions in the design and operational model. Finally, the underlying emission factors, system lifetime and discount rate for the investment are given in the last section of Table 6.6.

For the cases in which the system design is underdimensioned and not capable of serving the heat load at all times, the operational model is infeasible due to the violated heating balance in Equation 6.45. Thus, a "dummy" heat source at very high costs with regard to both objectives is added to the system in order to cover the residual heat load. Within the present case study, these costs are considered through a peak load boiler with high marginal generation costs and at the same time a low efficiency which induces a high gas consumption with respective emissions. This ensures that the operational model is feasible at all times whereas the "expensive" solutions are dominated during the optimization process.

Data clustering

As different components such as the CHP units and heat pump are based on a MILP formulation, the solution time for a single operational model is computationally expensive. Thus, similarly to the first case study, complexity in the operational model has to be reduced in order to decrease the overall runtime and allow for a higher number of evaluations in the design model. Following the approach described in Figure 4.4, within a first step, an operational model with a fixed dimensioning is optimized for an optimization period of one year. For this, the abovementioned setup which has also been used in another article [8] is analyzed regarding the cycles of the TES in scenario 2030-C. Figure 6.6 shows the performed cycle analyis which yields the respective depths of cycle (DoCs) and lengths of cycle (LoCs).

It becomes clear that most cycles have a duration of less than three days with only a minor share having a duration larger than one week. This indicates a similar pattern as in the first case study (cf. Figure 5.7). Likewise, a correlation between longer cycle durations and higher depths of cycle is indicated. Smaller intra-day and multi-day cycles seem to dominate in occurance due to the operation at the electricity market with its typical diurnal price pattern. This observation is supported by Figures 9.11 and 9.12 in the appendix which show the corresponding distributions. Further, this diurnal pattern could be confirmed in a respective autocorrelation analysis of the electricity price time series in Figure 9.13 in the appendix.
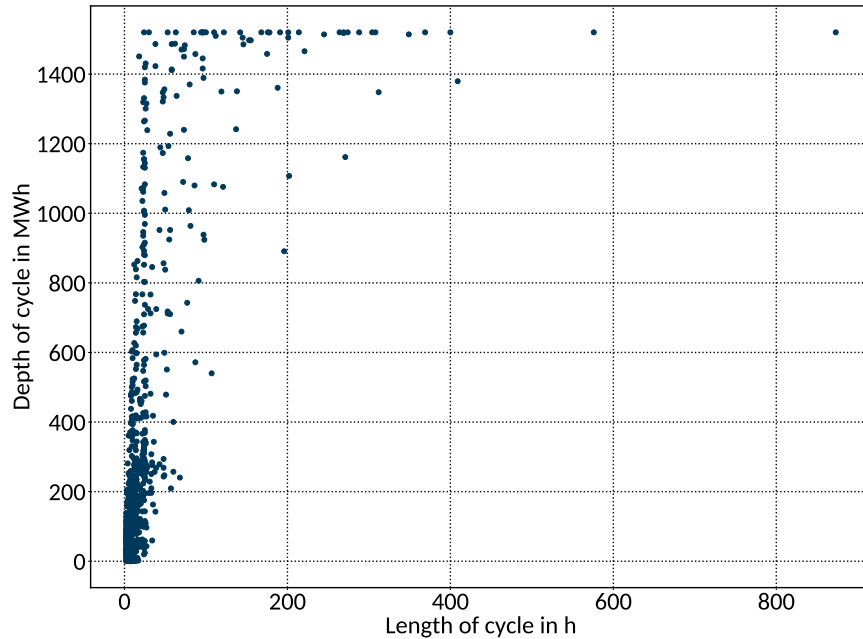
Figure 6.6: Depth and length of TES cycles for an optimization period of one year in scenario "2030-C". Figures 9.11 and 9.12 in the appendix show corresponding distributions for both quantities.

Consequently, a comparably low number of time steps per period which is set to 48 h is sufficient to model the system in its characteristics without neglecting the behaviour of the storage. For this, similarly to the second case study, the initial and final filling levels of the TES are set to be equal and in this case at a value of 50 % of the storage capacity.

The number of representative periods is determined by means of the MAE which is calculated for different cluster algorithms and a different number of periods. As in the first case study, duration curves are used due to their frequent usage and interpretability. Within Figure 6.7, the MAE between annual original and cluster heat load duration curves is shown for a different number of representative periods. Figures 9.14 in the appendix show corresponding measures for the electricity price in the energy system.

As within the first case study, the selected clustering algorithms perform differently whereby in this case the hierarchical algorithm delivers the best results when looking at the average error in terms of the heat load. Again, it can be seen that the accuracy already increases with a small number of periods while the value of adding more periods decreases after approximately eight to ten periods. As mentioned above, Figure 9.14 in the appendix show corresponding measures for the electricity price. Due to the strong diurnal pattern of the heat load, a good approximation of the temperature can be achieved with even less than ten periods whereby the deviations of the electricity price are comparably higher due to the higher fluctuations and high prices in the original data. Nonetheless, these only occur in a couple of hours per year which can be seen in Figure 9.9 in the appendix and can thus be neglected. In conclusion, an annual
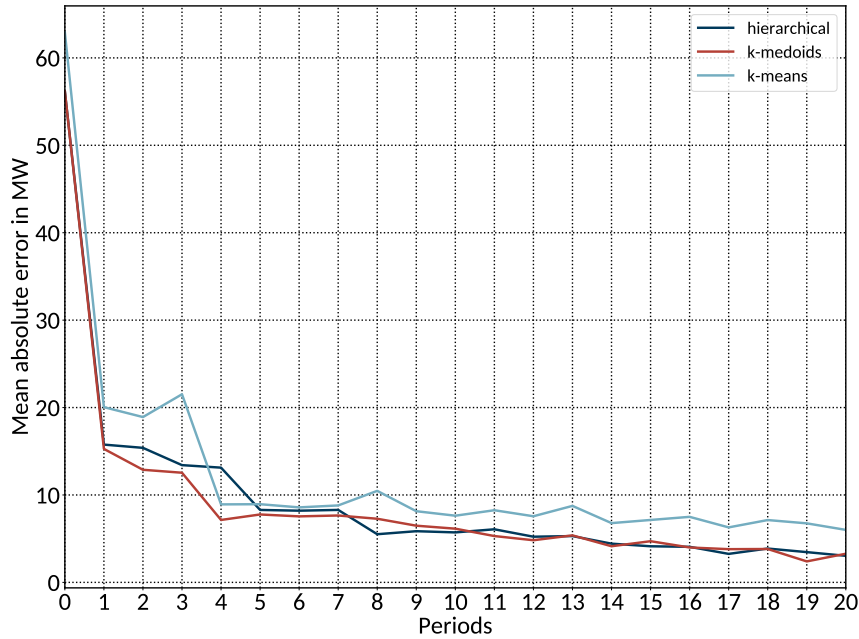
Figure 6.7: Mean absolute error between annual original and cluster heat load duration curves in scenario "2030-C" for a different number of representative periods of each 48 h.

time series can be expressed at a low MAE by only 7 periods of each 48 hours in order to express the real data. Finally, a summary of the statistical distributions for the selected representative periods is shown in a boxplot in Figure 6.8 for the clustered heat load. Figure 9.16 in the appendix shows the corresponding time series.

It can be seen that a diverse set of periods is derived to represent the heat load. For instance, periods 0, 1 and 4 seem to represent typical winter days with a high head load and a rather high variation whereas period 5 represents intermediate periods which could possibly occur during spring or autumn. Within, period 2, 3 and 6, typical summer periods with very low head loads are captured and the low variability in the data indicates that a major part of the heat load might be observed by the losses of the thermal grid. The representation of variability is supported by Figure 6.7 which indicates that already a small but diverse set of clusters would be sufficient to represent a large portion of the original data. Again, adding more periods only has a comparably minor influence with regard to the MAE.

In order to address the question which effect can be achieved through a representation of the original year in single cluster periods, the overall model runtime is analyzed for different representations of the original year. For this, different time slice lengths from one year represented in one entire period, two half-year periods, four quarter periods and twelve months are compared to a representation in cluster periods. In contrast to the period length of 48 h in 7 clusters chosen above, a period length of 72 h in 10 clusters is chosen for the following exemplary comparison. Hereby, a representation in clusters of 72 h can be
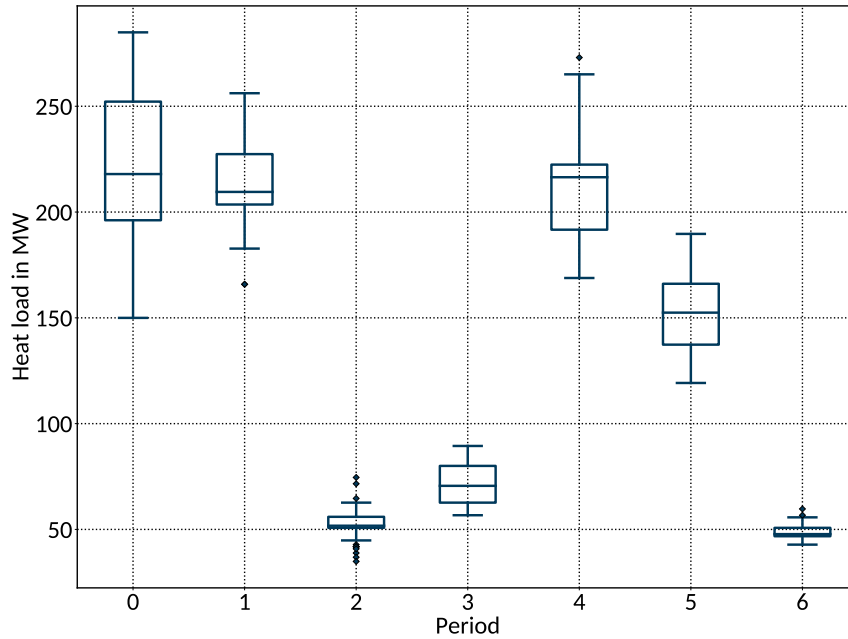
Figure 6.8: Boxplot of selected representative periods of each 48 h for the heat load in scenario "2030-C" using the hierarchical clustering algorithm.

compared to the one in 48 h hours as both capture diurnal patterns (cf. Figure 6.7 and Figure 9.15 in the appendix) whereas more and longer periods have the advantage of providing a broader range of data within the scope of a runtime comparison. Figure 6.9 shows the respective results on a logarithmic scale in order to highlight the differences. Using the gurobi solver in version 8.2 [189], the integer gap is set to 3 % for all problems for reasons of comparability.

It becomes clear that a significant runtime reduction can be achieved by means of a representation of an entire year in smaller time slices. Where a representation of one year within two half-years already reduces the runtime to about one third of the original problem, a reduction to about 14 % can be achieved by working with quarters. Further, when representing the year in single months, the runtime can be reduced to less than 5 % of the original problem. Finally, an even stronger improvement can be achieved when working with single cluster periods each having a respective weight. Using this approach allows a reduction to a total runtime of about 0.1 % of the original problem. This indicates the enormous contribution of data clustering algorithms to reduce complexity by reducing the overall problem size and thus resulting runtime.

An analysis of the resulting dispatch is shown in Figure 6.10 in annual shares of heat production for different technologies. It can be seen that the shares are similar for the different types of representation. Whereas almost no difference can be observed between annual, half-year, quarterly and monthly time slices, the results differ slightly compared to the clustering approach. Here, the shares of the CET and
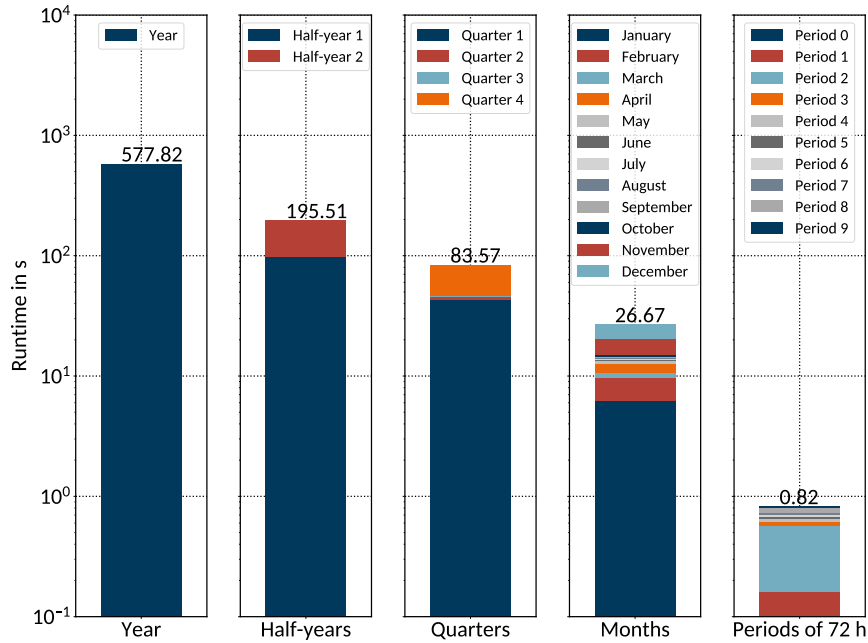
Figure 6.9: Total model runtime for a representation of one year in different time slice lengths.

EHB are almost equal whereas the ICE shows an increased production while at the same time the HP shares are reduced. This difference can be explained by deviations in single clusters which can possibly be weighted stronger than others. Further, the effect decreases when the weighting is distributed across an increasing number of clusters. Nonetheless, the difference is comparably small when compared to the overall runtime reduction and does not change the overall relations. For more information on the relation between the number of clusters and the resulting system design it is referred to [118] in this place.

In theory, this significant runtime reduction can be explained by the worst case runtime behaviour of the simplex algorithm which results from the number of iterations that are needed to solve a problem to optimality. For pure LPs, it is still assumed that the number of required iterations is an exponential function of the number of the problem matrice's rows m or columns n in the worst case [102, p.44]. Consequently, the reduction of the problem size directly affects the worst case behaviour of the algorithm that is used to solve the problem. As the simplex algorithm is also used to solve the relaxed problem repeatedly in the branch-and-bound algorithm that is used to solve MILP problems [101], both, the number of needed simplex iterations to solve a problem as well as the number explored nodes to satisfy the integer domains of the decision variables have an impact on the total solution time. In combination, this also explains the major runtime differences for representative periods of identical lengths. Finally, an empirical analysis of the discussed metrics for the different time slice representations is provided in Figure 6.11 using logarithmic scales.
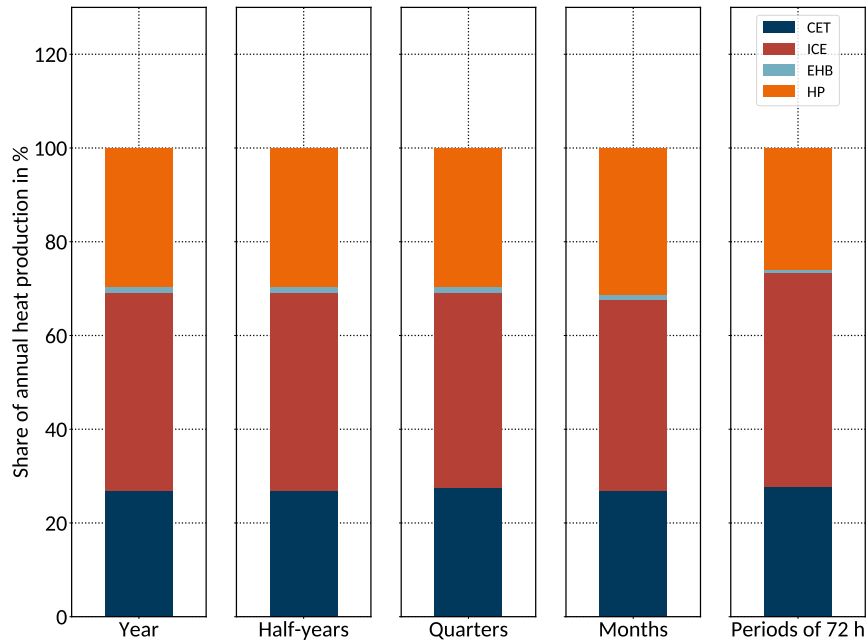
Figure 6.10: Annual heat production for a representation of one year in different time slice lengths.

It can be seen that the empirical analysis confirms the outlined theory as the number of simplex iterations raises overproportionally with the problem size. The required runtime strongly depends on the number of simplex iterations that are needed to solve the problem to optimality or to a specific gap. As explained above, for MILP problems, the total number of required simplex iterations is also influenced by the explored nodes in the branch-and-bound algorithm which is illustrated in Figure 9.20 in the appendix. Consequently, both metrics have to be taken into account for a detailed investigation of the required runtimes.

The empirical algorithm performance for this specific problem does not allow for a generalization as respective runtimes highly depend the individual problem structure given by the variable number and domains, constraints, and parameter range as well as the applied solution techniques of the specific solver. A detailed analysis for different solver types and problems is provided in [190, p.29. ff.] whereby in [102, p.47 f.] a more general approach is applied in combination with the simplex method and random problems. Nonetheless, a clear tendency can be stated as the empirical results of this case study show the same trend as described in theory and thus support the overall findings. In summary, it can be stated that data clustering algorithms provide a powerful instrument to reduce complexity and resulting runtimes. This allows for a quick and repeated solution of respective models in the evolutionary design optimization and thus is a significant improvement for the proposed combination of algorithms.
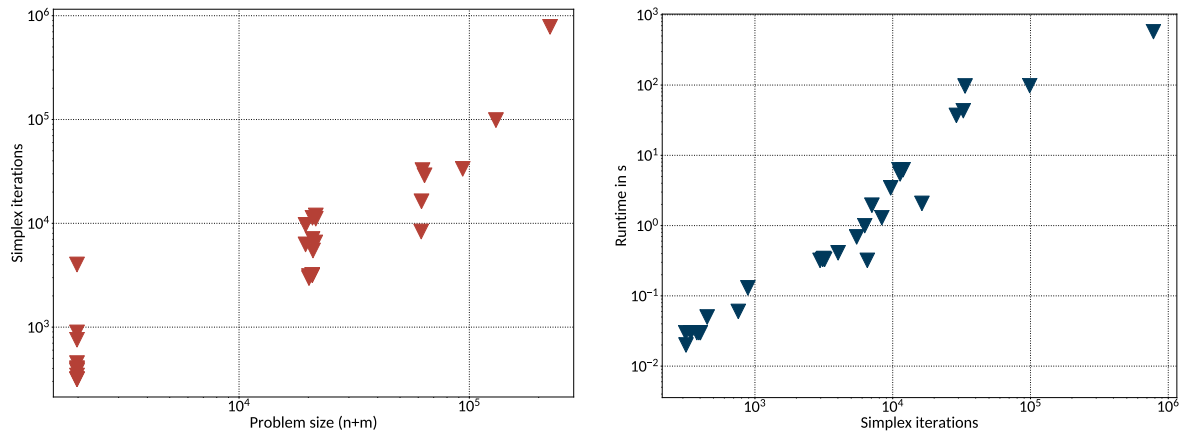
Figure 6.11: Relation between the number of total simplex iterations, problem size and solver runtime.

Algorithm setup

In contrast to the first case study, the prominent MOEA based on decomposition (MOEAD/D) [191, 192] is applied for the design optimization. Compared to traditional variants of evolutionary algorithms, this algorithm is especially suited for finding an even representation of an approximated Pareto front for multiple objectives beyond a number of 5-10 in total. The algorithm makes use of decomposition techniques and shares features with the weighted sum approach known from single-objective optimization. Some characteristics are similar to other approaches which are based on populations such as particle swarm optimization. The algorithm starts with an evenly distributed set of weight vectors in the objective space. Now for each of these vectors, a list of its T closest neighbours is created based on the Euclidean distances. Within the next step, a population of N individuals is created and evolved whereby each individual is associated with one of the defined weight vectors which are used to calculate single fitness values.

Compared to a parallel calculation within independent searches, the neighbourhood sets are used to structure the entire population. Selection and recombination is only happening in demes (isolated sub-populations), similar to cellular EAs [99, p.200]. Further, the location of the weight vectors and respective neighbouring sets are updated periodically. By doing this, within parallel searches, it is reflected what is discovered about the solution space [99, p.200]. Finally, in [193] and [194], it is demonstrated that MOEA/D outperforms NSGA-II on different test instances of the multi-objective travelling salesman problem at the same execution time. For the actual case study, the standard parameter set for a special variant of the algorithm called MOEA/D-DE is applied as described in [143]. This chosen algorithm variant makes use of the differential evolution (DE) operator. An overview of the applied parameters selection is provided in Table 6.7.

Table 6.7: Parameter selection for the multi-objective evolutionary algorithm MOEA/D-DE.

Parameter	Symbol	Unit	Value
Number of individuals in population	n_i	-	24
Number of islands	n_p	-	12
Number of generations	n_g	-	150
Method used to generate the weights	-	-	grid
Decomposition method	-	-	Tchebycheff
Number of weight vectors in neighborhood	T	-	20
Crossover parameter in the DE operator	CR	%	1
Mutant vector parameter for the DE operator	F	-	0.5
Distribution index for polynomial mutation	η_m	-	20
Chance that the neighbourhood is considered	δ	%	0.9
Maximum number of reinserted copies	n_r	-	2

Similarly to the first case study, an island model is used for a parallel optimization of different populations. As the number of decision variables amounts to five which is still low, a small population of only 24 individuals n_i is chosen. For the problem at hand, this number has delivered good results and allows a comparably little evaluations per generation which is of special interest with higher runtimes of single operational models resulting from expensive MILP problems. Moreover, a number of islands n_p of 12 is used to preserve a certain amount of diversity. The number of generations n_g is set to 150 in order to guarantee a sufficient exploitation of the search space. Moreover, the default values for the parameters T, CR, F, η_m, δ and n_r are chosen according to [143] and deliver good results when compared to other combinations of parameter settings. One shortfall of the MOEA/D-DE algorithm is that it takes more runtime than NSGA-II which was already noticed by [194] and could be confirmed in own experiments. Nonetheless, this higher runtime has been tested and lies within the range of approximately additional 20 % when compared to NSGA-II and is thus still acceptable.

As for the operational optimization, the default solver settings are changed to allow for a faster evaluation of single individuals. Since the CHP and heat pump implementations require the use of multiple binary variables, the mixed-integer gap is set to 3 % in this place to solve the operational model. Another improvement is the usage of more compact models which only contain parameters for average supply temperatures. As explained before, the usage of varying flow temperatures is proven to deliver only slightly different results [8] and thus assumed to have no significant influence on the design results.

6.4 Results and discussion

By applying the described model to the three future power market scenarios, results for perspective system designs are obtained. As described in the overview in Section 6.1, the selected scenarios represent different possible stages of future energy supply systems from conventional to increasingly renewable pathways. Different combinations of cost and revenue expressions can occur and directly influence the selected objectives. For instance, lower overall power prices in the first scenario along with a moderate price for CO_2 certificates in scenario A are likely to deliver different results than higher and more volatile power prices in scenario C-climate with simultaneously higher prices for CO_2 certificates. The obtained approximated Pareto-fronts are illustrated in Figure 6.12 for the three different scenarios. Again, it can be seen that the algorithm in the design optimization converges quickly towards the fronts in the single scenarios.
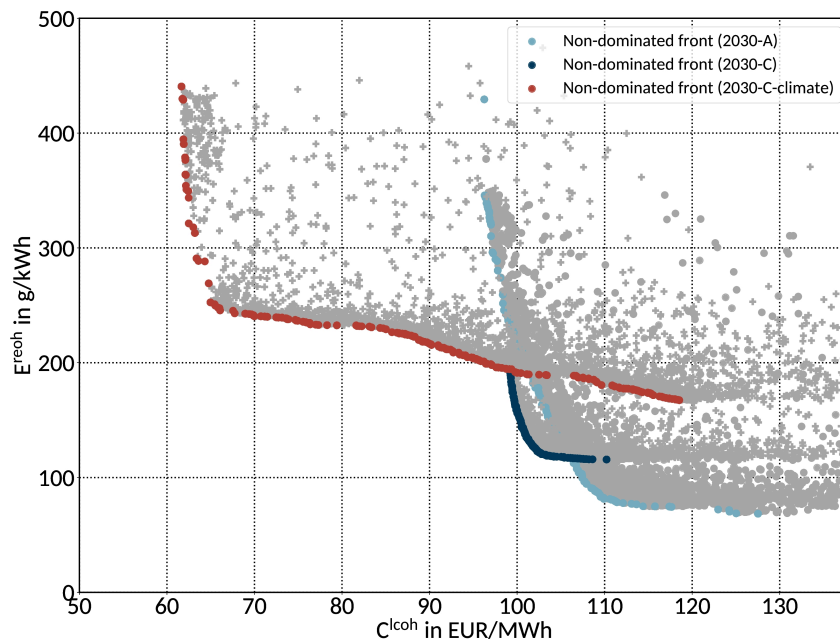
Figure 6.12: Pareto fronts for the analyzed future power system scenarios.

Overall, it becomes clear that different future pathways have a strong impact on the derived results. Different design cases lead to a very diverse set of solutions regarding both objectives as the fronts cover different areas of the objective space. Within scenario 2030-A, the levelized costs of heat are throughout above a value of 95 EUR/MWh while the relative emissions of heat are comparably low in certain areas of the front. In contrast, in the more renewable scenario 2030-C, the costs lie within a narrower range of approximately 100–110 EUR/MWh at emissions in the range of approximately 120-200 g/kWh. Finally, in scenario 2030-C-climate, lower LCOE from 60-120 EUR/MWh can be achieved in a large set of design cases but at a higher level of emissions in relation to the surrounding energy system. This diverse set of

solutions demonstrates that the actual pathway of the power system has a strong impact on the selected objectives and underlying system designs. Here, both the LCOH and and REOH lie in a valid range that is also found in other studies for levelized costs of heat [179] and power plant emissions [195, 196].

In the following, the single fronts are analyzed in detail by looking at the respective design variables for the different scenarios. As the capacity of the TES increases with lower emissions throughout all scenarios, only the develoment of the CHP and PtH capacities are illustrated depending on both objectives. This allows for a direct comparison of both technologies across the different scenarios which will be discussed in detail.

Scenario "2030-A"

Within Figure 6.13, the Pareto front and design parameters for scenario 2030-A are shown. It can be seen that the levelized costs of heat increase and emissions decrease with rising shares of CHP capacity while the shares of PtH capacity remain relatively constant for both objectives in the range from 95-108 EUR/MWh. Within the design case with lowest LCOH, no shares of CHP are included. Above this value, minor emission reductions can be achieved with increased shares of PtH. These are supported by higher shares of TES which show a strong correlation (cf. Figure 6.13 in the appendix). The overall level of achievable costs is throughout comparably high when compared to current and short-term production costs from another study on district heating systems [179]. This development can be explained by looking closer at the assumptions and model results of scenario 2030-A which are given by Figure 9.9 and 9.10 in the appendix and show the respective distributions for the electricity price and emissions. As the electricity prices are comparably low on average in relation to scenario 2030-C and 2030-C-climate, while the emissions are significantly higher due to the higher share of fossil power plants, this is directly reflected in the development of the CHP capacity.
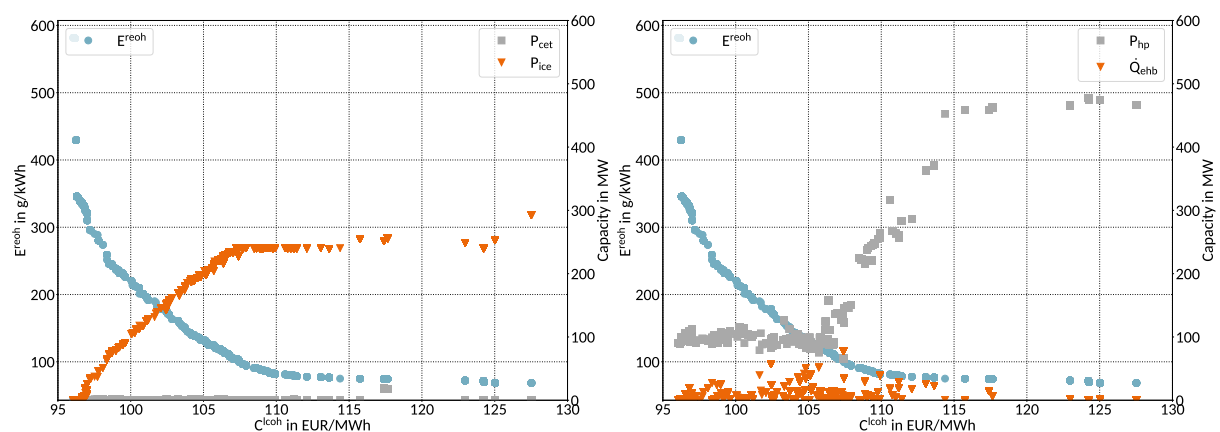
Figure 6.13: Pareto front and design parameters for scenario "2030-A".

Consequently, higher shares of CHP capacity reduce emissions in an energy system with on average high emissions. This results from the credit of electricity production according to Equation 6.32 and 6.38, respectively. Due to the on average lower emissions of the internal combustion engine which result from the respective pre-calculated characteristics (cf. Figure 6.5), the highest emission reduction can be achieved by means of higher ICE capacities. Even more emissions can be reduced by increasing the HP capacity in combination with higher shares of TES. In contrast to the increased shares of HP capacities, no EHB in seen in the system design which indicates a higher contribution of the HP in terms of both objectives. As the overall heat load can already be served by large compressor capacities for the heat pump with on average lower shares of direct electric heating, a significant over-dimensioning on the CHP site is needed in order to reduce the overall emissions. As the overall level of electricity market prices is low, these reductions come at the expense of higher levelized costs of heat as the utilized CHP units are not profitable under the given market conditions. Further, it can be seen that there is a clear technology priority towards the ICE when reducing the emissions by means of additional CHP capacity. As illustrated, within the chosen emission modeling approach, additional CHP capacity allows for a reduction of emissions when the surrounding energy system shows high average emissions. This reduction results from the credit of the electricity production in Equation 6.38. Thus, this assessment approach gives an advantage towards CHP regarding the emissions.

Scenario "2030-C"

As expected, this picture changes in scenario 2030-C which is shown in Figure 6.14 and characterized by higher shares of RE and consequently lower system emissions. Due to the on average higher electricity prices when compared to scenario 2030-A, the overall range of LCOH is comparably narrow and lies between approximately 98 EUR/MWh up to 110 EUR/MWh. This narrower range is also influenced by a reduced number of low electricity prices (cf. Figure 9.9 in the appendix) and demonstrates the strong impact of the revenues from CHP-based electricity production because the fuel costs are identical with scenario 2030-A. Within design case with lowest LCOH, already moderate shares of CHP are included. Similarly to scenario 2030-A, the CET is not seen in the system design whereas the ICE leads to lower overall emissions compared to scenario 2030-A. Again, the ICE is flexibilized by a comparably cheap TES and thus more attractive than the CET. Moreover, an emission reduction with higher shares of CHP indicates that the level of emissions in the surrounding energy system lies above the marginal emissions of the ICE and CET as the further is present in all design cases with lower levels of emissions.

The overall trend can be compared to scenario 2030-A as the shares of PtH capacity remain almost constant in the areas with low LCOE in which the CHP reduces the resulting emissions. Again, the HP is preferred over the EHB which can be explained by the cost assumptions which are shown in Table 6.2. Although the investment costs for a heat pump amount to almost two times of the investment costs for an
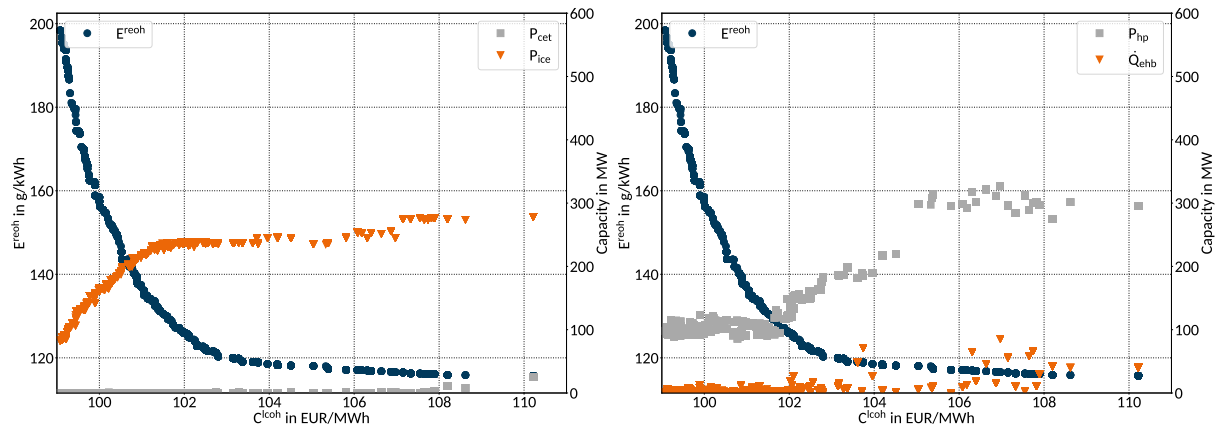
Figure 6.14: Pareto front and design parameters for scenario "2030-C".

electric boiler, the heat pump still has lower variable production costs. This is the case even if the share of other variable costs e.g. for maintenance are higher. This results from a comparably high coefficient of performance of approximately three units of heat for each unit of consumed electricity which creates an economic advantage for the heat pump. When no temperature restrictions are modelled the HP can be used to serve heat on high temperature levels which normally would be a technical advantage of an EHB (cf. [8] for a publication that deals with this topic). In summary, within scenario 2030-C as a rather green "business-as-usual" scenario, the ecologic advantage of CHP which results from a higher energy efficiency starts to vanish slightly. Furthermore, the shares of PtH from greener electricity remain almost constant with a rather slight impact on the emissions. As in scenario 2030-A, an increased utilization of thermal energy storage capacity can be observed towards lower emissions which can be seen in Figure 9.23 in the appendix. Finally, when looking at other approaches for an assesment of other emissions than the one that is chosen here (cf. Equations 6.32-6.38), this trend would be even stronger when only local emissions are accounted for as the shares of both, the CET and ICE would vanish with a lowering of emissions.

Scenario "2030-C-climate"

This trend of a reduced impact of CHP production on the emissions is also indicated in the results for scenario 2030-C-climate which are shown in Figure 6.15. Due to the lower overall system emissions and the significantly higher price for carbon of 100 EUR/t in this scenario, CHP is forced out of the system towards lower emissions. Further, it can be seen that the overall levelized costs of heat lie within a range of approximately 60- 120 EUR/MWh which indicates that comparably low LCOH can be achieved based on the electricity prices in the surrounding energy system. Larger shares of ICE with revenues from electricity production in overall high price regimes seem to compensate for the higher carbon price. Again, the CET is not seen in the system design as the ICE in combination with a TES provides the a higher

amount of flexibility while being more efficient. The designs with large shares of CHP consequently lead to high relative emissions of heat as the capability to produce heat exceeds the heat load in the DH system (cf. Table 6.6 and Equation 6.10). This means that the ICE operates in the electricity market whereby the maximum level of heat production is not required in the DH system and the remaining minimum heat production is buffered in the TES. As the shadow prices from the power system model are intepreted as electricity prices, these tend to overestimate in some areas. Thus, the chosen approach only allows to describe the general trend of the system. Further, these vanishing shares of CHP are directly related to the design objectives which increase and decrease, respectively.
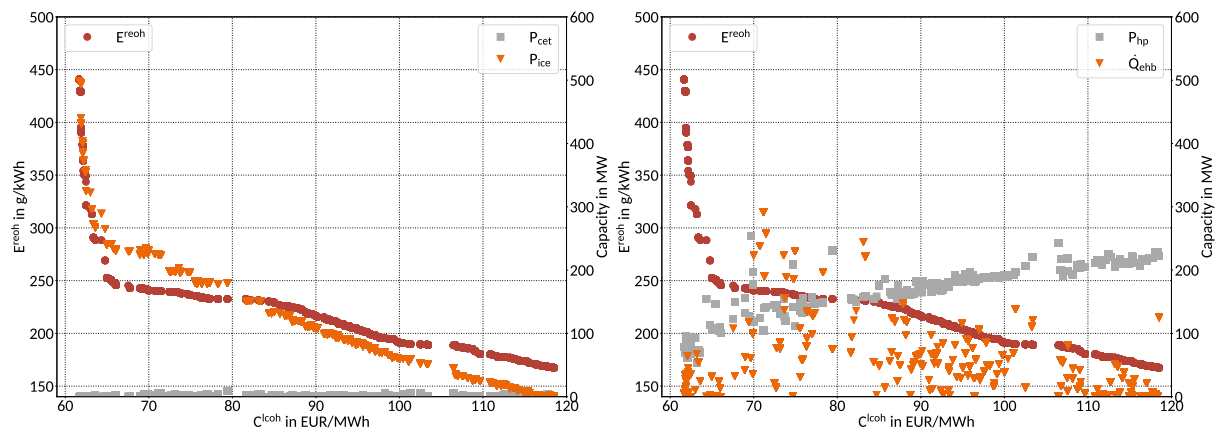
Figure 6.15: Pareto front and design parameters for scenario "2030-C-climate".

A clear trend towards more PtH which is represented by higher shares of HP can be observed with lower emissions, although there are certain areas in which shares of EHB are added and both seem to complement each other. This, again can be explained by the ratio of the investment and variable costs for both components. Whereas the HP has higher investment costs at comparably low variable cost, the opposite is the case for the electric heating boiler. Moreover, when compared directly, if the hours that are needed for an amortization of both assets are close by each other, they are indifferent to a certain degree regarding the economic dimension. This might be the case in situations when at the same time the ecological advantage is on a similar level due to a lower share of total utilization hours. Nonetheless, towards the lowest emissions, the HP dominates the EHB in most cases. This is also realized in the design case with lowest emissions which are realized by a HP in combination with a TES.

System operation

Within the modeling process, the operational model is validated extensively in its functionality for different design cases. Respective tests include the validation of load ranges for the different components as well as the utilization of the thermal storage in combination with the operation of different production units. Further, other constraints such as the equality of the first and last storage filling level are evaluated.

An exemplary test that demonstrates the behaviour of CHP and PtH units in combination with a TES is analyzed and illustrated in Figure 6.16 with a focus on the operation at the electricity market. For this, an exemplary design case with only an internal combustion engine, a heat pump and a thermal storage is chosen.
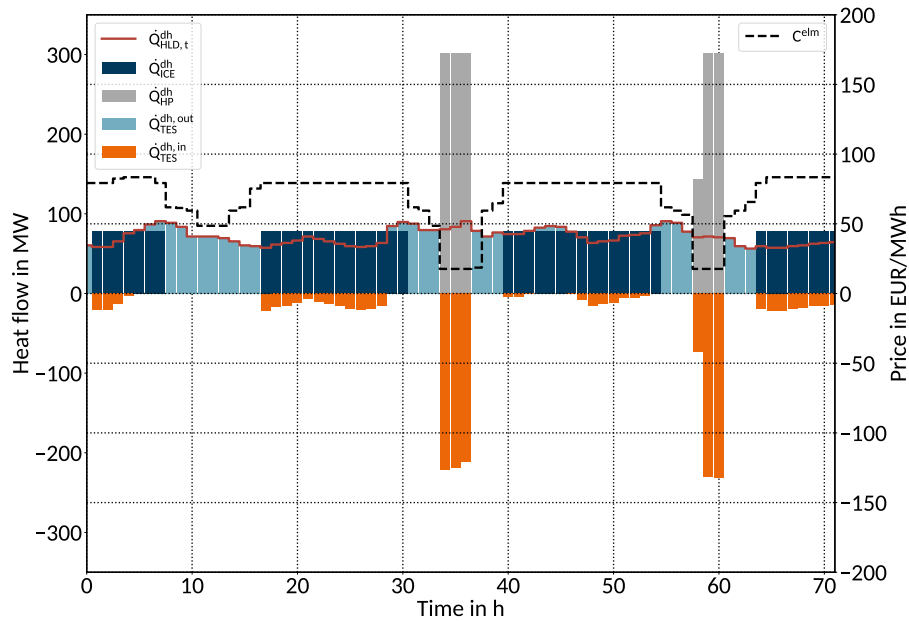
Figure 6.16: Unit commitment for a design case with an internal combustion engine, a heat pump and a thermal energy storage within a single cluster.

It becomes clear that the heating system orients its operation to the surrounding market environment. Regimes with higher prices are served by the ICE which is able to change its level of heat extraction during the operation from areas with full to minimum heat extraction (cf. Figure 6.5 for both operational characteristics). Further, regimes with low prices are served by the HP which is supported by the TES. The dispatch priority is again determined by the variable costs of both technologies in different operational areas which in turn influence the points in time when the units are producing. Consequently, this also has a direct impact on the resulting emissions as these increase with higher electricity prices (cf. Figure 9.25 in the appendix) through the mono-objective and cost-driven operational model. As indicated, the economical operation of both CHP and PtH units is supported by the TES which provides flexibility to the system. This allows to bridge over regimes with low electricity prices where the ICE is turned off and the HP is activated to serve the heat load and produce additional energy for the TES. Finally, due to the comparably low investment costs of the TES, its flexibility is utilized throughout all scenarios as it leverages the LCOE of the overall heating system. This can be seen from Figures 9.22-9.24 in the appendix which show respective minimum levels of TES in all scenarios.

The obtained system designs strongly depend on the chosen modeling approach and parametrization. For example, different operational regions of CHP plants for different design cases might influence which technology is seen in the results. As only one example, the PQ-diagrams for different sizes of CETs and ICEs are illustrated in Figure 6.17. It can be seen that within this case study, the ICE is capable of producing more heat and power based on the same installed electrical capacity. This advantage comes at the expense of less flexibility as an ICE is limited by a minimum heat production. Nonetheless, an additional TES with low investment costs is able to buffer this heat production in most cases and thus provides flexibility to the system. This is only one example for the complex interaction between single components within the modelled system.
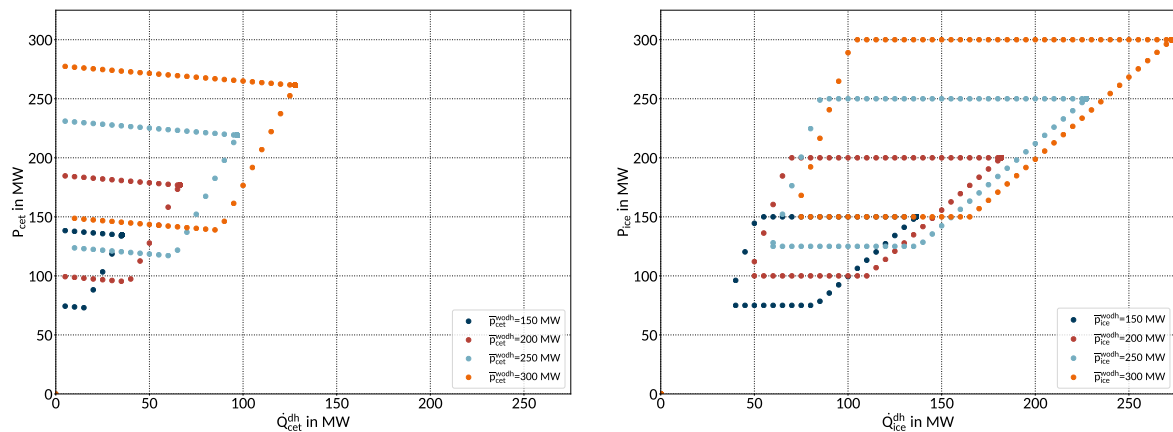
Figure 6.17: Comparison of PQ-diagrams for different design cases of CET and ICE.

As explained above, different design cases have a direct impact on the actual system operation and consequently lead to a diverse set of objective values. Operational characteristics are adapted for all design cases based on detailed thermodynamic modeling. Such complex models like the modeling of different CHP plants in PQ-diagrams have a strong impact on the overall model performance in terms of computational runtime. Thus, a trade-off between accuracy and runtime is considered in order to determine the overall trends while preserving an acceptable runtime. Besides another application of data clustering for the operational model, this is realized by working with less generations in the evolutionary algorithm. For the different scenarios at hand, runtimes from approximately 72 hours for scenario 2030-A up to almost 96 hours for scenario 2030-C-climate were achieved and found to deliver sufficient results for the chosen parameter set.

6.5 Case study conclusions

It is shown that the method can be applied to optimize design parameters on a future district heating system with regard to objectives that are relevant for both the operator and the environment. In the design optimization, another evolutionary algorithm, MOEA/D-DE is applied and has proven to deliver good results by indicating the general design trends regarding the chosen objectives. Again, the optimization is based on a detailed validated techno-economical operational model that is realized as a MILP with dynamically changed operational characteristics for arbitrary design cases. Further, the model includes different technologies including CHP, PtH and TES that are optimized in combination while regarding their interdependencies. Good assumptions for the surrounding DH system are capable of describing the general behaviour appropriately in terms of the operational characteristics [8]. The flexibility of the proposed hybrid method offers the possibility to pre-calculate characteristics for specific design cases and thus provides an advantage over other methods that operate on constant assumptions [197, 64, 65]. This fitting of operational characteristics for every design case allows for a higher level of detail and thus a better representation of single technologies in the model. For the case study at hand, the chosen algorithm setup delivers robust results when a trade-off between runtime and accuracy is found. Nonetheless, the runtimes are significantly higher than in the first case study because of the required integer variables in the operational model. This indicates that special emphasis should be put on the operational model which should have as much explanatory power as possible and be as detailed as required.

An analysis of the different Pareto-fronts demonstrates that possible future pathways of the energy supply system have a strong influence on the optimal heating system layout. Further, as mentioned earlier, a diverse set of design cases is obtained and opposed design trends can be identified between the different scenarios. In particular, it is demonstrated that the question whether the system is mainly driven by CHP or PtH units is influenced by the surrounding energy system. The case study demonstrates that the question, whether PtH is a viable alternative to CHP from an economical and ecological point of view, heavily depends on the surrounding energy system represented by the electricity price levels and carbon intensity. This is in line with other previous studies in this field [180]. In this respect, it is important to note that the evaluation approach of the emissions also has a strong influence on the investigated designs and should be selected carefully. Nonetheless, the method allows for a more detailed investigation of the interdependencies of objectives and design cases which in turn enables a better understanding of the problem. This is of special interest for decision makers who have to evaluate different system variants while dealing with requirements from different other stakeholders. Again, these solution sets obtained from a multi-objective optimization are superior compared to mono-objective variants from literature when specific investment decisions are evaluated. This can be relevant in the process of reshaping DH systems towards more efficient systems with higher shares of RE as described in [176].

From a practical perspective, it can be seen that there is no single heating system setup that performs well concerning both objectives under all scenarios. On the contrary, it could be demonstrated that there are certain tipping points that improve the postition of certain setups. When looking at the future scenarios, these could be interpreted as different points on a timeline. Scenario 2030-A could represent a situation in the nearer future, whereas scenario 2030-C-climate could be imagined as a situation in the longer future with significant penalties on carbon emissions. Following this idea, this circumstance should be taken into account when considering an investment into a specific heating system. For instance, if the policy perspective is a significantly higher price on carbon in the near future, the actual design should be adapted to this fact by rather following the results of scenario 2030-C-climate, even if the current framework conditions are closer by scenario 2030-A. In conclusion, the method helps to understand the role of CHP as a bridge technology in Germany [198, p.5] from an investor's perspective and thus delivers a valuable contribution to the public debate.

7 Case study - Multi-regional power system

This chapter describes the method application on the multi-regional power system of Kazakhstan. For this, an overview of the national energy system is provided followed by a detailed generic model description. Finally, a specific setup is chosen and optimized under three different future cost scenarios before the results are interpreted.

7.1 Case study overview

Kazakhstan is the largest of the former Soviet Union republics after Russia with more than 18 million inhabitants in 2018. The electricity sector in Kazakhstan can be divided into a northern, southern and western zone which stems from the energy zone division during Soviet Union era. Historically, the northern zone was integrated into the Siberian power zone, while the southern zone was part of the Central Asian power zone with Turkmenistan, Kyrgyzstan, Uzbekistan and Tajikistan. In 2016, the majority of electricity in Kazakhstan was generated by coal fired plants, covering 85.6% of total electricity generation, while hydropower generation covered 9% and gas generation 5.2% [199]. Only the remaining 0.2% were covered by RE [200]. Existing CHP units are operated mainly to serve the heat load and power is a byproduct because of the fixed coupling of heat and power generation. An overview of installed generation capacity in the year 2015 in 14 administrative regions is provided in Figure 7.1 based on the work of [88] and shows the distribution of gas and coal generation from the western to the eastern zones. A detailed map of the electricity network is provided in Figure 7.5 in the model parametrization and all related data is published in a respective study [98].

Kazakhstan holds large reserves of fossil energy sources where oil extraction is the main industry with exports forming the major part of the gross domestic product. The oil industry has taken a rapid development and expansion over the last two decades, which has resulted in a significant increase of electricity generation. Furthermore, gas based electricity generation forms a major part in the western zone with significant shares of gas turbines and gas based CHP plants. According to [201], Kazakhstan has around four trillion cubic meters of gas reserves. Nevertheless, gas consumption accounts only for 17.5% of the country's primary energy balance. Most reserves are located in the western part of Kazakhstan and a gas pipeline network connects the West with the South. However, no direct connection to the region of
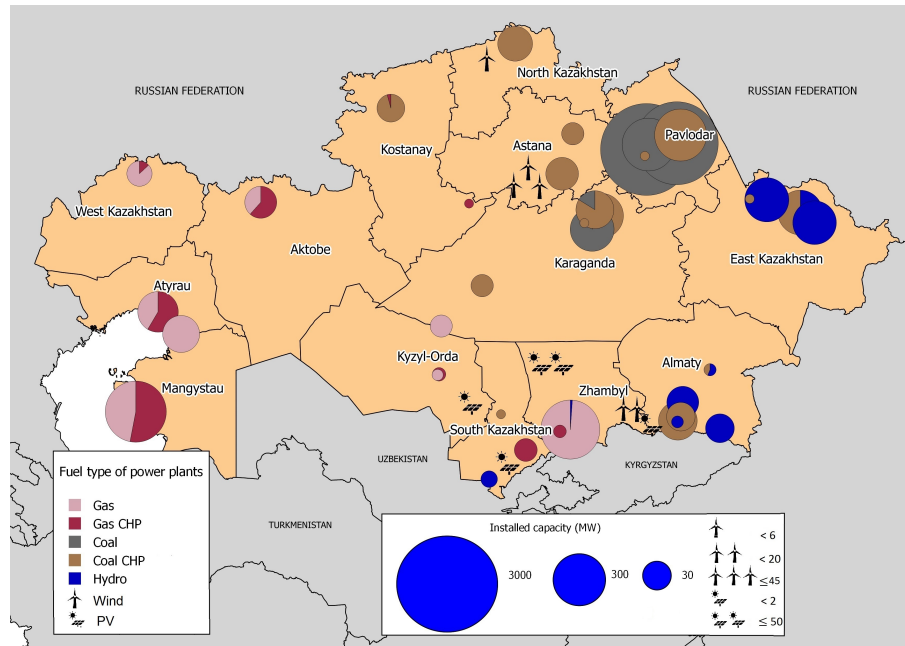
Figure 7.1: Energy system of Kazakhstan resolved in administrative regions [88].

Kostanay nor the North of Kazakhstan is established [89, p.8]. Consequently, prices for natural gas vary significantly within the country with comparably lower prices in the west [202].

The energy supply strategy of the government from the year 2013 aims to reduce greenhouse gas emissions, minimize energy costs and increase energy savings. A feed-in tariff scheme with separate standard rates for different technologies like wind, photovoltaic (PV), small hydropower and biogas plants was introduced in 2014. One of the main targets of the concept for the transition towards a green economy aims to reach 3% generation from RES until 2020. By 2030, it is expected that 4.6 GW of wind and 0.5 GW of solar capacities will be installed [203]. As pointed out in [204], [205], [206] and [207] the country has a significant potential for RE like wind, solar, hydro and biomass. Further, high shares of gas turbines in the power system allow for quick starts and high ramping rates in order to integrate higher shares of RE. Therefore, especially the western and central part of Kazakhstan present a good potential for an increased share of RES. This is particularly the case for wind power within coastal areas at the Caspian Sea. Nonetheless, the mandatory operation of the CHP plants imposes a restriction on the maximum possible level of RES penetration if no other measures like local TES and PtH options are taken to decouple the power from the heat generation.

The outlined characteristics point out the potential for an increased share of RES in the power system which could be investigated by means of respective models that capture their volatile characteristics. System designs with higher shares of RES could help to bridge the gap between demand and supply (cf. [89]), reduce the overall emissions and use the economical and ecological benefit of RE. As described

above, the power system is subject to different objectives like economical and environmental targets. For instance, a certain reduction of greenhouse gas emissions could be required from an international policy perspective where the local focus is put on the average electricity price. Further, when transforming the system towards higher shares of RE, questions like the optimal installed capacity in specific regions could arise. Consequently, in the following, the impact of higher shares of wind and solar energy in the power system of Kazakhstan is investigated with regard to the resulting average system emissions and levelized costs of electricity. For this, three different investment costs scenarios for wind and solar are considered based on price forecasts from literature. These costs are shown in Figure 7.2 where the installed wind and solar capacity in each region is a decision variable in the design optimization.
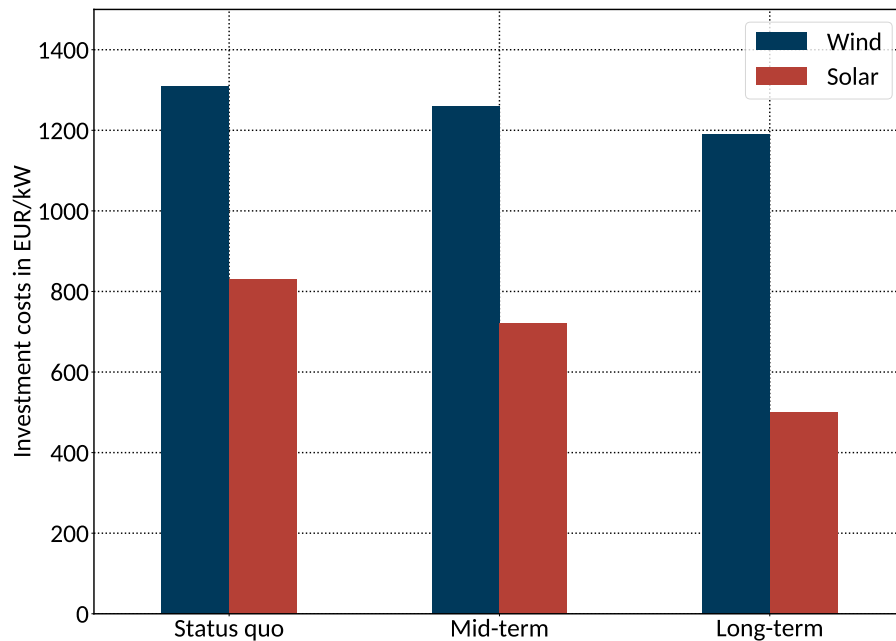
Figure 7.2: Investment costs for wind and solar within three different future scenarios based on [208].

It becomes clear that significant cost reductions are assumed for solar due to further technical development and scale effects. Likewise, moderate cost reductions for wind energy are assumed to be achieved even if the technology is already relatively mature. Further, different emission price levels starting from 25 EUR/t in the "Status quo" scenario, over 50 EUR/t in the "Mid-term" scenario up to 75 EUR/t in the "Long-term" scenario are assumed to model the increasing pressure to reduce greenhouse gas emissions. However, fuel prices are assumed to be constant due to the currently large availability and low prices for gas and coal in Kazakhstan. This assumption can be interpreted as rather conservative with regard to possibly increasing world market prices for fossil fuels. As the real price development cannot be projected correctly, the chosen scenarios represent a possible range of future developments and allow to assess their impact on the selected power system objectives. All additional assumptions will be discussed in the model outline and parametrization and are summarized in Tables 7.2 and 7.2.

7.2 Model creation and outline

At first, all needed sets and indices are defined in Expressions 7.1-7.6. As within the other case studies, this formulation holds for any number of technologies and an arbitrary number of time steps. Likewise, subsets and empty sets for the case of a non-existent unit are also covered with this approach. For the following model description, the same sign conventions as within the first and second case study are used (cf. Section 5.2).

$$t \in T \quad \text{Index and set of all time steps} \tag{7.1}$$
$$f \in F \quad \text{Index and set of all fossil power plants} \tag{7.2}$$
$$r \in R \quad \text{Index and set of all renewable power plants} \tag{7.3}$$
$$n \in N \quad \text{Index and set of nodes} \tag{7.4}$$
$$(n1, n2) \in L \quad \text{Index and set of transmission lines between nodes whereas} \tag{7.5}$$
$$L = \{(n_1, n_2) \,|\, (n_1, n_2) \in \{N \times N\} \wedge n_1 \neq n_2\} \tag{7.6}$$

Design model

The question of costs for an energy system transformation towards higher shares of RE has been analyzed in numerous studies. In this context, it is often asked at which point wind and solar are competitive without additional subsidies and how to dimension their shares in terms of economical or ecological objectives. For these types of questions, academic papers often use the metric of levelized costs of electricity (LCOE with symbol *lcoe*) in order to estimate the costs of generating technologies in different energy systems [209, 210, 211, 162]. LCOE represent the full life-cycle costs based on the fixed and variable costs of a single power generation technology or a combination of technologies per unit of electricity.

Two objective functions are chosen for the design optimization. The first objective minimizes the LCOE of the power system when higher shares of RE are integrated into the system. For the second objective, an environmental metric is chosen by minimizing the relative emissions of electricity (REOE with symbol *reoe*) in the system. As a result, the multi-objective design optimization can be described via Expression 7.7 as an unconstrained and linear multi-objective optimization problem.

$$min \left[C^{lcoe}, E^{reoe} \right] \tag{7.7}$$

The general formulation of the LCOE calculation in the first fitness function is shown in Equation 7.8 and outlined in the following. LCOE are defined as the ratio of the system costs C^{sys} for capacity investment

and operation and the aggregated discounted load (DCL with symbol dlc) W^{dcl}. The further is specified by means of Equation 7.9 and the latter via Equations 7.19 and 7.20.

$$C^{lcoe} = \frac{C^{sys}}{W^{dcl}} \tag{7.8}$$

As there are different definitions for the LCOE calculation (cf. [211, p.29]), it has to be noted that the one used here is similar to the one in [212] and differs compared to other methods e. g. as proposed in [213] and [214]. Further, no integration costs for RE as suggested in [215] are included as only general trends are shown and their effect can be treated qualitatively. Additional revenues for the heat production from CHP are omitted in order to reduce the number of assumptions. Finally, the system costs C^{sys} are modelled according to Equation 7.9 using different cost expressions for the investment and operation of the system over the expected lifetime.

$$C^{sys} = C^{cpx,total} + \sum_a \left(\frac{C^{opx,fix,total} + C^{opx,var,total}}{(1+i)^a} \right) \tag{7.9}$$

Similarly to the other case studies, investment costs for RE are modelled in the CAPEX occuring in the initial period which are outlined in Equation 7.10 and 7.11. These encompass possible cost expressions for all renewable generation technologies in all regions. As an example, installation costs for wind C^{inv}_{wind} are used for the installed wind capacity $\overline{p}^{res}_{n,wind}$ in a specific region.

$$C^{cpx,total} = C^{cpx,inv,res} \tag{7.10}$$

$$C^{cpx,inv,res} = \sum_n \sum_r \overline{p}^{res}_{n,r} c^{inv}_r \tag{7.11}$$

In contrast to conventional generation technologies with different ratios of investment to variable costs, wind, solar and hydro are characterized by comparably high fixed costs and almost non-existent variable costs. Thus, in the model, it is assumed that RE only have fixed annual costs and no additional variable costs. These fixed cost expressions are descibed via Equation 7.12 and 7.13.

$$C^{opx,fix,total} = C^{opx,fix,res} \tag{7.12}$$

$$C^{opx,fix,res} = \sum_n \sum_r \overline{p}^{res}_{n,r} c^{fix}_r \tag{7.13}$$

Occuring variable costs for the operation of fossil power plants in the system are modelled in Equations 7.14 to 7.18. In Equation 7.14, these are summed for all periods p with their respective weight or number

of occurances ω_p. Costs for fuel and emissions are considered by means of a fuel specific emission factor e_f^{fuel} for the summed fossil fuel consumption of all periods in Equation 7.15. In Equation 7.16, the fuel consumption of all plants is calculated for both CHP and regular power plants based on the actual electricity production per fuel and type and the underlying assumption that both plant types have different efficiencies. As the installed fossil generation capacity is constant in the different scenarios, it is assumed that no fixed costs occur as these have no impact on the obtained dispatch. Thus, if needed, respective costs for maintenance and other positions can be added to the variable fuel costs instead. Respective electricity productions are given by Equation 7.17 and 7.18.

$$C^{opx,var,total} = \sum_p \omega_p (C^{opx,var,fossil}) \tag{7.14}$$

$$C^{opx,var,fossil} = \sum_f Q_{p,f}(c_f^{fuel} + c_f^{var} + e_f^{fuel} c^{emi}) \tag{7.15}$$

$$Q_{p,f} = \sum_n (\frac{W_{p,n,f}^{chp}}{\eta_f^{chp}} + \frac{W_{p,n,f}^{pp}}{\eta_f^{pp}}) \tag{7.16}$$

$$W_{p,n,f}^{chp} = \sum_t (P_{p,n,f,t}^{chp,fix} + P_{p,n,f,t}^{chp,var})\tau \tag{7.17}$$

$$W_{p,n,f}^{pp} = \sum_t P_{p,n,f,t}^{pp}\tau \tag{7.18}$$

As explained above, in order to calculate the LCOE, the NPV is divided by the discounted overall electricity consumption W^{dcl} in the power system which is defined in Equation 7.19 based on the electricity load W^{load}. The actual discouting is required for an integration of the load in connection with the costs in Equation 7.8.

$$W^{dcl} = \sum_a (\frac{W^{load}}{(1+i)^a}) \tag{7.19}$$

$$W^{load} = \sum_p \omega_p (\sum_n \sum_t P_{p,n,t}^{load}\tau) \tag{7.20}$$

Within the second objective, the REOE are optimized as defined in Equation 7.21 by dividing the system's total emissions E^{total} by the overall electricity load W^{load} as defined in Equation 7.20.

$$E^{reoh} = \frac{E^{total}}{W^{load}} \tag{7.21}$$

The system's total emissions E^{total} are outlined in Equation 7.22 and 7.23. Again, these are calculated based on the fuel specific consumption $Q_{p,f}$ and specific emissions e_c^{fuel}.

$$E^{total} = \sum_p \omega_p (E^{fuel}) \tag{7.22}$$

$$E^{fuel} = \sum_f Q_{p,f} e_f^{fuel} \tag{7.23}$$

As becomes clear from the equations, only directly related operational emissions are tracked. This means that no upstream emissions for the installation of RE or other sources are considered as this would go beyond the scope of this thesis. For further reading about lifecycle assessment of emissions for different electricity generation technologies, it is referred to [195] in this place.

Operational model

Within the operational model, the overall operational costs of the power system are minimized under technical generation constraints and transmission restrictions between different regions. Input data consists of the regional electrical loads and technical as well as economical properties of fossil or renewable power plants. The model integrates economical data such as prices for fuel and CO_2 emissions as well as resulting marginal generation costs. Furthermore, regulatory framework mechanisms can be integrated on the input or output side of each unit if needed. After the optimization, output data is delivered in hourly time series which capture the power production and transmission in the network. Other metrics such as the system's emissions can be calculated in an optional postprocessing step. Figure 7.3 gives an overview of the basic structure and crucial input and output data.

For the operational optimization, a rather simple but still representative model of the power system is chosen. In contrast to the first two case studies, the optimization task is solved via LP whereby again an hourly time resolution is used. This allows for reduced runtimes for the multi-regional model when a higher number of decision variables is used in the design optimization. Again, the model is implemented in the Open Energy Modeling Framework [142, 9]. As opposed to [88], no DC load flow is used as a simplification and linearization of the real AC power flow. Instead, a simple transshipment model allows for reduced runtimes and a utilization in the surrounding design optimization.

All relations are represented in an abstract mathematical model of the system which is shown in Figure 7.4 for three exemplary regions. Single regions are represented by nodes which in turn represent electricity balances. Practically, this means that the electricity load in single nodes has to be covered at all points in time by means of all connected power plants and transmission lines. Fossil fueled power plants consist of conventional power plants which produce electricity only (marked by the symbol *conv*), CHP plants which have to serve a heat load throughout the year (marked by the symbol *fix*) and CHP plants which can be operated flexibly (marked by the symbol *var*). Feed-in from RE like hydro, wind and solar is
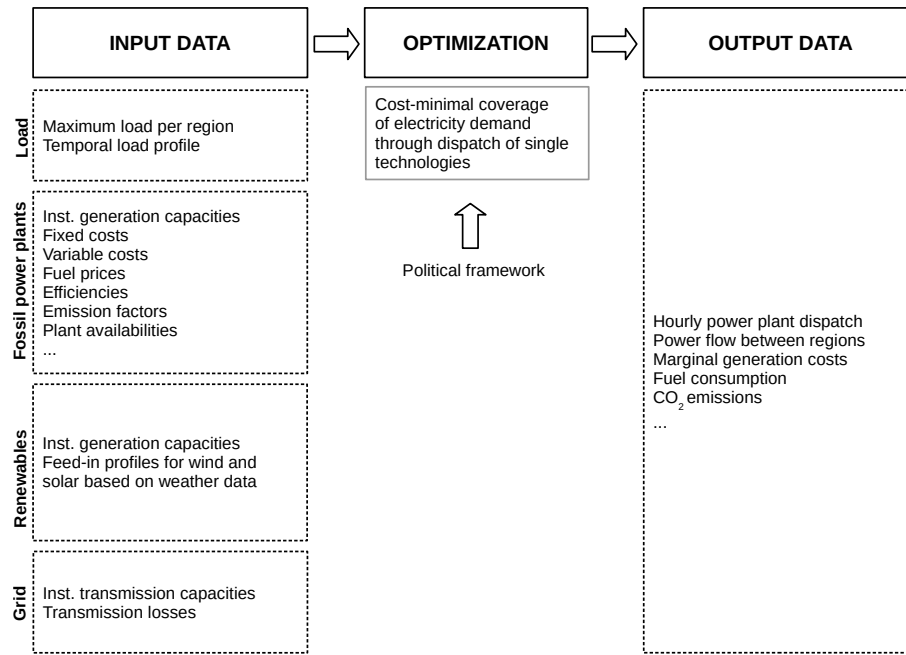
Figure 7.3: Structure of the operational model for the multi-regional power system case study.

modelled based on time-varying profiles. Finally, transmission capacities between regions are modelled by single variables in each direction with respective maximum capacities.

The objective function is described in Expression 7.24. It consists of single expressions for fuel and emission costs for the different types of power plants and reduces the overall costs to operate the electricity system. Mathematically, this is realized by a minimization of the sum of variable costs for all generation technologies over all nodes and time steps. Fuel consumption is calculated based on the assumption of an average efficiency per plant type (CHP or conventional) and fuel type as fuel costs are given per unit of fuel. Further, costs for emissions are calculated by means of a fuel-specific emission factor e_f^{fuel} and emission price c^{emi}. This explicit calculation of the marginal generation costs of each plant in the objective increases the overall model size. Consequently, in a reduced model formulation, these costs are pre–calculated and related to each plant in order to reduce the size and resulting runtime. Nonetheless, a more detailed model formulation is proposed here for the sake of clarity. Fixed costs for renewable power plants are not included in the operational model as these have no impact on the overall dispatch. However, these are added only in Equation 7.12 and 7.13 of the design model.

$$min\left[\sum_n\sum_f\sum_t(\frac{P_{n,f,t}^{chp,fix}+P_{n,f,t}^{chp,var}}{\eta_f^{chp}}+\frac{P_{n,f,t}^{conv}}{\eta_f^{pp}})\tau(c_f^{fuel}+e_f^{fuel}c^{emi})\right] \tag{7.24}$$

As mentioned above, the load coverage is a central constraint that has to be satisfied in any node at any point in time. This relation is expressed by a power balance in Equation 7.25 which assures that the
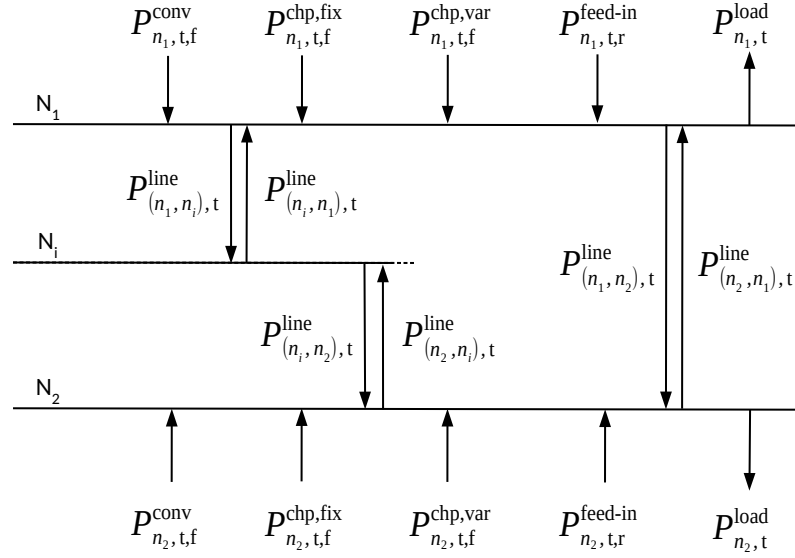
Figure 7.4: Abstract model for a multi-regional power system.

electrical demand is served by all fossil and renewable generation technologies. Additionally, imports or exports from or into a specific node can be used to exchange power between single nodes. Transmission losses are considered by means of an efficiency $\eta^{line}_{(n_1,n_2)}$ which can be set individually for each line.

$$
\begin{aligned}
P^{load}_{n,t} = \sum_f (P^{chp,fix}_{n,f,t} + P^{chp,var}_{n,f,t} + P^{conv}_{n,f,t}) + \sum_r P^{feed-in}_{n,r,t} \qquad & \forall\, n,t \qquad (7.25)\\
+ \sum_{(n_1,n_2=n)\in L} P^{line}_{(n_1,n_2),t}\eta^{line}_{(n_1,n_2)} - \sum_{(n_1=n,n_2)\in L} P^{line}_{(n_1,n_2),t}\eta^{line}_{(n_1,n_2)} &
\end{aligned}
$$

Heat driven and thus fixed CHP plants operate to serve a certain heat demand profile $\mu^{chp,fix}_{n,f}$ and maximum heat load $\overline{p}^{chp,fix}_{n,f}$ throughout the year which is modelled in Equation 7.26 for all nodes, fuel types and time steps.

$$
P^{chp,fix}_{n,f,t} = \mu^{chp,fix}_{n,f}\overline{p}^{chp,fix}_{n,f} \qquad \forall\, n,f,t \qquad (7.26)
$$

In contrast, flexible CHP plants can produce electricity up to their installed capacity $\overline{p}^{chp,var}_{n,f}$ depending on the residual electrical load which is described for all nodes, fuel types and time steps in Inequality 7.27.

$$
P^{chp,var}_{n,f,t} \le \overline{p}^{chp,var}_{n,f} \qquad \forall\, n,f,t \qquad (7.27)
$$

Likewise, conventional power plants that are not producing heat are modelled by means of Inequality 7.28 based on their installed electrical capacity $\overline{p}_{n,f}^{conv}$. It becomes clear that the representation of flexible CHP and conventional plants is identical and could also be formulated in one expression. Nonetheless, this explicit and mathematically redundant formulation is chosen to allow for a simple parameterization.

$$P_{n,f,t}^{conv} \leq \overline{p}_{n,f}^{conv} \qquad\qquad \forall\, n,f,t \qquad\qquad (7.28)$$

Renewable power power plants are modelled by means of Inequality 7.29. This is realized via a specific relative production profile $\mu_{n,r,t}^{res,feed-in}$ with regard to their installed generation capacity $\overline{p}_{n,r}^{res}$. Such a division into a relative production profile and installed capacity instead of absolute production values is chosen to allow for changing installed capacities in the design optimization.

$$P_{n,r,t}^{res,feed-in} \leq \mu_{n,r,t}^{res,feed-in}\overline{p}_{n,r}^{res} \qquad\qquad \forall\, n,r,t \qquad\qquad (7.29)$$

Finally, the grid is modelled in Inequality 7.29 by limiting the transmission capacities between two nodes to their respective upper line limit $\overline{p}_{(n_1,n_2)}^{line}$. As explained above, this represents the power flow between nodes for the economical optimum without a detailed physical representation of the grid. Occuring shortcuts on lines which are frequently used can thus be an indicator for technical adaptions on the transmission network and be discussed qualitatively.

$$P_{(n_1,n_2),t}^{line} \leq \overline{p}_{(n_1,n_2)}^{line} \qquad\qquad \forall\, (n_1,n_2),t \qquad\qquad (7.30)$$

In addition to the generation capacities, electrical load and transmission network, a "shortage" and "excess" variable is added to every node. Both variables have significantly higher costs than the most expensive plant in the network and assure that the problem is feasible under all parameter selections. This is especially important during the development phase when successively more components are added to the model. If the final model is set up, both, the "shortage" and "excess" variable should not be utilized as these would represent that either the load is not covered or electricity cannot be utilized in the network. Both situations would lead to an imbalance in Equation 7.25.

7.3 Model and algorithm setup

After the generic model description, a concrete instance for the power system of Kazakhstan is set up in the following. As for the other case studies, at first, all economic and technical model parameters are outlined followed by a description of the data clustering process. Finally, an overview of the algorithm setup is provided.

Model parametrization

The power system's LCOE and REOE are selected as objectives in the design optimization. As explained above, the spatial model resolution is similar to the one in [87] whereby assumptions on power plants are taken from [88, 98]. Within the design model, the installed generation capacity of wind and solar in every region are chosen as a decision variables. All design objectives and decision variables are summarized in Table 7.1 with their respective unit and range.

Table 7.1: Overview of design objectives and decision variables for the power system of Kazakhstan.

Model component	Symbol	Unit	Possible range
Objectives			
Levelized costs of electricity	C^{lcoe}	EUR/MWh	$\mathbb{R}^+$
Relative emissions of electricity	E^{reoe}	g/kWh	$\mathbb{R}^+$
Decision variables			
Installed wind capacity in node n	$\overline{p}^{res}_{n,wind}$	MW	0.001..1000
Installed solar capacity in node n	$\overline{p}^{wodh}_{n,solar}$	MW	0.001..1000

As outlined in the overview, three investment and emission cost scenarios are modelled in the design optimization. For this, different investment costs for RE are modelled based on assumptions on future price developments from a recent comprehensive meta-study [208]. Assumptions for wind energy are chosen from the "baseline" scenario for onshore turbines at medium specific capacity and medium hub height [208, p.14]. Assumptions for solar are chosen from the baseline scenario for utility-scale PV without tracking [208, p.21]. When comparing the current installation costs to price projections from 2013 [216], especially the costs for solar have dropped significantly lower with a massive cost reduction in the last years. Thus, both price trajectories assume the "best guess" price developments and are assumed to be rather moderate. Finally, an overview of parameters in the considered investment cost scenarios is provided in Table 7.2.

Within the first scenario "Status quo", current price structures for RE are used based on the values for the year 2020. Further, in the scenario "Mid-term", a lower price is assumed based on projections for the

Table 7.2: Overview of parameters within the considered investment cost scenarios.

Parameter	Unit	Value
Scenario "Status quo"		
Investment costs for wind	EUR/MW	1,310,000
Investment costs for solar	EUR/MW	830,000
Certificate price for CO_2	EUR/t CO_2	25
Scenario "Mid-term"		
Investment costs for wind	EUR/MW	1,260,000
Investment costs for solar	EUR/MW	720,000
Certificate price for CO_2	EUR/t CO_2	50
Scenario "Long-term"		
Investment costs for wind	EUR/MW	1,190,000
Investment costs for solar	EUR/MW	500,000
Certificate price for CO_2	EUR/t CO_2	75

year 2030 with stronger price reductions for solar than for wind energy due to the technical development and expected scale effects. Finally, scenario "Long-term" captures price projections for the year 2050 with even lower investment costs for their possible long-term development. Respective certificate price for CO_2 emissions are expected to start from a low level of 25 EUR/t up to a rather moderate level of 75 EUR/t within the scenario "High". The high emission price in the "High" scenario results in increased marginal generation costs for fossil power plants and thus could also be interpreted as an increased fuel price.

Different generation capacities have briefly been illustrated within Figure 7.1 in the overview and are outlined in Tables 9.3, 9.4 and 9.5 in the appendix for coal, gas and hydropower, respectively. Currently installed wind and solar capacities are provided in Tables 9.6 and 9.7 of the appendix but are rather negligible except for some installations in the Akmola and Zhambyl regions (cf. Figure 7.1). Current generation capacities are dimensioned to match the maximum system load in all regions without the need of importing electricity from other countries. The maximum electricity load in each region is given in Table 9.8 in the appendix whereby the distribution is similar to the respective installed generation capacities.

Transmission capacities between different regions are aggregated for voltage levels from 110 kV to 500 kV and the results are shown in Table 9.2 in the appendix. Within the model, on average of 5 % transmission losses are assumed for every line and implemented via a specific effiency as described in Equation 7.25 above. A respective spatial overview of the network can be found in Figure 7.5 and reveals that the entire transmission grid consists of two separated networks. Whereas the western zone is connected

to Russia but not to the rest of Kazakhstan, the eastern and southern zone with their centers Astana and Almaty are interconnected on higher voltage levels. A possible connection of the western and other markets is discussed in the scenario section in [89] but here only treated qualitatively. Further, it is assumed that all cross-border connections to neighbouring countries (Russia, Uzbekistan, and Kyrgyzstan) are not utilized which means that no electricity is exported to or imported from other countries. This approach of assumed self-sufficiency is adopted from [89, p.19] and allows to reduce the number of assumptions on the model. Such uncertain assumptions are electricity prices for imported electricity or varying electrical imports due to structural changes in the economy of surrounding countries. As a result for the transmission model, two independent interconnected multi-regional systems are optimized as yet no transmission lines connect the western zone with the eastern and southern zone.
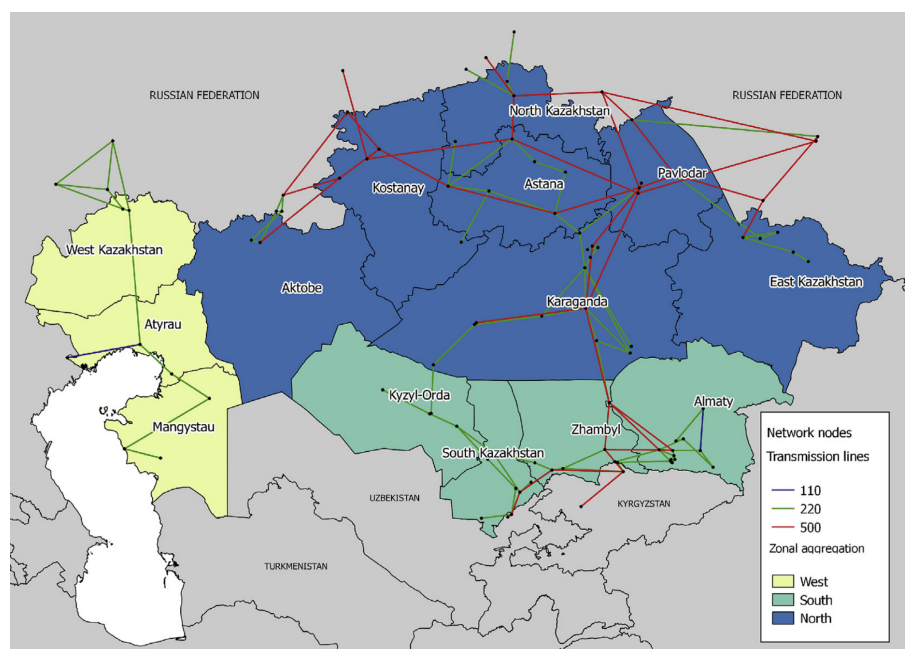
Figure 7.5: High voltage transmission network in Kazakhstan resolved in administrative regions [88].

All other assumptions on the power system and resulting model parameters are set constant over the three scenarios and summarized in Table 7.3. Fixed costs for wind and solar are set to relative values with regard to the installed generation capacity according to [208]. Fuel price assumptions are set to the average values between 2013 and 2030 from [89] and converted with respective exchange rates between 2013 and 2020 which indicate a massive inflation between both years [217]. As mentioned above, the assumption of constant future fuel prices is rather conservative in this context. Further, additional fixed costs for the operation of fossil power plants are not considered as these would require to recalculate the marginal generation costs of each plant on the operational model which would induce a high computational effort in the design optimization.

Table 7.3: Overview of other model parameters in the case study.

Parameter	Unit & reference	Value
Fixed operational costs		
Operational costs for wind	% of total investment costs	3
Operational costs for solar	% of total investment costs	1.7
Variable operational costs		
Fuel price for coal	EUR/MWh	2.65
Fuel price for gas	EUR/MWh	7.7
Efficiencies		
Efficiency for coal power plants	%	32
Efficiency for gas power plants	%	34
Efficiency for coal CHP	%	42
Efficiency for gas CHP	%	44
Other		
Emission factor for coal energy input	t CO_2/MWh	0.335
Emission factor for gas energy input	t CO_2/MWh	0.2012
Lifetime	a	20
Discount rate	%	5

Instead, this effect is regarded qualitatively by considering that it gives a competetive edge to fossil power plants in the model. Plant efficiencies for different types of fossil power plants are chosen from [98] and used to calculate the marginal generation costs within the objective function of the operational model. It becomes clear that the efficiencies for CHP plants are comparably high when compared to pure power plants which are designed for power generation only. Nonetheless, the dataset from [98] and respective assumptions are the only source for a closed power system dataset of Kazakhstan and consequently adopted in this case study. Emission factors for coal and gas are based on [218] and given for the energy input whereas a typical plant lifetime of 20 years along with a discount rate of 5 % are selected similarly to other studies [39, 178, 179]. Finally, regional power production data for wind and solar is gathered for typical wind and solar sites based on a data portal for global renewable electricity generation which builds on the data from [219] and [220]. Thus, production profiles for wind and solar plants which are not installed in the current power system are already included in the operational model.

Data clustering

Although the operational model is described as a LP without additional integer constraints, the spatial resolution of 14 regions on an hourly basis for an entire year would result in a significant solution run-times. Consequently, the model data is clustered in order to reduce the computational effort in the design optimization. Here, the type and amount of modeling data differs significantly from the first two case studies. Whereas in the first two case studies only a few time series such as electricity prices or marginal system emissions are aggregated, multiple time series for 14 regions have to be considered in the clustering process. These include the electrical load, fixed must-run CHP capacities, wind and solar feed-in profiles as well as feed-in from hydropower.

In contrast to the first two case studies, no storage is present in the current energy system of Kazakhstan. This means that no cycle analyis has to be applied in order to select the adequate cluster period length. Within [118], energy systems with higher shares of RE and storage are identified to deliver a poor performance with regard to time series aggregation. This is due to the lacking representation of the original period sequences in the clusters which does not allow to include long term storage properly. However, this issue of representing seasonal storage when typical periods are used is addressed in another subsequent study [141]. As especially the electricity demand shows a diurnal pattern, often type days are used to create reduced but representative models at lower runtimes [121, 96, 123, 221]. Thus, in this case study, the cluster length is set to 24 hours in order to represent the year as no seasonal storage effects have to be modelled.

As the process of data clustering is computationally expensive, special focus has to be put on the question whether the time series of the original problem are represented correctly. For this, again, different error metrics are applied on the duration curves of the original and clustered data. As both, the electricity load and solar production show a clear diurnal pattern, the emphasis is put on feed-in from wind power due to the stochastic nature and resulting high variability. Hydropower plants are assumed as must-run capacities in the model and thus have no impact on the error metric. As an example for the verification of the wind power production, cluster results for different numbers of representative periods in the Zhambyl region are shown in Figure 7.6.

It becomes clear that a certain number of periods is needed to represent the original period correctly. The hierarchical clustering algorithm outperforms both, the k-medoids and k-means algorithm significantly for a number of less than 13 periods. Similarly to the time series clustered in the first two case studies, a significant improvement of accuracy can be achieved within the first periods, especially when looking at the error of the hierarchical clustering. The representation of wind energy with its stochastic nature represents the "bottleneck" in terms of accuracy when compared to the other time series. Thus, a total number of 7 periods is chosen in the following to represent the original data. Similar figures for the solar production and electrical load in the Zhambyl region are provided in Figure 9.28 and Figure 9.29 in the
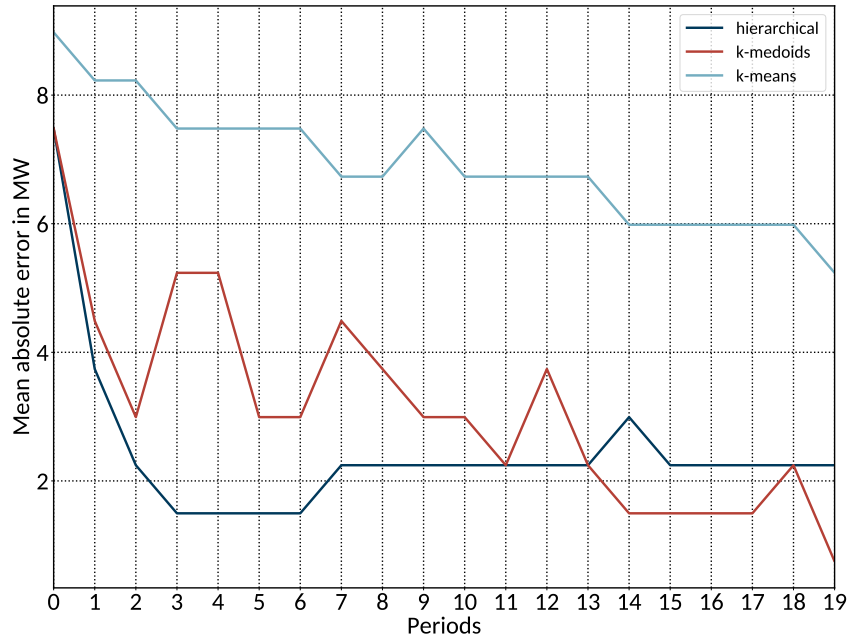
Figure 7.6: Mean absolute error between annual original and cluster wind feed-in duration curves in the Zhambyl region for a different number of representative periods of each 24 h.

appendix and confirm the strong diurnal pattern of both time series. Finally, a summary of the statistical distributions for the wind power feed-in in the Zhambyl region is shown in a boxplot in Figure 7.7.

It becomes clear that a large portion of variability can be captured in only 7 representative periods. Whereas period 1 and period 2 represent rather windy days at almost maximum capacity, period 0 represents days with a lower average production but higher variability e.g. through wind gusts. Intermediate days are represented by period 3-5 whereas days with almost no power production from wind energy are represented by period 6 with a low overall range and average value. A respective representation of the solar feed-in in the Zhambyl region indicates significantly lower variability within single clusters and can be found in Figure 9.30 in the appendix. Due to the typical symmetrical bell-shaped solar production curve, far less periods are needed to represent the original period (cf. Figure 9.29 in the appendix).

Algorithm setup

In contrast to the first two case studies, another prominent MOEA is applied for the design optimization. Within this case study, the Non-dominated Sorting Particle Swarm Optimization (NSPSO) algorithm which was initially proposed in [222] is chosen. Based on the initial Particle Swarm Optimization (PSO) algorithm for mono-objective problems [223, 224], the NSPSO algorithm extends basic PSO by a better utilization of particles' personal bests and created offspring in order to reach more effective comparisons in terms of non-domination. In contrast to the original PSO algorithm, NSPSO compares the best of all
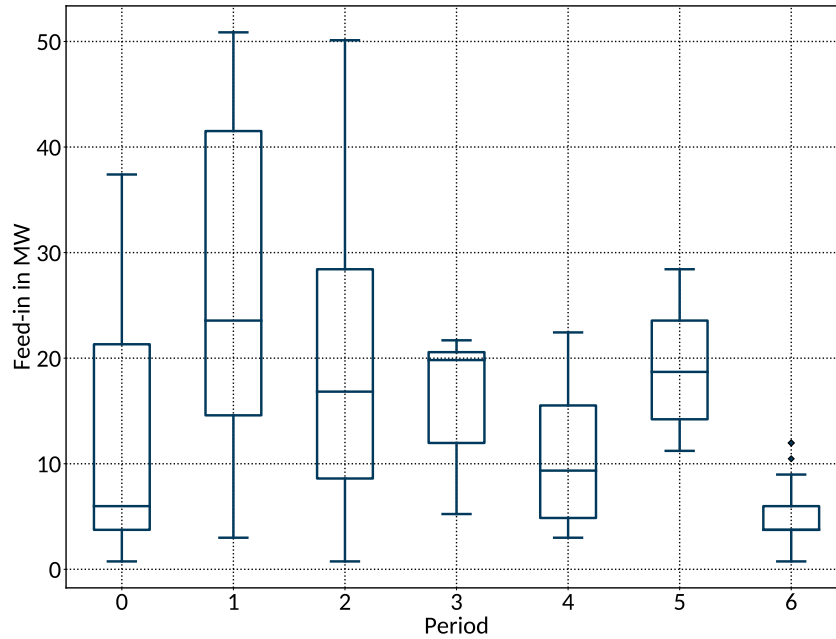
Figure 7.7: Boxplot of selected representative periods of each 24 h for the wind feed-in in the Zhambyl region using the hierarchical clustering algorithm.

particles' and their offspring in the population instead of comparing between a single particle's personal best and its offspring [222]. The algorithm requires a sufficient population size to cover the search space in order to deliver a good convergence. Similarly to NSGA-II, the concept of non-dominated sorting is applied and the algorithm performs well on well-known difficult test functions [222].

Different methods can be used to prevent a clustering of solutions in the search process. In contrast to metrics such as the crowding distance or niche count, the maxmin fitness function is used to rank individuals in evolving populations. Herefore, NSPSO is adopted to rank by the maximin function [225] in contrast to the initial algorithm [222] which uses the the non-dominated sorting procedure from NSGA-II. This adaption to the maximin function has proven to deliver a remarkable convergence and diversity of solutions on well known test problems for MOEAs and outperforms the well-known NSGA II in most performance measures [225]. Within this case study, again, the standard parameter set of the algorithm as described in [143] is applied as multiple tests for different population sizes and islands have proven to deliver good results. An overview of the parameter selection is provided in Table 7.4.

Similarly to the first two case studies, different populations are optimized parallelly based on an island model. As the number of decision variables in the design optimization amounts to 28 resulting from 14 regions with each wind and solar capacities to be build, a larger population size of 60 individuals n_i is chosen. This also considers the fact that minimum population size is required for NSPSO in order to deliver good results. For the problem at hand, this allows a reasonable evaluation runtime in combination

Table 7.4: Parameter selection for the multi-objective evolutionary algorithm NSPSO.

Parameter	Symbol	Unit	Value
Number of individuals in population	n_i	-	60
Number of islands	n_p	-	12
Number of generations	n_g	-	50
Inertia weight of particles	ω	-	0.95..10
Force in the direction of its previous best position	c_1	-	0.01
Force in the direction of its global best	c_2	-	0.5
Velocity scaling factor	χ	-	0.5
Velocity coefficient (maximum particle velocity)	v_{max}	-	0.5
Leader selection range parameter	LSR	-	2

with the rather complex operational LP model which captures more decision variables due to the multi-regional approach and different technologies. Moreover, a number of islands n_p of 12 is used to preserve a high amount of diversity. This aims at finding a rather diverse set of solutions by parallel runs which also confirm each other mutually. The number of generations n_g is set to a comparably low value of 50 in contrast to the first case studies. Moreover, the default values for the parameters ω, c_1, c_2, χ, v_{max} and LSR are chosen according to [143] and deliver good results for different generation sizes and number of evolutions.

Within the operational optimization, the default solver settings are used as the problem is defined as an LP and generally solves faster than a respective MILP variant in which a possible mixed-integer gap can be set. Due to the reduced complexity by means of the data clustering approach, solving times for single cluster periods amount to less than 5 seconds for a period of 24 hours. This achieved solution time of the operational model is sufficient to allow for a repeated evaluation in the design optimization. The formulation as an LP offers a clear advantage over the previous MILP models with their inherent characteristics of possibly longer runtimes. Consequently, the evaluation time of single periods in individuals and thus the overall runtime can be influenced significantly by the chosen model type.

7.4 Results and discussion

Results for possible system designs are obtained by applying the model with the described scenarios. As described in the overview in Section 7.1, the selected scenarios represent renewable investment cost scenarios from the current prices in the year 2020 towards future price estimations for the years 2030 and 2050. Further, it is assumed that the price for CO_2 emissions rises from 25 EUR/t in the scenario "Status quo", to 50 EUR/t and 75 EUR/t in the scenario "Mid-term" and "Long-term", respectively. This assumption aims at modeling, both, a consideration of a moderate penalty for emissions from power generation and at the same time a possible increase of marginal generation costs for fossil power plants. As a result, the competitive position of RE improves from scenario "Status quo" towards scenario "Long-term" due to the lower investment costs and higher marginal costs for fossil fuels. The obtained Pareto-fronts for the three different scenarios are shown in Figure 7.8. As within the other case studies, it becomes clear that the algorithm converges quickly towards the fronts in the single scenarios while minimizing both, the LCOE and REOE.
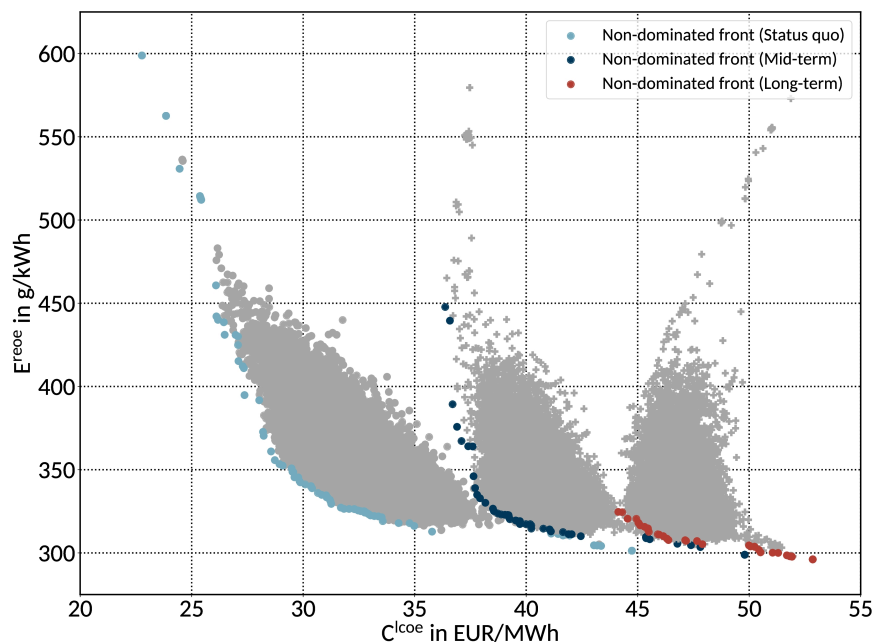
Figure 7.8: Pareto fronts for the analyzed future price scenarios.

It can be seen that the obtained design solutions cover a broad range of objective values across the selected scenarios. In scenario "Status quo", solutions with high levels of REOE up to approximately 600 g/kWh and overall low LCOE decrease to significantly lower levels at the expense of higher LCOE. This drop in emissions is comparably lower in the "Mid-term" scenario with generally lower REOE but higher LCOE. Finally, this trend continues in the "Long-term" scenario with significantly lower REOE and almost doubled LCOE. Here, the achievable emission reduction is comparably low in relation to the

other scenarios with significantly lower LCOE. A further analysis of the design parameters reveals the relation between system design and both objectives.

Scenario "Status quo"

Within Figure 7.9, the Pareto front and design parameters are shown for the "Status quo" scenario with high investment costs for RE and low prices for emissions. For this, in the following scenario results, the scale of the ordinate is adjusted in order to highlight individual trends in the data.
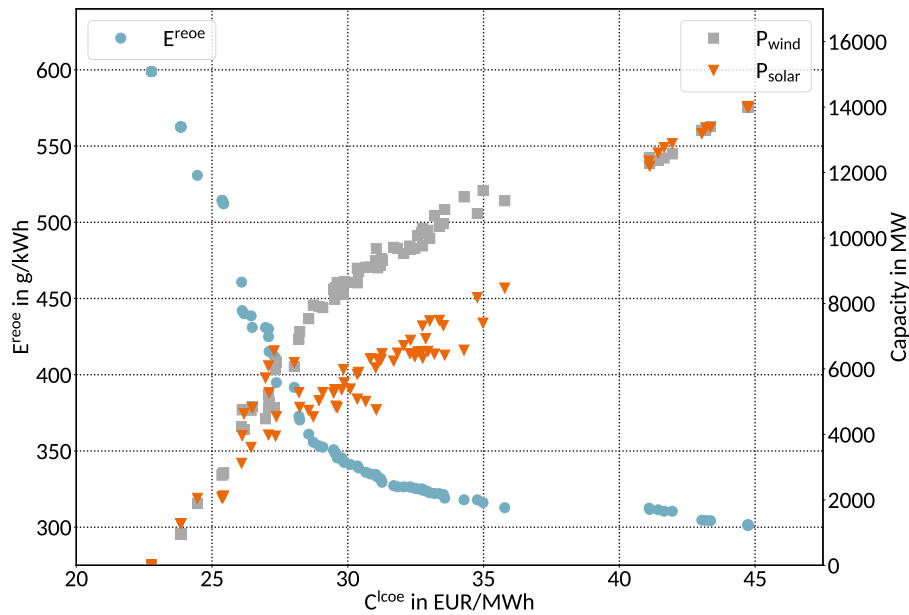
Figure 7.9: Pareto front and design parameters for scenario "Status quo".

As indicated in Figure 7.8, a diverse set of design solutions from a system with mainly fossil power plants to a system with high shares of RE is obtained. When looking at both objectives, the current system with almost no installed renewable capacities has the lowest LCOE but at the same time also the highest REOE. This is due to the fact that the current prices for fossil fuels are very low in Kazakhstan as the country is rich in coal, gas and oil resources. As a result, current investment costs for RE are still in a range where they cannot compete with these very low fuel prices when looking only at the LCOE. Nonetheless, the shape of the Pareto-front reveals that a large share of the emissions can already be reduced by a minor share of RE in the system while only having a slight increase of the LCOE. This significant drop of almost 50 % of the initial emissions is located between LCOE of approximately 23 EUR/MWh and 30 EUR/MWh and can be achieved with approximately 8 GW of wind and 6 GW of solar in the system. Above LCOE of 30 EUR/kWh, higher shares of RE still lead to lower REOE but at the expense of substantially higher LCOE. This can be explained by the diminishing marginal utility when adding more RE to the system.

This increasing share of RE cannot steadily be absorbed by the system beyond a certain point due to the volatile generation profile and possibly limited grid capacities.

Scenario "Mid-term"

The cost optimal share between fossil and renewable generation capacities changes in the "Mid-term" scenario which is shown in Figure 7.10.
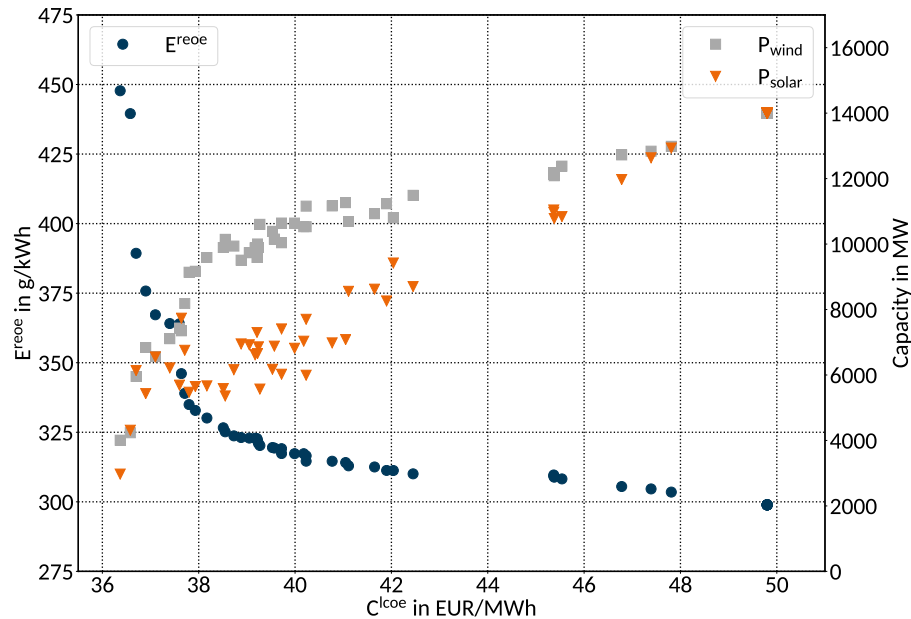
Figure 7.10: Pareto front and design parameters for scenario "Mid-term".

Here, the investment cost degression for RE and higher emission prices enforces a specific share of RE in the system in order to reach the lowest LCOE. This constant share of renewable generation also explains the overall lower emissions which amount to at most 450 g/kWh for the design case with the lowest share of RE. As in the scenario "Status quo", only a slight increase of the share of RE reduces the REOE significantly whereby this effect decreases with higher shares of RE which mostly affect the increasing LCOE. Nonetheless, this only minor decrease of investment costs and increase of the carbon price illustrate their strong impact on the overall benefit and resulting system design. Furthermore, this relation is illustrated with current fuel prices where the additional carbon price has only a minor effect compared to possibly higher future fuel prices. As already indicated in the "Status quo" scenario, significantly higher shares of wind than solar are added to the system in the middle range of LCOE from approximately 38 EUR/MWh to 47 EUR/MWh. This higher share of wind indicates a higher systemic value of wind in these design cases as the relation of costs and temporal as well as spatial availability seems to be better than for solar.

Scenario "Long-term"

As expected, this trend continues in the "Long-term" scenario which is shown in Figure 7.11 and indicates even higher shares of RE.
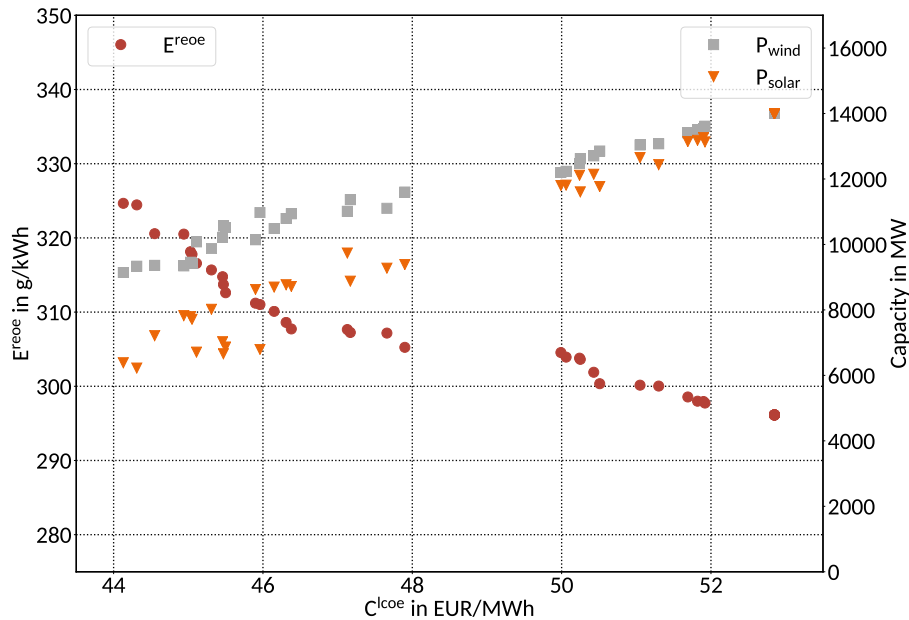
Figure 7.11: Pareto front and design parameters for scenario "Long-term".

As in the scenario "Mid-term", the design solutions with the lowest LCOE already contain a large share of RE. Further, the level of LCOE decreases significantly towards the minimal emissions that are imposed to the system due to fossil must-run CHP capacities. Consequently, the effect of increasing the share of RE has a minor impact on the REOE whereas it affects the LCOE significantly due to the diminishing marginal utility of adding more capacity to the system. As mentioned above, the overall level of LCOE almost doubles when compared to the "Status quo" scenario which can be explained by the overall higher emission prices and the high share of fossil must-run capacities. These are mainly fueled by coal (cf. Table 9.3 and Table 9.4 in the appendix) and consequently affect both, the REOE and LCOE in terms of emissions and investment as well as variable operational costs. The generally flat shape of the Pareto front reveals the comparably low but costly potential for further emission reductions. As mentioned above, this results from the high share of fossil based must-run CHP in the system. This share poses a lower barrier to the system as it does not allow for a substitution by renewable heat. If such a substitution would be allowed in the model, this shape would look differently and allow for further reductions to significantly lower emission levels. In this context, the resulting LCOE would depend on the actual costs for the allowed alternative generation technologies.

System operation

The operational model has been tested successfully for plausibility in numerous test calculations and confirms results of respective other scientific publications [87, 88, 98]. A large share of fossil regular and must-run capacities can be seen when analyzing single design cases with regard to their annual system operation. As illustrated in Figure 7.1 above, a large share of coal fueled CHP power plants is located within the populated regions in the north-eastern, central and southern part of the country. Especially the regions Pavlodar, North Kazakhstan, Akmola with the capital Astana, Karaganda and Almaty are characterized by large coal plants. In contrast, in the western region, mainly gas is used as an energy carrier whereby the relative emissions for gas amount to approximately 60 % when compared to coal (cf. Table 7.3). This reveals that a significant reduction of emissions can be achieved in the heat and power production in eastern and southern Kazakhstan. This could be either realized by a respective fuel switch to lower-emission fuels in the CHP plants or by switching to renewable heat generation technologies. Finally, as an example for the high fossil shares, Figure 7.12 shows the operational results for the design case at lowest LCOE in the "Status quo" scenario for the Akmola region. For this, the obtained design results for the clustered data are inserted into the unclustered original operational model.
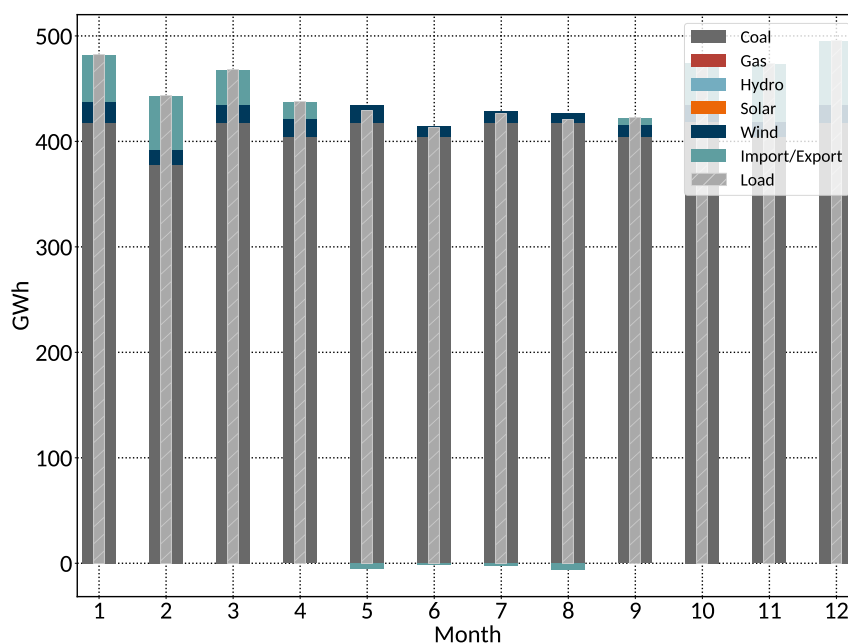
Figure 7.12: Dispatch within the Akmola region at lowest LCOE in scenario "Status quo".

It becomes clear that the major share of electricity demand is covered by coal fired plants and only a minor share is covered by 45 MW of installed wind power capacity (cf. Table 9.6 in the appendix). Due to the large share of installed coal capacities at very low variable costs, only minor shares of electricity are imported or exported which indicates that electricity production from coal is the cheapest option in

most periods of the year. This situation changes with rising shares of RE in the scenarios "Mid-term" and "Long-term" which give a competitive edge to RE due to reduced investment costs and high prices on fossil emissions. The lower Figure 7.13 shows the respective dispatch for the design case with the lowest LCOE in the scenario "Long-term".
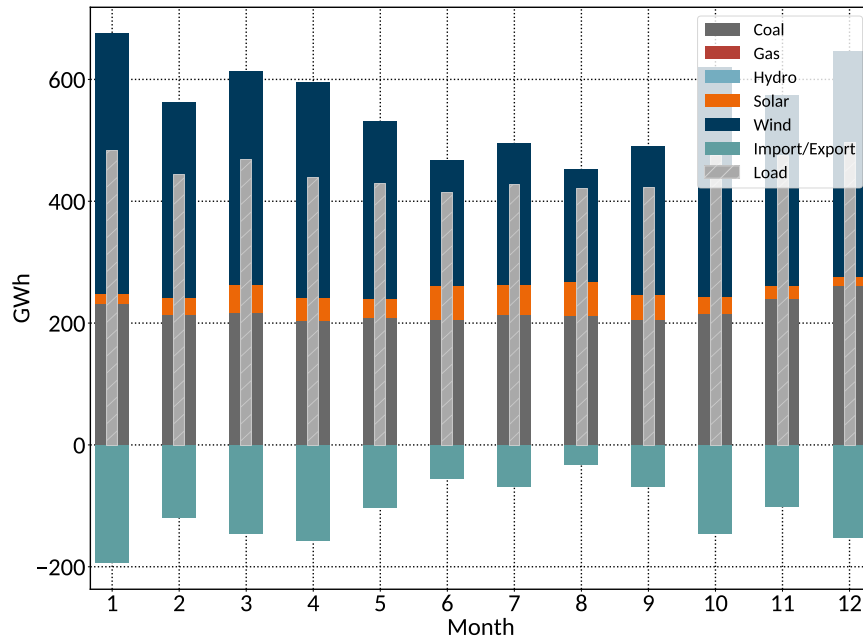
Figure 7.13: Dispatch in the Akmola region at lowest LCOE in scenario "Long-term".

Large shares of coal-based generation are substituted by renewable generation capacities due to the good potentials for solar and wind in the region. A major share of wind is utilized when compared to the installed solar capacities which can be explained for the significant potential for wind energy in the region [206]. This large amount of production even leads to an overproduction and resulting exports to other regions with lower potentials for RE and consequently higher average marginal electricity costs. Further, it can be seen that still a large portion of coal production remains in the power system. This can be explained by the large share of must-run CHP in the power system. The overall installed CHP capacity in the region amounts to 562 MW and has to be operated at a minimal load of 50 % due to mandatory heat production (cf. Table 9.3 in the appendix). As explained above and indicated in the Pareto fronts of the different scenarios, this large share of CHP imposes a lower bound for the REOE in the model as the resulting emissions can not be substituted by higher shares of RE. This could be changed by respective sector coupling measures such as electric heating boilers in combination with TES based on electricity from RE.

Classification of results

Finally, the results are related to the current power system design with a high share of fossil power plants and only 20 % RE which is mainly based on hydropower. For this, the initial and unoptimized system design is related to the obtained results in each future scenario. Further, the contribution of RE to the overall electricity consumption is calculated for the solution with the lowest levelized costs of electricity and lowest relative emissions of electricity in each scenario. Additionally, the share is calculated for a solution next to the area within the respective Pareto front where the marginal utility of reducing emissions dimishes and already a major share of emissions is reduced. Finally, a comparison of the different results is provided in Figure 7.14 wheres the initial system design in each scenario is highlighted by respective markers and auxiliary lines.
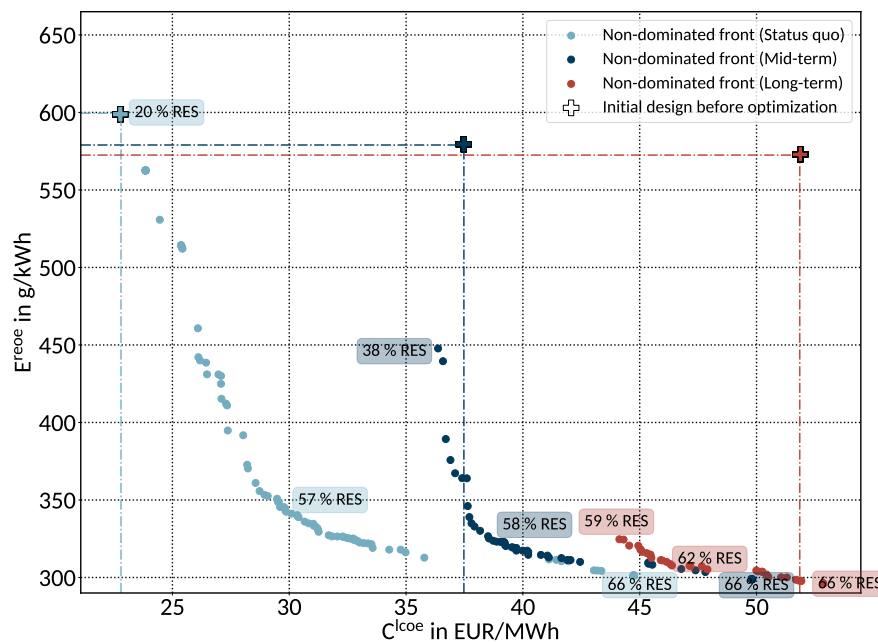
Figure 7.14: Comparison of optimized with initial system designs. Shares of electricity production from renewable energy sources (RES) are provided for specific solutions.

A comparison reveals that a diverse set of design solutions is found in each scenario whereby the Pareto-optimal system designs heavily depend on the surrounding market environment. Main drivers in the analyzed future scenarios are the capital costs for renewable generation and respective energy policy with applied emission prices. As mentioned above, in the "Status quo" scenario, the initial system design with about 20 % RE achieves the lowest LCOE at the expense of the highest emissions. Significant emission reductions at moderate electricity costs can be achieved by increasing the share of RE towards more than approximately 57 % of the overall electricity consumption. Increased shares up to 66 % of RE allow for a further reduction but at relatively higher costs. As for the "Mid-term" scenario, the current

fossil system is outperformed by the generated solutions and consequently not contained within the Pareto front. The solution with lowest LCOE already serves 38 % of the overall power consumption by means of wind, solar and hydropower. Again, a large portion of emissions is reduced at approximately 58 % of RE with a further reduction to about 66 % in the solution with the lowest emissions. Within the "Long-term" scenario, the renewable shares increase to 59 %, 62 % and 66 % , respectively. This indicates that significantly higher shares of renewable generation in the future power system of Kazakhstan will be beneficial in an economical and environmental sense even under conservative assumptions.

7.5 Case study conclusions

The developed method can be applied to a multi-regional model of a national power system. For this, the power system of Kazakhstan is modelled with different types of conventional and renewable power plants and the overall transmission system. A detailed operational optimization model is embedded in a MOEA that optimizes design parameters on the operational model. In contrast to the preceding case studies, the techno-economical operational model is realized as a LP that operates on clustered power system data. Again, a preliminary data clustering is applied to reduce the system complexity and allow for improved runtimes. Here, the clustering of load and volatile renewable energy generation data for multiple regions is proven to be highly beneficial. As a result, effects like energy exchange due to spatially distributed volatile renewable energy production can be modelled at acceptable runtimes. With regard to the design optimization, another prominent MOEA is applied to demonstrate the general applicability of the proposed method. The Non-dominated Sorting Particle Swarm Optimization (NSPSO) algorithm has proven to deliver robust results with well-known parameter sets, population sizes of 60 individuals and only 50 generations. As within the other case study applications, a massive parallel optimization on different islands shows good performance (cf. Section 4.2) and independent optimization results confirm the overall validity of the stochastic nature of the chosen algorithm. Nonetheless, special emphasis should be put on the development of the operational model and data clustering because a good trade-off between model accuracy and runtime has to be found to allow for a high number of evaluations in the design part.

The results for the different future cost scenarios show that the economical environment has a strong impact on the derived solutions. Different pathways for current and future investment costs of RE as well as different prices for operational emissions lead to diverse sets of design solutions. Moreover, valuable insights between system objectives, given by the levelized costs of electricity and relative emissions of electricity, and design variables, which are the installed wind and solar capacity, can be gained. For example, it can be demonstrated that a large amount of emissions can already be reduced at low costs in the current system. This can be achieved with shares of approximately only 35 % wind and solar energy in combination with the already existing 20 % of energy generation from hydropower. In the "Mid-term" and "Long-term" scenarios, this trend continues and higher shares of RE are already present

in the solutions with the lowest LCOE. Further, it can be seen that certain technical designs are more beneficial than others because throughout all scenarios certain optimal shares of wind and solar can be found. This reflects the temporal and spatial dimension as well as the system value of variable renewable generation. The exact progression of design parameters can be of special interest for decision makers to enable an identification of "tipping points" or "no regret solutions". This highlights the advantages of the proposed method that lie in the creation of design pathways between different stakeholder objectives when compared to approaches with only one objective and different scenarios [87, 88, 98, 226]. In summary, this case study shows that the method provides deeper insights into the relation between both objectives and existing as well as obtained system designs.

From a practical point of view, it can be stated that low LCOE and emissions in the future power system of Kazakhstan can only be achieved with significant shares of RE. As it turned out, systems with higher shares of fossils energy become uneconomical with decreasing investment costs for RE and increasing costs for emissions from fossil fuels. While the further is most likely to happen because of further costs regressions for power generation from wind and solar [208], the latter might arise through increased efforts to mitigate climate change resulting in respective energy policies. Increasing fossil fuel prices resulting from a depletition of resources or other price raising effects were not even considered in the present case study. As a consequence, the obtained results can be interpreted as conservative with regard to the market position of RE. Further, in the model, the Pareto-optimal share of renewable generation is limited by the current transmission grid and the lack of electrical storage or sector coupling measures like power to heat with thermal energy storage. As demonstrated by other studies [227, 228, 229], an application of respective measures is likely to support the cost-optimal integration of higher shares of RE in the power system. This effect could be a consideration for further research including an extension of the grid, large scale electrical storage and sector coupling measures. This could also involve the consideration of integration costs for RE as described in different studies [230, 231, 232, 233, 234] because these might cause additional costs for very high shares of RE in the system [215]. In conclusion, the significant and yet almost unexploited potential for RE in Kazakhstan [205, 235] is identified and confirmed.

8 Final discussion

This chapter discusses the main findings of the thesis with regard to the method development and its application. The focus is put on the added value of the proposed method in comparison to existing methods. Specific highlights are discussed based on respective results from the case studies. Initially, the added value is discussed with regard to the formulated research questions. After this, the main conclusions of the thesis are summarized. Finally, a critical reflection of the work is provided and ideas for future research are outlined.

8.1 Research results

The main objective of this thesis is the development of a new method that optimizes design and operation of arbitrary energy systems with regard to multiple objectives. The research questions reflect the method development and its application in three case studies carried out throughout this thesis. The questions in the first part relate to the method development, while the questions in the second part relate to the method application and specific highlights.

1. a) How can the design and operation of energy systems be optimized for multiple objectives?

The developed hybrid method combines two well established optimization methods in order to optimize the design and operation of arbitrary energy systems with different energy carriers across various sectors. For the system operation, specifically the economic dispatch or unit commitment problem, linear programming (LP) or mixed-integer linear programming (MILP) is applied. This operational problem is formally specified as the slave problem. For the actual design optimization, flexible multi-objective evolutionary algorithms (MOEA) are applied in order to change parameters or variable bounds on the operational LP or MILP. This design problem is also referred to as the master problem where the respective LP/MILP is an individual in the evolving population of the MOEA. The re-evaluation of many individuals in the master problem can be computationally expensive, therefore data clustering can be applied for larger slave problems in an optional pre-processing stage. Finally, the result is a set of Pareto efficient design cases. Through this the optimal system operation is taken into account for all solutions based on

an optimization regarding one objective. A detailed outline of the proposed hybrid method on different levels is provided in Chapter 4 along with specific details for an effective implementation.

1. b) What advantages offers the proposed method over existing methods?

Strengths of both types of algorithms are used on each level of the method. In the slave problem, the operation of an energy system is optimized with regard to one objective based on the rationale that an energy system's dispatch follows the economic priciple in the vast majority of cases. In this context, the formulation as LP/MILP offers the advantage of being deterministic and solving the problem to optimality. Due to the linear description of the problem, large numbers of decision variables and constraints can be handled and solutions are found in acceptable computational runtimes. Nonetheless, the linear properties also restrict the model capabilities when non-linearities have to be captured. These can be encountered in many real-world applications and consequently also within the slave problems constraints and objectives. Here, the method can provide an advantage by dealing with the non-linearities in the pre- and post-processing stage of the operational model, which has been demonstrated in the first two case studies. Moreover, the method is capable of a "real" Pareto-optimization in the design part in contrast to other widely used methods for example the prominent ϵ-constraint method. The latter requires additional decisions to be made, which might lead to infeasibility for complex problems with many values. This is outlined in detail in Section 3.3 based on the definition of different problem types in Section 3.1. Finally, due to the abstraction to arbitrary evolutionary algorithms types, the master problem can be solved flexibly by different algorithms and the slave problem is principally not limited to be modelled as a linear optimization problem.

1. c) Which design patterns and concepts are valuable for a performant implementation?

The hybrid optimization approach is realized in a generic software architecture that allows for a coupling of different algorithms and arbitrary energy systems. The developed architecture is independent of its actual implementation and uses an object-oriented design. The main advantage is that this flexible structure allows to model arbitrary energy systems as instances of the same basic class structure. Moreover, a separation of model and data is achieved through an object-oriented design, as model instances can be created by passing datasets into the constructor of respective classes. To increase the overall optimization performance, the concept of parallelism can be applied. Through this both the operational and the design optimization benefit from significantly reduced runtimes. Initially, the objective function value calculations are accelerated in the operational optimization by a parallel period optimization for the case of multiple cluster periods. This type of parallelization can be beneficial when the actual solution runtime for different periods is computationally expensive and a runtime reduction by parallel execution is higher than the runtime induced by a memory overhead due to multiprocessing or multithreading. Another type

of parallelism is used to simultaneously evaluate multiple design models in the applied evolutionary algorithms. This is realized by working with parallel populations on different islands within the MOEA, which results in a linear acceleration of the overall solution runtime. The general concept of parallelization and its application in the architecture is outlined in detail in Section 4.2.

2. a) How can non-linear relations be considered within specific applications?

The question how non-linear relations can be taken into account in specific models is addressed in the first case study, which applies the method to a detailed model of a CAES plant. Both concepts of using non-linear expressions in the pre-processing and post-processing phase of the operational model are applied. The former is applied in order to model non-linear investment costs for turbomachinery based on a reference approach for the underlying cost assumptions. These logarithmically shaped cost curves are post-processed from operational results, as the installed turbomachinery capacity is an upper bound in the operational model and a decision variable in the design optimization (cf. Section 5.2). This demonstrates how parameters from the linear model can be used as input arguments for non-linear expressions in the fitness calculation. Likewise, non-linear expressions can be handled in the pre-processing phase by pre-calculating parameters for the operational model. Here, in contrast to the post-processing variant, parameters on the linear model are determined by applying a set of different functions with design variables as input arguments. This allows for a dynamic adaption of the operational plant characteristics in the design optimization based on the actual sizing of the different components. Finally, both variants of calculation lower the burden of handling of non-linearities through a flexible adaption during the design stage that offers a high degree of flexibility to the modeller.

2. b) How can model complexity and resulting runtimes be reduced?

In the case studies, three different cluster algorithms are applied in order to aggregate time series for one or multiple locations. The applied algorithms are k-means, k-medoids and hierarchical clustering. The used dataset is chosen based on a suitable performance indicator for the difference between the obtained duration curves of the original and clustered data. This performance indicator is also the basis for the decision about the number of clusters to be chosen. The cluster length, meaning the number of time points (e.g. hours) represented by a single cluster, is explained separately. For this, a special data clustering process for systems with energy storage is proposed in Section 4.2 based on cycle detection and analysis for the original time series. In general, the concept of data clustering can be interpreted as an option to decompose the original problems into smaller representative sub-problems. This has a significant influence on the overall runtime, because the worst case runtime for LP or MILP problems exponentially depends on the dimension of the problem. In particular, this is of special interest for MILP problems which often show long search trees in the branch and bound algorithm. Finally, in the second

case study, it is demonstrated that the runtime can be reduced to a thousandth of the original while almost preserving the original dispatch.

2. c) How can obtained results be related to existing system designs?

A comparison between existing system designs and obtained model results is provided in the third case study for the power system of Kazakhstan. Levelized costs of electricity and relative system emissions are used as design objectives. The current system design with a high share of fossil power plants is compared to the set of Pareto-optimal system designs. This comparison of existing design cases with results for different scenarios in the solution space offers valuable insights to the decision maker. For instance, in the case study it is demonstrated that the current system design is progressively outperformed by renewable energy systems, with increasing marginal generation costs for fossil power plants and decreasing investment costs for RE as main drivers. Further, possible pathways between both objectives can be described and it is found that a large portion of emissions can already be reduced with comparably low shares of RE in the system at overall moderate costs. The progression of design parameters with regard to multiple objectives can be of special interest for decision makers to identify robust pathways of energy system designs. An improved data basis displays its strength, particularly in the presence of multiple stakeholders with conflicting objectives which is often the case in policy design. In conclusion, this again highlights the advantages of the method when compared to approaches with only one objective and different scenarios as it provides new and possibly unexpected insights.

2. d) Which algorithms and parameter sets are valuable in terms of different applications?

In the selected case studies, three different MOEAs are applied in the design part and combined with either linear programming or mixed-integer programming models in the operational part. The prominent Nondominated Sorting Genetic Algorithm (NSGA-II) is applied in the CAES case study, while the Multi-objective Evolutionary Algorithm based on Decomposition (MOEAD/D) is used for the second case study that models a district heating system. In the third case study, Non-dominated Sorting Particle Swarm Optimization (NSPSO) is applied to optimize the system design. This diverse set of algorithms ranging from genetic algorithms to population based methods demonstrates that the general function principle of the hybrid method is independent of the specific algorithm. All algorithms are proven to deliver robust results for the different applications. The typical search behaviour of evolutionary approaches that is described in Section 3.3 is also reflected in the algorithm parametrization. During the exploration phase in the first generations of the optimization phase, a large share of the search space is explored (cf. Figure 9.7 in the appendix). In the following exploitation phase, the individuals "spread" close to the latest non-dominated front as the number of non-dominated individuals increases with a specific diversity on the front (cf. Figure 9.8 in the appendix). Both phases require less then 100 generations in total to deliver

good results in the case studies. As already stated in research question 1.c), the concept of parallelization enables a broader set of solutions. The population size depends on the actual problem at hand and the ratio between the number of design decision variables and individuals is chosen as 2/24 for the first case study, 5/24 for the second case study and 28/60 for the third case study. In the operational part, it is proven to be benefial to work in an integer gap of up to 3 % on computationally intensive MILP models.

2. e) Which range of applications can be identified for the proposed method?

The general applicability of the method for a wide range of applications from detailed technical to large and spatially resolved models is demonstrated in the different case studies. The scientific value is elaborated for the general method in comparison to existing methods as well as for special capabilities with regard to different applications. The application to the detailed modeling of compressed air energy storage has shown that it is principally possible to model single technologies on a high level of technical and economical detail. The relevance of the current method for a diverse set of sector coupling technologies is demonstrated through the application to a municipal heating system in the second case study. In the third case study, an increased number of spatially distributed technologies is modelled using the power system of Kazakhstan. Different combinations of objectives and design variables are proven to deliver valuable insights into respective interrelations between both. However, these are only exemplary applications and the method theoretically allows for other energy systems, numbers and types of objectives, decision variables and technical, temporal and spatial resolution. As one example, the chosen hourly time resolution is common in the field of energy modeling, but the method could potentially use time resolutions of minutes or seconds. Nonetheless, the model type is still limited to be discrete when the operational optimization is based on an LP or MILP model. Finally, as with all computer models, a trade-off between accuracy and computational effort is required in order to obtain meaningful results in acceptable runtimes.

8.2 Main conclusions

The developed method for the multi-objective optimization of design and operation is proven to perform well for a broad range of energy systems. Here, the strengths of MOEAs are used in design optimization whereas the strengths of LP/MILP are used in operational optimization. The former is capable of dealing with non-linearities in the pre- and post-processing stage of the operational model and enables a real Pareto-optimization of the design parameters. The latter offers the advantage of being deterministic and solving the problem to optimality. Further, problems with large numbers of decision variables and constraints can be solved in acceptable computational runtime. When used in combination, the re-evaluation of operational models allows for a continuous adaption of parameters in the pre- and post-processing phase and therefore a dynamic alignment of the parametrization on the operational model. Because the

repeated evaluation of multiple operational models can be computationally expensive, cluster methods may be applied to reduce the dimensionality of the underlying data.

The concepts of object-orientation and parallelization are found to be valuable for a concrete method implementation. Object-orientation allows for a division into independent units which can be used by themselves while parallelization enables significant runtime reductions when applied to the optimization of the system design and operation. Hereby, the combination of software that was developed throughout the course of this study with other packages into a new set of packages is proven to perform well. Different combinations of algorithms are possible in the design and operational part. Within the different case studies, the prominent MOEAs NSGA-II, MOEA\D-DE and NSPSO are applied in the design optimization, where the linear and (mixed-integer) programs in the operational part are solved by respective free and open or commercial solvers. k-means, k-medoids and hierarchical clustering are applied to decompose the original problem into smaller sub-problems for the data clustering in the operational part. This results in a significant improvement of the overall computational performance.

In the first case study, a compressed air energy storage system is optimized from an operator's perspective on the German spot market. Chosen design objectives are the system's net present value and storage efficiency. The chosen technology representation is based on a detailed techno-economical operational model that includes partial load conditions. Moreover, non-linear cost effects as well as operational characteristics that are dynamically changed for different design cases are considered. It can be demonstrated that different market environments have a strong impact on the derived solutions and that different design cases lead to very diverse solutions regarding both objectives. From a practical point of view, it can be shown that no CAES plant can survive in the current day-ahead market in Germany. This situation might change with increasing spreads in future power systems or additional remuneration shemes like capacity payments or revenues from other markets such as control reserve.

In the second case study, which models a municipal heating system in northern Germany, the impact of different future power system scenarios on the levelized costs of heat and system emissions is analyzed. It is demonstrated that the method can be applied to optimize design parameters of respective sector coupling systems with regard to objectives that are relevant for both the operator and community. Different technologies including CHP, PtH and thermal energy storage are optimized based on detailed models while considering their interdependencies. Again, it is shown that different future pathways have a strong influence on the optimal heating system layout as a diverse set of design cases is obtained for the different scenarios. From a practical perspective, it can be observed that no single heating system setup performs well concerning both relative costs and emissions of heat under all scenarios. As a consequence, the question whether the system is mainly driven by CHP or PtH units heavily depends on the surrounding incentives, penalties and emissions in the power system.

In the third case study, a multi-regional power system model for the country of Kazakhstan investigates the impact of higher shares of wind and solar with regard to the levelized costs of electricity and emissions. For this, three future scenarios are modelled based on forecasts for renewable investment costs and emission prices. It is demonstrated that the method can be applied to a multi-regional model of a national power system including different types of conventional and renewable power plants as well as the overall transmission system. By investigating the impact of different future scenarios, it becomes clear that the economical environment has a strong impact on the derived system designs. For the current system, it can be demonstrated that a large amount of emissions can already be reduced at low costs with moderate shares of wind and solar. In the selected future scenarios, this trend continues and significantly higher shares of RE are already present in the solutions with the lowest costs. From a practical point of view, it is shown that low generation costs and emissions can be achieved with significant shares of RE in the power system. Here, the possibility to substitute fossil based CHP must-run capacities by means of renewable heat was not even considered. Other air pollutant emissions may be reduced by effective scrubbers at lower costs than through RES. This highlights the significant and yet almost unexploited potential for RE in Kazakhstan.

Arbitrary multi-sectoral energy systems can be defined on a high level of flexibility by means of the proposed method. This is demonstrated by a diverse set of exemplary applications ranging from local electrical energy storage, over municipal district heating systems to national power systems with transmission networks across multiple regions. As a result, the method allows to answer a wide array of questions arround the design and operation of energy supply systems in technical, economical and environmental dimension, while preserving criteria from different perspectives in the optimization process. A conversion of future energy systems towards more complex cross-sectoral and decentralized structures demands for new tools in order to investigate possible future pathways. In conclusion, the developed method can contribute to create a solid base of alternatives for a thorough scientific discussion from different perspectives as it provides new insights into the interdependencies of respective energy systems.

8.3 Critical reflection

Despite the outlined advantages of the developed method, it also has some drawbacks which either result from the method itself or its application to the selected case studies. First of all, the operational optimization is mono-objective due to the realization as LP or MILP, which is a rational assumption for most real systems that are operated based on one command value. However, this does not allow for a real multi-objective dispatch with regard to the system design. As a result of the chosen optimization approaches, sometimes ambigous solutions exist with regard to the design objectives. As one example, it is possible that different economic dispatch solutions for a heating system exist for the same objective value, although the dispatch solutions differ in their resulting emissions. One option to address this is-

sue would be the inclusion of external costs in the operation by monetizing the operational emissions of different units. This has been realized in the second and third case studies through a certificate price for CO_2. However, in theory, this effect dimishes with decreasing cluster lengths and a therefore decreasing probability for ambigous solutions regarding single objectives in the operational part.

When looking at the different case studies, the assumption of „perfect foresight" with regard to the spot market prices and heat demand is rational but generally optimistic. The market prices and heat load are stochastic and subject to uncertainty, therefore the real dispatch is based on forecasts and will differ with respective deviations. Nonetheless, this problem occurs for all design cases and cannot be addressed generally as the actual operative setting is highly individual. For example, it could be the case that the heating system is embedded in a larger portfolio of power plants and forecast errors are balanced by other flexibility options. However, for the present case studies, the assumption is valid and easy to communicate when considering the fact that the results are generally optimistic. For a comparison of different technical setups across multiple scenarios, the general relations and ranking of solutions are not affected. Thus, the general assumption of „perfect foresight" can be justified in cases where only general relations between different technical concepts are investigated. Likewise, the assumption of constant annual results over the system's lifetime is unlikely to occur in reality because energy supply systems and respective markets are changing constantly. This is for example the case in the first case study, where constant costs and revenues are assumed for the calculation of the net present value. However, this assumption is not related to the method itself because it would principally be possible to integrate varying conditions over the lifetime of the investigated system. Again, for a comparison of different setups while focusing on the interrelations between objectives and design variables, it is sufficient to work with equal boundary conditions in order to not discriminate against single setups or included technologies.

Specific features can be observed when looking at the analyzed applications. The advantage of pre-processing parameters for the operational model requires expert knowledge in order to translate the detailed characteristics into linear characteristics that depend on the actual equipment size. Here, it is important to mention that the characteristics have an influence one the convergence behaviour of the MOEA. Thus, it is proven to be more effective when the pre-processing is tested separately before an integration in the design optimization. Moreover, the flexibility of MOEAs, which is based on their stochastic nature and the absence of derivatives, comes at the expense of requiring multiple runs because these do not deliver the real optimum in order to confirm the results. Finally, the data clustering demands for a special focus as it directly affects the obtained design results.

8.4 Further research

As indicated in the algorithm setup in the design optimization parts in Section 5.3, Section 6.3 and Section 7.3, different assumptions on population sizes, number of islands and generations are made based on various test runs with different configurations. This rather rough assessment of adquate parameter sets could be improved by applying a parameter optimization for the problem at hand. In this connection, the population size, numer of islands and other parameters such as the crossover or mutation probability become a decision variable and are optimized regarding one or more criteria. As objectives, the hyper-volume indicator introduced in Section 3.3 or the number of non-dominated individuals could be used as objectives for a fixed number of generations on the problem. This would allow for structured and considerably better parameter estimations with regard to specific problems in a multi-objective meta-optimization layer. Further, an iterative creation of Pareto fronts as proposed in [80] could be applied by re-inserting solutions from former optimization runs as starting points. This can be of special interest for sparse fronts with large uncovered areas. Additionally, other MOEAs can be studied regarding their performance in the design optimization.

Regarding the operational optimization, an improvement could be achieved by looking at more advanced modeling techniques. In order to address the optimistic assumption of "perfect foresight", uncertainty can be included in the operational model through the application of robust optimization or stochastic programming. The further is capable of tackling uncertain parameters within certain bounds and the latter is based on probability distributions that can be estimated or are known in advance. The general idea is to maximize the expectation for a function of decisions and random variables, for example varying electricity prices or stochastic wind feed-in, in order to obtain more realistic results. For this, different formulations such as the representation of uncertainty within scenarios, two-stage or multi-stage formulations can be chosen depending on the problem knowledge and goal. A recent literature review provides an overview of the fundamentals and developments of stochastic programming in unit commitment [236]. These formulations can also be combined with a rolling forecast or time window which is discussed in other studies [237, 238]. Moreover, special emphasis can be put on compact model formulations to decrease the runtime. This has already been applied in the third case study, where the generation from fossil power plants is modelled by only one generation variable instead of linking it to the fuel consumption, which requires an additional variable. This applies the principle of Occam's razor to obtain a reduced model and could be applied equally for other operational models.

When focussing on the method results in combination with the applied data clustering, the impact of different cluster numbers and actual cluster sizes on the design results can be investigated more thoroughly. The cluster selection and treatment can have a significant impact on the design results [118]. This influence could be quantified with additional calculations for different applications to provide a better understanding of the respective interrelations. Further, in the present study, seasonal storage has

not been integrated in combination with cluster methods, although promising approaches have been proposed lately [141]. Another suggestion for future research could be the comparison of model results with real system designs. As becomes clear from Figure 7.14 in the third case study, the distance between real designs and model results can be interpreted as a measure for the improvement of existing designs. Generic concepts to measure this distance mathematically could help to describe this relation using precise metrics. Thinking further, the method can be transferred to other types of energy systems or even other domains like production lines or logistic chains, because the general concept is applicable to a broad range of technical systems. Finally, a combination with other methods such as the application of machine learning in the operational part is generally possible.

Nomenclature

The nomenclature includes abbbreviations, symbols and subscripts including formulations from different modelling sections. For the sake of brevity, symbols for parameters and variables are explained only once by the index for all units $u \in U$ if they are used in a similar fashion for different types of units e.g. CAES or CHP plants.

Abbreviations

4GDH   4th generation district heating

BOP   Balance of plant

BPT   Back-pressure turbine

CAES   Compressed air energy storage

CAPEX   Capital expenditure or capital expense

CAS   Compressed air storage

CDOM   Combined design and operational model

CET   Combined cycle extraction turbine

CHP   Combined heat and power

COP   Coefficient of performance

DCH   Discounted heat

DCL   Discounted load

DE   Differential evolution

DER   Distributed energy resources

DH	District heating
DM	Design model
DoC	Depth-of-cycle
EA	Evolutionary algorithm
ED	Economic dispatch
EGIX	European Gas Index
EHB	Electric heating boilers
GA	Genetic algorithm
HDOM	Hybrid design and operational model
HLD	Heat load
HP	Heat pump
ICE	Internal combustion engine
IP	Investment planning
IQR	Interquartile range
LCOE	Levelized costs of electricity
LCOH	Levelized costs of heat
LoC	Length-of-cycle
LP	Linear program
MAE	Mean absolute error
MCDOM	Multi-objective combined design and operational model
MDM	Multi-objective design model
MES	Multi-regional energy system
MHDOM	Multi-objective hybrid design and operational model

MILP	Mixed-integer linear program
MINLP	Mixed-integer nonlinear optimization problem
MOEA	Multi-objective evolutionary algorithms
MOEA/D	Multiobjective evolutionary algorithm based on decomposition
MOM	Multi-objective operational model
MOP	Multi-objective optimization problem
NPV	Net present value
NSGA	Nondominated sorting genetic algorithm
NSPSO	Non-dominated sorting particle swarm optimization
oemof	Open energy modelling framework
OM	Operational model
OPEX	Operational expenditure or operational expense
OREV	Operational revenue
PF	Power flow
PLB	Peak load boiler
PLB	Peak load boilers
PSO	Particle swarm optimization
PtH	Power to heat
PV	Photovoltaic
PWL	Piecewise linear
RE	Renewable energies
REOE	Relative emissions of electricity
REOH	Relative emissions of heat

RMSE Root-mean-square error

SOS Special ordered set

TES Thermal energy storage

UC Unit commitment

UML Unified modelling language

Greek Symbols

α_i Auxiliary coefficient

α_i Coefficient of performance

β Power loss factor

ϵ Auxiliary coefficient

$\eta^{ref,caes}$ Reference efficiency of other plant

μ Relative share of quantity

ω_p Weight of period

τ Time increment

Roman Symbols

$c_{t,p}^{elm}$ Spot market electricity price

$c_{t,p}^{emi}$ Price for emissions

$c_{t,p}^{fuel}$ Fuel market price

$C_{u,t,p}^{elm}$ Total costs at electricity market

$c_{u,t,p}^{var}$ Variable costs

$C_u^{cpx,bop}$ Total balance of plant costs within CAPEX

$c_u^{inv,ref}$ Investment costs of reference system

C_u^{inv} Investment costs of component u

$C_u^{opx,ins}$	Total insurance costs within OPEX
$C_u^{opx,mnt}$	Total maintenance costs within OPEX
$C_u^{opx,per}$	Total personell costs within OPEX
e^{system}	Specific emissions of the surrounding electricity system
e_c^{fuel}	Specific fuel emissions for a CHP unit
$R_{u,t,p}^{elm}$	Total revenues at electricity market
s_c^{ins}	Share of insurance costs
s_c^{per}	Share of maintenance costs
s_c^{per}	Share of personell costs
s_u^{bop}	Share of balance of plant costs
v_k^{cas}	Volume of compressed air storage
$\overline{p}_u$	Installed electrical capacity or upper bound
$\overline{p}_u^{ref}$	Installed electrical capacity of reference system
$\dot{Q}_{k,t,p}^{exp,in}$	Fuel supply within expansion part
$\overline{q}_s^{heat}$	Heat quantity of storage

Subscripts

a	Year
b	Peak load boiler
c	CHP unit
d	Heat demand
e	Electric boiler
g	Heat production unit
h	Heat pump

n	Node
p	Representative period
s	Thermal storage
t	Time step
u	General unit $u \in U$ with $U = K \cup G$

Superscripts and Identifiers

0	Initial value
a..d	Specific coefficient
abs	Absolute quantity
ann	Annual
b	y-intersect
bop	Balance of plant
cas	Compressed air storage
cmp	Compression part
cond	Condenser
cpp	Conventional power plant
cpx	Capital expenditures
dh	District heating
dhs	Dummy heat source
el	Electrical power
elm	Electricity market
emi	Emissions
er	Edge region

exp	Expansion part
$feed-in$	Feed from renewables
fg	Flue gas
fix	Fixed value
$fuel$	Fuel related
$init$	Initial value
ins	Insurance
inv	Investment
m	Slope
mnt	Maintenance
opr	Pressure above minimum
opx	Operational expenditures
orv	Operational revenues
$pers$	Personell
ref	Reference unit
res	Renewable energy sources
$start$	Start related
sys	System
tmp	Temporal
var	Variable quantity
$wodh$	Without district heating

List of Figures

List of Tables

Bibliography

[1] S. Pfenninger, A. Hawkes, and J. Keirstead, "Energy systems modeling for twenty-first century energy challenges," *Renewable and Sustainable Energy Reviews*, vol. 33, pp. 74 – 86, 2014. [Online]. Available: https://doi.org/10.1016/j.rser.2014.02.003

[2] S. J. Davis, N. S. Lewis, M. Shaner, S. Aggarwal, D. Arent, I. L. Azevedo, S. M. Benson, T. Bradley, J. Brouwer, Y.-M. Chiang, C. T. M. Clack, A. Cohen, S. Doig, J. Edmonds, P. Fennell, C. B. Field, B. Hannegan, B.-M. Hodge, M. I. Hoffert, E. Ingersoll, P. Jaramillo, K. S. Lackner, K. J. Mach, M. Mastrandrea, J. Ogden, P. F. Peterson, D. L. Sanchez, D. Sperling, J. Stagner, J. E. Trancik, C.-J. Yang, and K. Caldeira, "Net-zero emissions energy systems," *Science*, vol. 360, no. 6396, 2018. [Online]. Available: https://doi.org/10.1126/science.aas9793

[3] D. R. Biggar and M. Reza Hesamzadeh, *The Economics of Electricity Markets*. John Wiley & Sons, 2014.

[4] C. Harris, *Electricity Markets: Pricing, Structures and Economics*. John Wiley & Sons. Second Edition, 2006.

[5] A. J. Wood, B. F. Wollenberg, and G. Sheble, *Power Generation, Operation and Control*. John Wiley & Sons. Third Edition, 2013.

[6] D. Kirschen and G. Strbac, *Fundamentals of Power System Economics*. John Wiley & Sons, 2004.

[7] S. Pfenninger, L. Hirth, I. Schlecht, E. Schmid, F. Wiese, T. Brown, C. Davis, B. Fais, M. Gidden, H. Heinrichs, C. Heuberger, S. Hilpert, U. Krien, C. Matke, A. Nebel, R. Morrison, B. Müller, G. Plessmann, M. Reeg, J. C. Richstein, A. Shivakumar, I. Staffell, T. Tröndle, and C. Wingenbach, "Opening the black box of energy modelling: strategies and lessons learned," *ArXiv e-prints*, Jul. 2017. [Online]. Available: https://doi.org/10.1016/j.esr.2017.12.002

[8] C. Boysen, C. Kaldemeyer, S. Hilpert, and I. Tuschy, "Integration of flow temperatures in unit commitment models of future district heating systems," *Energies*, vol. 12, no. 6, 2019. [Online]. Available: https://doi.org/10.3390/en12061061

[9] S. Hilpert, C. Kaldemeyer, U. Krien, S. Günther, C. Wingenbach, and G. Plessmann, "The open energy modelling framework (oemof) - a new approach to facilitate open science in energy system modelling," *Energy Strategy Reviews*, vol. 22, pp. 16 – 25, 2018. [Online]. Available: http://www.sciencedirect.com/science/article/pii/S2211467X18300609

[10] F. Wiese, S. Hilpert, C. Kaldemeyer, and G. Pleßmann, "A qualitative evaluation approach for energy system modelling frameworks," *Energy, Sustainability and Society*, vol. 8, no. 1, p. 13, Apr 2018. [Online]. Available: https://doi.org/10.1186/s13705-018-0154-3

[11] H.-K. Ringkjøb, P. M. Haugan, and I. M. Solbrekke, "A review of modelling tools for energy and electricity systems with large shares of variable renewables," *Renewable and Sustainable Energy Reviews*, vol. 96, pp. 440 – 459, 2018. [Online]. Available: http://www.sciencedirect.com/science/article/pii/S1364032118305690

[12] D. Connolly, H. Lund, B. Mathiesen, and M. Leahy, "A review of computer tools for analysing the integration of renewable energy into various energy systems," *Applied Energy*, vol. 87, no. 4, pp. 1059 – 1082, 2010. [Online]. Available: http://www.sciencedirect.com/science/article/pii/S0306261909004188

[13] A. A. Bazmi and G. Zahedi, "Sustainable energy systems: Role of optimization modeling techniques in power generation and supply—a review," *Renewable and Sustainable Energy Reviews*, vol. 15, no. 8, pp. 3480 – 3500, 2011.

[14] B. Saravanan, S. Das, S. Sikri, and D. P. Kothari, "A solution to the unit commitment problem—a review," *Frontiers in Energy*, vol. 7, no. 2, pp. 223–236, Jun 2013. [Online]. Available: https://doi.org/10.1007/s11708-013-0240-3

[15] I. Abdou and M. Tkiouat, "Unit commitment problem in electrical power system: A literature review," *International Journal of Electrical and Computer Engineering (IJECE)*, vol. 8, p. 1357, 06 2018.

[16] S. Stoft, *Power System Economics: Designing Markets for Electricity*. Wiley, 2002. [Online]. Available: https://books.google.de/books?id=DrTEsqJRKrYC

[17] P. Mancarella, "Mes (multi-energy systems): An overview of concepts and evaluation models," *Energy*, vol. 65, pp. 1 – 17, 2014. [Online]. Available: http://www.sciencedirect.com/science/article/pii/S0360544213008931

[18] M. Geidl, "Integrated modeling and optimization of multi-carrier energy systems," Ph.D. dissertation, ETH Zurich, 2007.

[19] M. Geidl, G. Koeppel, P. Favre-Perrod, B. Klockl, G. Andersson, and K. Frohlich, "Energy hubs for the future," *IEEE Power and Energy Magazine*, vol. 5, no. 1, pp. 24–30, Jan 2007.

[20] D. Simon, *Evolutionary Optimization Algorithms*. John Wiley & Sons, 2013.

[21] P. Gabrielli, M. Gazzani, E. Martelli, and M. Mazzotti, "Optimal design of multi-energy systems with seasonal storage," *Applied Energy*, 2017. [Online]. Available: http://www.sciencedirect.com/science/article/pii/S0306261917310139

[22] A. Rieder, A. Christidis, and G. Tsatsaronis, "Multi criteria dynamic design optimization of a small scale distributed energy system," *Energy*, vol. 74, pp. 230 – 239, 2014. [Online]. Available: //www.sciencedirect.com/science/article/pii/S0360544214007026

[23] O. Erdinc and M. Uzunoglu, "Optimum design of hybrid renewable energy systems: Overview of different approaches," *Renewable and Sustainable Energy Reviews*, vol. 16, no. 3, pp. 1412 – 1425, 2012. [Online]. Available: http://www.sciencedirect.com/science/article/pii/S1364032111005478

[24] A. Alarcon-Rodriguez, G. Ault, and S. Galloway, "Multi-objective planning of distributed energy resources: A review of the state-of-the-art," *Renewable and Sustainable Energy Reviews*, vol. 14, no. 5, pp. 1353 – 1366, 2010. [Online]. Available: http://www.sciencedirect.com/science/article/pii/S1364032110000146

[25] M. Fadaee and M. Radzi, "Multi-objective optimization of a stand-alone hybrid renewable energy system by using evolutionary algorithms: A review," *Renewable and Sustainable Energy Reviews*, vol. 16, no. 5, pp. 3364 – 3369, 2012. [Online]. Available: http://www.sciencedirect.com/science/article/pii/S1364032112001669

[26] H. Park and R. Baldick, "Integration of compressed air energy storage systems co-located with wind resources in the ercot transmission system," *International Journal of Electrical Power & Energy Systems*, vol. 90, pp. 181 – 189, 2017. [Online]. Available: http://www.sciencedirect.com/science/article/pii/S0142061516300667

[27] D. Wolf, A. Kanngießer, M. Budt, and C. Doetsch, "Adiabatic compressed air energy storage co-located with wind energy - multifunctional storage commitment optimization for the german market using gomes," *Energy Systems*, vol. 3, no. 2, pp. 181–208, Jun 2012. [Online]. Available: http://dx.doi.org/10.1007/s12667-011-0044-7

[28] H. Lund and G. Salgi, "The role of compressed air energy storage (caes) in future sustainable energy systems," *Energy Conversion and Management*, vol. 50, no. 5, pp. 1172 – 1179, 2009. [Online]. Available: http://www.sciencedirect.com/science/article/pii/S0196890409000429

[29] H. Lund, G. Salgia, B. Elmegaard, and A. Andersen, "Optimal operation strategies of compressed air energy storage (caes) on electricity spot markets with fluctuating prices. journal: Applied thermal engineering." 2009.

[30] M. Abbaspour, M. Satkin, B. Mohammadi-Ivatloo, F. H. Lotfi, and Y. Noorollahi, "Optimal operation scheduling of wind power integrated with compressed air energy storage (caes)," *Renewable Energy*, vol. 51, pp. 53 – 59, 2013. [Online]. Available: http://www.sciencedirect.com/science/article/pii/S0960148112005733

[31] B. C. Cheung, R. Carriveau, and D. S. Ting, "Multi-objective optimization of an underwater compressed air energy storage system using genetic algorithm," *Energy*, vol. 74, pp. 396 – 404, 2014. [Online]. Available: http://www.sciencedirect.com/science/article/pii/S0360544214008251

[32] B. Li and J. F. DeCarolis, "A techno-economic assessment of offshore wind coupled to offshore compressed air energy storage," *Applied Energy*, vol. 155, pp. 315 – 322, 2015. [Online]. Available: http://www.sciencedirect.com/science/article/pii/S0306261915007448

[33] J. Zhang, K. Li, M. Wang, W. Lee, and H. Gao, "A bi-level program for the planning of an islanded microgrid including caes," pp. 1–8, Oct 2015.

[34] H. Daneshi and A. K. Srivastava, "Security-constrained unit commitment with wind generation and compressed air energy storage," *IET Generation, Transmission Distribution*, vol. 6, no. 2, pp. 167–175, February 2012.

[35] F. de Bosio and V. Verda, "Thermoeconomic analysis of a compressed air energy storage (caes) system integrated with a wind power plant in the framework of the ipex market," *Applied Energy*, vol. 152, pp. 173 – 182, 2015. [Online]. Available: http://www.sciencedirect.com/science/article/pii/S0306261915000689

[36] E. Drury, P. Denholm, and R. Sioshansi, "The value of compressed air energy storage in energy and reserve markets," *Energy*, vol. 36, no. 8, pp. 4959 – 4973, 2011, pRES 2010. [Online]. Available: http://www.sciencedirect.com/science/article/pii/S0360544211003665

[37] A. N. Ghalelou, A. P. Fakhri, S. Nojavan, M. Majidi, and H. Hatami, "A stochastic self-scheduling program for compressed air energy storage (caes) of renewable energy sources (ress) based on a demand response mechanism," *Energy Conversion and Management*, vol. 120, pp. 388 – 396, 2016. [Online]. Available: http://www.sciencedirect.com/science/article/pii/S0196890416303399

[38] Y. Gu, J. McCalley, M. Ni, and R. Bo, "Economic modeling of compressed air energy storage," *Energies*, vol. 6, no. 4, pp. 2221–2241, 2013. [Online]. Available: http://www.mdpi.com/1996-1073/6/4/2221

[39] C. Kaldemeyer, C. Boysen, and I. Tuschy, "Compressed air energy storage in the german energy system – status quo & perspectives," *Energy Procedia*, vol. 99, pp. 298 – 313, 2016, 10th International Renewable Energy Storage Conference, IRES 2016, 15-17 March 2016, Düsseldorf, Germany. [Online]. Available: http://www.sciencedirect.com/science/article/

pii/S1876610216310815

[40] ——, "A generic unit commitment formulation for compressed air energy storage plants as mixed integer linear program," *Materials Today*, 2018, 5th International Conference on Nanomaterials and Advanced Energy Storage Systems, INESS 2017, 9-11 August 2017, Astana, Germany. [Online]. Available: http://www.sciencedirect.com/science/article/pii/S1876610216310815

[41] A. Kanngießer, "Entwicklung eines generischen Modells zur Einsatzoptimierung von Energiespeichern für die techno-ökonomische Bewertung stationärer Speicheranwendungen," Ph.D. dissertation, Technische Universität Dortmund, 2014.

[42] H. Khani and R. D. Zadeh, "Energy storage in an open electricity market with contribution to transmission congestion relief," pp. 1–5, July 2014.

[43] Y. Li, S. Miao, X. Luo, and J. Wang, "Optimization model for the power system scheduling with wind generation and compressed air energy storage combination," *International Conference on Automation and Computing (ICAC)*, vol. 22, pp. 300–305, Sept 2016.

[44] Y. Li, S. Miao, S. Zhang, B. Yin, X. Luo, M. Dooner, and J. Wang, "A reserve capacity model of aa-caes for power system optimal joint energy and reserve scheduling," *International Journal of Electrical Power & Energy Systems*, vol. 104, pp. 279 – 290, 2019. [Online]. Available: http://www.sciencedirect.com/science/article/pii/S0142061518309992

[45] R. Madlener and J. Latz, "Economics of centralized and decentralized compressed air energy storage for enhanced grid integration of wind power," *Applied Energy*, vol. 101, pp. 299 – 309, 2013, sustainable Development of Energy, Water and Environment Systems. [Online]. Available: http://www.sciencedirect.com/science/article/pii/S0306261911006362

[46] B. Mauch, P. M. Carvalho, and J. Apt, "Can a wind farm with caes survive in the day-ahead market?" *Energy Policy*, vol. 48, pp. 584 – 593, 2012, special Section: Frontiers of Sustainability. [Online]. Available: http://www.sciencedirect.com/science/article/pii/S0301421512004740

[47] X. Wang, C. Yang, M. Huang, and X. Ma, "Multi-objective optimization of a gas turbine-based cchp combined with solar and compressed air energy storage system," *Energy Conversion and Management*, vol. 164, pp. 93 – 101, 2018. [Online]. Available: http://www.sciencedirect.com/science/article/pii/S0196890418301985

[48] E. Yao, H. Wang, L. Wang, G. Xi, and F. Maréchal, "Multi-objective optimization and exergoeconomic analysis of a combined cooling, heating and power based compressed air energy storage system," *Energy Conversion and Management*, vol. 138, pp. 199 – 209, 2017. [Online]. Available: http://www.sciencedirect.com/science/article/pii/S0196890417300857

[49] A. Yucekaya, "The operational economics of compressed air energy storage systems under uncertainty," *Renewable and Sustainable Energy Reviews*, vol. 22, pp. 298 – 305, 2013. [Online]. Available: http://www.sciencedirect.com/science/article/pii/S1364032113000786

[50] S. Bracco, G. Dentici, and S. Siri, "Economic and environmental optimization model for the design andÂ the operation of a combined heat and power distributed generation system in an urban area," *Energy*, vol. 55, pp. 1014 – 1024, 2013. [Online]. Available: http://www.sciencedirect.com/science/article/pii/S0360544213003046

[51] M. S. Mahbub, M. Cozzini, P. A. Østergaard, and F. Alberti, "Combining multi-objective evolutionary algorithms and descriptive analytical modelling in energy scenario design," *Applied Energy*, vol. 164, pp. 140 – 151, 2016. [Online]. Available: http://www.sciencedirect.com/science/article/pii/S0306261915014920

[52] S. Fazlollahi, S. L. Bungener, G. Becker, and F. Maréchal, "Multi-objectives, multi-period optimization of district heating networks using evolutionary algorithms and mixed integer linear programming (milp)," vol. 30, pp. 262 – 266, 2012. [Online]. Available: http://www.sciencedirect.com/science/article/pii/B9780444595195500538

[53] S. Fazlollahi, P. Mandel, G. Becker, and F. Maréchal, "Methods for multi-objective investment and operating optimization of complex energy systems," *Energy*, vol. 45, no. 1, pp. 12 – 22, 2012, the 24th International Conference on Efficiency, Cost, Optimization, Simulation and Environmental Impact of Energy, ECOS 2011. [Online]. Available: http://www.sciencedirect.com/science/article/pii/S0360544212001600

[54] S. Fazlollahi and F. Maréchal, "Multi-objective, multi-period optimization of biomass conversion technologies using evolutionary algorithms and mixed integer linear programming (milp)," *Applied Thermal Engineering*, vol. 50, no. 2, pp. 1504 – 1513, 2013. [Online]. Available: http://www.sciencedirect.com/science/article/pii/S1359431111006636

[55] S. Fazlollahi, G. Becker, and F. Maréchal, "Multi-objectives, multi-period optimization of district energy systems: Ii—daily thermal storage," *Computers & Chemical Engineering*, vol. 71, pp. 648 – 662, 2014. [Online]. Available: http://www.sciencedirect.com/science/article/pii/S0098135413003384

[56] ——, "Multi-objectives, multi-period optimization of district energy systems: Iii. distribution networks," *Computers & Chemical Engineering*, vol. 66, pp. 82 – 97, 2014, selected papers from ESCAPE-23 (European Symposium on Computer Aided Process Engineering - 23), 9-12 June 2013, Lappeenranta, Finland. [Online]. Available: http://www.sciencedirect.com/science/article/pii/S0098135414000507

[57] S. Fazlollahi, G. Becker, A. Ashouri, and F. Maréchal, "Multi-objective, multi-period optimization of district energy systems: Iv – a case study," *Energy*, vol. 84, pp. 365 – 381, 2015. [Online]. Available: http://www.sciencedirect.com/science/article/pii/S0360544215002856

[58] C. I. Weber, "Multi-objective design and optimization of district energy systems including poly-generation energy conversion technologies," Ph.D. dissertation, École Polytechnique Fédérale de Lausanne, Lausanne, 2008.

[59] A. Christidis, C. Koch, L. Pottel, and G. Tsatsaronis, "The contribution of heat storage to the profitable operation of combined heat and power plants in liberalized electricity markets," *Energy*, vol. 41, no. 1, pp. 75 – 82, 2012, 23rd International Conference on Efficiency, Cost, Optimization, Simulation and Environmental Impact of Energy Systems, {ECOS} 2010. [Online]. Available: //www.sciencedirect.com/science/article/pii/S0360544211004348

[60] I. Dimoulkas, M. Amelin, and F. Levihn, "District heating system operation in power systems with high share of wind power," *Journal of Modern Power Systems and Clean Energy*, vol. 5, no. 6, pp. 850–862, Nov 2017. [Online]. Available: https://doi.org/10.1007/s40565-017-0344-6

[61] D. Böttger, M. Götz, M. Theofilidi, and T. Bruckner, "Control power provision with power-to-heat plants in systems with high shares of renewable energy sources – an illustrative analysis for germany based on the use of electric boilers in district heating grids," *Energy*, vol. 82, pp. 157 – 167, 2015. [Online]. Available: http://www.sciencedirect.com/science/article/pii/S0360544215000419

[62] I. Dimoulkas and M. Amelin, "Constructing bidding curves for a chp producer in day-ahead electricity markets," *2014 IEEE International Energy Conference (ENERGYCON)*, pp. 487–494, May 2014. [Online]. Available: 2014IEEEInternationalEnergyConference(ENERGYCON)

[63] ——, "Probabilistic day-ahead chp operation scheduling," *2015 IEEE Power & Energy Society General Meeting*, pp. 1–5, July 2015. [Online]. Available: https://doi.org/10.1109/PESGM.2015.7285962

[64] C. Milan, M. Stadler, G. Cardoso, and S. Mashayekh, "Modeling of non-linear chp efficiency curves in distributed energy systems," *Applied Energy*, vol. 148, pp. 334 – 347, 2015. [Online]. Available: http://www.sciencedirect.com/science/article/pii/S0306261915003372

[65] S. Mashayekh, M. Stadler, G. Cardoso, and M. Heleno, "A mixed integer linear programming approach for optimal {DER} portfolio, sizing, and placement in multi-energy microgrids," *Applied Energy*, vol. 187, pp. 154 – 168, 2017. [Online]. Available: http://www.sciencedirect.com/science/article/pii/S0306261916316051

[66] B. Morvaj, R. Evins, and J. Carmeliet, "Optimising urban energy systems: Simultaneous system sizing, operation and district heating network layout," *Energy*, vol. 116, pp. 619 – 636, 2016.

[Online]. Available: http://www.sciencedirect.com/science/article/pii/S0360544216314207

[67] ——, "Optimization framework for distributed energy systems with integrated electrical grid constraints," *Applied Energy*, vol. 171, pp. 296 – 313, 2016. [Online]. Available: http://www.sciencedirect.com/science/article/pii/S0306261916304159

[68] ——, "Decarbonizing the electricity grid: The impact on urban energy systems, distribution grids and district heating potential," *Applied Energy*, vol. 191, pp. 125 – 140, 2017. [Online]. Available: http://www.sciencedirect.com/science/article/pii/S0306261917300661

[69] J. P. J. Navarro, K. C. Kavvadias, S. Quoilin, and A. Zucker, "The joint effect of centralised cogeneration plants and thermal storage on the efficiency and cost of the power system," *Energy*, vol. 149, pp. 535 – 549, 2018. [Online]. Available: http://www.sciencedirect.com/science/article/pii/S0360544218302536

[70] M. Sameti and F. Haghighat, "A two-level multi-objective optimization for simultaneous design and scheduling of a district energy system," *Applied Energy*, vol. 208, pp. 1053 – 1070, 2017. [Online]. Available: http://www.sciencedirect.com/science/article/pii/S0306261917313272

[71] G. Taljan, G. Verbič, M. Pantoš, M. Sakulin, and L. Fickert, "Optimal sizing of biomass-fired organic rankine cycle chp system with heat storage," *Renewable Energy*, vol. 41, pp. 29 – 38, 2012. [Online]. Available: http://www.sciencedirect.com/science/article/pii/S0960148111005647

[72] A. Vandermeulen, B. van der Heijde, D. Vanhoudt, R. Salenbien, and L. Helsen, "Modesto - a multi-objective district energy systems toolbox for optimization," *The 5th International Solar District Heating Conference*, pp. 140–147, 2018. [Online]. Available: https://lirias.kuleuven.be/retrieve/509049

[73] S. Samsatli and N. J. Samsatli, "A multi-objective milp model for the design and operation of future integrated multi-vector energy networks capturing detailed spatio-temporal dependencies," *Applied Energy*, vol. 220, pp. 893 – 920, 2018. [Online]. Available: http://www.sciencedirect.com/science/article/pii/S0306261917313375

[74] M. G. Prina, M. Cozzini, G. Garegnani, D. Moser, U. F. Oberegger, R. Vaccaro, and W. Sparber, "Smart energy systems applied at urban level: the case of the municipality of bressanone-brixen," *International Journal of Sustainable Energy Planning and Management*, vol. 10, pp. 33–52, 2016. [Online]. Available: https://doi.org/10.5278/ijsepm.2016.10.4

[75] M. G. Prina, M. Cozzini, G. Garegnani, G. Manzolini, D. Moser, U. F. Oberegger, R. Pernetti, R. Vaccaro, and W. Sparber, "Multi-objective optimization algorithm coupled to energyplan software: The eplanopt model," *Energy*, vol. 149, pp. 213 – 221, 2018. [Online]. Available: http://www.sciencedirect.com/science/article/pii/S0360544218302780

[76] M. G. Prina, L. Fanali, G. Manzolini, D. Moser, and W. Sparber, "Incorporating combined cycle gas turbine flexibility constraints and additional costs into the eplanopt model: The italian case study," *Energy*, vol. 160, pp. 33 – 43, 2018. [Online]. Available: http://www.sciencedirect.com/science/article/pii/S0360544218312957

[77] H. Yousefi, M. H. Ghodusinejad, and A. Kasaeian, "Multi-objective optimal component sizing of a hybrid ice+pv/t driven cchp microgrid," *Applied Thermal Engineering*, vol. 122, pp. 126 – 138, 2017. [Online]. Available: http://www.sciencedirect.com/science/article/pii/S1359431116320038

[78] Y. Hu, Z. Bie, T. Ding, and Y. Lin, "An nsga-ii based multi-objective optimization for combined gas and electricity network expansion planning," *Applied Energy*, vol. 167, pp. 280 – 293, 2016. [Online]. Available: http://www.sciencedirect.com/science/article/pii/S0306261915013902

[79] P. Stadler, A. Ashouri, and F. Maréchal, "Model-based optimization of distributed and renewable energy systems in buildings," *Energy and Buildings*, vol. 120, pp. 103 – 113, 2016. [Online]. Available: http://www.sciencedirect.com/science/article/pii/S0378778816302079

[80] C. A. Kang, A. R. Brandt, and L. J. Durlofsky, "Optimizing heat integration in a flexible coal and natural gas power station with co2 capture," *International Journal of Greenhouse Gas Control*, vol. 31, pp. 138 – 152, 2014. [Online]. Available: http://www.sciencedirect.com/science/article/pii/S1750583614002813

[81] ——, "A new carbon capture proxy model for optimizing the design and time-varying operation of a coal-natural gas power station," *International Journal of Greenhouse Gas Control*, vol. 48, pp. 234 – 252, 2016. [Online]. Available: http://www.sciencedirect.com/science/article/pii/S1750583615301390

[82] J. Deane, A. Chiodi, M. Gargiulo, and B. P. Gallachóir, "Soft-linking of a power systems model to an energy systems model," *Energy*, vol. 42, no. 1, pp. 303 – 312, 2012, 8th World Energy System Conference, WESC 2010. [Online]. Available: http:////www.sciencedirect.com/science/article/pii/S0360544212002551

[83] M. Geidl and G. Andersson, "Operational and topological optimization of multi-carrier energy systems," pp. 6 pp.–6, Nov 2005.

[84] G. Abdollahi and M. Meratizaman, "Multi-objective approach in thermoenvironomic optimization of a small-scale distributed cchp system with risk analysis," *Energy and Buildings*, vol. 43, no. 11, pp. 3144 – 3153, 2011. [Online]. Available: http://www.sciencedirect.com/science/article/pii/S0378778811003446

[85] H. Bilil, G. Aniba, and M. Maaroufi, "Multiobjective optimization of renewable energy penetration rate in power systems," *Energy Procedia*, vol. 50, pp. 368 – 375, 2014. [Online].

Available: http://www.sciencedirect.com/science/article/pii/S1876610214007802

[86] L. Li, P. Liu, Z. Li, and X. Wang, "A multi-objective optimization approach for selection of energy storage systems," *Computers & Chemical Engineering*, vol. 115, pp. 213 – 225, 2018. [Online]. Available: http://www.sciencedirect.com/science/article/pii/S0098135418303223

[87] M. Assembayeva, N. Zhakiyev, and Y. Akhmetbekov, "Impact of storage technologies on renewable energy integration in kazakhstan," *Materials Today: Proceedings*, vol. 4, no. 3, Part A, pp. 4512 – 4523, 2017, 4th International Conference on Nanomaterials and Advanced Energy Storage Systems (INESS 2016), August 11-13, 2016, Almaty, Kazakhstan. [Online]. Available: http://www.sciencedirect.com/science/article/pii/S2214785317305813

[88] M. Assembayeva, J. Egerer, R. Mendelevitch, and N. Zhakiyev, "A spatial electricity market model for the power system: The kazakhstan case study," *Energy*, vol. 149, pp. 762 – 778, 2018. [Online]. Available: http://www.sciencedirect.com/science/article/pii/S036054421830238X

[89] J. Egerer, R. Mendelevitch, and C. von Hirschhausen, "A lower carbon strategy for the electricity sector of kazakhstan to 2030/50: Scenarios for generation and network development; technical report," vol. 85, 2014. [Online]. Available: http://EconPapers.repec.org/RePEc:diw:diwpok:pbk85

[90] C. A. Kang, A. R. Brandt, and L. J. Durlofsky, "Optimal operation of an integrated energy system including fossil fuel power generation, co2 capture and wind," *Energy*, vol. 36, no. 12, pp. 6806 – 6820, 2011. [Online]. Available: http://www.sciencedirect.com/science/article/pii/S0360544211006748

[91] S. Samsatli, N. J. Samsatli, and N. Shah, "Bvcm: A comprehensive and flexible toolkit for whole system biomass value chain analysis and optimisation - mathematical formulation," *Applied Energy*, vol. 147, pp. 131 – 160, 2015. [Online]. Available: http://www.sciencedirect.com/science/article/pii/S0306261915001142

[92] S. Samsatli and N. J. Samsatli, "A general spatio-temporal model of energy systems with a detailed account of transport and storage," *Computers & Chemical Engineering*, vol. 80, pp. 155 – 176, 2015. [Online]. Available: http://www.sciencedirect.com/science/article/pii/S0098135415002008

[93] S. Samsatli, I. Staffell, and N. J. Samsatli, "Optimal design and operation of integrated wind-hydrogen-electricity networks for decarbonising the domestic transport sector in great britain," *International Journal of Hydrogen Energy*, vol. 41, no. 1, pp. 447 – 475, 2016. [Online]. Available: http://www.sciencedirect.com/science/article/pii/S0360319915300574

[94] K.-K. Cao, F. Cebulla, J. J. Gómez Vilchez, B. Mousavi, and S. Prehofer, "Raising awareness in model-based energy scenario studies - a transparency checklist," *Energy, Sustainability*

and Society, vol. 6, no. 1, p. 28, 2016. [Online]. Available: http://dx.doi.org/10.1186/s13705-016-0090-z

[95] R. Morrison, "Energy system modeling: Public transparency, scientific reproducibility, and open development," *Energy Strategy Reviews*, vol. 20, pp. 49 – 63, 2018. [Online]. Available: https://www.sciencedirect.com/science/article/pii/S2211467X17300949

[96] S. Fazlollahi, S. L. Bungener, P. Mandel, G. Becker, and F. Maréchal, "Multi-objectives, multi-period optimization of district energy systems: I. selection of typical operating periods," *Computers & Chemical Engineering*, vol. 65, pp. 54 – 66, 2014. [Online]. Available: http://www.sciencedirect.com/science/article/pii/S0098135414000751

[97] R. T. Marler and J. S. Arora, "The weighted sum method for multi-objective optimization: new insights," *Structural and Multidisciplinary Optimization*, vol. 41, no. 6, pp. 853–862, Jun 2010. [Online]. Available: https://doi.org/10.1007/s00158-009-0460-7

[98] M. Assembayeva, J. Egerer, R. Mendelevitch, and N. Zhakiyev, "Spatial electricity market data for the power system of kazakhstan," *Data in Brief*, vol. 23, p. 103781, 2019. [Online]. Available: http://www.sciencedirect.com/science/article/pii/S2352340919301325

[99] A. Eiben and J. Smith, *Introduction to Evolutionary Computing (Second Edition)*. Springer-Verlag, 2015.

[100] D. H. Wolpert and W. G. Macready, "No free lunch theorems for optimization," *IEEE Transactions on Evolutionary Computation*, vol. 1, no. 1, pp. 67–82, April 1997. [Online]. Available: https://doi.org/10.1109/4235.585893

[101] J. Kallrath, *Gemischt-ganzzahlige Optimierung: Modellierung in der Praxis (2. Auflage)*. Springer-Verlag, 2013.

[102] R. J. Vanderbei, *Linear Programming - Foundations and Extensions*. Spri, 2014.

[103] L. Suhl and T. Mellouli, *Optimierungssysteme: Modelle, Verfahren, Software, Anwendungen (2. Auflage)*. Springer-Verlag, 2009.

[104] K. Deb, "Multi-objective optimization using evolutionary algorithms: An introduction," *Multi-objective Evolutionary Optimisation for Product Design and Manufacturing*, pp. 3–34, 2011. [Online]. Available: https://doi.org/10.1007/978-0-85729-652-8_1

[105] M. T. M. Emmerich and A. H. Deutz, "A tutorial on multiobjective optimization: fundamentals and evolutionary methods," *Natural Computing*, vol. 17, no. 3, pp. 585–609, Sep 2018. [Online]. Available: https://doi.org/10.1007/s11047-018-9685-y

[106] P. J. Fleming, R. C. Purshouse, and R. J. Lygoe, "Many-objective optimization: An engineering design perspective," *International Conference on Evolutionary Multi-Criterion Optimization*, vol. Evolutionary Multi-Criterion Optimization, pp. 14–32, 2005.

[107] R. Marler and J. Arora, "Survey of multi-objective optimization methods for engineering," *Structural and Multidisciplinary Optimization*, vol. 26, no. 6, pp. 369–395, Apr 2004. [Online]. Available: https://doi.org/10.1007/s00158-003-0368-6

[108] G. Mavrotas, "Effective implementation of the Îμ-constraint method in multi-objective mathematical programming problems," *Applied Mathematics and Computation*, vol. 213, no. 2, pp. 455 – 465, 2009. [Online]. Available: http://www.sciencedirect.com/science/article/pii/S0096300309002574

[109] G. Mavrotas and K. Florios, "An improved version of the augmented μ-constraint method (augmecon2) for finding the exact pareto set in multi-objective integer programming problems," *Applied Mathematics and Computation*, vol. 219, no. 18, pp. 9652 – 9669, 2013. [Online]. Available: http://www.sciencedirect.com/science/article/pii/S0096300313002166

[110] N. Riquelme, C. V. Lücken, and B. Baran, "Performance metrics in multi-objective optimization," *Latin American Computing Conference (CLEI)*, pp. 1–11, Oct 2015. [Online]. Available: https://doi.org/10.1109/CLEI.2015.7360024

[111] J. Bader and E. Zitzler, "Hype: An algorithm for fast hypervolume-based many-objective optimization," *Evolutionary Computation*, vol. 19, no. 1, pp. 45–76, 2011. [Online]. Available: https://doi.org/10.1162/EVCO_a_00009

[112] E. Zitzler, L. Thiele, M. Laumanns, C. M. Fonseca, and V. G. da Fonseca, "Performance assessment of multiobjective optimizers: an analysis and review," *IEEE Transactions on Evolutionary Computation*, vol. 7, no. 2, pp. 117–132, April 2003. [Online]. Available: https://doi.org/10.1109/TEVC.2003.810758

[113] A. Auger, J. Bader, D. Brockhoff, and E. Zitzler, "Hypervolume-based multiobjective optimization: Theoretical foundations and practical implications," *Theoretical Computer Science*, vol. 425, pp. 75 – 103, 2012, theoretical Foundations of Evolutionary Computation. [Online]. Available: http://www.sciencedirect.com/science/article/pii/S0304397511002428

[114] L. While and L. Bradstreet, "Applying the wfg algorithm to calculate incremental hypervolumes," *2012 IEEE Congress on Evolutionary Computation*, pp. 1–8, June 2012. [Online]. Available: https://doi.org/10.1109/CEC.2012.6256171

[115] L. While, L. Bradstreet, and L. Barone, "A fast way of calculating exact hypervolumes," *IEEE Transactions on Evolutionary Computation*, vol. 16, no. 1, pp. 86–95, Feb 2012.

[116] K. Nowak, M. Märtens, and D. Izzo, "Empirical performance of the approximation of the least hypervolume contributor," *Lecture Notes in Computer Science*, vol. 8672, 2014. [Online]. Available: https://doi.org/10.1007/978-3-319-10762-2_65

[117] N. Beume, C. M. Fonseca, M. Lopez-Ibanez, L. Paquete, and J. Vahrenhold, "On the complexity of computing the hypervolume indicator," *IEEE Transactions on Evolutionary Computation*, vol. 13, no. 5, pp. 1075–1082, Oct 2009.

[118] L. Kotzur, P. Markewitz, M. Robinius, and D. Stolten, "Impact of different time series aggregation methods on optimal energy system design," *Renewable Energy*, vol. 117, no. Supplement C, pp. 474 – 487, 2018. [Online]. Available: http://www.sciencedirect.com/science/article/pii/S0960148117309783

[119] M. V. Shcherbakov, A. Brebels, N. Shcherbakova, A. Tyukov, T. Janovsky, and V. A. Kamaev, "A survey of forecast error measures," *World Applied Sciences Journa*, vol. 24, pp. 171–176, 2013.

[120] D. L. Davies and D. W. Bouldin, "A cluster separation measure," *IEEE Transactions on Pattern Analysis and Machine Intelligence*, vol. PAMI-1, no. 2, pp. 224–227, April 1979.

[121] F. Domínguez-Muñoz, J. M. Cejudo-López, A. Carrillo-Andrés, and M. Gallardo-Salazar, "Selection of typical demand days for chp optimization," *Energy and Buildings*, vol. 43, no. 11, pp. 3036 – 3043, 2011. [Online]. Available: http://www.sciencedirect.com/science/article/pii/S037877881100329X

[122] K. Poncelet, H. Höschle, E. Delarue, A. Virag, and W. D'haeseleer, "Selecting representative days for capturing the implications of integrating intermittent renewables in generation expansion planning problems," *IEEE Transactions on Power Systems*, vol. 32, no. 3, pp. 1936–1948, May 2017.

[123] P. Nahmmacher, E. Schmid, L. Hirth, and B. Knopf, "Carpe diem: A novel approach to select representative days for long-term power system modeling," *Energy*, vol. 112, pp. 430 – 442, 2016. [Online]. Available: http://www.sciencedirect.com/science/article/pii/S0360544216308556

[124] J. M. F. Rager, "Urban energy system design from the heat perspective using mathematical programming including thermal storage," Ph.D. dissertation, École Polytechnique Fédérale de Lausanne, Lausanne, 2015. [Online]. Available: http://dx.doi.org/10.5075/epfl-thesis-6731

[125] D. Whitley and J. P. Watson, "Complexity theory and the no free lunch theorem," pp. 317–339, 2005. [Online]. Available: https://doi.org/10.1007/0-387-28356-0_11

[126] D. Izzo, M. Ruciński, and F. Biscani, "The generalized island model," *Studies in Computational Intelligence*, vol. 415, 2012.

[127] R. Storn and K. Price, "Differential evolution – a simple and efficient heuristic for global optimization over continuous spaces," *Journal of Global Optimization*, vol. 11, no. 4, pp.

341–359, Dec 1997. [Online]. Available: https://doi.org/10.1023/A:1008202821328

[128] Z. Konfrst, "Parallel genetic algorithms: advances, computing trends, applications and perspectives," *18th International Parallel and Distributed Processing Symposium*, pp. 162–, April 2004.

[129] E. Alba and M. Tomassini, "Parallelism and evolutionary algorithms," *IEEE Transactions on Evolutionary Computation*, vol. 6, no. 5, pp. 443–462, Oct 2002.

[130] M. E. Aydin and V. Yigiit, "Parallel simulated annealing," *Parallel Metaheuristics: A New Class of Algorithms*, pp. 267–287, 2005. [Online]. Available: https://onlinelibrary.wiley.com/doi/abs/10.1002/0471739383.ch12

[131] R. Gämperle, S. Müller, and P. Koumoutsakos, "A parameter study for differential evolution," *International Conference on Advances in Intelligent Systems, Fuzzy Systems, Evolutionary Computation*, 2002.

[132] H. Pedersen and M. Erik, "Good parameters for differential evolution," *Hvass Laboratories. Technical Report no. HL1002*, 2010.

[133] E. Mezura-Montes and A. G. Palomeque-Ortiz, "Parameter control in differential evolution for constrained optimization," *2009 IEEE Congress on Evolutionary Computation*, pp. 1375–1382, May 2009.

[134] R. A. Sarker, S. M. Elsayed, and T. Ray, "Differential evolution with dynamic parameters selection for optimization problems," *IEEE Transactions on Evolutionary Computation*, vol. 18, no. 5, pp. 689–707, Oct 2014.

[135] K. Zielinski, P. Weitkemper, R. Laur, and K.-D. Kammeyer, "Parameter study for differential evolution using a power allocation problem including interference cancellation," *IEEE Congress on Evolutionary Computation*, 2006.

[136] M. Andersson, S. Bandaru, and A. H. Ng, "Tuning of multiple parameter sets in evolutionary algorithms," *Proceedings of the Genetic and Evolutionary Computation Conference*, pp. 533–540, 2016. [Online]. Available: http://doi.acm.org/10.1145/2908812.2908899

[137] A. Eiben and S. Smit, "Parameter tuning for configuring and analyzing evolutionary algorithms," *Swarm and Evolutionary Computation*, vol. 1, no. 1, pp. 19 – 31, 2011. [Online]. Available: http://www.sciencedirect.com/science/article/pii/S2210650211000022

[138] J. Dambrowski and S. Pichlmaier, "Mathematical methods for classification of state-of-charge time series for cycle lifetime prediction," *Advanced Automotive Battery Conference Europe 2012*, 2012.

[139] F. Witte and C. Kaldemeyer, "Cycle detection in time series: Cydets," May 2019. [Online]. Available: https://doi.org/10.5281/zenodo.2806946

[140] A. Christidis, "Thermische Speicher zur Optimierung des Betriebs von Heizkraftwerken in der Fernwärmeversorgung," Ph.D. dissertation, Technische Universität Berlin, 2019.

[141] L. Kotzur, P. Markewitz, M. Robinius, and D. Stolten, "Time series aggregation for energy system design: Modeling seasonal storage," *Applied Energy*, vol. 213, pp. 123 – 135, 2018. [Online]. Available: https://www.sciencedirect.com/science/article/pii/S0306261918300242

[142] oemof developer group, "oemof - open energy modelling framework (v0.2.1)," 2018. [Online]. Available: https://doi.org/10.5281/zenodo.1203601

[143] F. Biscani and D. Izzo, "esa/pagmo2: pagmo 2.13.0," Jan. 2020. [Online]. Available: https://doi.org/10.5281/zenodo.3603747

[144] Zenodo.org, "About Zenodo," 2020. [Online]. Available: https://about.zenodo.org/

[145] C. Kaldemeyer, "Customized version of oemof 0.2.3dev," 2020. [Online]. Available: https://doi.org/10.5281/zenodo.3702453

[146] ——, "(A)pplication (s)tarter for (o)emof solph (m)odels," 2020. [Online]. Available: https://doi.org/10.5281/zenodo.3726565

[147] ——, "(E)volutionary (c)omputing for (o)emof solph (m)odels," 2020. [Online]. Available: https://doi.org/10.5281/zenodo.3726919

[148] ——, "ZNES Clustering," Mar. 2020. [Online]. Available: https://doi.org/10.5281/zenodo.3726585

[149] ——, "Compressed Air Energy Storage (CAES) Model," 2020. [Online]. Available: https://doi.org/10.5281/zenodo.3726583

[150] C. Kaldemeyer and C. Boysen, "Heat Component Models," 2020. [Online]. Available: https://doi.org/10.5281/zenodo.3726582

[151] C. Kaldemeyer, "ZNES Plotting," 2020. [Online]. Available: https://doi.org/10.5281/zenodo.3726586

[152] E. Jones, T. Oliphant, P. Peterson *et al.*, "Scipy: Open source scientific tools for python," 2019. [Online]. Available: http://www.scipy.org/

[153] J. Wang, K. Lu, L. Ma, J. Wang, M. Dooner, S. Miao, J. Li, and D. Wang, "Overview of compressed air energy storage and technology development," *Energies*, vol. 10, no. 7, 2017. [Online]. Available: https://www.mdpi.com/1996-1073/10/7/991

[154] M. Nakhamkin, L. Andersson, E. Swensen, J. Howard, R. Meyer, R. Schainker, R. Pollak, and B. Mehta, "Aec 110 mw caes plant: Status of project." 1992.

[155] D. Wolf, "Methods for design and application of adiabatic compressed air energy storage based on dynamic modeling," Ph.D. dissertation, Fraunhofer-Institut fuer Umwelt-, Sicherheits- und Energietechnik (UMSICHT), 2011.

[156] A. Dietrich, "Assessment of Pumped Heat Electricity Storage Systems through Exergoeconomic Analyses," Ph.D. dissertation, TU Darmstadt, Darmstadt, 2017. [Online]. Available: http://tuprints.ulb.tu-darmstadt.de/6752/

[157] A. Bejan, G. Tsatsaronis, and M. Moran, *Thermal Design and Optimization*, ser. Wiley-Interscience publication. Wiley, 1995. [Online]. Available: https://books.google.de/books?id=sTi2crXeZYgC

[158] R. Turton, *Analysis, Synthesis, and Design of Chemical Processes*, ser. Prentice-Hall international series in the physical and chemical engineering sciences. Prentice Hall, 2009. [Online]. Available: https://books.google.de/books?id=YEJHAQAAIAAJ

[159] I. Tuschy, "Druckluftspeicherkraftwerke als Option zur Netzintegration erneuerbarer Energiequellen: Ein Vergleich der Konzepte," *Tagungsband zum 40. Kraftwerkstechnischen Kolloquium*, 2008.

[160] M. H. E. Steck, "Entwicklung und Bewertung von Algorithmen zur Einsatzplanerstellung virtueller Kraftwerke," Ph.D. dissertation, Technische Universitaet Muenchen, 2013.

[161] A. Christidis, E. Mollenhauer, G. Tsatsaronis, G. K. Schuchardt, S. Holler, D. Böttger, and T. Bruckner, "EnEff-Wärme: Einsatz von Wärmespeichern und Power-to-Heat-Anlagen in der Fernwärmeerzeugung," *Forschungsbericht*, 2017.

[162] IRENA, "Electricity storage and renewables for island power - a guide for decision makers," 2012. [Online]. Available: http://www.irena.org/DocumentDownloads/Publications/Electricity%20Storage%20and%20RE%20for%20Island%20Power.pdf

[163] P. Hochloff, J. von Appen, T. Trost, N. Gerhardt, M. Puchta, M. Jentsch, M. Schreiber, K. Rohrig, B. Meyer, M. Wendorff, A. Hashemi, A. Kanngießer, A. Grevé, and C. Doetsch, "Metastudie energiespeicher," 2015. [Online]. Available: http://www.umsicht.fraunhofer.de/de/presse-medien/2015/metastudie-energiespeicher.html

[164] P. Rundel, B. Meyer, M. Meiller, I. Meyer, R. Daschner, M. Jakuttis, M. Franke, S. Binder, and A. Hornung, "Speicher für die Energiewende," *Fraunhofer Institut für Fertigungstechnik und angewandte Materialforschung*, 2013.

[165] P. Elsner, M. Fischedick, and D. Sauer, *Flexibilitätskonzepte für die Stromversorgung 2050: Technologien – Szenarien – Systemzusammenhänge*, 2015.

[166] B. Zakeri and S. Syri, "Electrical energy storage systems: A comparative life cycle cost analysis," *Renewable and Sustainable Energy Reviews*, vol. 42, pp. 569 – 596, 2015. [Online]. Available: http://www.sciencedirect.com/science/article/pii/S1364032114008284

[167] A. Gillhaus, F. Crotogino, and S. Hübner, "Verbesserte Integration grosser Windstrommengen durch Zwischenspeicherung mittels CAES," 2007.

[168] Powernext, "Pegas reference prices - publication of the european gas index (egix) to increase transparency on the market," 2019. [Online]. Available: https://www.powernext.com/sites/default/files/download_center_files/20190603_PEGAS_Reference_Price_EGIX.pdf

[169] J. Conrad, C. Pellinger, and M. Hinterstocker, "Gutachten zur Rentabilität von Pumpspeicherkraftwerken," *Forschungsstelle für Energiewirtschaft (FFE)*, 2014.

[170] F. Crotogino, K.-U. Mohmeyer, and R. Scharf, "Huntorf caes: More than 20 years of successful operation." [Online]. Available: http://www.uni-saarland.de/fak7/fze/AKE_Archiv/AKE2003H/AKE2003H_Vortraege/AKE2003H03c_Crotogino_ea_HuntorfCAES_CompressedAirEnergyStorage.pdf

[171] R. Jiang, H. Yin, K. Peng, and Y. Xu, "Multi-objective optimization, design and performance analysis of an advanced trigenerative micro compressed air energy storage system," *Energy Conversion and Management*, vol. 186, pp. 323 – 333, 2019. [Online]. Available: http://www.sciencedirect.com/science/article/pii/S0196890419302626

[172] K. Deb, A. Pratap, S. Agarwal, and T. Meyarivan, "A fast and elitist multiobjective genetic algorithm: Nsga-ii," *IEEE Transactions on Evolutionary Computation*, vol. 6, no. 2, pp. 182–197, Apr 2002.

[173] K. De Jong, "Parameter setting in eas: a 30 year perspective," *Studies in Computational Intelligence*, vol. 54, pp. 1–18, 04 2007.

[174] A. M. Vogelsang, "Mehrzieloptimierung von solarthermischen Parabolrinnenkraftwerken unter Berücksichtigung variabler Vergütungsschemata mit Hilfe technischer Auslegungsparameter," Ph.D. dissertation, Europa-Universität Flensburg, 2014.

[175] P. Havel and T. Simovic, "Optimal planning of cogeneration production with provision of ancillary services. journal: Electric power systems research." 2012.

[176] H. Lund, S. Werner, R. Wiltshire, S. Svendsen, J. E. Thorsen, F. Hvelplund, and B. V. Mathiesen, "4th generation district heating (4gdh): Integrating smart thermal grids into future sustainable energy systems," *Energy*, vol. 68, pp. 1 – 11, 2014. [Online]. Available: http://www.sciencedirect.com/science/article/pii/S0360544214002369

[177] S. Hilpert, M. Söthe, and C. Wingenbach, "ANGUSII Scenarios: German Energy System 2030," Jul. 2019, The work has been funded by the Federal Ministry of Economic Affairs, Germany. [Online]. Available: https://doi.org/10.5281/zenodo.3346905

[178] C. Boysen, C. Kaldemeyer, and I. Tuschy, "Druckluftspeicherkraftwerk Schleswig-Holstein - Untersuchung zur Eignung Schleswig-Holsteins als Modellstandort für die Energiewende. Forschungsergebnisse 5." 2017.

[179] ——, "Elektrizitätsnetzgekoppelte Fernwärmeversorgung 2020 - Untersuchung von Flexibilitätsoptionen in der Wärmeversorgung. Forschungsergebnisse 9." 2019.

[180] I. Tuschy, C. Boysen, C. Kaldemeyer, and C. Kapp, "Kraft-Wärme-Kopplung oder Power-to-Heat – Netzgekoppelte Wärmeversorgung bei einem steigenden Anteil erneuerbarer Energien," *Tagungsband zum 50. Kraftwerkstechnischen Kolloquium*, 2018.

[181] E. Mollenhauer, A. Christidis, and G. Tsatsaronis, "Evaluation of an energy- and exergy-based generic modeling approach of combined heat and power plants," *International Journal of Energy and Environmental Engineering*, vol. 7, no. 2, pp. 167–176, 2016. [Online]. Available: http://dx.doi.org/10.1007/s40095-016-0204-6

[182] F. Salgado and P. Pedrero, "Short-term operation planning on cogeneration systems: A survey," *Electric Power Systems Research*, 2007.

[183] B. Bach, J. Werling, T. Ommen, M. Münster, J. M. Morales, and B. Elmegaard, "Integration of large-scale heat pumps in the district heating systems of greater copenhagen," *Energy*, vol. 107, pp. 321 – 334, 2016. [Online]. Available: http://www.sciencedirect.com/science/article/pii/S0360544216304352

[184] A. Bischi, L. Taccari, E. Martelli, E. Amaldi, G. Manzolini, P. Silva, S. Campanari, and E. Macchi, "A detailed milp optimization model for combined cooling, heat and power system operation planning," *Energy*, vol. 74, pp. 12 – 26, 2014. [Online]. Available: http://www.sciencedirect.com/science/article/pii/S0360544214001765

[185] M. B. Blarke, "Towards an intermittency-friendly energy system: Comparing electric boilers and heat pumps in distributed cogeneration," *Applied Energy*, vol. 91, no. 1, pp. 349 – 365, 2012. [Online]. Available: http://www.sciencedirect.com/science/article/pii/S030626191100643X

[186] H. Wang, W. Yin, E. Abdollahi, R. Lahdelma, and W. Jiao, "Modelling and optimization of chp based district heating system with renewable energy production and energy storage," *Applied Energy*, vol. 159, pp. 401 – 421, 2015. [Online]. Available: http://www.sciencedirect.com/science/article/pii/S0306261915010909

[187] T. Schütz, R. Streblow, and D. Müller, "A comparison of thermal energy storage models for building energy system optimization," *Energy and Buildings*, vol. 93, pp. 23 – 31, 2015. [Online]. Available: http://www.sciencedirect.com/science/article/pii/S037877881500136X

[188] A. Bloess, W.-P. Schill, and A. Zerrahn, "Power-to-heat for renewable energy integration: A review of technologies, modeling approaches, and flexibility potentials," *Applied Energy*, vol. 212, pp. 1611 – 1626, 2018. [Online]. Available: https://www.sciencedirect.com/science/article/pii/S0306261917317889

[189] Gurobi Optimization, "Gurobi - the most powerful mathematical optimization solver," 2020. [Online]. Available: http://www.gurobi.com

[190] J. Gearhart, K. Adair, R. Detry, J. Durfee, K. Jones, and N. Martin, "Comparison of open-source linear programming solvers," *Sandia National Laboratories*, vol. Sandia Reports, no. SAND2013-8847, 2013.

[191] Q. Zhang and H. Li, "Moea/d: A multiobjective evolutionary algorithm based on decomposition," *IEEE Transactions on Evolutionary Computation*, vol. 11, no. 6, pp. 712–731, Dec 2007.

[192] H. Li and Q. Zhang, "Multiobjective optimization problems with complicated pareto sets, moea/d and nsga-ii," *IEEE Transactions on Evolutionary Computation*, vol. 13, no. 2, pp. 284–302, April 2009.

[193] W. Peng, Q. Zhang, and H. Li, "Comparison between moea/d and nsga-ii on the multiobjective travelling salesman problem," *Studies in Computational Intelligence*, vol. 171, 2007.

[194] N. Qamar, N. Akhtar, and I. Younas, "Comparative analysis of evolutionary algorithms for multi-objective travelling salesman problem," *International Journal of Advanced Computer Science and Applications*, vol. 9, 01 2018.

[195] R. Turconi, A. Boldrin, and T. Astrup, "Life cycle assessment (lca) of electricity generation technologies: Overview, comparability and limitations," *Renewable and Sustainable Energy Reviews*, vol. 28, pp. 555 – 565, 2013. [Online]. Available: http://www.sciencedirect.com/science/article/pii/S1364032113005534

[196] IPCC Working Group III, "Mitigation of climate change, annex iii: Technology - specific cost and performance parameters," 2014. [Online]. Available: https://www.ipcc.ch/report/ar5/wg3/

[197] M. Casisi, P. Pinamonti, and M. Reini, "Optimal lay-out and operation of combined heat & power (chp) distributed generation systems," *Energy*, vol. 34, no. 12, pp. 2175 – 2183, 2009, eCOS 2007. [Online]. Available: http://www.sciencedirect.com/science/article/pii/S0360544208002594

[198] J. Nitsch, T. Pregger, T. Naegler, D. Heide, D. L. de Tena, F. Trieb, Y. Scholz, K. Nienhaus, N. Gerhardt, M. Sterner, T. Trost, A. von Oehsen, R. Schwinn, C. Pape, H. Hahn, M. Wickert,

and B. Wenzel, "Langfristszenarien und Strategien für den Ausbau der erneuerbaren Energien in Deutschland bei Berücksichtigung der Entwicklung in Europa und global," 2012.

[199] "Annual report of joint-stock company kazakhstan electricity grid operating company (kegoc) - 2016," 2016. [Online]. Available: http://www.kase.kz/files/emitters/KEGC/kegcp_2015_eng.pdf

[200] "Operation of electric power industry in kazakhstan in 2013," 2015. [Online]. Available: http://kegoc.kz/

[201] "Kazenergy 2015: The national energy report," 2015. [Online]. Available: http://www.kazenergy.com/images/NationalReport15_English.pdf

[202] KazTransGas (KTG), "Annual report 2015," 2015. [Online]. Available: http://www.kaztransgas.kz/files/ktg_annual_report_2015.pdf

[203] "Concept for transition of the republic of kazakhstan to green economy," 2013. [Online]. Available: http://gbpp.org/wp-content/uploads/2014/04/Green_Concept_En.pdf

[204] M. Karatayev and M. L. Clarke, "Current energy resources in kazakhstan and the future potential of renewables: A review," *Energy Procedia*, vol. 59, pp. 97 – 104, 2014, european Geosciences Union General Assembly 2014, EGU Division Energy, Resources & the Environment (ERE). [Online]. Available: http://www.sciencedirect.com/science/article/pii/S1876610214017214

[205] M. Karatayev, S. Hall, Y. Kalyuzhnova, and M. L. Clarke, "Renewable energy technology uptake in kazakhstan: Policy drivers and barriers in a transitional economy," *Renewable and Sustainable Energy Reviews*, vol. 66, pp. 120 – 136, 2016. [Online]. Available: http://www.sciencedirect.com/science/article/pii/S1364032116303847

[206] M. Karatayev and M. L. Clarke, "A review of current energy systems and green energy potential in kazakhstan," *Renewable and Sustainable Energy Reviews*, vol. 55, pp. 491 – 504, 2016. [Online]. Available: http://www.sciencedirect.com/science/article/pii/S1364032115011570

[207] D. Bogdanov, A. Toktarova, and C. Breyer, "Transition towards 100power and heat supply for energy intensive economies and severe continental climate conditions: Case for kazakhstan," *Applied Energy*, vol. 253, p. 113606, 2019. [Online]. Available: http://www.sciencedirect.com/science/article/pii/S0306261919312802

[208] I. Tsiropoulos, D. Tarvydas, and A. Zucker, "Cost development of low carbon energy technologies - scenario-based cost trajectories to 2050," *Joint Research Centre of the European Commission.*, 2018.

[209] EIA, "Annual energy outlook 2015: with projections to 2040," 2017.

[210] P. L. Joskow, "Comparing the costs of intermittent and dispatchable electricity generating technologies," *American Economic Review*, vol. 101, no. 3, pp. 238–41, May 2011. [Online]. Available: http://www.aeaweb.org/articles?id=10.1257/aer.101.3.238

[211] C. Kost, S. Shammugam, V. Jülch, H.-T. Nguyen, and T. Schlegl, "Levelized cost of electricity renewable energy technologies," *Fraunhofer Institute for Solar Energy Systems ISE*, 2018.

[212] P. Konstantin, *Praxisbuch Energiewirtschaft - Energieumwandlung, -transport und -beschaffung im liberalisierten Markt (3. Auflage)*. Springer-Verlag, 2013.

[213] G. Allan, M. Gilmartin, P. McGregor, and K. Swales, "Levelised costs of wave and tidal energy in the uk: Cost competitiveness and the importance of "banded" renewables obligation certificates," *Energy Policy*, vol. 39, no. 1, pp. 23 – 39, 2011. [Online]. Available: http://www.sciencedirect.com/science/article/pii/S0301421510006440

[214] C. S. Lai and M. D. McCulloch, "Levelized cost of energy for pv and grid scale energy storage systems," *Computing Research Repository*, 2016. [Online]. Available: http://arxiv.org/abs/1609.06000

[215] F. Ueckerdt, L. Hirth, G. Luderer, and O. Edenhofer, "System lcoe: What are the costs of variable renewables?" *Energy*, vol. 63, pp. 61 – 75, 2013. [Online]. Available: http://www.sciencedirect.com/science/article/pii/S0360544213009390

[216] A. Schröder, F. Kunz, J. Meiss, R. Mendelevitch, and C. von Hirschhausen, "Current and prospective costs of electricity generation until 2050," *Deutsches Institut für Wirtschaftsforschung (DIW) Data Documentation*, 2013.

[217] XE, "Current and historical rate tables," 2020. [Online]. Available: https://www.xe.com/currencytables/?from=KZT&date=2020-01-20

[218] Landesamt für Umwelt Brandenburg, "CO2 - Emissionsfaktoren nach Energieträgern," 2020. [Online]. Available: https://lfu.brandenburg.de/cms/detail.php/bb1.c.523833.de

[219] I. Staffell and S. Pfenninger, "Using bias-corrected reanalysis to simulate current and future wind power output," *Energy*, vol. 114, pp. 1224 – 1239, 2016. [Online]. Available: http://www.sciencedirect.com/science/article/pii/S0360544216311811

[220] S. Pfenninger and I. Staffell, "Long-term patterns of european pv output using 30 years of validated hourly reanalysis and satellite data," *Energy*, vol. 114, pp. 1251 – 1265, 2016. [Online]. Available: http://www.sciencedirect.com/science/article/pii/S0360544216311744

[221] J. Ortiga, J. Bruno, and A. Coronas, "Selection of typical days for the characterisation of energy demand in cogeneration and trigeneration optimisation models for buildings," *Energy Conversion and Management*, vol. 52, no. 4, pp. 1934 – 1942, 2011. [Online]. Available:

http://www.sciencedirect.com/science/article/pii/S0196890410005315

[222] X. Li, "A non-dominated sorting particle swarm optimizer for multiobjective optimization," *Lecture Notes in Computer Science*, vol. 2723, pp. 37–48, 2003.

[223] R. Eberhart and J. Kennedy, "A new optimizer using particle swarm theory," *Proceedings of the Sixth International Symposium on Micro Machine and Human Science*, pp. 39–43, Oct 1995.

[224] J. Kennedy and R. Eberhart, "Particle swarm optimization," *Proceedings of the International Conference on Neural Networks*, vol. 4, pp. 1942–1948 vol.4, Nov 1995.

[225] X. Li, "Better spread and convergence: Particle swarm multiobjective optimization using the maximin fitness function," *Lecture Notes in Computer Science*, vol. 3102, pp. 117–128, 2004.

[226] J. Egerer, R. Mendelevitch, and C. von Hirschhausen, "A Lower Carbon Strategy for the Electricity Sector of Kazakhstan to 2030/50: Scenarios for Generation and Network Development," 2014. [Online]. Available: http://www.diw.de/documents/publikationen/73/diw_01.c.478677.de/diwkompakt_2014-085.pdf

[227] T. Brown, D. Schlachtberger, A. Kies, S. Schramm, and M. Greiner, "Synergies of sector coupling and transmission reinforcement in a cost-optimised, highly renewable european energy system," *Energy*, vol. 160, pp. 720 – 739, 2018. [Online]. Available: http://www.sciencedirect.com/science/article/pii/S036054421831288X

[228] C. Bussar, P. Stoecker, Z. Cai, L. M. Jr., D. Magnor, P. Wiernes, N. van Bracht, A. Moser, and D. U. Sauer, "Large-scale integration of renewable energies and impact on storage demand in a european renewable power system of 2050 - a sensitivity study," *Journal of Energy Storage*, vol. 6, pp. 1 – 10, 2016. [Online]. Available: http://www.sciencedirect.com/science/article/pii/S2352152X16300135

[229] J. Hoersch and T. Brown, "The role of spatial scale in joint optimisations of generation and transmission for european highly renewable scenarios," *14th International Conference on the European Energy Market (EEM)*, pp. 1–7, June 2017. [Online]. Available: https://doi.org/10.1109/EEM.2017.7982024

[230] M. Milligan, E. Ela, B.-M. Hodge, B. Kirby, D. Lew, C. Clark, J. DeCesaro, and K. Lynn, "Integration of variable generation, cost-causation, and integration costs," *The Electricity Journal*, vol. 24, no. 9, pp. 51 – 63, 2011. [Online]. Available: http://www.sciencedirect.com/science/article/pii/S1040619011002636

[231] H. Holttinen, P. Meibom, A. Orths, B. Lange, M. O'Malley, J. O. Tande, A. Estanqueiro, E. Gomez, L. Soeder, G. Strbac, J. C. Smith, and F. van Hulle, "Impacts of large amounts of wind power on design and operation of power systems, results of iea collaboration," *Wind Energy*, vol. 14, no. 2,

pp. 179–192, 2011. [Online]. Available: https://onlinelibrary.wiley.com/doi/abs/10.1002/we.410

[232] H. Holttinen, M. OMalley, J. Dillon, D. Flynn, A. Keane, H. Abildgaard, and L. Söder, "Steps for a complete wind integration study," *46th Hawaii International Conference on System Sciences*, pp. 2261–2270, Jan 2013.

[233] M. Joos and I. Staffell, "Short-term integration costs of variable renewable energy: Wind curtailment and balancing in britain and germany," *Renewable and Sustainable Energy Reviews*, vol. 86, pp. 45 – 65, 2018. [Online]. Available: http://www.sciencedirect.com/science/article/pii/S1364032118300091

[234] R. Sims, P. Mercado, W. Krewitt, G. Bhuyan, D. Flynn, H. Holttinen, G. Jannuzzi, S. Khennas, Y. Liu, L. J. Nilsson, and et al., "Integration of renewable energy into present and future energy systems," *Renewable Energy Sources and Climate Change Mitigation: Special Report of the Intergovernmental Panel on Climate Change*, p. 609–706, 2011. [Online]. Available: https://doi.org/10.1017/CBO9781139151153.012

[235] S. Ahmad, A. Nadeem, G. Akhanova, T. Houghton, and F. Muhammad-Sukki, "Multi-criteria evaluation of renewable and nuclear resources for electricity generation in kazakhstan," *Energy*, vol. 141, pp. 1880 – 1891, 2017. [Online]. Available: http://www.sciencedirect.com/science/article/pii/S0360544217319618

[236] M. Haberg, "Fundamentals and recent developments in stochastic unit commitment," *International Journal of Electrical Power & Energy Systems*, vol. 109, pp. 38 – 48, 2019. [Online]. Available: http://www.sciencedirect.com/science/article/pii/S014206151832547X

[237] T. Ommen, W. Brix Markussen, and B. Elmegaard, "Comparison of linear, mixed integer and non-linear programming methods in energy system dispatch modelling. journal: Energy." 2014.

[238] J. M. Zepter and J. Weibezahn, "Unit commitment under imperfect foresight - the impact of stochastic photovoltaic generation," *Applied Energy*, vol. 243, pp. 336 – 349, 2019. [Online]. Available: http://www.sciencedirect.com/science/article/pii/S0306261919306026

[239] M. Sameti and F. Haghighat, "Optimization approaches in district heating and cooling thermal network," *Energy and Buildings*, vol. 140, pp. 121 – 130, 2017. [Online]. Available: http://www.sciencedirect.com/science/article/pii/S0378778816312245

[240] H. Lund, B. Möller, B. Mathiesen, and A. Dyrelund, "The role of district heating in future renewable energy systems," *Energy*, vol. 35, no. 3, pp. 1381 – 1390, 2010. [Online]. Available: http://www.sciencedirect.com/science/article/pii/S036054420900512X

[241] J. A. M.-V. Gerardo Guerra, "Optimal sizing and operation of energy storage systems considering long term assessment," *AIMS Energy*, vol. 6, p. 70, 2018.

[242] O. J. Isebor and L. J. Durlofsky, "Biobjective optimization for general oil field development," *Journal of Petroleum Science and Engineering*, vol. 119, pp. 123 – 138, 2014. [Online]. Available: http://www.sciencedirect.com/science/article/pii/S0920410514001090

Appendix

A Related research

This thesis was developed during my time as a research associate at the Center for Sustainable Energy Systems (ZNES) of the Flensburg University of Applied Sciences and Europa-Universität Flensburg from 2015 to 2020. During this time, I was financed by several third party research projects with companies and organisations from the public and private sector. A brief overview of the most relevant research activities is provided below.

Research projects

Project „ANGUS II - Integration unterirdischer Speichertechnologien in die Energiesystemtransformation am Beispiel des Modellgebietes Schleswig-Holstein" (2018 - 2020)

Project „Elektrizitätsnetzgekoppelte Fernwärmeversorgung - Untersuchung technischer, wirtschaftlicher und ökologischer Konzepte zur elektrizitätsnetzgekoppelten Wärmebereitstellung" (2016 - 2018)

Project „Druckluftspeicherkraftwerk Schleswig-Holstein - Machbarkeitsanalyse zur Eignung Schleswig-Holsteins als Standort für ein Druckluftspeicherkraftwerk" (2014 - 2016)

Project „Open Energy Modelling Framework - A free and open toolbox to model energy supply system" (2014 - ongoing)

Peer-reviewed articles

Kaldemeyer, C.; Hilpert, S.; Assembayeva, M. & Prina, M. G., Multi-objective optimal design and operation of energy supply systems - Integration of wind and solar into the power system of Kazakhstan. Energies, 2020 [to be submitted]

Krien, U.; Schönfeld, P.; Hilpert, S.; Kaldemeyer, C.; Plessmann, G. & Launer, J., oemof.solph - A model generator for linear and mixed-integer linear optimization of energy systems. Software Impacts, 2020 [submitted]

Prina, M. G.; Casalicchio, V.; Kaldemeyer, C.; Manzolini, G; Moser, D.; Wanitschke, A. &Sparber, W., Multi-objective investment optimization for energy system models in high temporal and spatial resolution. Applied Energy, 2020

Boysen, C.; Kaldemeyer, C.; Hilpert, S. & Tuschy, I., Integration of Flow Temperatures in Unit Commitment Models of Future District Heating Systems. Energies, 12, 2019

Hilpert, S.; Kaldemeyer, C.; Krien, U.; Günther, S.; Wingenbach, C. & Plessmann, G. The Open Energy Modelling Framework (oemof) - A new approach to facilitate open science in energy system modelling. Energy Strategy Reviews, 22, 16-25, 2018

Wiese, F.; Hilpert, S.; Kaldemeyer, C. & Pleßmann, G. A qualitative evaluation approach for energy system modelling frameworks. Energy, Sustainability and Society, 8, 13, 2018

Kaldemeyer, C.; Boysen, C. & Tuschy, I. A Generic Unit Commitment Formulation for Compressed Air Energy Storage Plants as Mixed Integer Linear Program. Materials Today, 2018

Kaldemeyer, C.; Boysen, C. & Tuschy, I. Compressed Air Energy Storage in the German Energy System – Status Quo & Perspectives Energy Procedia. 99, 298-313, 2016

Other articles

Tuschy, I.; Boysen, C.; Kaldemeyer, C. & Kapp, C. Kraft-Wärme-Kopplung oder Power-to-Heat - Netzgekoppelte Wärmeversorgung bei einem steigenden Anteil erneuerbarer Energien. Erschienen im Tagungsband zum 50. Kraftwerkstechnischen Kolloquium Technische Universität Dresden, 2018

Research reports

Boysen, C.; Kaldemeyer, C. & Tuschy, I., Elektrizitätsnetzgekoppelte Fernwärmeversorgung 2020 - Untersuchung von Flexibilitätsoptionen in der Wärmeversorgung. Forschungsergebnisse 9. Zentrum für nachhaltige Energiesysteme (ZNES), 2019

Boysen, C.; Kaldemeyer, C. & Tuschy, I. Druckluftspeicherkraftwerk Schleswig-Holstein - Untersuchung zur Eignung Schleswig-Holsteins als Modellstandort für die Energiewende. Forschungsergebnisse 5. Zentrum für nachhaltige Energiesysteme (ZNES), 2017

Posters and other presentations

Kaldemeyer, C.; Boysen, C. & Tuschy, I., "The Technology Perspective of Compressed Air Energy Storage in the German Energy System", 11th International Renewable Energy Storage Conference, Düsseldorf, 2017

Kaldemeyer, C.; Boysen, C. & Tuschy, I., "A Generic Unit Commitment Formulation for Compressed Air Energy Storage Plants", INESS 5th International Conference on Nanomaterials and Advanced Energy Storage Systems, Astana, 2017

Kaldemeyer, C.; Boysen, C. & Tuschy, I., "Compressed Air Energy Storage in the German Energy System Status Quo & Perspectives", 10th International Renewable Energy Storage Conference, Düsseldorf, 2016

Hilpert, S.; Kaldemeyer, C.; Krien, U.; Günther, S., "solph - An Open Multi-Purpose Optimisation Library for Flexible Energy System Analysis", 12th Conference on Sustainable Development of Energy, Water and Environment Systems Dubrovnik, Croatia, 2017

Wingenbach, C.; Hilpert, S.; Günther, S.; Kaldemeyer, C., Modelling of energy, material and commodity flows based on bipartite, directed graphs and linear and non-linear programs", 12th Conference on Sustainable Development of Energy, Water and Environment Systems Dubrovnik, Croatia, 2017

Oral presentations

"Integration of varying flow temperatures in unit commitment models of future district heating systems", 4th International Conference on Smart Energy Systems and 4th Generation District Heating, Aalborg, Denmark, 2018

"Research activities at the Center for Sustainable Energy Systems (ZNES) Flensburg, Germany", Burabay Forum: Cooperation between bordering regions of Kazakhstan and Russia, Astana, Kazakhstan, 2017

"Modelling a compressed air energy storage (CAES) as a complex oemof component", oemof User Meeting, Berlin, 2017

"The Open Energy Modelling Framework (oemof) - Toolboxes and applications", Open Energy Modelling Workshop, Frankfurt, 2017

"Open Energy Modelling Framework (oemof) - A modular open source framework to model energy supply systems", 6. Fachtagung des Fördervereins Energie- und Umweltmanagement (EUM), Flensburg, 2016

"Forschungsprojekt Druckluftspeicherkraftwerk Schleswig-Holstein", Energiespeichertagung Schleswig-Holstein, Reußenköge, 2015

Supervised theses

Bachelor thesis, Adrian Grimm, "Zukünftige technische Anforderungen für Windenergieanlagen zur Erbringung von Regelleistung in Deutschland", 2018

Master thesis, Mario Kropshofer, "Entwicklung einer Methodik zur wirtschaftlichen und technischen Optimierung des deutschen Netzausbaus in der Hoch- und Höchstspannungsebene", 2017

Master thesis, Timo Rogge, "Entwicklung eines Betriebsmodells für dezentrale Batteriespeichersysteme zum kombinierten Einsatz für Eigenverbrauchssteigerung und Primärregelleistung am Beispiel des Pilotprojektes SunBESSy", 2016

Teaching

Master course "Introduction to Energy System Modelling and Optimisation", Europa-Universität Flensburg, Summer semester, 2016

Tutorial "Thermodynamics", Flensburg University of Applied Sciences, Winter semester, 2015

B Figures
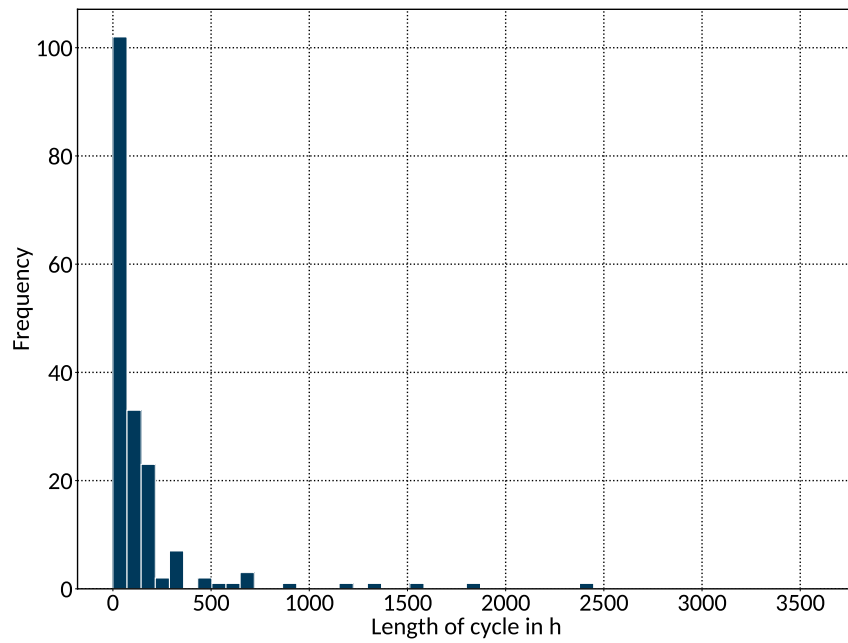
Figure 9.1: Histogram of CAES cycle lengths. A bin width of 72 h is chosen to group a total of 181 cycles.
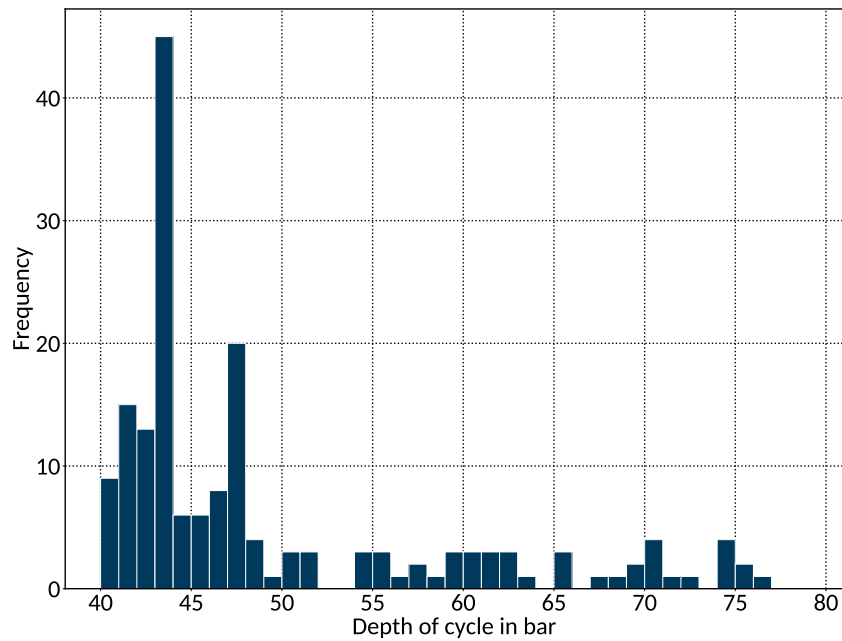

Figure 9.2: Histogram of CAES cycle amplitudes. A bin width of 1 bar is chosen to group a total of 181 cycles.
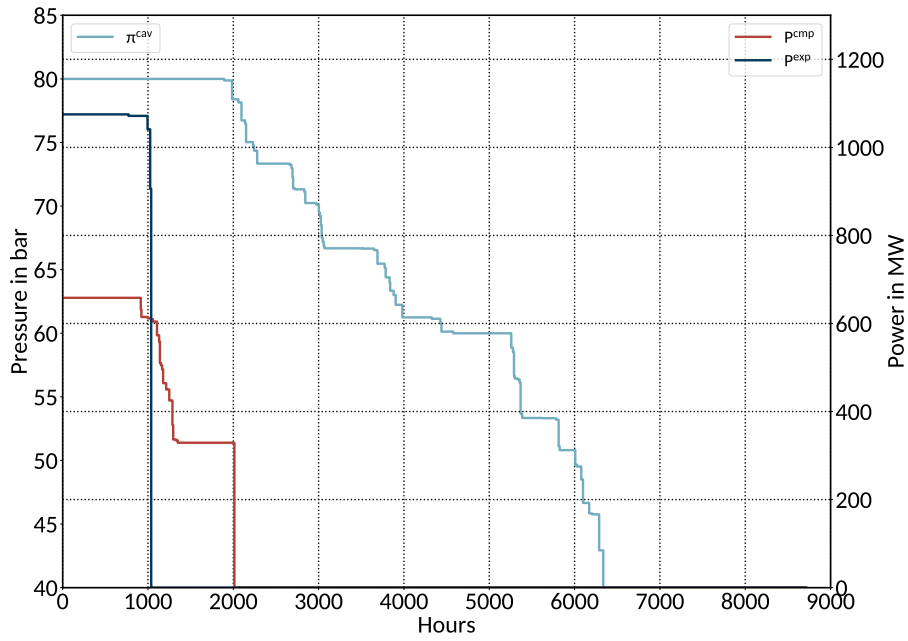
Figure 9.3: Duration curves for expansion, compression and storage part for a design case with a low efficiency of 57.92 %.
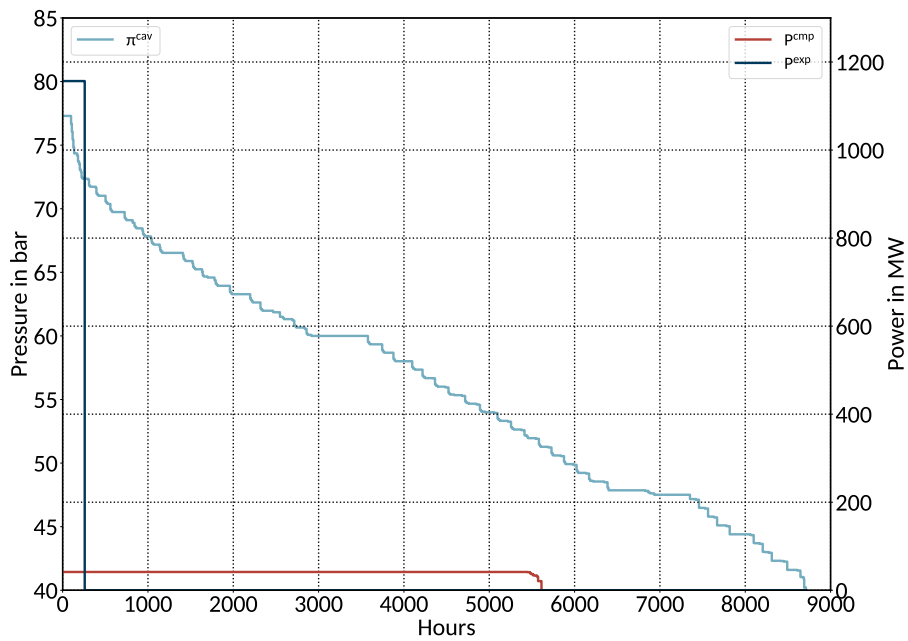

Figure 9.4: Duration curves for expansion, compression and storage part for a design case with a high efficiency of efficiency of 70.59 %.
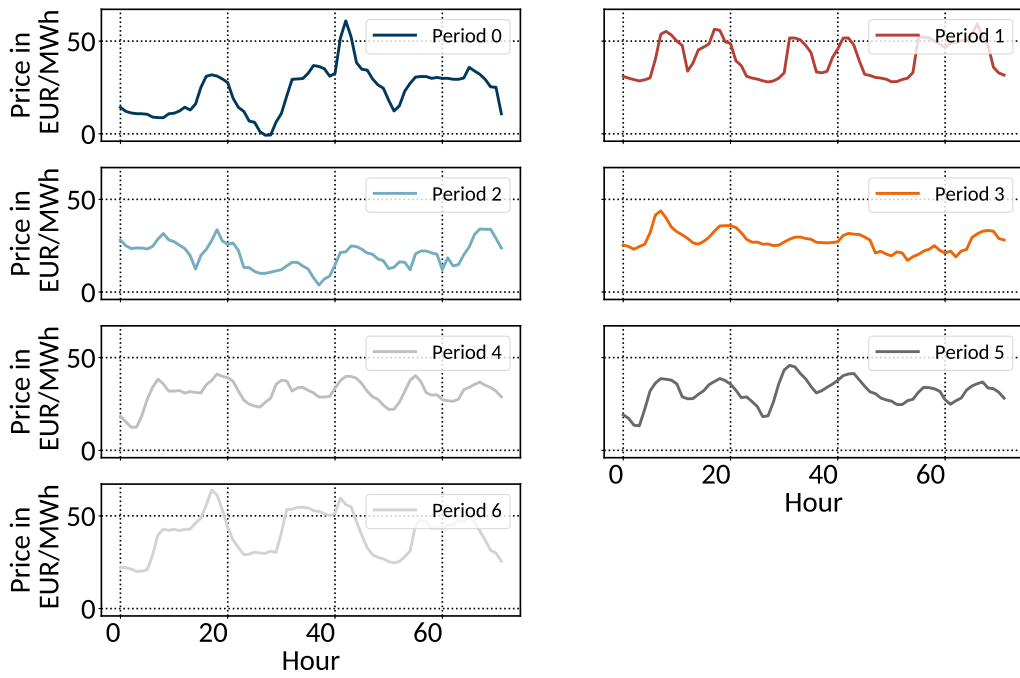
Figure 9.5: Selected representative periods of each 72 h for the electricity price using the k-medoids clustering algorithm.
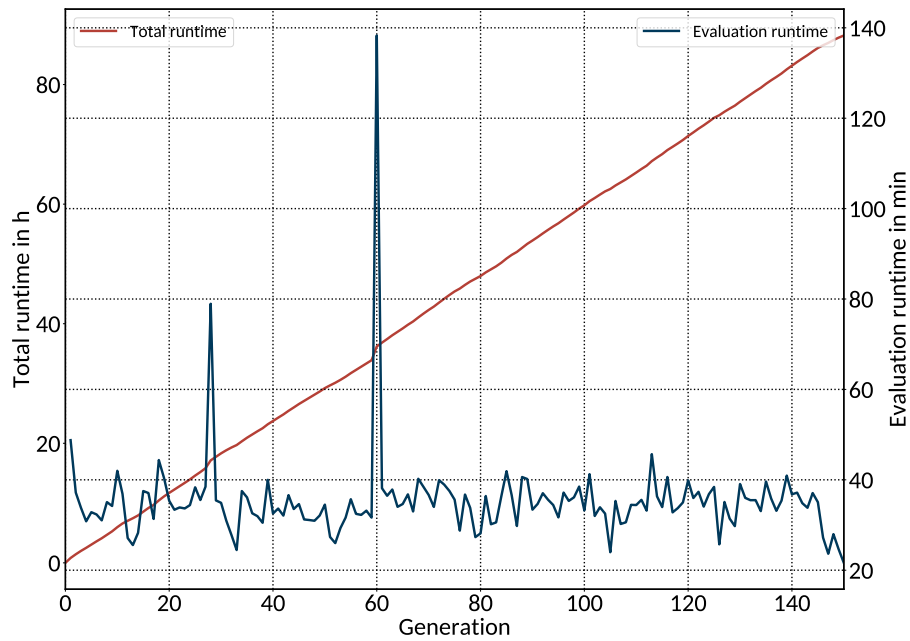

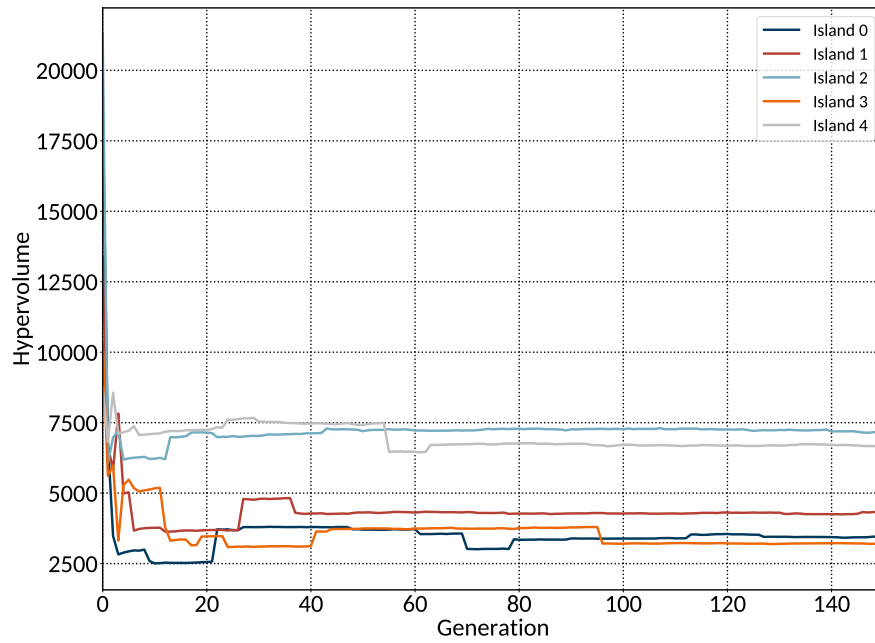**Figure 9.6:** Total algorithm and fitness evaluation runtime over evolutionary process.

Figure 9.7: Hypervolume over evolutionary process for five different islands each having one population of 32 individuals.
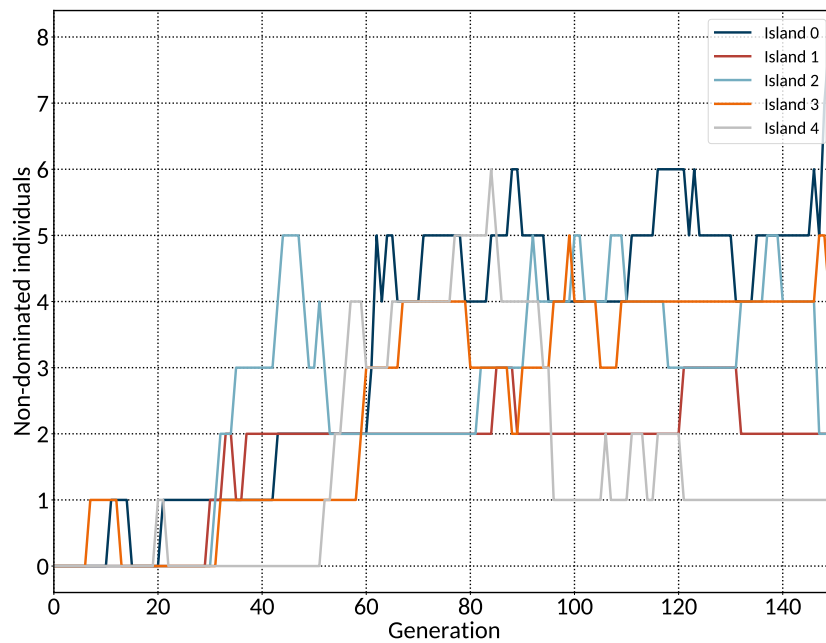

Figure 9.8: Non-dominated individuals over evolutionary process for five different islands each having one population of 32 individuals.
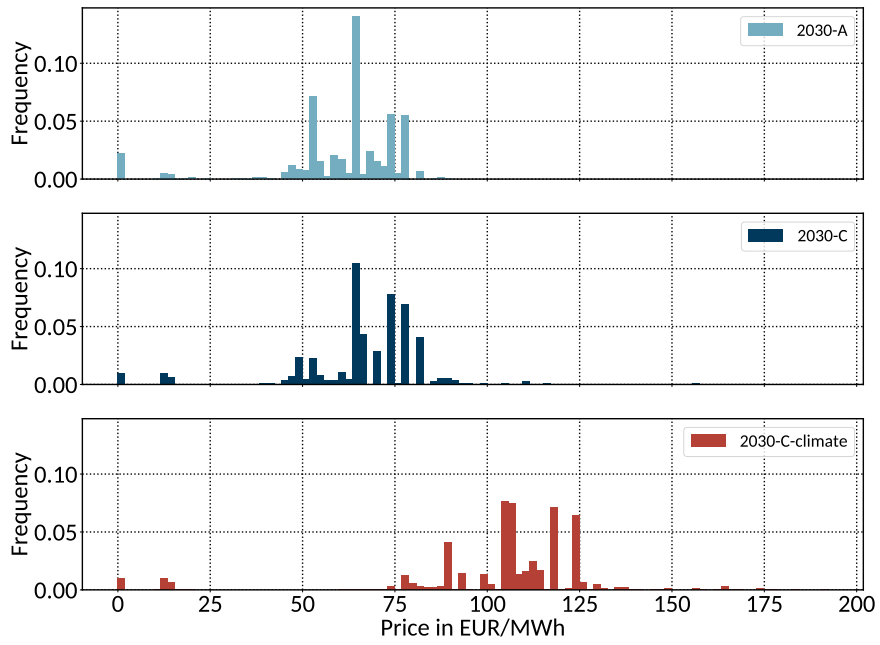
Figure 9.9: Histogram of marginal generation costs within the three selected power system scenarios.
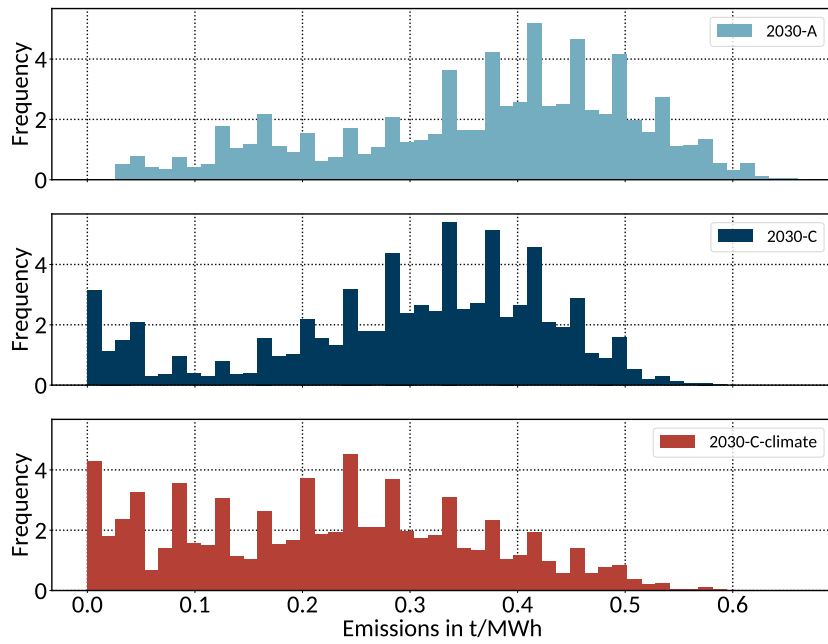

Figure 9.10: Histogram of emissions within the three selected power system scenarios.
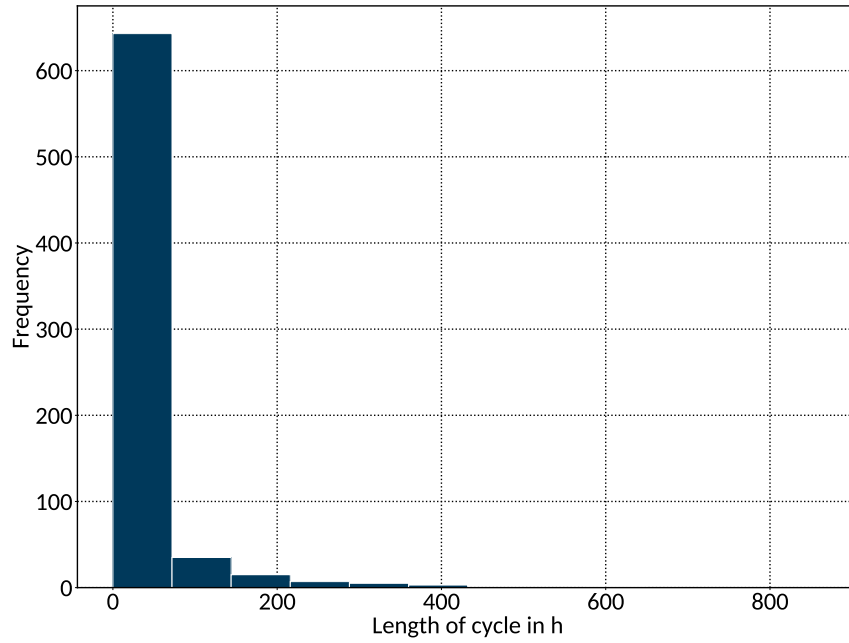
Figure 9.11: Histogram of TES cycle lengths. A bin width of 72 h is chosen to group a total of 709 cycles.

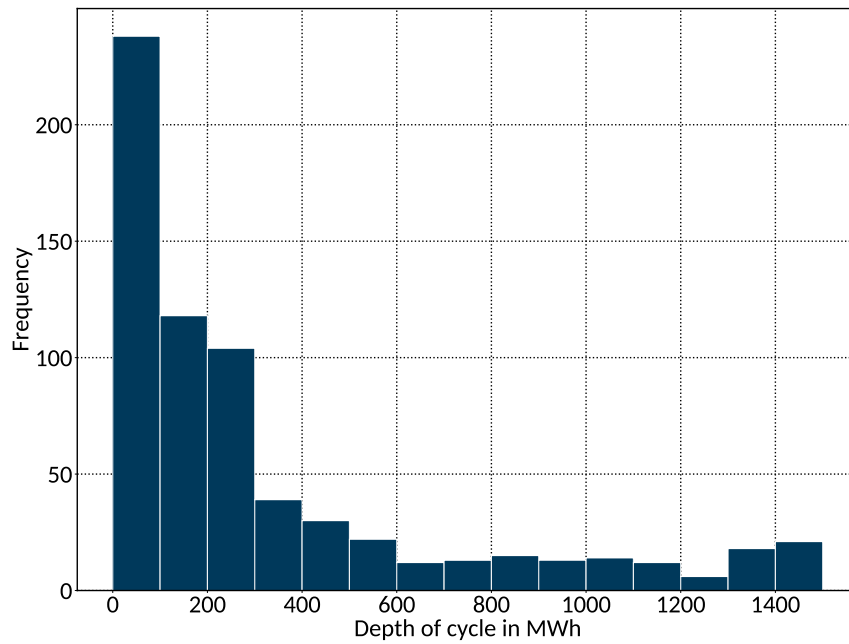**Figure 9.12:** Histogram of TES cycle amplitudes. A bin width of 100 MWh is chosen to group a total of 709 cycles.
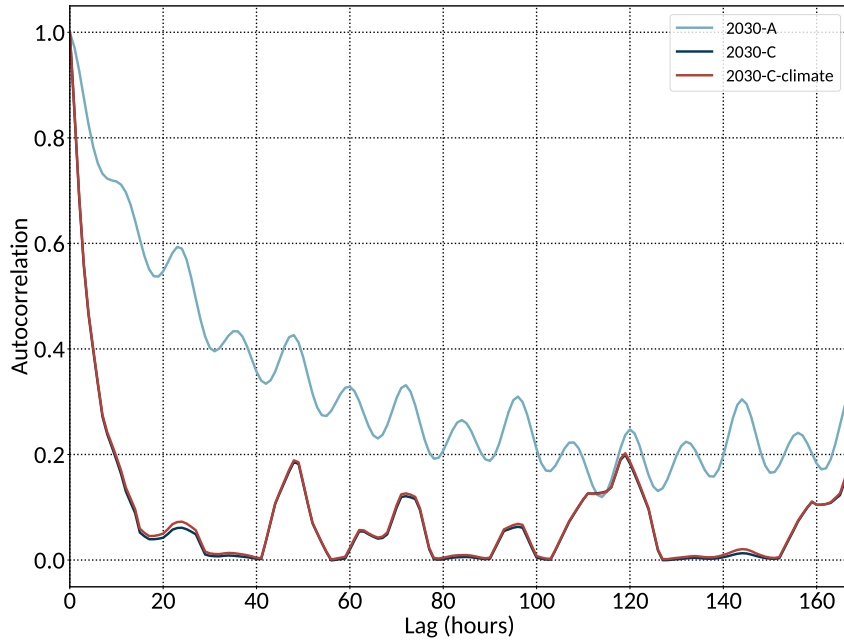
Figure 9.13: Autocorrelation of electricity prices within different power system scenarios.
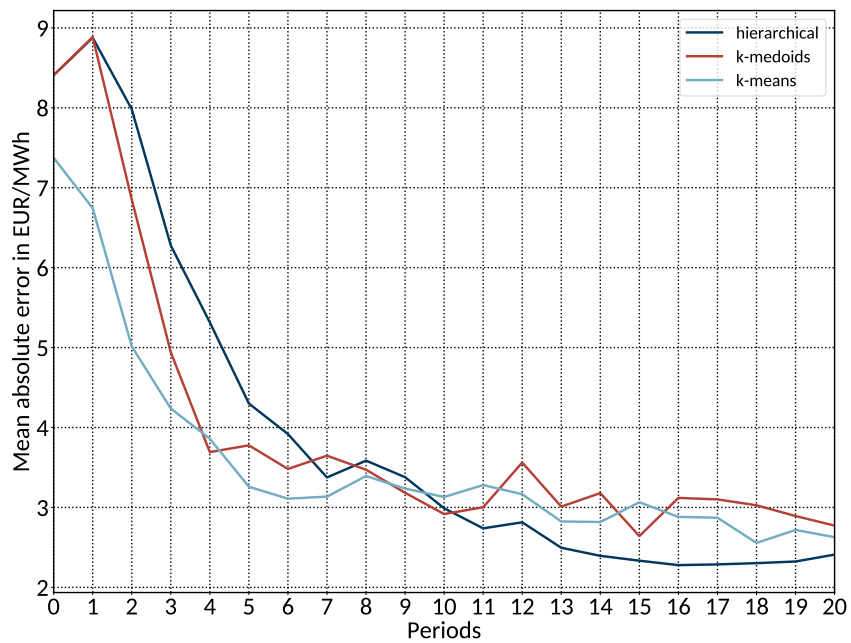
Figure 9.14: Mean absolute error between annual original and cluster electricity price duration curves in scenario "2030-C" for a different number of representative periods of each 48 h.

Figure 9.15: Mean absolute error between annual original and cluster heat load duration curves in scenario "2030-C" for a different number of representative periods of each 72 h.
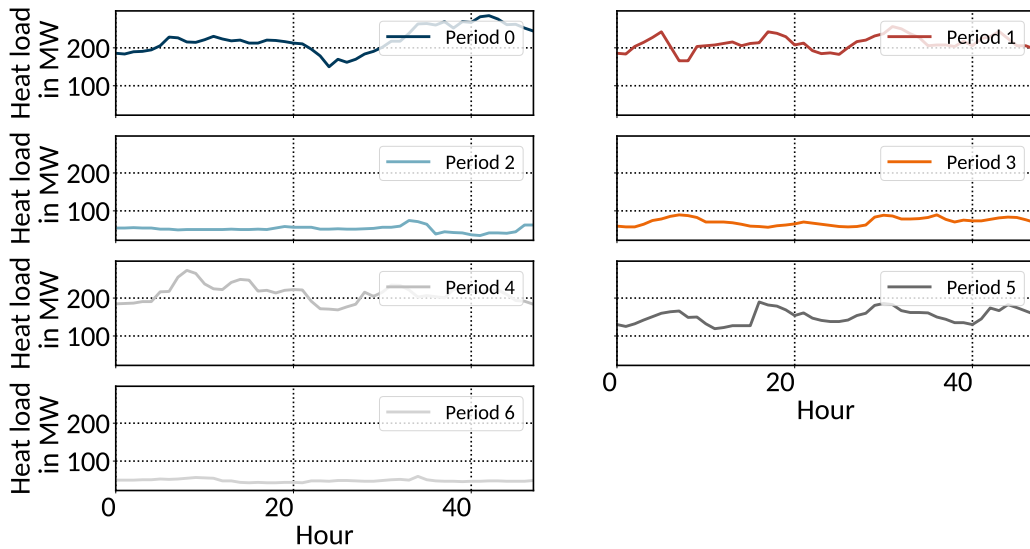
Figure 9.16: Selected representative periods of each 48 h in scenario "2030-C" for the heat load using the hierarchical clustering algorithm.
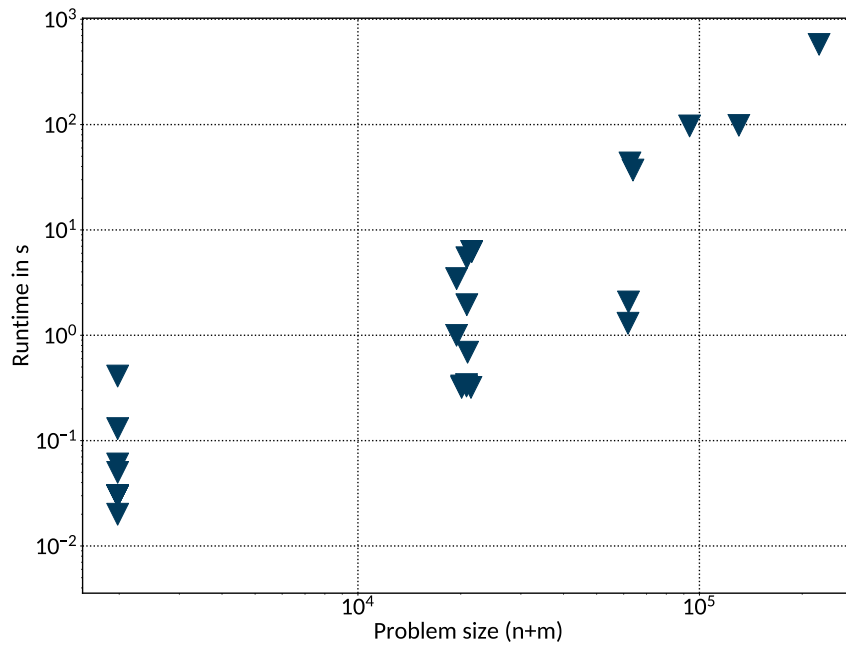
Figure 9.17: Correlation of model runtime and problem size given by the sum of the matrix dimensions.
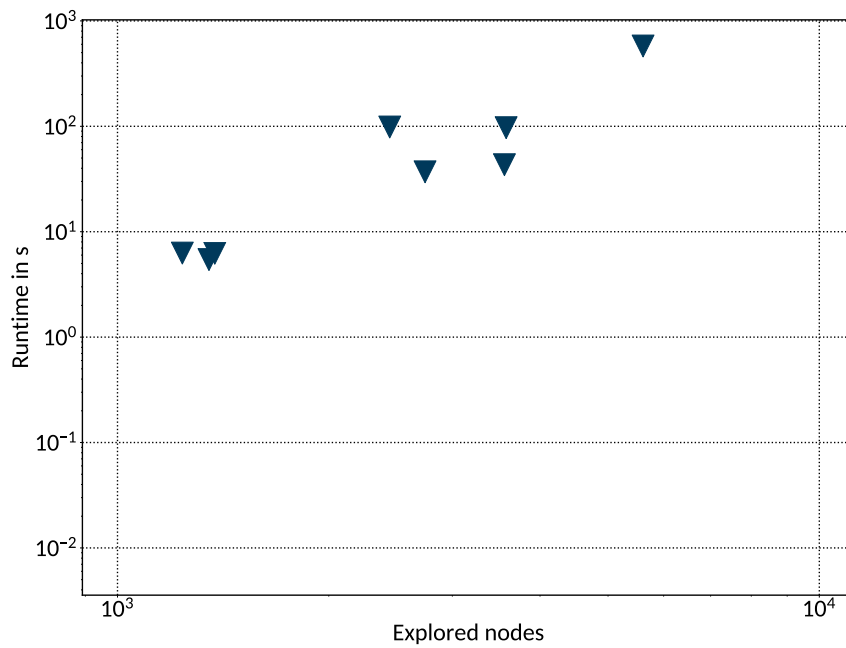
Figure 9.18: Correlation of model runtime and explored nodes within the branch-and-bound algorithm.
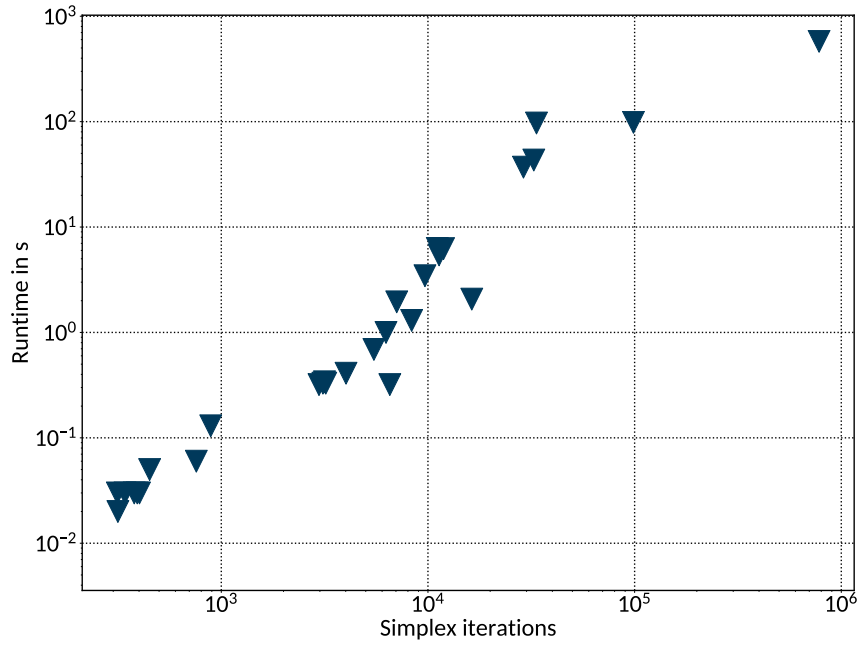
Figure 9.19: Correlation of model runtime and total number of simplex iterations.
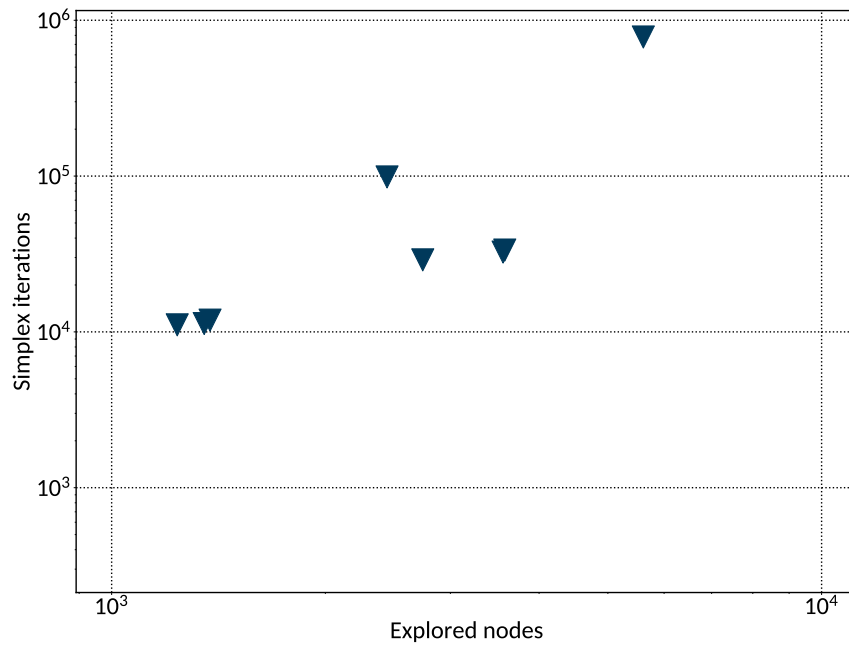
Figure 9.20: Correlation of explored nodes and total number of simplex iterations.
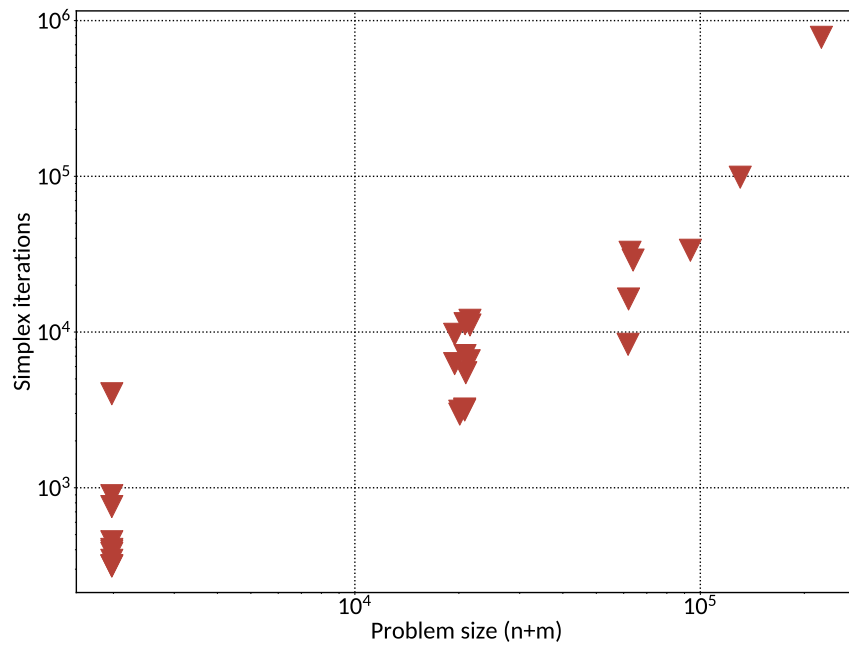
Figure 9.21: Correlation of the number of total simplex iterations and problem size.
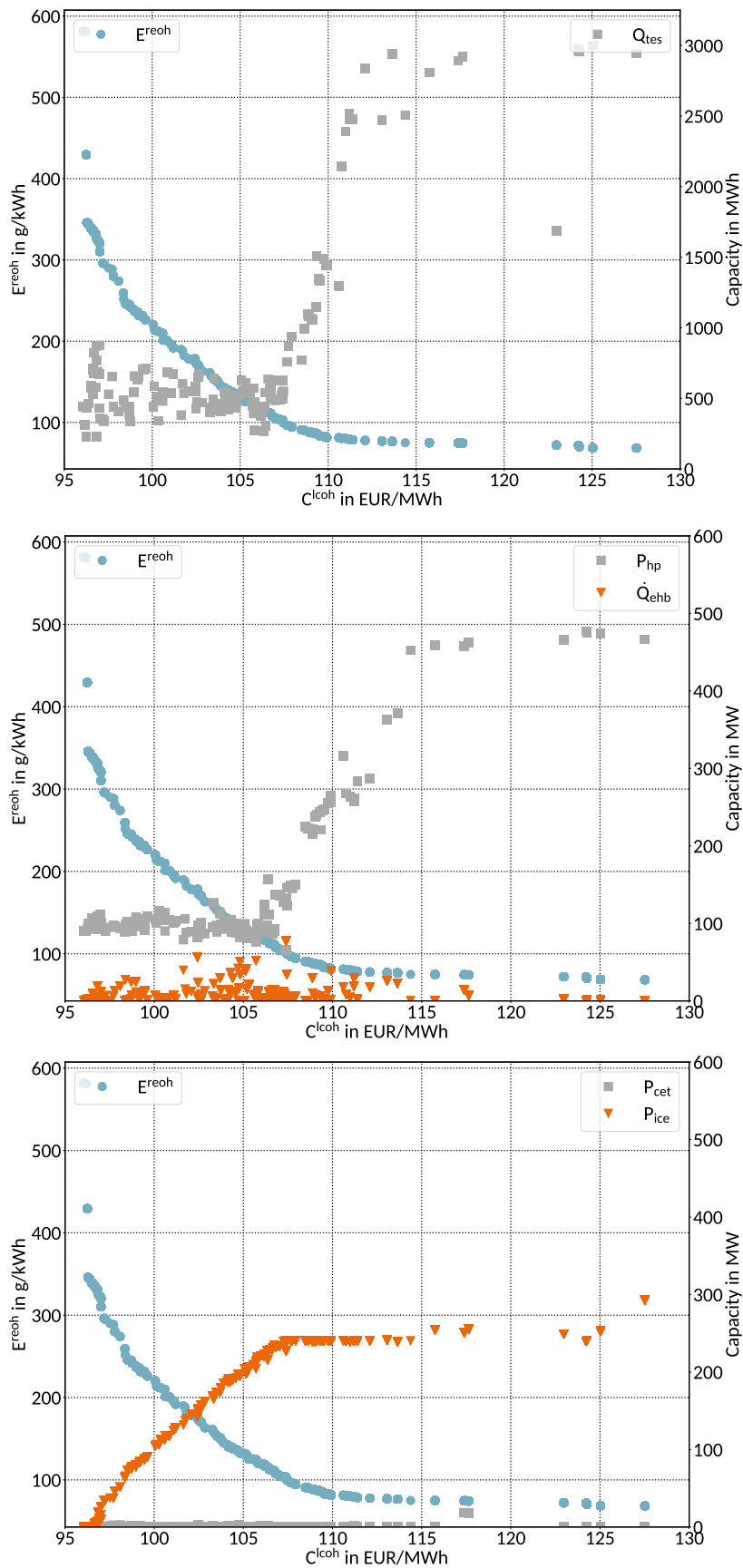
Figure 9.22: Pareto front and design parameters for scenario "2030-A".
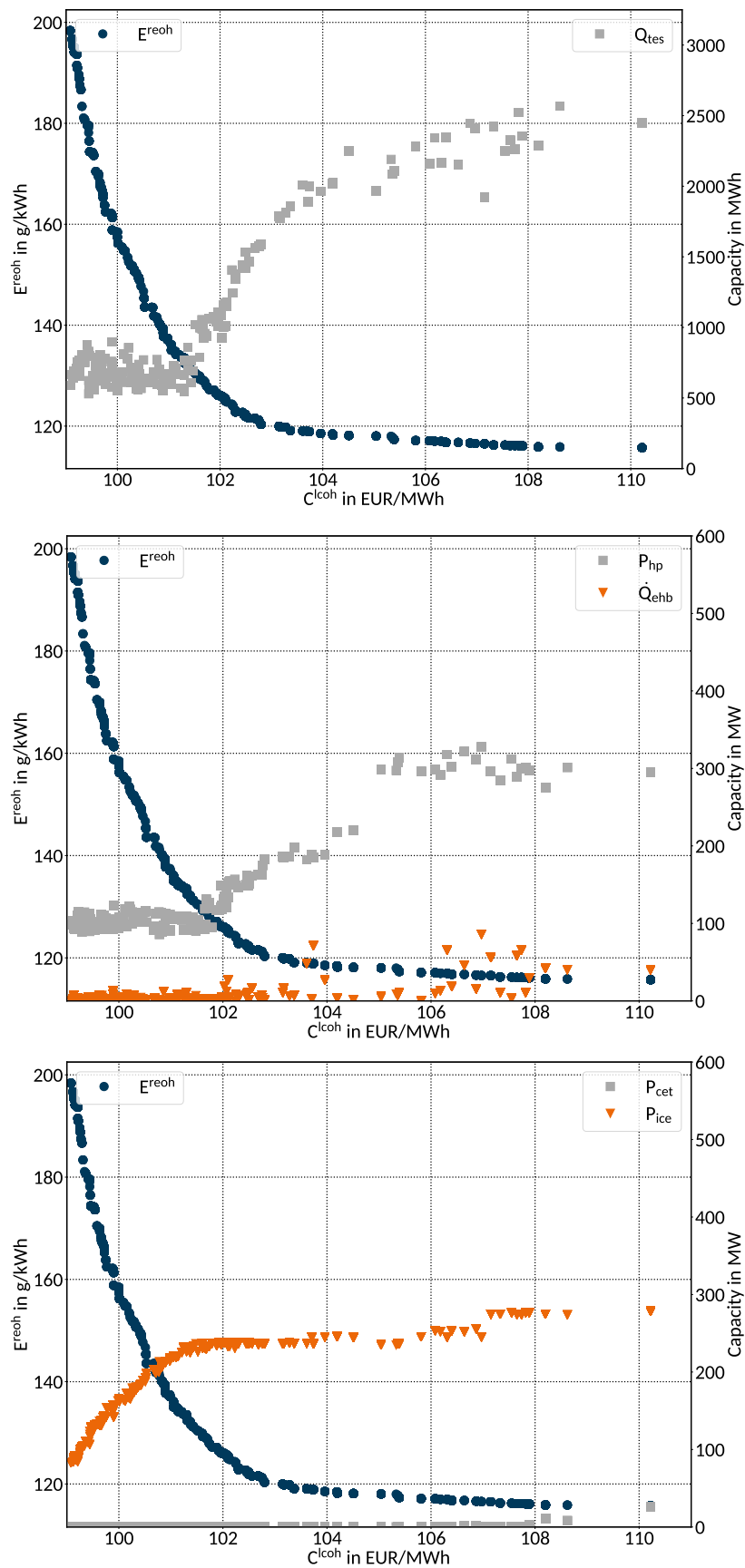
Figure 9.23: Pareto front and design parameters for scenario "2030-C".
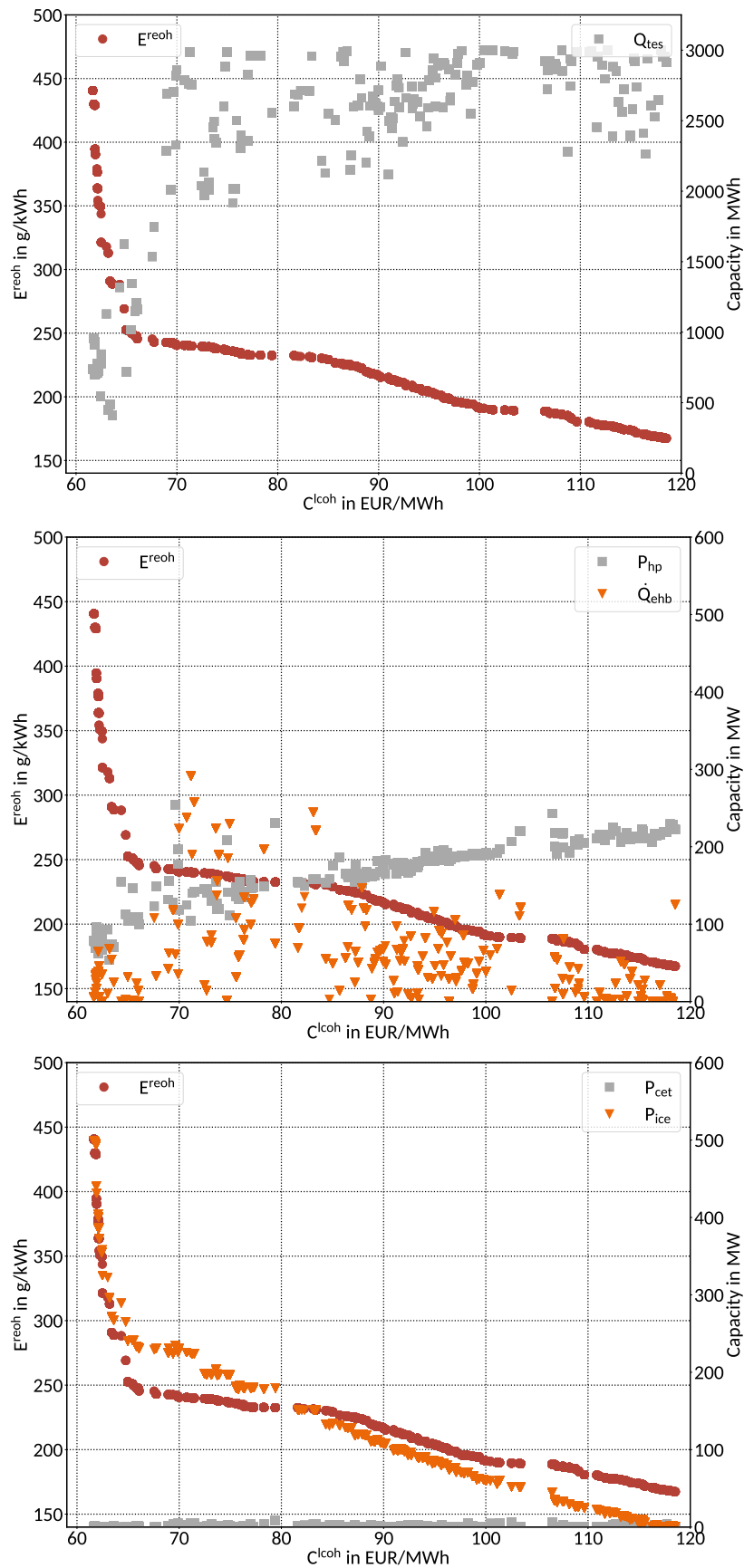
Figure 9.24: Pareto front and design parameters for scenario "2030-C-climate".
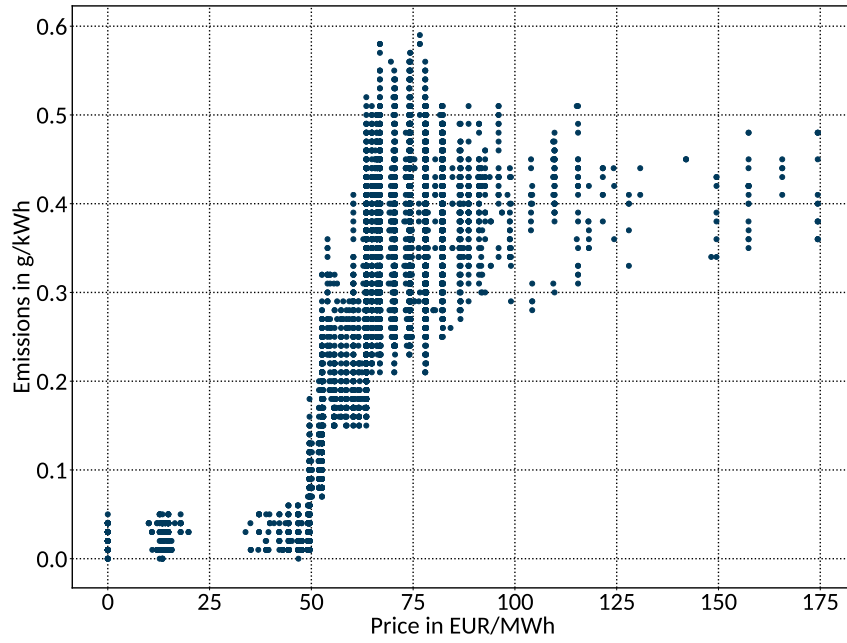
Figure 9.25: Correlation of electricity price and system emissions within scenario "2030-C".
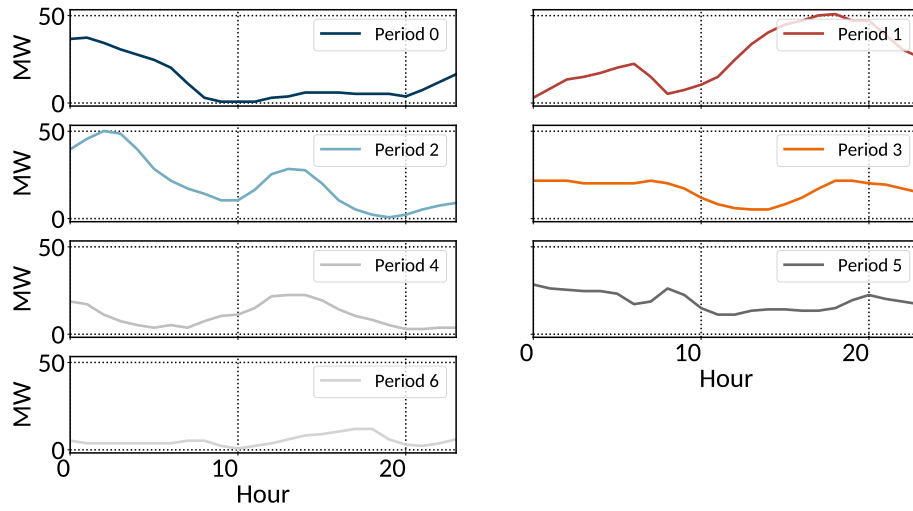
Figure 9.26: Boxplot of selected representative periods of each 72 h for the wind feed-in in the Zhambyl region using the hierarchical clustering algorithm.
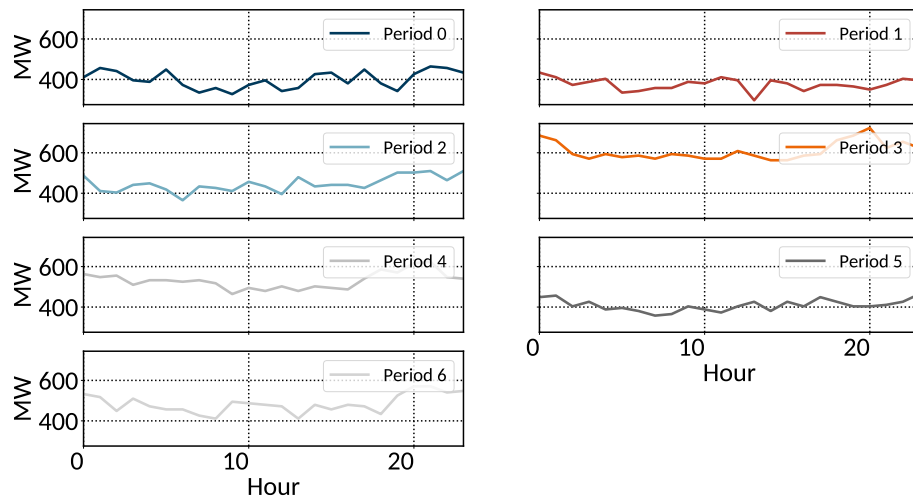
Figure 9.27: Boxplot of selected representative periods of each 72 h for the electricity load in the Zhambyl region using the hierarchical clustering algorithm.
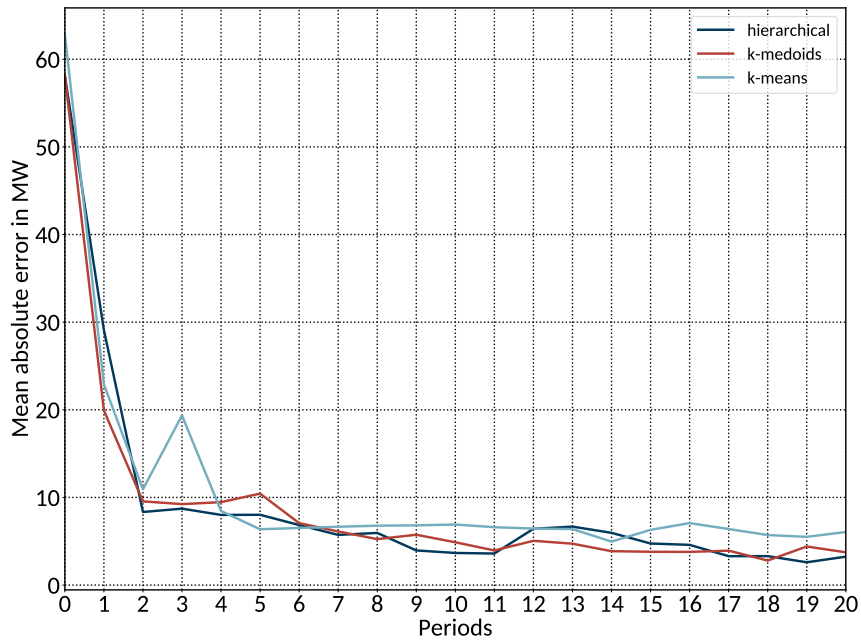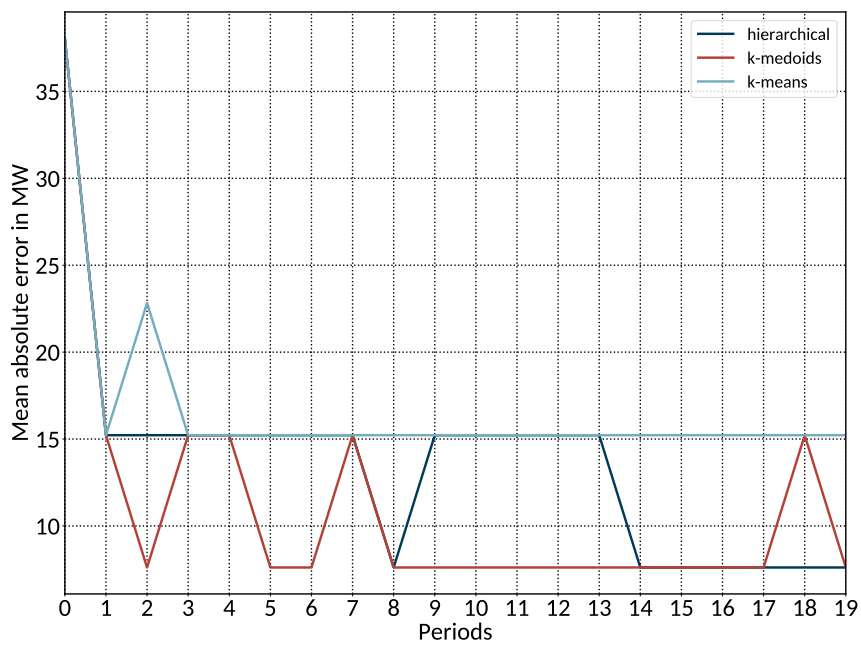

Figure 9.28: Mean absolute error between annual original and cluster load duration curves in the Zhambyl region for a different number of representative periods of each 24h.
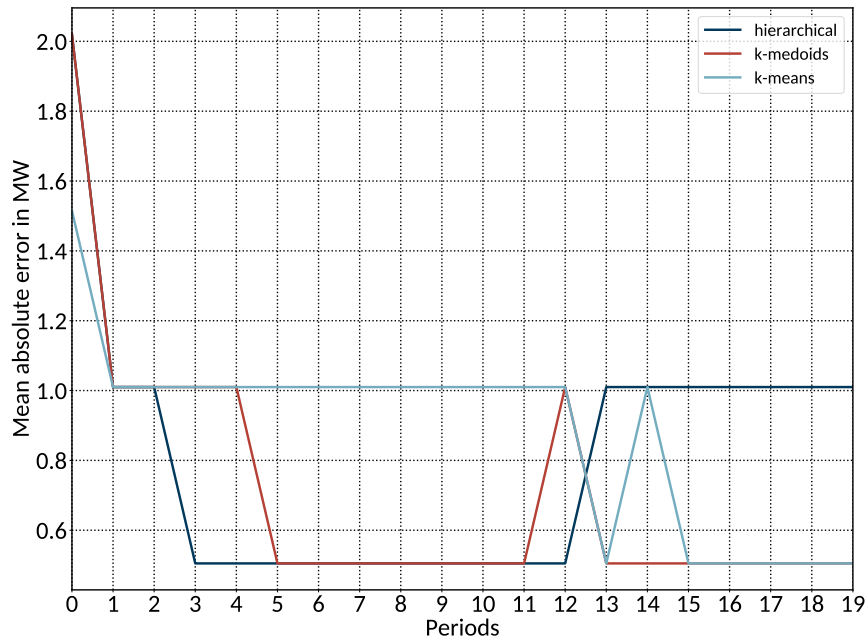
**Figure 9.29:** Mean absolute error between annual original and cluster solar feed-in duration curves in the Zhambyl region for a different number of representative periods of each 24h.
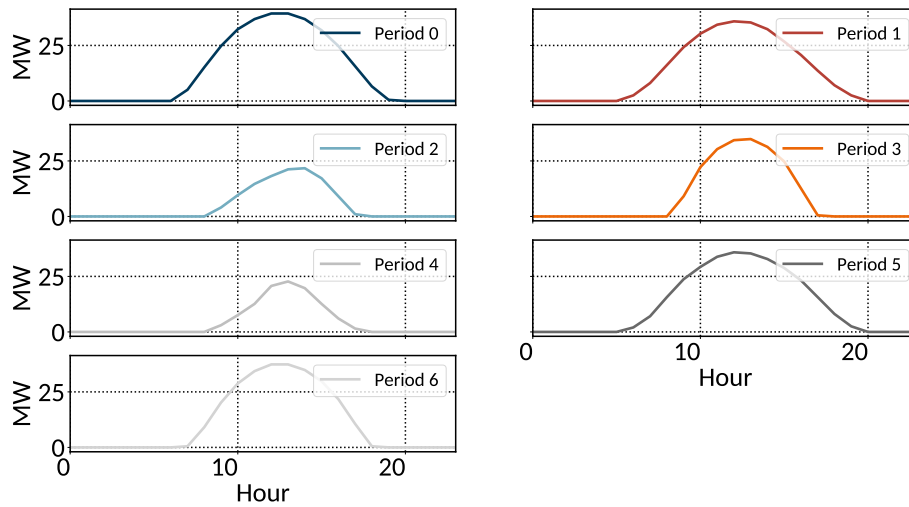
Figure 9.30: Boxplot of selected representative periods of each 72 h for the solar feed-in in the Zhambyl region using the hierarchical clustering algorithm.

C Tables

Table 9.1: Top ten of the most used metrics in evolutionary multi-objective optimization from 2005 to 2013. Table according to [110] with own adaptions.

Ranking	Citations	Metrics	Aspects	Sets
1	91	Hypervolume	Accuracy, Diversity	Unary
2	26	Generational distance	Accuracy	Unary
3	23	Epsilon family	All	Binary
4	17	Inverted generational distance	Accuracy, Diversity	Unary
4	17	Spread: Delta indicator	Diversity	Unary
4	17	Two set coverage	All	Binary
5	9	ONVG	Cardinality	Unary
5	9	R-Metric	All	Binary
6	8	Convergence measure	Accuracy	Unary
7	6	Convergence metric	Accuracy	Unary
7	6	D1R	Accuracy, Diversity	Unary
7	6	Spacing	Diversity	Unary
8	5	M3* metric	Diversity	Unary
9	4	M1* metric	Accuracy	Unary
10	3	Diversity metric	Diversity	Unary
10	3	Entropy metric	Diversity	Unary
10	3	Spread measure	Diversity	Unary

Table 9.2: Overview of grid lines between different regions.

From region	To region	Capacity in MW
AKM	KUS	2880
AKM	SEV	1780
AKM	PAV	2540
AKM	KAR	680
AKT	KUS	1100
ALM	ZHA	2880
ATY	MAN	680
ATY	ZAP	340
KAR	PAV	2880
KAR	ALM	2540
KAR	KZY	340
PAV	VOS	340
YUZ	ZHA	1780
YUZ	KZY	680
KUS	AKM	2880
SEV	AKM	1780
PAV	AKM	2540
KAR	AKM	680
KUS	AKT	1100
ZHA	ALM	2880
MAN	ATY	680
ZAP	ATY	340
PAV	KAR	2880
ALM	KAR	2540
KZY	KAR	340
VOS	PAV	340
ZHA	YUZ	1780
KZY	YUZ	680

Table 9.3: Overview of coal power plants in different regions.

Region	Type	Capacity in MW	Efficiency in %	Min. in %	Max. in %
AKM	CHP	562	42	50	100
AKM	N	0	32	0	100
AKT	CHP	0	42	0	100
AKT	N	0	32	0	100
ALM	CHP	827	42	50	100
ALM	N	0	32	0	100
ATY	CHP	0	42	0	100
ATY	N	0	32	0	100
KAR	CHP	1558	42	50	100
KAR	N	663	32	0	100
KUS	CHP	267	42	50	100
KUS	N	0	32	0	100
KZY	CHP	0	42	0	100
KZY	N	0	32	0	100
MAN	CHP	0	42	0	100
MAN	N	0	32	0	100
PAV	CHP	1977	42	50	100
PAV	N	6450	32	0	100
SEV	CHP	434	42	50	100
SEV	N	0	32	0	100
VOS	CHP	405	42	40	100
VOS	N	0	32	0	100
YUZ	CHP	17	42	50	100
YUZ	N	0	32	0	100
ZAP	CHP	0	42	0	100
ZAP	N	0	32	0	100
ZHA	CHP	0	42	0	100
ZHA	N	0	32	0	100

Table 9.4: Overview of gas power plants in different regions.

Region	Type	Capacity in MW	Efficiency in %	Min. in %	Max. in %
AKM	CHP	0	44	0	100
AKM	N	0	34	0	100
AKT	CHP	91	44	34	100
AKT	N	320	34	0	100
ALM	CHP	25	44	40	100
ALM	N	0	34	0	100
ATY	CHP	338	44	40	100
ATY	N	733	34	0	100
KAR	CHP	0	44	0	100
KAR	N	177	34	0	100
KUS	CHP	16	44	30	100
KUS	N	0	34	0	100
KZY	CHP	67	44	40	100
KZY	N	48	34	0	100
MAN	CHP	705	44	40	100
MAN	N	625	34	0	100
PAV	CHP	0	44	0	100
PAV	N	0	34	0	100
SEV	CHP	0	44	0	100
SEV	N	0	34	0	100
VOS	CHP	0	44	0	100
VOS	N	0	34	0	100
YUZ	CHP	190	44	20	100
YUZ	N	0	34	0	100
ZAP	CHP	30	44	40	100
ZAP	N	198	34	0	100
ZHA	CHP	60	44	40	100
ZHA	N	1230	34	0	100

Table 9.5: Overview of hydropower plants in different regions.

Region	Capacity in MW	Efficiency in %
BUS-AKM	0	100
BUS-AKT	0	100
BUS-ALM	746.2	95
BUS-ATY	0	100
BUS-KAR	0	100
BUS-KUS	0	100
BUS-KZY	0	100
BUS-MAN	0	100
BUS-PAV	0	100
BUS-SEV	0	100
BUS-VOS	1740	92
BUS-YUZ	102.5	100
BUS-ZAP	0	100
BUS-ZHA	14.90	93

Table 9.6: Overview installed wind capacity in different regions.

Region	Capacity in MW
BUS-AKM	45
BUS-AKT	0
BUS-ALM	9
BUS-ATY	0
BUS-KAR	0
BUS-KUS	0
BUS-KZY	0
BUS-MAN	0
BUS-PAV	0
BUS-SEV	3.5
BUS-VOS	0
BUS-YUZ	0
BUS-ZAP	0
BUS-ZHA	74.8

Table 9.7: Overview installed solar capacity in different regions.

Region	Capacity in MW
BUS-AKM	0
BUS-AKT	0
BUS-ALM	2
BUS-ATY	0
BUS-KAR	0
BUS-KUS	0
BUS-KZY	0.4
BUS-MAN	0
BUS-PAV	0
BUS-SEV	0
BUS-VOS	0
BUS-YUZ	2
BUS-ZAP	0
BUS-ZHA	50.5

Table 9.8: Overview maximum and annual load in different regions.

Region	Max. load in MW	Annual load in TWh
BUS-AKM	738	5.38
BUS-AKT	658	4.19
BUS-ALM	1801	10.33
BUS-ATY	643	4.02
BUS-KAR	2262	15.35
BUS-KUS	990	5.44
BUS-KZY	292	1.6
BUS-MAN	825	4.86
BUS-PAV	2520	16.89
BUS-SEV	348	1.74
BUS-VOS	1389	8.64
BUS-YUZ	752	4.29
BUS-ZAP	291	1.76
BUS-ZHA	761	3.96

D Code listings

```python
1  class ExampleDesignModel(DesignModel):
2      """Examplary design model class."""
3
4      def __init__(self, ctx):
5          """Initialize with required attributes.
6
7          Parameters
8          ----------
9          ctx : dictionary to instantiate as parent object
10          """
11          DesignModel.__init__(self, ctx)
12
13      def fitness(self, x):
14          """Select and return fitness functions.
15
16          Parameters
17          ----------
18          x : list with vector of design variables
19          """
20          # set design variables
21          self.set_design_variables(x)
22          self.update_design_variables()
23
24          # pre-process model (optional)
25
26          self.optimize_operation()
27
28          # post-process model (optional)
29
30          # define and return objectives
31          f1 = self.calculate_net_present_value()
32          f2 = self.calculate_efficiency()
33
34          return [f1, f2]
```

Algorithm 9.1: Exemplary definition of a design model.

E Other

Current state of research

This subsection contains a detailed analysis of the literature listed in Section 2.2 i.e. single entries within Table 2.2, Table 2.3 and Table 2.4. For the sake of brevity, these are summarized within Section 2.2.

Compressed air energy storage

In [30] the operation of a conventional gas-fired power units is optimized in combination with wind power and compressed air energy storage. The modelling is realized within a mixed integer non-linear program and implements detailed constraints such as ramping rates and up- and downtimes. Two objective functions are used and either profits maximized or costs minimized. As a result, it is found that significantly higher profits from operation and slightly lower costs in a market environment could be achieved by the use of CAES.

A thermo-economic analysis of a compressed air energy storage system integrated with a wind power plant within the italian spot market for electricity is proposed in [35]. The study involves the analysis of off-design conditions and different operating strategies as well as a detailed modelling of all components. For the case study of southern Italy, it can be demonstrated that the inclusion of a storage option is only cost-effective when it solves local grid imbalances.

The storage model proposed in [30] is used in reduced form as a mixed-integer program within [37] which evalues the value of CAES within a system of renewable energy sources. Extended into a stochastic program, the model includes the uncertainty of electricity prices and variable renewable feedin which can be balanced by the storage in combination with a demand response mechanism which shifts load depending on electricity prices. Overall, the validity of the model is shown by applying four different case studies.

Another optimization model for CAES in combination with wind generation is proposed within [43]. The model is again formulated for the scheduling of the wind farm in combination with the storage in order to optimize the overall profit which depends on the time-wise utilization of gas and electricity prices. It uses chance-constrained programming and investigates a diabatic concept by using the data of the plant in Huntorf, Germany. Overall, the general functionality of the model can be proven by applying the respective case study.

The role of CAES in the future sustainable energy system of Denmark is investigated in [28] from a system and operator perspective. Both, spot market prices and markets for ancilliary services are analyzed with the result that only both markets in combination might indicate potential feasibility from an investors

perspective. An analysis for the German market is proposed in own studies with similar results [39] whereas the model is implemented as mixed-integer linear program and published in another article [40].

Within [29] different operation strategies on electricity spot markets are analyzed for potential CAES operators. In such an operation mode, energy is stored when electricity prices are low and fed into the grid again when electricity are high. Three optimal computer-based methodologies are compared along with two more realistic practical approaches. Results for a Danish case study indicate that even with pratical approaches 80-90% of the optimal earnings can be achieved.

Similarly to [29], in [46] the economic viability of coupling a wind farm with CAES in the day-ahead electricity market is investigated. Therefore, the study assumes a setting when renewable portfolio standards are not present and wind competes in the market. The modelling is hereby realized in an optimization model by means of dynamic programming. Again, results show that the wind–CAES system would not be able to cover annualized capital costs using historical market prices. Even with moderately higher carbon prices in future, the economic viability of the system cannot be achieved.

The integration of offshore wind farms coupled to a compressed air energy storage is also investigated in [32]. By deciding about design components such as grid-tied cable capacities and component sizes of the storage, the model optimizes for the minimum levelized cost of electricity. Derived results indicate that the usage of CAES is significantly more expensive as a backup gas-turbine, even at a very ambitous price for carbon. Thus, the results agree with the ones resulting from [46].

An integration of CAES into the transmission system of Texas with the aim of integrating higher shares of wind energy is investigated in [26]. A mixed integer program is used to model the thermal generation and storage in combination with demand and a simplified transmission network. As wind generation is balanced with CAES their system behaviour is changed towards baseload generators by shifting power generation between peaks and valleys. However, the fossil generation decreases significantly due to the gas used to operate the gas turbine of the diabatic storage plant.

The operational economics of CAES under uncertainty are analyzed within [49] by means of mixed-integer linear program in combination with a probabilistic model to estimate forward hourly electricity and natural gas prices. A case study for Turkey is applied along with economic analyses on the economic performance of the system. Annual profits are analyzed for various simulations for the period from 2011 to 2041 with the result that the investment would be economically viable for the given market environment. Moreover, a sensivity analysis is applied and different design layouts are compared in terms of their economic performance.

In addition to this, studies on single concepts in multiple market environments have been published in different articles. For example, in [38] a detailed production cost model as mixed-integer linear program is proposed and applied to a case study to investigate the value of CAES in systems with large shares of

wind power. In hourly and five-minute time-wise resolution, the economic performance is analyzed in the day-ahead, real-time and control reserve markets with the result that other business cases than solely arbitrage on day-ahead markets lead to a significantly higher profitability.

Another detailed model which is capable of integrating energy and control reserve markets is suggested in [34]. Among proposing detailed unit commitment constraints, the proposed model includes security constraints for the grid and evaluates the integration of wind generation by means of an energy storage system. Case studies with different numbers of busses are presented to validate the overall model. Moreover, a literature review analyzes studies in terms of CAES in the perspective of locational pricing, business economics and other contexts.

A model for an adiabatic CAES for the case of an open electricity market is proposed in [42]. The focus here is on the investigation of benefits in terms of transmission congestion relief and the model again realized as mixed-integer program. As a result, it can be demonstrated that utility commands should be forecasted and integrated within the model to create benefit from the storage system technically on the system side and financially on the operator side.

Even more flexible models for different technical concepts within multiple market environments are proposed in other studies. A generic optimization model within different market environments for storage systems at a high level of detail is developed and described [41]. In contrast to other works, the model also deals with the topics of (non-linear) costs functions of CAES due to a changing efficiency for different load conditions. Among the works in [27] which focus on CAES in combination with wind energy, the model is used to investigate CAES within different economical contexts.

Another model for different concepts within energy and control reserve markets in suggested in [36]. By applying the model within different U.S. markets, the added value of providing control reserve, the dynamic behaviour and the sensitivity of CAES net revenues depending design and performance parameters is investigated. Results indicate that diabatic concepts can be economcally feasible and reserve market revenues have a significant positive influence on the profitability. Against this, adiabatic concepts are not beneficial in terms of an investment due to their hight investment costs.

Similarly, in [45] diabatic and adiabatic concepts are investigated within the German energy and tertiary control reserve market. In combination with wind energy, the centralized and decentralized possibility of integrating the storage is analyzed by applying an optimization model. As shown within other studies, the study concludes that plants can only be operated economically if both the spot market and market for control reserve is utilized. Moreover, a centralized integration of storage expectably seems to be more viable than a decentralized. Moreover, diabatic concepts are more profitable than adiabatic ones due to their cost structure.

A detailed component-based model of an adiabatic concept is presented in [44] as a mixed-integer non-linear program and along with a reduced linearized form. The model is used to l jointly shedule energy and reserves reserve within a standardized test system with multiple busses. The impacts of the storage on the energy and reserve schedules within the power system are analyzed as well as overall operation costs and curtailment of wind turbines. Results show that the system reserve demand cannot be served alone by the system and provided reserve services may increase the overall reserve demand.

Own research works related to the techno-economic modelling and assessment of CAES are based on a mixed-integer multi-concept and -market model. The model is capable of modelling diabatic and adiabatic concepts and is applied in [39] to model two concepts. As a market environment, the German day-ahead spot market and tertiary control reserve market are chosen. Results indicate that the diabatic concept can be economically viable when both spot market and tertiary control reserve markets are utilized. Nevertheless, this is likely to change in future due to a shrinking volume of tertiary control reserve markets due to other technologies that are capable of providing the same service. The full model is published in [40] along with a case study for other concepts.

Only a small number of research works related to CAES with a focus on multiple objectives has been published yet. A design optimization of a combined cooling, heating and power based compressed air energy storage system in terms of thermodynamic and economic objectives is published in [48]. A steady state model based on an exergoeconomic analysis is used within an multi-objective evolutionary algorithm to assess the impact of typical design parameters on the objectives and find beneficial designs. Among other insights, it can be demonstrated that the turbine, compressor and turbine inlet heat exchangers are crucial to obtain a higher exergy efficiency while remaining cost-effective.

Similarly, in [47] design parameters of a combined cooling, heating and power system combined with a solar collector and compressed air energy storage are optimized. Objectives within the evolutionary optimization algorithm are in this case the investment cost and exergetic efficiency of the system. Moreover, within a sensitivity analysis, the effects of technical parameters are evalutated for both maximum heating and cooling conditions.

Design parameters of a small-scale underwater compressed air energy storage system are optimized in [31]. Within the concept, it is assumed that the equipment such as the compressor and turbine is located on-shore while air accumulators are placed at depth. Within a multi-objective evolutionary algorithm the storages energy, exergy, and economics are analyzed. Preferred system designs for different interest rates are studied and additionally the round-trip efficiency and operating profit determined.

A combined approach which optimizes the design and operation of a microgrid with a CAES is proposed in [33]. The microgrid is prepresented by am island test system and consists of a wind turbine, photovoltaic array, diesel generators complemented by a storage. All design variables are changed within a genetic algorithm whereas the unit commitment is realized within an embedded mixed-integer linear pro-

gram. Finally, the proposed dispatch strategy is compared to other existing approaches with the result that it outperforms all other methods. Finally, all studies are summarized and differentiated with regard to different criteria in Table 2.2.

District heating systems

The advantages of heat and power sector coupling have been discussed in numerous studies within the last decades. Hereby, most studies focus on the potential to create flexibility in the the power sector by means of the heat sector in order to integrate higher shares of volatile renewable energies. This mostly affects the spot market for electricity and the markets for control reserve with power to heat technologies in combination with thermal storages or fossil power plants. Moreover, existing and future district heating infrastructure is particularly suitable in this context.

A holistic concept for the conversion of district heating and cooling systems within future renewable energy supply systems is proposed and scientifically claimed by Lund et al. [176] with a strong focus on the question on how such systems can be decarbonized towards 100% renewable systems. Therefore, single future challenges in this field are tackled and the next generation of district heating systems (so called 4th generation district heating systems) are significantly more efficient and smartly connected with power and gas infrastructures. By the creation of an annual conference in the year 2014, meanwhile numerous articles have been published in this field.

Optimization approaches applied to district heating and cooling thermal networks are outlined in [239]. The review article analyses and discusses different types of optimization problems, constraints and techniques as well as the optimization tools that are used in the field of in district energy systems. Among other criteria, it is distinguished between the number of objectives, the type of district heating system and the applied solver.

Various articles within the field of heat and power sector coupling based on linear mathematical models and respective approaches are illustrated in [188], wheras the focus lies on heat supply for the household sector. In summary, it is demonstrated that power and heat technologies can cost efficiently conribute to decarbonize existing energy supply systems by substituting fossil fuels through renewable electricity and heat. Moreover, the usage of heat pumps and passive heat storages on a domestic level level is found to have a large potential in terms of emission reduction.

Formulations on CHP plants within respective optimization models are studied within [182] and [181]. Whereas [182] provides an overview of commonly used generic formulations within (mixed-integer) linear models, the focus in [181] is the proposal and analytical justification of a generic model for CHP plants on a high level of detail. Therefore, respective calculations of the approximated model are com-

pared to detailed thermodynamical analysis with the results that the general characteristics of a power plant can be adequately adressed within a simplified techno-economic model.

The integration potentials for renewables by means of district heating systems in computational models have been analysed in different studies. As one example [240] investigates the development of district heating systems within the danish energy system in 100% renewable scenarios until the year 2060. As one key result, district heating systems are identified as strategically important to cover heat demands in urban areas. Hereby, such central systems and specifically heating grids are decarbonized gradually until the year 2060. In contrast, for decentral heat supply on a domestic level heat pumps are recommended due to comparably low costs and induced emissions which is in line with the findings from [176].

Capabilities of a typical urban district heating grid to balance volatile wind power feed-in are analyzed in [60]. Within the study, the optimal unit commitment of different heat supply technologies is analyzed for different levels of wind power feed-in in terms of the overall effect related to the operational costs. It could be demonstrated that respective systems are able to provide a high level of flexibility and can contribute significantly to the intergration of renewable energy into the power system. Morover, the dimensioning of the thermal storage in relation to the overall renewable and fossil generation capacity is evaluated. The overall findings are hereby in line with [240].

Similar questions related to the question on how renewable power generation can be balanced within the Germany energy system are addressed within [61]. Hereby, in particular the influence of electric heaters on the system costs and emissions is analyzed for the period from 2012 until 2025. In accordance with [60] the general capability of district heating systems to balance variable renewables can be demonstrated with a focus on control reserve markets. By utilizing power to heat technologies in times of high renewable power generation, fossil based power plants can be decoupled from must-run capacities providing negative control reserve which reduces induced emissions.

Relations between CHP plants in combination with thermal storages and the overall efficiency and costs of the electricity system are evaluated in [69]. Besides the variation of the share of renewable and fossil generation capacities, the capacity of thermal storages and feed-flow temperature of thermal power plants is varied. Results confirm a positive integration effect for renewable power generation which is in line with the findings from [60] and [61]. Moreover, it can be demonstrated that CHP plants are able to reduce the efficiency of the overall system as well as the overall system costs. In line with expectations, increased capacities of thermal storages lead to higher shares of integrated renewables.

The integration of flow temperatures in UC models of future DH systems has been analyzed within an own paper [8] which has been proposed and presented at the conference by Lund et al. (2014) mentioned above [176]. The study investigates the effect of introducing varying supply temperatures in mixed-integer linear programming models based on a case study of a municipal district heating system. Moreover, it is analyzed how the temperature integration approach affects unit commitment and technology assessment

for different temperature levels and scenarios. In conclusion, it could be demonstrated that the effect of changing temperature on a technology assessment is comparably small as opposed to adaptions in the regulatory framework which directly affect the objective function.

Within Milan et al. (2015) the modeling of non-linear CHP efficiency curves in distributed energy systems is analized [64]. The authors claim that in this context detailed system models are required in order to make optimal decisions on investment and operation. As fuel cells and micro-turbine units share non-linear properties especially when modelling part-load behaviour, the study implements two approximation variants within a MIP problem. Results indicate that part load operation has mainly been found important for fuel cell units whereas the micro-turbine is found almost exclusively in full load. Thus the application of the new approaches to the micro-turbine is found to be not as relevant as to the fuel cell for the considered unit sizes and building types.

One recent approach to optimize district heating systems in terms of different objectives, is the toolbox "modesto" which is developed at the department of mechanical engineering at KU Leuven [72]. The software is meant to be a multi-objective district energy systems toolbox for optimization and allows for different components to be optimized in (sub) networks whereas the overall problem is represented as a (mixed-integer) linear program. In this context, the term "multi-objective" means the general capability of exchanging the objective function to optimize for different metrics such as emissions, costs or energy. Thus, the toolbox still uses mono-objective optimization and does not allow to optimize for multiple objectives simulaneously.

Within [70] a two-level optimization approach is proposed to optimize the design and operation of district heating systems. It uses mixed-integer linear programming and consists of a master level which includes mainly design variables, and a slave level which integrating operational variables. The method uses weighted sums to integrate economical and ecological metrics in the objective and is successfully applied to a case study.

Complexity reduction approaches for the optimal design and operation optimization of multi-energy systems involving seasonal energy storage are investogated within [21]. Therefore, new mixed integer linear programming methodologies are proposed which allow the consideration of long term horizons at hourly resolution while the complexity of the optimization problem is significantly reduced. Moreover, the methodologies are compared to results for clustered models and full horizon optimizations indicating that the results are corresponding.

As opposed to various studies on the systemic effects and economy of district heating systems, research on the business economy of single systems from an operators perspective is scarce. Hereby, in particular the work of [59] and related publications of this work group such as [22] have to be mentioned. Within [59] the contribution of heat storages on the business economy of the district heating operation is investigated using the case study of a district heating system in the area of Berlin. Results indicate that thermal

storages have a significant positive impact on the business economy of the entire district heating infrastructure. In contrast to the assumption of "perfect foresight" used in [59], studies [62] and [63] focus on the question on how uncertainty concerning wind feed-in and electricity prices can be addressed by means of a stochastic optimization model of the district heating system.

Optimal sizing of a biomass-fired organic rankine cycle combined heat and power system with heat storage is presented along with a respective methodology in [71]. The focus is on investor based assessment along with the investigation of heat storage benefits. Within a hybrid optimization approach, the operation is optimized using mixed-integer linear programming whereas the non-linear sizing optimization embeds the operational optimization within a loop. Overall, fuel prices for an economical operation could be estimated and the existence of a heat storage be proven to be uneconomical due to the assumption of fixed feed-in tariffs.

The optimal design and operation of technologies in multi-energy microgrids with electricty, heating, and cooling loads is described in [65]. The model extends the DER-CAM model which is developed at the university of Berkeley is adapted by new mixed-integer formulations and uses multiple nodes instead of a single node to balance the demand and supply side. Results indicate that the inclusion of multiple nodes is required to model distributed energy systems in order to correctly estimate the occurring investment costs.

A multi-objective model for the design and operational optimization of combined heat and power distributed generation systems is proposed in [50]. The authors use mixed-integer programming in combination with the method of weighted sums in order to integrate multiple criteria within the objective function. The model is applied to a case study of limited urban area where buildings Are connected by a heat network and equipped with small-size CHP plants. Furthermore, it can be demonstrated that the model is capable of showing the potential in terms of economical and ecological benefits.

Within [22] the interdependencies between heat storages and district heating networks are analyzed regarding economic and ecological criteria. Therefore, a multi-criteria objective function which includes profit and operational emissions is applied within within a mixed-integer linear optimization by means of the weighted sum method. Besides the operational optimization design parameters such as the type of supply, transport and storage facilities are optimized simultaneously along with subsequent a sensivity analysis. Results show that newly installed storage facilities are favored over a network expansion regarding both objectives due to the strong effect of decoupling heat demand and electricity production.

A framework that couples a descriptive analytical model for medium to large-scale energy systems with a multi-objective evolutionary algorithm is proposed by [51]. The framework enables identify Pareto-optimal sets of configurations regarding different competing objectives and is applied to the case of Aalborg municipality within a case study. While confirming the finding of previous works, an entire set of additional optimal solutions could be generated and the effectiveness of the approach be proven.

Multi-objective optimization of optimal design and operation of urban distributed energy systems as well as optimal heating network layouts is studied in [66]. A mixed integer linear programming model was used along with the ε-constraint method for multi-objective optimisation to minimize total cost and carbon emissions. Within a case study for residential and commercial building different design results are presented which show that emissions savings can be improved significantly over a standard solution for the same cost by means of the proposed method. Moreover, an adaption of the model by power flow and grid upgrade options using three different methods (including one bi-level method with an evolutionary algorithm) is proposed in [67]. It can be shown that all methods produce interpretable results and have their fields of application depending on the acceptable runerime and level of accuracy. In another work, one of the methods is used on the decarbonization of urban grids [68].

Generic bi-level multi-objective approaches for the simultaneous design and operational optimization of disctrict heating systems have been applied by Fazlollahi et al. in a series of publications [52, 53, 55, 56, 57, 96, 54] based on previous work at the same institute [58]. A first method consisting of a district heating system represented in a MILP model optimized cost-wise with regard to the opration which is embedded within a multi-objective evolutionary algorithm optimizing design parameters of the system in terms of multiple objectives was proposed in conference contribution [52] and leading to a subsequent journal publication [53]. The same model has later been applied for the integration of biomass resources within [54].

An application of the multi-objective approach to district heating optimization using data which is clustered by a method proposed before by the autor [96] is realized within [55]. Thermo-economic simulation models are used to adapt the LP/MILP models depending on the assertion of objectives within the multi-objective evolutionary algorithm. Decision variables are the maximum size of equipment e.g. the thermal storage capacity and the type of storage. Objective-wise, a simulaneous minimization of total annual cost along with induced emissions and a maximization of the total system efficiency is realized. Results indicate that all objectives could be improved moderately by means of the method application.

In [56] the model is further developed to optimize network structures such as pipeline layouts between consumers and producers. Objectives are similar to previous work from [55] and the operational optimization (called slave optimization in this context) is explained in detail using a layer structure. In conclusion, it could be demonstrated that the developed method is applicable using an illustrative example. In another study [57] the previous work from [56] and [96] is combined to optimize a district heating system for an urban are including a respective transmission network. Objectives are again the total annual cost, induced emissions and system efficiency which all could be improved significantly. Finally, all studies are summarized and differentiated with regard to different criteria in Table 2.3.

Multi-regional and other systems

Especially for the country of Kazakhstan three relevant modelling papers have been published within the last decade. Within a collaboration of the DIW Berlin and the Nazarbayev University in Astana, lower carbon strategies for the electricity sector of Kazakhstan for the years 2030 and 50 are modelled [89]. Hereby, a two-stage CDOM optimizes both, the operation of all generation facilities and and the investment in grid expansion in order to evaluate economical pathways for the future electricity sector of Kazakhstan. Further, within another study the impact of storage technologies on renewable energy integration in Kazakhstan is analyzed within an operational model that is realized as an LP [87]. Within another study, a spatially resolved electricity market model for the power system is published [88]. The model is designed to provide a transparent tool in order to assess the changes in the national electricity system in a technical, economic, and environmental dimension and provides all data in another subsequent paper [98].

A procedure for estimating the optimal sizing of photovoltaic and energy storage units has been proposed in [241] whereas the storage optimization and operation is realized from a utility's perspective. Moreover, the storage optimization seeks for a maximization of the technical benefits for the distribution system by means of a general parallel GA which embeds a simulator for the distribution system. Hierarchical clustering is applied to reduce the problem size and find typical daily power curves e.g. for PV units.

Within [84] a thermoenvironomic optimization of a small-scale distributed combined cooling, heating, and power (CCHP) system with risk analysis is realized within a multi-objective approach . A GA has been applied to optimize three objective functions including the exergetic efficiency, total levelized cost rate of the system product and the cost rate of environmental impact. In this context only the design is optimized with regard to the different objectives which makes a MDM. Furthermore, risk analysis is used to make a decision based on the final optimal solution.

In [19] an operational and topological optimization of multi-carrier energy systems i proposed based on their concept of energy hubs which includes multiple energy carriers such as electricity, natural gas, and district heat. While previous studies focused on sole operational optimization of such systems [83] within this paper the couplings between different systems are optimized. This combined optimization of energy systems allows to determine optimal interfaces between different energy infrastructures and is illustrated by means of three exemplary case studies.

Another study proposes a multi-objective optimization approach for the selection and dimensioning of energy storage systems [86]. Within different case studies storage systems are analyzed for different applications such as grid-scale applications in centralized energy systems and services within DER are analyzed. The model is implemented as a MIP problem whereas and adapted form of the ε-constraint

method is applied to regard multiple objectives such as the storages' discharge duration, levelized costs of storage and environmental impact.

A combination of a multi-objective evolutionary algorithm and a descriptive analytical model has been proposed in the field of energy scenario design [51]. As scenarios are typically based on a mix of different energy sources and at the same time different competing objectives exist it is possible to automatically identify a set of Pareto-optimal configurations. Within a case study for the disctrict heating of Aalborg in northern Denmark the proposed method is applied for the contrasting goals of cost and carbon emissions. Results indicate that the method delivers additional insights compared to a previous single optimization investigation as it yields additional optimal solutions with regard to the defined objectives.

The optimal design of multi-energy systems with seasonal storage is analyzed in [21]. For this, novel MILP methodologies which allow for a consideration of an annual time horizon at hourly resolution are applied which are able to significantly reduce the problem complexity. It could be shown that the proposed approaches deliver similar results as an optimization at full scale. Finally, a multi-energy system which is based on a neighborhood in Zurich, Switzerland, is optimized with regard to total annual costs and emissions in order to perform a sensitivity analysis on different features of the system designby applying the well known ε-constraint method.

An optimal sizing of a combined cooling, heating and power microgrid using multi-objective optimization has been studied within [77]. The CCHP is designed to satisfy the demand in power, heating and cooling for a large office building located in Tehran. Costs, energy efficiency and emissions are optimized within a multi-objective genetic algorithm which embeds a simulation-based operational model. Results indicate that a solar-dominated system has a considerable advantages in energy saving and emissions over a conventional based system.

Renewable energy penetration rates in power systems which are optimized regarding multiple objectives are analyzed in [85]. Within a case study approach a multi-objective evolutionary algorithm is applied to optimize both the annualized renewable energy cost and the system reliability simultaneously. Hereby, conventional backup capacities are installed in the current system and the the rate of renewables is optimized with regard to both objectives. Obtained results for the case study demonstrate that the use of various renewable resources namely PV and wind is able to satisfy both objectives to a large extent. Nevertheless, the capacity expansion has not been extented to conventional capacities since this would require an operational model.

A multi-objective model for operation and the design of future integrated multi-carrier energy networks at a high spatial and temporal resolution has been proposed with [73] after applying the approach to different research questions. The multi-objective optimization is realized by means of a weighted sum approach and the energy system representation described by the concept of "value webs" [73] which shows characteristics as energy hubs [19], MES [17] or other graph-based descriptions [9]. Within the

proposed concept article [73] different scenarios involving different primary energy sources to satisfy demands for heat, electricity and mobility across different sectors were examined for Great Britan.

The respective model has been used for the evaluation of biomass value chains within different bioenergy system pathways within [91]. Moreover in [92] the model has been adapted to generically encompass conversion, transport and storage infrastructures along with a decomposition approach which reduces the complexity of the design optimization. Finally, in another paper the model is applied to the energy system of Great Britain for a decabonization by means of an optimal design and operation of a potential future integrated wind-hydrogen-electricity network [93].

Within Mashayakekh at al. (2017) a mixed integer linear programming approach for the sizing, and placement of DER portfolio in multi-energy microgrids [65] is proposed. Within a multi-node modeling approach that includes electrical power and heat flow equations, the model allows to perform an optimal siting while considering physical and operational constraints of different components. Within a case study, the model is compared to a single-node version for an example microgrid. Results indicate that multi-node approaches are superior within the process of sizing DER portfolios when compared to single-node approaches as they tend to underestimate the overall investment costs.

Optimal operation of an integrated energy system including fossil fuel power generation, carbon capture and wind is analyzed in [90]. Within a nonlinear hourly model for the system the operating profit is maximized for a period of 24 hours by means of given energy prices and wind generation data. Moreover, a carbon emission constraint is modelled to limit the amout of emissions to a maximal value. As a result, it could be demonstrated that via optimal flexible operation the effective operating cost of respective systems can be substantially reduced with an additional consideration of emission constraints.

In another study the authors have extended their model to simultaneously determine the optimal design and and operation for a flexible coal–natural gas power station with carbon capture [80]. Hereby, a similar coal-fired power station is undergoing a retrofit including a carbon capture unit powered by a specially designed combined cycle gas turbine. Moreover, the focus lies on a detailed modelling and optimization of the heat recovery steam generator contained within the CCGT within different electricity markets. Within a bi-objective method a mixed-integer nonlinear programming formulation delivers the optimal operation which is embeded within an external design optimization which is realized via a specific PSO variant based in preliminary works from [242]. Finally, Pareto frontiers are obtained for the minimization of capital requirement and the maximization of the net present value and offer more information for the decision maker than a sole operational optimization as [90]. A similar investigation of the same authors uses the same methods as in [80] with a stronger focus on the detailed modelling [81].

Multi-objective design and operational optimization of distributed and renewable energy systems in build-ings has been proposed in [79]. The authors make use of a hybrid multi-objective optimization approach for the sizing of thermal and electrical energy systems with regard to thermo-economic performance in-

dicators. Within the approach the operation is optimized using a MILP and model-predictive control. Additionally, design variables are optimized by an evolutionary algorithm which embeds the linear program along with clustered data which reduces the complexity and resulting runtime. Within a case study different sizes of the components are analyzed regarding two objectives which are investment costs and self-consumption share.

Within [78] the authors proposed a multi-objective optimization approach for combined gas and electricity network expansion planning. For this, within a hybrid method a hard mixed integer non-linear stochastic problem is embedded within an evolutionary algorithm along with a preference-based decision making approach to select the final solution from the set of optimal solutions with regard to both objectives. Both investment cost and production cost are optimized simultaneously while regarding criteria which ensure network security. In addition, wind power generation is addressed in the model in its stochastic nature. Finally, the method is tested against different reference systems and found to be effective.

A soft-linking of a power systems model to an energy systems model is proposed in [82]. This soft-linking is realized to gain insights from the power systems model strong points and transfer them into the energy systems model. Obtained results hereby help to improve and develop a deeper understanding of results from the energy systems model. The authors' main motivation stems from the idea that there is not one specific energy modeling tool which is able to address all aspects of the real energy system in detail. In contrast, according to the authors insights and progress can rather be achieved by looking a the results of different specialized modelling tools rather than trying to cover all aspects within one comprehensive modelling tool.

Within another study [74] energy systems are modelled at urban level by for the municipality of Bressanone (Brixen) in northern Italy. Various energy scenarios including PV on roof tops, heat pumps and electrical and thermal energy storages are applied within a case study with the aim to improve the system in terms of costs and emissions. Here, the EES and a TES attached to a heat pump are further evaluated to utilize the generated excess electricity from PV. Within a hybrid approach two simulation models have been embedded within a MOEA in order to optimize different system configurations with regard to costs and emissions. Besides demonstrating the value which has been added by the approach results clearly highlight the benefits of coupling the electricity and heat sector.

A generalization of the approach from [74] has been proposed by Prina et al. (2018a) [75] along with another case study application [75]. Within the case study the coupling of a MOEA namely NSGAII to the EnergyPLAN simulation software is described in detail using the same objectives as in [74] for the energy system of South Tyrol. Hereby, special emphasis is put on the energy efficiency in buildings whereas energy efficiency costs are be described for different building types having respective construction periods and locations. Overall, the advantages of an optimization approach which covers economical, technical and environmental aspects are demonstrated within the selected case study.

Another study of the same authors [75] for the case study of Italy uses the same approach to incorporate CCGT flexibility constraints and related additional costs into the model proposed in [76]. As the energy system of Italy is dominated by high capacities of CCGT this modelling of costs which are related to start-up and partial load conditions is needed to describe the system adequately. Results indicate that the consideration of CCGT cycling costs within energy system modells is crucial in future because these are strongly affected by increasing shares of intermittent renewable generation in future. Moreover, these rising costs can open favorable business models for other technologies offering load modulation such as EES. Finally, all studies are summarized and differentiated with regard to different criteria in Table 2.4.